Heat and Mass Transfer

Nickolai M. Rubtsov
Kirill Ya. Troshin
Michail I. Alymov

Catalytic Ignition of Hydrogen and Hydrogen-Hydrocarbon Blends Over Noble Metals

Springer

Heat and Mass Transfer

This book series publishes monographs and professional books in all fields of heat and mass transfer, presenting the interrelationships between scientific foundations, experimental techniques, model-based analysis of results and their transfer to technological applications. The authors are all leading experts in their fields.

Heat and Mass Transfer addresses professionals and researchers, students and teachers alike. It aims to provide both basic knowledge and practical solutions, while also fostering discussion and drawing attention to the synergies that are essential to start new research projects.

Nickolai M. Rubtsov · Kirill Ya. Troshin ·
Michail I. Alymov

Catalytic Ignition of Hydrogen and Hydrogen-Hydrocarbon Blends Over Noble Metals

Springer

Nickolai M. Rubtsov
Merzhanov Institute of Structural
Macrokinetics and Materials Science
Russian Academy of Sciences
Moscow, Russia

Kirill Ya. Troshin
N. N. Semenov Federal Research Center for
Chemical Physics
Russian Academy of Sciences
Moscow, Russia

Michail I. Alymov
Merzhanov Institute of Structural
Macrokinetics and Materials Science
Russian Academy of Sciences
Moscow, Russia

ISSN 1860-4846 ISSN 1860-4854 (electronic)
Heat and Mass Transfer
ISBN 978-3-031-28415-1 ISBN 978-3-031-28416-8 (eBook)
https://doi.org/10.1007/978-3-031-28416-8

This Springer imprint is published by the registered company Springer Nature Switzerland AG
The registered company address is: Gewerbestrasse 11, 6330 Cham, Switzerland

I love science more than money.

Johann Wolfgang Döbereiner

Preface

One of the reasons for writing this book was that 200 years ago in 1822, Johann Wolfgang Döbereiner published his pioneering work on the catalytic action of platinum on the oxidation of alcohol to acetic acid, although the term "catalysis" was introduced by Jöns Jakob Berzelius noticeably later in 1835. Döbereiner was the first, who noted that *the platinum was not used up by the reaction but could be used again* to acidify fresh, perhaps limitless, quantities of alcohol. It is the definition that carries the essence of the contemporary meaning of the catalysis.

Another phrase of Döbereiner "*I love science more than money*" also remained in history, and something tells the authors that few modern scientists can repeat these words sincerely.

In this book, the issues on noble metal influence on gaseous combustion are examined, which have been partly considered in our previous books *Key Factors of Combustion, From Kinetics to Gas Dynamics* (2017, Springer Aerospace technology, Springer International Publishing) and *Initiation and Flame Propagation in Combustion of Gases and Pyrophoric Metal Nanostructures* (2021, Fluid Mechanics and Its Applications, Springer Nature Switzerland AG). We drew attention to the fact that our seemingly disparate experimental data presented in these books were significantly supplemented and rethought; in addition, a number of new results were obtained, both experimental and theoretical ones. In our opinion, the entire cycle of our research on the effects of noble metals (platinum, palladium, ruthenium and rhodium) on the ignition and combustion of hydrogen and hydrogen-hydrocarbon mixtures (C1–C6) should be presented sequentially and summarized in a separate monograph.

Catalysis by noble metals is usually studied when the metal is deposited on a substrate, while the action of the catalyst itself should be separated from the processes of interaction of the metal and the reaction being studied with the substrate. Nevertheless, relatively few studies have been devoted to catalysis on the surfaces of pure metals. This book is one of such studies.

The book is aimed at the consideration of the essential problems of catalysis with noble metals in combustion; it presents the original results obtained by the authors in 2014–2022. This book focuses on the new data on combustion processes having practical applications and includes fire safety issues in the use of noble metals in

hydrogen recombiners for NPP, as well as in catalytically stabilized (CS) combustion technology including stimulation of combustion of hydrogen-blended hydrocarbons, synthesis of carbon nanotubes and determination of catalytic ignition limits in noble metal-hydrogen-hydrocarbon systems.

The studies presented in each paragraph are set out in the common scientific article format, namely introduction, experiment and discussion of the results.

The book is useful for experienced students and qualified scientists in the area of experimental and numerical studies of combustion processes.

A cellular combustion regime of 40% H_2–air mixture in the presence of a Pt wire over the interval 270–350 °C was observed for the first time. It is shown that the regime is caused by the catalytic action of Pt-containing particles formed by decomposition of volatile platinum oxide in the gas phase.

It was shown that the temperature of the initiated ignition at 40 Torr over heated Pd foil is ~100 °C lower than over Pt foil. Even the minimum temperature value (623 °C) is sufficient to ignite $2H_2 + O_2$ mixture; i.e., the influence of a catalytic $H_2 + O_2$ reaction over the noble metals is negligible in case of initiated ignition. The presence of water vapor prevents ignition. For thermal ignition at 180 Torr and 288 °C over Pd foil, the catalytic activity of the surface is higher than that over Pt foil. The activity of Pd foil reveals itself in both the occurrence of local ignition centers on the foil, from which combustion wave propagates, and the dark catalytic reaction of consumption of the flammable mixture.

It was shown that in the reaction of hydrogen combustion, metallic Pt acts as a heat source similar to, e.g., a tungsten wire heated by an external source. However, in the case under investigation, Pt is heated with an internal source, namely a surface catalytic reaction. It must be also taken into account that the composition of the surface layer changes during ignitions from Pt oxide (PtO_2) to another composition, exhibiting properties different from PtO_2.

Hydrogen and deuterium combustion over Rh, Ru, Pd and Pt wires at total pressures up to 200 Torr and initial temperatures up to 500 °C was investigated in order both to establish the dependencies of catalytic ignition limits over noble metal surfaces on temperature and to indicate the governing factors of the problem of gas ignition by a catalytic surface. It was revealed that Rh, Ru and Pd surfaces treated with $2H_2 + O_2$ ignitions show the defects in the form of openings, which are located on etching patterns; the etching substances are active intermediates of H_2 oxidation. It was found that before ignition catalytic wire is not heated up uniformly; initial centers of the ignition occur. It was shown that Rh is the most effective catalyst of $2H_2 + O_2$ ignition, the lowest ignition temperature over Rh-coated Pd wire (Rh/Pd) was 210 °C, for Ru/Pd and Pd—300 °C, for Pt wire—410 °C at total pressures less than 200 Torr. The hysteresis phenomenon is observed over Ru/Pd, Pt and Pd wires; namely, the ignition limit value measured over the wire, which is not treated with ignitions (a procedure of increasing temperature from a state of no ignition), is higher than the value measured with a procedure of decreasing temperature from a state of catalytic ignition. It was shown that Rh is the most effective catalyst of $2D_2 + O_2$ ignition, in this case the lowest ignition temperature over Rh-coated Pd wire (Rh/Pd) was 100 °C. It is more accurate to speak about ignition over noble

metals hydrides/deuterides; thus, the lowest ignition limit of $2D_2 + O_2$ over rhodium deuteride was 100 °C; thus, D_2 is more flammable than H_2 over Rh and Pd. The obtained results indicate the existence of a "kinetic inverse isotope effect", which affects the reactivity of MeH and MeD, where Me = Rh, Pd.

It was shown that the initiation of the thermal ignition process is always determined by the presence of reactive centers on the surface, the properties of which are determined by both surface defects having an excess of free energy and their catalytic properties; the ignition process includes stages of warming-up, local ignition and flame propagation. The chemical activity of various sites of the surface changes from one ignition to another. The basic feature of the ignition process lies in the fact that the ignition occurs at separate sites of surface at uniform temperature of the reactor surface. Therefore, combustion originates on the surface of the reactor even under conditions of almost homogeneous warming-up of a flammable gas mixture. It was found that the qualitative model based on the reactive compressible Navier–Stokes equations allows obtaining both the mode of the emergence of primary ignition centers on the wire followed by a local ignition and the mode of a dark catalytic reaction of the consumption of the initial reagent.

It was shown experimentally that the ignition temperature of the 40% H_2 + air mixture over metallic Pd (70 °C, 1 atm) was ~200 °C lower than over the Pt surface (260 °C, 1 atm). In addition, Pd wire initiates the ignition of (30–60% H_2 + 70–40% $CH_4)_{stoich}$ + air mixtures; Pt wire of the same size cannot ignite these mixtures at reactor temperatures below 450 °C. This means that Pd wire is more effective in initiation of the ignition than Pt wire. The cellular structure of the flame front during ignition in the presence of Pd wire was not observed in contrast to the results obtained on the Pt surface. Therefore, Pd is more suitable than Pt for hydrogen recombiners in nuclear power plants (NPP) because the catalytic particles do not appear in the gas phase. The experimental value of the effective activation energy of the process was estimated as (3.5 ±1) kcal/mol, which is characteristic of surface processes. This indicates the significant role of the dark reaction of H_2 and O_2 consumption on the Pd surface observed directly at low pressures. The presence of this reaction reduces the probability of accidental explosion compared to the Pt surface. It was found that in the presence of leucosapphire, there was no system of emission bands of H_2O^* in the range 570–650 nm, and a possible explanation of this effect was given. The appearance of an additional source of excited water molecules emitting in the range 900–970 nm was explained.

It was experimentally shown that the temperature of the catalytic ignition limit over Pd at $P = 1.75$ atm, measured with a bottom-up approach by temperature, of the mixtures 30% methane + 70% hydrogen + air ($\theta = 0.9$, $T = 317$ °C) and 30% propane + 70% H_2 + air ($\theta = 1$, $T = 106$ °C) markedly drops after subsequent ignitions to $T = 270$ °C for H_2–CH_4 mix and to $T = 32$ °C for the H_2–C_3H_8 blend. Equivalence ratio θ is a fraction of fuel in the mix with air: $\theta H_2 + 0.5\,(O_2 + 3.76\,N_2)$. The ignition limit returns to the initial value after treatment of the reactor with O_2 or air; i.e., a hysteresis phenomenon occurs. The ignition limit of the mixtures 30% (C2, C4, C5, C6) + 70% H_2 + air ($\theta = 0.6$, 1.1, 1.2, 1.2, correspondingly) over Pd amounts to 25–35 °C at $P = 1.75$ atm; the hysteresis effect is missing. It was found

that the lean 30% C_2H_6 + 70% H_2 + air mix ($\theta = 0.6$) shows the lowest temperature of the ignition limit: 24 °C at 1 atm. The estimate of the effective activation energy of the ignition of the mixes over Pd is ~2.4 ±1 kcal/mol that is characteristic of a surface process. Thus, the usage of Pd catalyst allows igniting H_2–hydrocarbon mixtures at 1–2 atm at initial room temperature without external energy sources. It was shown experimentally that the ignition temperature of the 40% H_2 + air mixture over metallic Pd (70 °C, 1 atm) was ~200 °C lower than over the Pt surface (260 °C, 1 atm). In addition, Pd wire initiates the ignition of the (30–60% H_2 + 70–40% $CH_4)_{stoich}$ + air mixtures; Pt wire of the same size cannot ignite these mixtures at reactor temperatures below 450 °C. This means that Pd wire is more effective in initiation of ignition than Pt wire.

It was found that the ignition temperatures of hydrogen–oxygen and hydrogen–methane–oxygen mixes at low pressure over heated Pd, Pt, Nichrome and Kanthal wires at 40 Torr increase with a decrease in H_2concentration; only a heated Pd wire shows the pronounced catalytic action. Numerical calculations allowed revealing the role of an additional branching step $H + HO_2 \rightarrow 2OH$.

The peculiarities of ignition of premixed stoichiometric n-pentane-air mixtures were studied in a rapid mixture injection static reactor in the presence of metallic Pt and Pd in the region of negative temperature coefficient (NTC). It is shown that in the absence of noble metals, thermoacoustic oscillations occur within NTC region. However, in the presence of Pt catalyst surface, which reacts with oxygen at the flame temperature and generates catalytic centers propagating into volume, thermoacoustic regimes of thermal ignition disappear. In other words, the catalytic Pt surface eliminates a certain inhibition stage of kinetic mechanism after the occurrence of the cool flame and NTC phenomenon vanishes; the stage may be, e.g., the decomposition of some intermediate slow-reacting peroxide on Pt surface with the formation of a more reactive radical. In the presence of the catalytic surface (Pd), which does not react at the flame temperature and does not generate catalytic centers propagating into volume, NTC phenomenon occurs.

Thus, the detected regularities must be taken into account in numerical simulations of NTC phenomenon. In other words, thermoacoustic oscillations and NTC phenomenon must both disappear in calculations after excluding a certain reaction or a series of reaction steps from the mechanism. The step must include the superficial reaction of an active intermediate of combustion on Pt surface, in which more active intermediates are formed from a low-active one.

It was found that the ignition delay (induction) period during the combustion of (70–40% hydrogen + 30–60% propane) + air mixtures over palladium at a total pressure of 1–2 atm first decreases with a decrease in temperature and then increases until the ignition limit is reached, i.e., the NTC phenomenon in catalytic combustion occurs. The effective activation energy E of the process is 2.2 ±1 kcal mol^{-1} that is characteristic of a surface process. Therefore, the NTC phenomenon detected in this work is closely related to the surface state of Pd. In the sample treated with ignitions, defects in the form of holes were found, which are focused on the etching patterns with active intermediates of the process. In this process, PdO particles are formed during the oxidation of the Pd surface and decompose to Pd and O_2 at the temperature

of flame products. Thus, Pd is consumed in the chemical etching reaction with active combustion intermediates. It should limit the applicability of palladium in ignition devices.

It was shown that at total pressures up to 200 Torr, the catalytic ignition areas over the Rh and Pd surfaces are larger for $2H_2 + O_2$ mixtures than for $(H_2 + CH_4)_{stoich} + O_2$ and $(H_2 + C_4H_8)_{stoich} + O_2$ mixtures; the mixtures containing more than 50% hydrocarbons do not ignite. This behavior is directly related to the formation of a carbon-containing film on the noble metal surface. The fuel in the mixtures is consumed in a dark reaction. In the case of the synthesis of carbon nanotubes by this method, the noble metal plays both the role of a catalyst for the growth of nanostructures and a heating element; for this, the presence of hydrogen and oxygen in the gas mixture is necessary. It has been shown that the dark reaction in $(80\%\ H_2 + 20\%\ C_4H_8)_{stoich} + O_2$ mixture leads to the formation of carbon nanotubes with a mean diameter in the range of 10–100 nm.

It was shown that in the reactor, treated with ignitions, the ignition temperature of the mixture 70% H_2 + 30% methane with air over rhodium surface is 62 °C. The result indicates the potential of using rhodium catalyst to markedly lower the ignition temperature of the fuels based on hydrogen–methane mixtures.

The critical condition for volume reaction is experimentally revealed. The volume process occurs at 45% H_2, but it is missing at $\leq$ 40% H_2. If $H_2 \leq 40\%$, only a slow surface reaction occurs; this phenomenon is qualitatively described by our calculations. It was revealed that the effective activation energies both of "upper" and "lower" limits of H_2 + methane oxidation over the range of linearity are roughly equal (2.5 ± 0.6) kcal/mol; it means that the key reactions, responsible for the occurrence of "upper" and "lower" ignition limits, are almost certainly the same. It was shown that for Rh/Pd catalyst, the chain development process has most likely heterogeneous nature because the effective activation energy is < 3 kcal/mol.

Rh has been found to be a more effective catalyst than Pd for the studied combustion processes. The effective activation energies of catalytic ignition depend not only on the nature of the catalyst, but also on the chemical nature of the hydrocarbon in the mixture. Thus, catalytic ignition is initiated by exothermic surface ignition of hydrogen oxidation reaction in the presence of catalyst, hydrocarbon on the surface is consumed in reactions involving hydrogen oxidation intermediates that do not lead to branching of chains, and then the combustion propagates into volume. It was found that in a reactor not treated with ignition, the ignition temperature of the mixture of 70% H_2 + 30% methane-air above the Pd surface at a pressure of 1.75 atm is 310 °C and above Rh surface—105 °C. In the ignition-treated reactor, the ignition temperature of this mixture above the Pd surface at a pressure of 1.75 atm is 270 °C and above the Rh surface is 62 °C. The obtained result also indicates the prospect of using rhodium catalyst for lowering the ignition temperature of methane and hydrogen-based fuels.

It was shown that under conditions of our experiments not the chemical nature of the catalyst but that of C_2 hydrocarbon in the mix with H_2 is the determining factor of catalytic ignition. The catalytic ignition limits of synthesis gas over Rh/Pd are qualitatively different from the dependencies for combustible hydrogen-hydrocarbon fuel.

The "lower" catalytic limit dependence has a distinct maximum, which indicates a more complex mechanism of the catalytic process; Arrhenius dependence of ln $[H_2]_{lim}$ on $1/T$ could not be applied. Therefore, the interpretation of the "upper" and "lower" limits of catalytic ignition given in the literature should be clarified. The relatively long delay periods of catalytic ignition of hydrogen—n-pentane mixes (tens of seconds) and the absence of the dependence of the periods on the initial temperature allow us to conclude that the catalytic ignition of hydrogen—n-pentane mixes is determined by the speed of transfer of the hydrocarbon molecules to the surface of the catalytic wire.

Thus, in the oxidation of hydrogen-hydrocarbon blends for "short" hydrocarbons, the main factor determining catalytic ignition is the oxidation reaction of hydrogen on the catalytic surface. With an increase in the number of carbon atoms in the hydrocarbon, the factors associated with the chemical structure, that is, the reactivity of the hydrocarbon in catalytic oxidation, begin to play a significant role; and then the oxidation rate is already determined by the speed of transfer of the hydrocarbon molecules to the catalyst surface.

It was shown that the ignition limits of $2H_2 + O_2$ and $(80\%H_2 + 20\%CH_4)_{stoich} + O_2$ mixes over Pt wire do not depend on the applied voltage without discharge up to 1200 V. It was shown that for $(80\%H_2 + 20\%CH_4)_{stoich} + O_2$ mix, the application of an electric field (1200 V) leads to the disappearance of Pt-containing particles formed by decomposition of volatile platinum oxide in gas phase from the reaction volume, which indicates that these particles are charged. This may be due to the chemiionization phenomenon observed in the combustion of hydrocarbons. It was shown that in combustion of $(80\%H_2 + 20\%CH_4)_{stoich} + O_2$ mix, carbon nanotubes practically do not form as distinct from combustion of $(H_2 + C_4H_8)_{stoich} + O_2$ mix.

It was established that an exemplary flame propagation process in a conditional room containing an indoor space with two openings and a flammable material inside shows a wide variety of combustion modes depending on the geometry of this complex volume. The preliminary numerical calculation of the expected flame propagation patterns may not always be successful. Thus, a real experiment under laboratory conditions, assuming the possibility of scaling the process, seems to be the most informative one.

It was shown that under certain conditions, Pt catalyst can suppress combustion and thereby show the opposite effect due to the high efficiency of Pt surface coated with a Pt oxide layer in the reaction of chain termination. Therefore, kinetic factors could be determining ones even under conditions of high turbulence.

The value of effective activation energy of the dark reaction of H_2 oxidation over Pd is evaluated as $E = 4.1 \pm 1$ kcal/mol that is characteristic of a surface process. The value is close to one determined in the literature for the temperature dependence of H_2 fraction at the ignition limit over Pd surface in mixtures with O_2, which is equal 3.5 ± 1 kcal/mol. It was shown that the rate of chain termination determines the value of the critical diameter for flame penetration through Pt or Pd cylinders;

the efficiency of Pd surface in chain termination reaction is much greater than that of Pt. Therefore, the action of noble metals on the processes of hydrocarbons oxidation is an effective tool to identify important reaction sets in their kinetic mechanism.

Moscow, Russia Nickolai M. Rubtsov
Moscow, Russia Kirill Ya. Troshin
Moscow, Russia Michail I. Alymov

Acknowledgments The authors would like to thank his co-authors and inspirers Ph.D. Boris S. Seplyarsky, Ph.D. Victor I. Chernysh leading engineer George I. Tsvetkov (Institute of Structural Macrokinetics and Materials Science of Russian Academy of Sciences), Prof. Eugene F. Lebedev, Doctor of Science V. A. Zeigarnik, Doctor of Science A. V. Gavrikov (Joint Institute of High Temperatures of Russian Academy of Sciences), scientist A. B. Ankudinov (A. A. Baikov Institute of Metallurgy and Materials Science, RAS) for the support, which cannot be overestimated, and jeweler E. A. Baturin for the production of high-quality samples.

Contents

Chapter 1
Introduction

Abstract It is shown that the gaseous process, called self-ignition (although in fact it is thermal ignition), proceeds heterogeneously in space and its regularities are determined not only by the initial temperature of the flammable gas, but also by the material and the state of the surface (the presence of defects or action of catalysts, which initiate primary active centers). This means that classical models that do not take into account surface heterogeneity and gas-dynamic features of the propagation of the reaction front, do not describe even qualitatively the emergence and development of the process of thermal ignition and should at least be supplemented.

Keywords Platinum · Hydrogen · Combustion · Heterogeneous · Nonuniform · Self ignition · Ignition limits

These were times when neither mobile phones nor computers had yet been invented, the ideas about greenhouse gases and global warming did not occur to anyone, scientists devoted their work to sponsors—dukes and conts, but they (the scientists) could say completely sincerely "*I love science more than money*".

By the beginning of the nineteenth century, the most important physical properties of platinum had become well understood and formed the basis for several different applications, but one of its main properties namely its remarkable catalyst function had yet to be discovered. In 1818, Sir Humphrey Davy, who was asked to study protective lamps in coal mines, discovered that methane and oxygen on hot platinum wires could emit a significant amount of heat in the dark reaction [1]. It could be said that in fact both Humphrey Davy and his cousin Edmund made preliminary reports on the effect of platinum on the oxidation of methane and alcohol, but neither of them sought to interpret their results in any detail [2]. However, in Germany, this topic was taken up by Döbereiner, whose study of the effect of platinum on hydrogen became the key to the discovery of the phenomenon of catalysis. Johann Wolfgang Döbereiner was born in 1780 in Hof an der Saale, Bavaria. Initially, he intended to pursue a career in real estate management, but instead, at the age of 14, he got a job at a local pharmacy. After completing a three-year apprenticeship, he embarked on a five-year journey that included periods of careful informal study of chemistry and mineralogy in Karlsruhe and Strasbourg. A series of pharmaceutical and technological works followed, each of which increased his scientific experience

N. M. Rubtsov et al., *Catalytic Ignition of Hydrogen and Hydrogen-Hydrocarbon Blends Over Noble Metals*, Heat and Mass Transfer,
https://doi.org/10.1007/978-3-031-28416-8_1

and reputation, but none provided financial security. Indeed, by 1810 he found himself unemployed, in debt and with a large family to support. He was saved from this predicament by the offer of the Department of Chemistry and Technology at the University of Jena. Jena was located in the land of Saxe-Weimar, whose ruler, Duke Karl August, was considered a very enlightened patron of both art and science. He was acutely aware of the practical value of science for his staff, and when searching for a candidate for the department, he indicated a person with "scientific genius with practical flair". Döbereiner immediately responded to his offer. In addition to his official duties as a professor, he served as a consultant on a wide range of issues, added the post of inspector of mines to his portfolio and in 1820 was appointed a privy councilor. Always a practical man, Döbereiner in his will ordered that his body be buried without a coffin and that two fruit trees be planted on the grave "so that the products of the decay of my corpse may turn into organic matter and appear in another guise in new life".

Karl August brought Goethe to Weimar in 1775, and a close relationship was established between the three men. Karl August and Goethe provided Döbereiner with the best conditions the state could afford; Döbereiner, for his part, remained in Jena for the rest of his life, despite offers of more lucrative and prestigious chairs as his reputation grew. Carl August became godfather to two of Döbereiner's children and Goethe to one. Goethe once wrote a poem for Döbereiner when he was ill, and another of his poems preceded Döbereiner's book about his platinum research. After Döbereiner's death in 1849, a statue was erected in the city of Jena in his memory. In addition to his extensive work in applied chemistry, Döbereiner's reputation now builds on three aspects of his career. He was a very successful teacher and a few years before, despite considerable personal expenses, conducted courses in practical experimental chemistry some years before Liebig's more famous courses at Giessen. Secondly, during the 1820s he developed his theory of "triads", an early predecessor towards the Periodic Table. And thirdly, there was his important pioneering work on platinum catalysis.

The precursor to Döbereiner's work on platinum is to be found in Humphry Davy's researches related to the miner's safety lamp. Davy discovered that a spiral of platinum wire near a lit wick in a lamp would catalyze the ongoing oxidation of coal gas (methane) with sufficient force to incandescent after the wick goes out. At least, that's how his experiment could be described now; but at that time Davy was most interested in the nature of combustion and safety in mines. He recognised that the addition of the platinum spiral was a useful modification to the miner's lamp, but of the phenomenon he had observed, he simply remarked that it was "more like magic than anything I have seen … it depends upon a perfectly new principle in combustion" [2].

Humphry's cousin Edmund Davy, working at the Cork Institution, was then carrying out a series of researches on the chemistry of platinum. In the course of this, he found that platinum sulphate could be reduced by alcohol to platinum in finely divided form. The platinum powder, which Davy observed, reacted strongly with alcohol vapour at room temperature, remaining white hot until all the alcohol was consumed. "This mode of igniting metal", he remarked, "seems to be quite a new fact in the history of chemistry; but the means of keeping it in a state of

ignition is only another illustration of the facts previously pointed out by Sir H. Davy" [3]. Edmund Davy's article was published in a German translation in 1821, and Döbereiner immediately began to repeat his experiments. The context, however, was crucially different. Döbereiner was then interested in the chemistry of alcohol, not platinum, so he emphasized not so much the glow of platinum powder as its ability to induce the oxidation of alcohol to acetic acid. He explained this ability in terms of the platinum electrochemically activating the alcohol towards reaction with oxygen. He also noted that the platinum was not used up by the reaction but could "be used again to acidify fresh, perhaps limitless, quantities of alcohol;—a circumstance which permits its use for the large-scale preparation of acetic acid" [2]. In the event, Döbereiner did get as far as designing an "Essiglampe", but did not exploit the reaction commercially.

Döbereiner published his results in 1822. He spent Christmas that year with Goethe in Weimar and, among other experiments, demonstrated to him the effect of Edmund Davy's platinum powder on alcohol. He continued to work on the properties of that powder during the winter, investigating also the properties of a form of finely divided platinum produced by ignition of ammonium chloroplatinate and extending the range of gases and vapours studied to include hydrogen.

The experiments that finally caught the imagination of the scientific world were carried out in the summer of 1823. Döbereiner prepared some platinum powder by ignition of ammonium chloroplatinate and exposed it to hydrogen. As he had expected, nothing happened. He then admitted some air to the hydrogen, and "there now followed in a few moments that strange reaction: the volume of the gases diminished and after ten minutes all the oxygen in the admitted air had condensed with the hydrogen to water" [2]. Substitution of pure oxygen for the air made the reaction vigorous enough to char the filter paper holding the platinum powder.

Döbereiner was so taken by the experiments that he repeated them "at least thirty times" that day, and "always with the same result". He proposed a mechanism analogous to that used in his 1821 experiments on the oxidation of alcohol: "The entire phenomenon must be regarded as an electrical one, whereby the hydrogen forms an electrical chain with the platinum". He quickly sent a report on his work to Goethe and the editors of three scientific journals; it was published a month later (the speed of publication, which modern information technology does not seem to be able to match). Then Döbereiner created an even more spectacular version of his experiment. Instead of the previous static arrangement, he directed a fine jet of hydrogen at the platinum from a distance of 4 cm, so that it was mixed with air before reaching its target. This had the effect of making the platinum immediately white hot and igniting the hydrogen jet. More excited letters were dispatched, commenting that "this experiment is most surprising and amazes every observer when one tells him that it is the result of a dynamic interaction between two types of matter, one of which is the lightest and the other the heaviest of all known bodies" [2].

In a small book published in October 1823 and dedicated to Carl August, in which he summarised his summer's experiments, Döbereiner suggested that the mechanism was "probably of a quite special nature, i.e. neither mechanical nor electrical nor magnetic" [4].

Döbereiner's work caused "a great sensation and excited the liveliest interest" in Paris, according to Liebig who was studying there at the time. French chemists Tenard and Dulong, who had previously investigated the decomposition of ammonia by heated metals and hydrogen peroxide, started working immediately; by September 15, they were able to submit to the Academy of Sciences a document extending Döbereiner's work to other forms of platinum and other metals [2]. Further papers followed, but the nature of the phenomenon remained obscure. On 29th November Liebig wrote to Döbereiner that, at a dinner for a group of leading scientists, "your beautiful and as yet inexplicable discovery was discussed in the most glowing terms". In the same letter, serious, albeit tactful, reservations were expressed regarding the mechanism originally proposed by Döbereiner.

News of Döbereiner's work reached England via a letter from the French chemist J.N.P. Hachette to Michael Faraday. By the end of September, Faraday repeated the experiment and in his laboratory journal unequivocally attributed this phenomenon to the adsorption capacity of fine platinum. At that time he could not continue his research, but ten years later he returned to this topic with great success. Other English chemists have also conducted experiments to study this phenomenon. Thus, Döbereiner's experiments aroused great interest and prompted many chemists in different countries to conduct further research. This was reflected in a brief overview of the events of the year prepared by the Swedish chemist Jöns Jakob Berzelius. In 1821 Berzelius had taken upon himself the monumental task of reviewing the advances of physical science during the previous year and presenting them in a series of annual reports. These owed their siderable influence to the fact that they were also published in German translation, initially by C.G. Gmelin and then by Friedrich Wöhler.

When writing his review of 1835, Berzelius was able to reflect on a wide variety of experimental and theoretical researches that had what he realised was a simple phenomenon in common [2]. He gave this phenomenon the name "catalysis", emphasizing at the same time that this name is intended to identify a specific phenomenon, and not to give a single explanation (the action of the "catalytic force") for all cases of this phenomenon. Döbereiner immediately turned his discovery to practical ends. One of those ends was eudiometry: he was able to demonstrate its value in eudiometry at the Halle conference, and Michael Faraday was using it routinely for this purpose by the end of the year. He also used platinum to prepare sulphuric acid by catalytic oxidation of sulphur dioxide to sulphur trioxide, independently of Peregrine Phillips who patented the process in England in 1831, but he did not establish the technique on a large scale.

Indeed, the application most associated with Döbereiner is the lighter. Like Humphrey Davy with his protective lamp, Döbereiner refused to patent his invention, published all the designs and rejected a major proposal of an Englishman named Robinson for monopoly rights with the words "I love science more than money" [5]. By 1828 about 20,000 Döbereiner lighters were in use in England and Germany alone, and it eventually found its way into most European countries. In spite of the invention of the safety match in 1848 by one of his former students, R.C. Böttger, the Döbereiner lighter was still in use at the beginning of the First World War. The part of its attraction lay in the scope it offered to the imaginative decorator: Döbereiner himself suggested that one could "embellish it with two alchemical symbols, namely

the lion and the snake, and so arrange it that the snake takes the place of the capillary tube for the stream of hydrogen and the open jaws of the lion sitting opposite the snake hold the platinum" [6].

Currently, the field of application of noble metals is so wide that it is not possible to outline it within the framework of one monograph. Below we will consider the studies that are most closely related to the issues discussed in this book.

It is evident that the various challenges in the safety of producing, transporting and storing hydrogen supplies need to be addressed before widespread use of hydrogen as fuel. One of the main problems is accidental ignition, since hydrogen has much wider flammability limits than most conventional fuels [7]. One of the typical sources of ignition is a hot surface. Thus, it is quite urgent to be able to prevent conditions, under which the ignition can occur, when a hydrogen-oxidizer mixture contacts with a hot surface. As is known, the hydrogen-air mixture entering the combustion chamber is susceptible to pre-ignition when it contacts a hot surface, such as the primary inlet valve. It is difficult to ignite hydrogen-air mixture by compression, and some additional ignition assist, for instance a glow plug, is required [8]. Therefore, it is clear that the design of the engines requires information about hot surface ignition.

The catalytic combustion of hydrogen is of noticeable interest because it is used in the boilers that operate at relatively low temperatures and can generate heat for household applications without CO_2 and NO_x emissions [9]. For hydrogen combustion process, the catalysts should possess both, oxygen storage capacity and thermal stability; these should provide that hydrogen oxidation should occur without explosion. That can be achieved using noble metals, which have high adsorption capability of hydrogen and oxygen at low temperatures [10].

Catalytic converters are applied in exhaust gas treatment system in automobiles and trucks; these utilize the oxidation to reduce toxic emissions. In order to stimulate the oxidation, noble metals such as Pt, Rh, Ru and Pd are used as catalysts. Pt based catalysts are not effective enough with methane; however, Pd catalyst provides higher methane conversion [11]. The peculiarities of catalytic action of noble metals have been under discussion. Noble metals affect the flammability of hydrogen–methane blends differently. For instance, we have earlier shown that the ignition temperature of the mixture 40% H_2–air over Pd Metal (70 °C, 1 atm) is ~ 200° less than over the Pt surface (260 °C, 1 atm) [12]. In addition, Pd ignites stoichiometric mixes (30 ÷ 60% H_2 + 70 ÷ 40% CH_4) + air [$\theta = 1$, equivalence ratio θ is a fraction of fuel in the mix with air: $\theta H_2 + 0.5\ (O_2 + 3.76N_2)$]; metallic Pt cannot ignite these up to 450 °C, i.e. Pd is more effective than Pt. We have also shown that the cellular structure of a flame front at ignition with Pd is not observed in contrast to Pt surface (see Chap. 2). Thus, Pd seems to be more usable for hydrogen recombiners in NPP, because no catalytic particles as ignition centers formed by decomposition of volatile oxide can appear in gas phase in contrast to Pt [13]. The experimental value of the effective activation energy of catalytic ignition over Pt is ~ 18 kcal/mol and is close to one of $H + O_2$ branching step [7]; the value over Pd is ~ 3.5 kcal/mol that is characteristic of surface processes [12]. It indicates the noticeable role of the dark reaction of consumption of H_2 and O_2, also referred to as "flameless combustion", which is observed at low pressures [14]. The occurrence of that reaction reduces the probability of an accidental explosion. All above listed works will be detailed below.

A number of experimental investigations have been performed to study the hydrogen ignition by a hot surface. Williams et al. [15] proposed a model for the catalytic combustion of hydrogen at high temperatures. Warnatz and coworkers [16] studied the catalytic combustion and ignition of hydrogen using detailed kinetic mechanisms for both surface and gas-phase reactions. Deutschmann et al. [17] studied the ignition of different fuels on different catalyst materials. They showed by numerical calculations that one or the other reactant almost covers the surface before ignition. It is clear that the detailed mechanisms of catalytic reactions involving noble metals at this level of scientific development are purely illustrative in nature and the numerical results obtained by the authors are devoid of the field of application. In a series of experiments with very thin catalytic wires, Rinnemo et al. [18] determined the critical ignition temperature of hydrogen–oxygen mixtures as a function of the mixture ratio. Kalinchak et al. [19] presented an analysis for the catalytic ignition using a simplified model for the heterogeneous chemistry. The results in addition to the fact that quantitative calculations have only conditional value, reveal a lack of universality of the ignition temperature concept and the need for a more profound understanding of the problem, because experimental features of hydrogen ignition over noble metals remain unsufficiently studied.

It is known that hydrogen and deuterium form binary intermetallic hydrides/deuterides with palladium, thus, the features of ignition over the surfaces of hydrides of noble metals have been a subject of investigation in this work. Unlike many known metallic hydrides, very little macroscopic deformation of the palladium lattice occurs, and the mechanical properties of the hydride are very similar to those of pure metal. There have been almost 150 years of active research into the palladium hydride/deuteride system up to now. Numerous literature reviews have been published on the system [20]. In the middle of the last century, the first diffraction patterns of β-PdH and β-PdD were recorded [21]. There is the "inverse isotope effect" observed [22] whereby heavier hydrogen isotopes have a higher critical temperature at similar H/D/T loading. Similar "inverse isotope effects" can also be found in the rate of diffusion of hydrogen isotopes through the palladium lattice. At low temperatures, hydrogen isotope exhibit an "inverse isotope effect" (where heavier isotopes diffuse faster than their lighter counterparts).

According to the above, the present book focuses on experimental studies of hydrogen and deuterium combustion over Rh, Ru, Pd and Pt metals in order to establish the dependencies of catalytic ignition limits over noble metal surfaces on temperature and to indicate the governing factors of the problem of gas ignition by a catalytic surface. A macrokinetic study of the chemical properties of the two lighter hydrogen isotopes (protium and deuterium) dissolved in rhodium and palladium, namely the study of the influence of hydrides and deuterides of noble metals on hydrogen and deuterium combustion, is performed.

In this regard, it is curious to note the existence of a rather scandalous problem of "cold fusion" raised in [23]. The article introduced the possibility of room-temperature fusion during electrolysis with a palladium cathode in a $LiOD/D_2O$ electrolyte solution. The article [24] published in Nature 30 years later summarizes the substance of the problem. The authors state that, really, the 1989 claim of 'cold fusion' was publicly heralded as the future of clean energy generation. However,

subsequent failures to reproduce the effect heightened skepticism of this claim in the academic community, and effectively led to the disqualification of the subject from further study. Motivated by the possibility that such judgement might have been premature, the authors [24] embarked on a multi-institution program to re-evaluate cold fusion to a high standard of scientific rigor. In [24], the efforts described, which have yet to yield any evidence of such an effect. Nonetheless, a by-product of the investigations has been to provide new insights into metal hydrides and low-energy nuclear reactions, and the authors contend that there remains much interesting science to be done in this underexplored parameter space.

One of the major concerns over economic growth and social development nowadays is the constantly increasing energy demand [25]. The study of U.S. Energy Information Administration has forecasted an increase of 28% in the world's energy consumption from 2015 to 2040 [26]. While there is a constant progress year by year for the development of renewable energies, the use of fossil sources (petroleum, coal and natural gas) is still dominant, and remains indispensable in the near future [27]. Among the fossil energy resources, the natural gas presents a particular interest because of its higher energy content (55.7 kJ g^{-1} if fully based on methane as its main component) than coal (39.3 kJ g^{-1}) and petroleum (43.6 kJ g^{-1}) as well as its reduced CO_2 emission (50% less than coal and 30% less than petroleum). Moreover, the proven natural gas reserves worldwide are abundant, reaching about 193.5 trillion cubic meters at the end of 2017 [28]. As a result, natural gas has accounted for the largest increment (24%) in the main energy consumption in the past decade until 2017, and has been suggested as a substitute for oil and coal as a future leading energy source for the next 20 years [29]. In response to this, there is a rapidly growing number of research and development efforts yearly on the deployment of natural gas for their use in various sectors including industrial, residential, power, transport and many others [30]. Besides the natural gas fields, the synthetic natural gas (SNG) can also be derived from coal gasification, CO_2 methanation and biomass gasification/digestion [31, 32].

The conventional flame combustion of natural gas occurs typically at above 1400 °C and releases harmful pollutants (such as NO_x, CO and polyaromatic hydrocarbons). The impact of NO_x on human health (respiratory diseases) has been widely recognized [33]. Its emission also has harmful environmental impacts including the formation of photochemical smog and acid rain [34].

It may be discovered that as compared to the conventional flame combustion, the presence of catalysts enables a decrease in the working temperature (<1400 °C). Depending on the target application, the operational temperature for catalytic methane combustion can be further divided into a relatively lower range (about 300–700 °C) and a relatively higher one (about 700–1400 °C). The low-temperature catalytic methane combustion becomes more attractive due to the remarkable abatement of pollutant emissions and the prolonged catalyst lifetime. For instance, the reusability and the reproducibility of catalysts, especially for noble metal catalysts, are shortened at high temperatures. In this field, developing catalysts with high catalytic activity, low light-off temperature and good thermal stability even for such low temperature operations is still a challenging issue. A great number of researches have been devoted to catalyst development [35, 36] and reactor design [37–39] for

catalytic methane combustion. Noble metal catalysts (e.g. Pt, Pd and Rh) have been widely investigated owing to their high catalytic activity. Most reported studies of catalytic oxidation employ supported Pt and Pd [40–45], where the support is mainly a more accessible metal oxide such as aluminium oxide [46–49], cerium oxide [50, 51], and silicon dioxide [52] or metal such as nickel [53], and zirconium [54, 55]. While such configurations are relevant for practical applications, they come with the complexity of the role played by the support and uncertainty of mechanisms explaining the interchanging reactions between noble metals, support, and gaseous reactants. Only a handful of papers are reported for pure unsupported noble metals reacting with a limited range of hydrocarbon fuels [56]. This book also deals with the problem.

In this regard, it is worth mentioning the possibility of a transition to green energy, which implies the abandonment of conventional hydrocarbon fuels, and which boils down to the fact that emissions from human activities pollute nature and must be dealt with. The main argument against this untimely transition is the fact that the humanity does not possess sufficiently powerful sources of energy (except for nuclear weapons, which will hopefully not be used for any purpose) to influence the climate. Such campaigns are usually born in the offices of corrupted officials and are associated with the money laundering on such projects. A good illustration of this is the campaign to ban chlorine-containing freons that allegedly destroy the ozone layer, which ended with the signing of the Montreal Protocol. To substantiate this dubious claim, Rowland and Molina published unconvincing kinetic schemes and in order to dispel all doubts, they were given the Nobel Prize. However, despite the ban, the ozone gap over Antarctica found in 1985 remains now almost as large as it was when the Montreal Protocol was signed in 1987. It is excessive to note that the global industrial factories and, especially, refrigeration units, are missing in Antarctica. However, the production of widely used chlorine-substituted halons such as promising combustion inhibitor and a coolant dufluorodichloromethane was stopped and essentially there was a replacement of one generation of freons with another one in the interests of certain American business groups. Really, for consumers it led to a significant increase in the cost of the equipment and prices for installation and service works [57].

In a similar vein, the imposition of hydrogen energy occurs, and the fact that conventional fuels are fossil ready-made fuels and hydrogen is a product that requires significant costs to obtain it is taken out of consideration [58]. According to Ref. [35], the decades-long increase in the average temperature of the Earth's surface, which is associated with anthropogenic emissions of greenhouse gases, primarily CO_2, into the atmosphere, is stimulating interest in the wider use of "carbon-free" energy sources, in particular, hydrogen. However, hydrogen is not a primary source of energy, but only an energy carrier, and the transition to "hydrogen energy" is associated not only with high capital and operating costs for its production, but also with significant additional consumption of fossil resources and, accordingly, additional CO_2 emissions into the atmosphere. Therefore, the global positive environmental and economic impact of such a transition is not obvious.

This book focuses on lowering the combustion temperature of hydrocarbons not only with noble metal catalysts, but also with hydrogen additives. At the same time, the issues of chemical mechanisms and gasdynamic factors in the oxidation of fuels

on the catalyst, the catalytic ignition areas for Pt, Pd, Ru and Rh, the identification of the most effective catalyst for the use in hydrogen recombinators, the applicability of noble metals for the synthesis of nanotubes are touched upon. The book also discusses the modes of spatial development of gas ignition on the catalytic surface and the possibility of synthesis of nanotubes on the catalyst surface associated with these modes when using hydrogen–hydrocarbon gas mixtures.

We will linger in more detail on some of the listed above issues.

It should be noted that the vast majority of gas phase combustion reactions has branched chain nature. It is determined by fundamental chemical laws. In the branched chain reaction, active particles, namely free radicals, are produced, the number of which grows quickly, it is called the branching of the chain. It is therefore enough for one single free radical to be produced (for example, thermally) for the radicals to multiply, which leads to a rapid reaction of the chain ignition type. Heat evaluation accelerates chain branching and vice versa, this feedback plays a marked role, even in close proximity to concentration combustion limits [59].

In the case of the chain explosion there are two possibilities:

(1) the rate of branching exceeds that of active particles termination, which results in very rapid development of the reaction chains;
(2) the rate of termination is greater than that of branching, so that the chains cannot develop and the reaction cannot even take place (if, as is usual, the rate of free radical formation is quite low). For instance, phosphorous vapor may stay below the limit for days and in contact with oxygen without even a trace of reaction processes being observed. The transition from a completely inert state to a violent reaction (explosion) can easily be caused by, for example, increasing the pressure of the oxygen or the dimensions of the reactor etc. [60]. Similar limit phenomena were observed by Hinshelwood [61] in the case of pressures which exceed a certain "second upper limit" (e.g. in the case of the reaction of water formation of oxygen and hydrogen). The second upper limit was explained on a basis of the ideas put forward by Semenov and Hinshelwood regarding competition of the process of chain termination in the volume in the case of termolecular collisions and the process of chain branching.

We draw the reader's attention that, firstly, free radicals are chemically highly active particles and therefore react far more readily with molecules than molecules react with one another. Secondly, the free valence cannot disappear in the course of the reaction between a free radical and a molecule, which means that at least one product of the reaction is a free radical. This radical again reacts with the nearest molecule, so that another free radical is formed, and thus a long chain of changes can take place. Therefore, three cases are possible:

(a) During the reaction between radical and molecule, a monoradical can form, which leads to the formation of an unbranched chain, e.g.

$$.CH_3 + CH_3CHO \rightarrow CH_4 + .CH_3CO$$
$$.CH_3CO \rightarrow .CH_3 + CO \text{ etc.}$$

(b) If the main chain of the reaction is unbranched but if, due to monomolecular breakdown of reaction products free radicals and, consequently, new chains can form, then it is usual to speak of a degenerate branching. As an example, we can consider formation of alkyl hydroperoxides:

$$\begin{aligned} .R + O_2 &\rightarrow .RO_2 \\ .RO_2 + RH &\rightarrow ROOH + .R \\ ROOH &\rightarrow .RO + .OH \end{aligned}$$

(c) During the course of the reaction, instead of one free valence, three are formed; each valence starts a new chain. The result is the occurrence of a (rather simplified) branched chain reaction [62]:

$$\begin{aligned} .OH + H_2 &= H_2O + .H\ (k_1); \\ .H + O_2 &= .OH + .O.\ (k_2)\ ; \\ .O. + H_2 &= .OH + .H\ (k_3); \\ .H + \text{wall} &= H_s(k_4)\ \text{chain termination}; \\ .H + O_2 + M &= .HO_2 + M\ (k_5); \\ .HO_2 + H_2 &= H_2O_2 + .H\ (k_6), \end{aligned}$$

Reactions (1)–(3) correspond to the following overall process:

$$.H + O_2 + 3H_2 \rightarrow 2H_2O + 3.H$$

Notice that the hydrogen–oxygen system is an attractive object of study because its detailed reaction mechanism is well understood (in contrast, for example, to hydrocarbon oxidation), because it is the simplest realistic combustion system, and because of its potential role as fuel.

In reaction (5), M is any particle that diverts excess energy from the relatively low-active HO_2 radical, reactions of which at low temperatures and pressures lead mainly to the termination of reaction chains. Under these conditions, the proportion of HO_2 entering the reaction (6) is small. At conventional combustion temperatures of H_2 exceeding 1000 K, the branching rate of the chains realized in the reactions (1)–(3) exceeds the reaction rate (5), and even more so exceeds the rate of termolecular chain termination.

Due to the branched-chain nature of H_2 oxidation, the developing combustion can occur in different kinetic modes with different critical conditions. Branched-chain character of the process also determines its exposure to the impurities of substances, reacting with active intermediate particles to form products that are not able to participate in the development of chains and, thus, lead to chain termination, to suppression of combustion.

One of the features of hydrogen oxidation is the presence of three critical ignition pressures (so-called ignition limits), which form self-ignition area in P–T coordinates.

The chain nature of the lower two limits is generally recognized (the reactions 4 and 5 correspondingly). The nature of the third limit, covering pressures above 0.4 atm and increasing with a decrease in the initial temperature, is still being discussed. It can be seen from the reaction scheme, that the rates of branching reactions and development of chains (1)–(3) are proportional to the first degree of concentration of initial reagents. Fast reaction (5) is proportional to the square of their concentration. Therefore, at these temperatures, above a certain pressure, the termolecular termination reaction (5) prevails over branching, and ignition is not possible. This is the second limit of self-ignition. Above 850 K, the second and third limits are not observed, since the reaction (6) plays a significant role, regenerating atomic hydrogen and thereby leveling the chain termination caused by the termolecular reaction (5).

Let us illustrate aforesaid by a simplified example.

As we stated, chain reactions take place through the formation of active particles. During a reaction, the amount of these particles may increase. First, active particles may be formed as a result of thermal motion, independently of the chain reaction, since reagent molecules may dissociate upon colliding with one another; the rate for this process can be high enough only for high temperatures. Second, branching of the chain may occur, that is, an elementary process involving one active atom or radical that yields two atoms (or free radicals). Branching always occurs due to the reaction energy. For example, the reaction $H + H_2 \rightarrow 3H$ is possible from the standpoint of the material balance. However from the standpoint of energy this reaction it is not possible, but the reaction $H + 3H_2 + O_2 \rightarrow 3H + 2H_2O$, on the other hand, is possible. The rate of formation of active particles in this way, as is seen from above, is proportional to their concentration. The presence of a source of active particles is extremely important and determines the main features of chain kinetics. The appearance of active particles can initiate branching that is formation of multiple numbers of active particles if it is possible thermodynamically. Besides, always there are processes, which cause their loss. The rate of removal of active centers from the reaction by collisions with stable molecules or by diffusion to the vessel walls also is proportional to the concentration of active centers. When the rate of chain branching becomes greater than the rate of chain termination, there are explosion conditions; when the conditions do not exist, the explosion is impossible. Essentially, the same type of concept holds for thermal explosion (or thermal ignition). When the rate of thermal energy release is greater than the rate of thermal energy loss, the condition of explosion is realized. However, this is not the case for chemical catalysis by noble metals. The increase in the temperature of the catalytic wire in the hydrogen-containing combustible mixture primarily leads to the formation of primary active centers on the wire that initiate combustion, which then spreads into the volume. A number of experimental evidence in favor of this statement is given below in this book.

Thus, for our simplified model, the equation for the time variation of the concentration of active centers can be written in the form

$$d[H]/dt = w_0 + f.[H] - g.[H]$$

w_0 is the very small rate of origination of active centers from molecular reagents and $f = k_2.[O_2]$ and $g = k_4$ for heterogeneous chain termination or $k_5.[O_2]$ for homogeneous chain termination on the second ignition limit [7, 60]. Writing $f - g = \phi$ we obtain $d[H]/dt = w_0 + \phi .[H]$ Note that the rate of origination of active centers w_0 is very small, so that in experiment we can hardly measure either change in the concentration of active centers or heat of the reaction. A change in the external conditions (temperature, pressure) causes changes in both f and g. Since no activation energy is required for loss of an active hydrogen atom H the constant characterizing the formation of new active centers by chain branching typically have stronger temperature dependence than the rate of chain termination. Thus, the difference $f - g$ changes sign as the temperature is raised. At low temperatures, it is negative and at high temperatures, it is positive. Thus, depending on the sign of $f - g$ the type of solution changes drastically. The temperature, at which ϕ equals zero, is the critical temperature below which an explosion is impossible. These qualitative considerations explain the existence of an explosion region for an explosive mixture at fixed initial pressure when the initial temperature passes through a critical value corresponding to $\phi = 0$.

As we stated above, the nature of the third ignition limit of $H_2 + O_2$ self-ignition has been under discussion up to now. Below some relevant issues are highlighted and the results are presented, which show that the features of ignition of H_2 in air in the area of the third ignition limit P_3 depend not only on the mixture composition, but also on the material of reactor surface and on the amount of chemically active additive. It is established that the process of ignition of H_2–air mixtures at atmospheric pressure begins with primary center occurrence on the most chemically active site of surface, which initiates flame propagation. In other words, the nature of the third ignition limit is determined by a number of factors, including the catalytic properties and the state of surfaces of both the reactor and other objects in the reactor.

It is known that the data on spatial development of spontaneous ignition of combustible gases at contact with heated surface are of practical and scientific interest in connection with the use of hydrogen as fuel in engines and other power devices. Experimental investigations of ignition are performed, as a rule, in static conditions when the mixture under investigation is quickly transferred into a heated vacuumized reactor. Ignition of hydrogen (H_2) at low pressures (<10 Torr) in heated reactor in the vicinity of the lower pressure limit is assumed to occur uniformly over reactor volume [60]. It is shown in [63] that uniform ignition of $2H_2 + O_2$ mixture can be observed only for pressures < 10 Torr (at pressures lower than 10 Torr the experiments were not performed). With an increase in total pressure of gas mixture in conditions of quick gas transfer the time of warming up decreases, because the velocity of gas flow must be increased to obtain larger pressure in the reactor. By the time of completion of gas transfer, the medium forms in the reactor, in which different parts of the gas mixture have the different history of warming-up [64]. This serves to ignition of the gas mixture near heated reactor surface. It means that with pressure growth the problem on uniform ignition in heated reactor transforms into a problem on ignition with heated surface [65–68]. As is established in [68] ignition of stoichiometric and rich mixtures of propane and pentane with air at 1 atm in heated reactor begins with

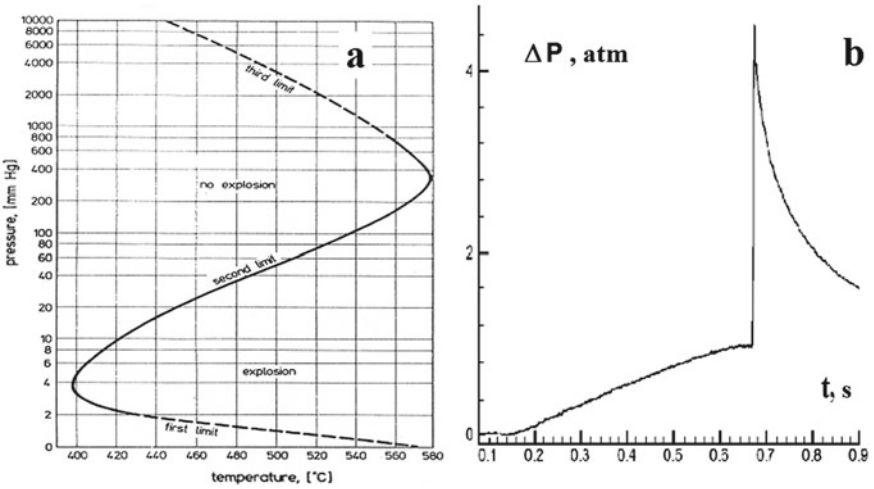

Fig. 1.1 **a** Spontaneous ignition area of $2H_2 + O_2$ mixtures [10]; **b** Pressure dependence in ignition of 40% H_2 in air (1 atm, 684 K)

occurrence of a primary ignition center on the most chemically active site of surface, i.e. includes the steps of warming up, local ignition and flame propagation.

In the work [63] spatial development of ignition of stoichiometric mixtures of H_2, methane and isobutene with oxygen was studied over total pressures 10–100 Torr and T = 750 – 1000 K by means of high-speed color cinematography. It was established that the features of spatial development of ignition are determined by material and state of reactor surface. Numerical modeling [13] showed that the flow of active centers from surface to volume leads to non-uniform development of ignition over reactor volume.

Promoting action of platinum (Pt) coating of reactor surface on the rate of H_2 oxidation is studied in [69]. It was shown in [70] that such action of Pt is caused by heterogeneous development of reaction chains that enhances probability of the ignition near surface. Hence, another factor influencing uniformity of ignition is the material of reactor surface.

As is known [7, 71], the area of spontaneous ignition of $2H_2 + O_2$ mixture can be presented as follows. The increase in reactor temperature above 820 K causes marked increase in the pressure of upper (second) pressure combustion limit and then to its disappearance. At pressures about 1 atm the third pressure limit of spontaneous ignition (P_3) occurs, in this case the pressure of the third limit increases with a decrease in temperature (Fig. 1.1a). As is suggested in [72], P_3 has thermal nature over Pyrex glass surface, but if reactor walls are coated with potassium chloride (KCl) P_3 is of chain nature. According to [73], the third pressure limit of ignition in heated reactor has chain nature in all cases. The short review of works on H_2 combustion at higher pressures and elevated temperatures can be found in [74].

The information below refers to the experimental investigation of spatial development of H_2–air mixtures ignition in the heated reactor over total pressures up to 2 atm by means of quick gas transfer with the use of high-speed color cinematography as well as at establishment of the influence of both propene additives [75] and surface state on the temperature of the third pressure limit of ignition. The experiments were performed with H_2–air mixtures in the range of 1–2 atm and T = 500–800 K. Gas mixtures of 40% H_2 + 60% air with (0–2%) propene (C_3H_6) additive were used in experiment and were prepared previously. In a number of experiments additive of 1–2% carbon tetrachloride (CCl_4) was used for visualization of H_2 flame. It should be noticed that CCl_4 additive in amounts less than 5% does not influence on H_2 combustion [7]. Experiments were performed in a heated stainless steel reactor of cylindrical shape of 25 cm in length and 12 cm in diameter equipped with demountable covers and an optical quartz window in one of the covers. Accuracy of temperature measurements was 0.3°. Combustion process was recorded by means of Casio Exilim F1 Pro color high-speed digital camera (30–1200 frames per second), sensitive over the spectral range of 420–740 nm through the optical quartz window. The pumped and heated reactor was quickly filled with the gas mixture from a high pressure buffer volume to necessary pressure. An electromagnetic valve was used to open and close gas communications. Because of sharp difference of pressures in the buffer volume and reactor there was a gas movement in the reactor that according to Ref. [64] led to the reduction of time of establishment of uniform temperature distribution (Fig. 1.1b). In [64] direct measurements of dynamics of temperature change in the center of the reactor by means of thin thermocouples were performed in similar conditions. It was shown that the time of warming up of gas mixture does not exceed 0.3 s. In this case, the formula considering only conductive heat exchange gives considerably greater value about tens of seconds. Pressure in the course of bleeding-in and combustion was recorded by means of a pressure transducer. At the moment of the valve opening a light-emitting diode was turned on, its flash was recorded by the camera. It allowed determining a delay time of ignition τ from a shot sequence independently for each separate ignition.

All experiments on high-speed registration of spontaneous ignition have shown that an initial center of ignition originates on the reactor surface; in each subsequent experiment under the same conditions, the site of origin of the initial center varies (Fig. 1.2a). Before each experiment, the reactor was washed by warm distilled water. Bright points in Fig. 1.2a are caused by emission of hot soot particles in the flame zone. It means that chemical activity of various sites of surface changes from one ignition to another [12–14]. It should be noted that at initial stages of combustion process the development of an initial single center leads to the propagation of the flame front of hemispherical shape. Hence, the velocity of flame propagation can be determined directly from experimental sequences of video images. It is obvious that the observed pattern of combustion origination corresponds to a regime of ignition with heated surface [13]. The basic feature of ignition process lies in the fact that ignition occurs at separate sites of surface at uniform temperature of the surface of the reactor.

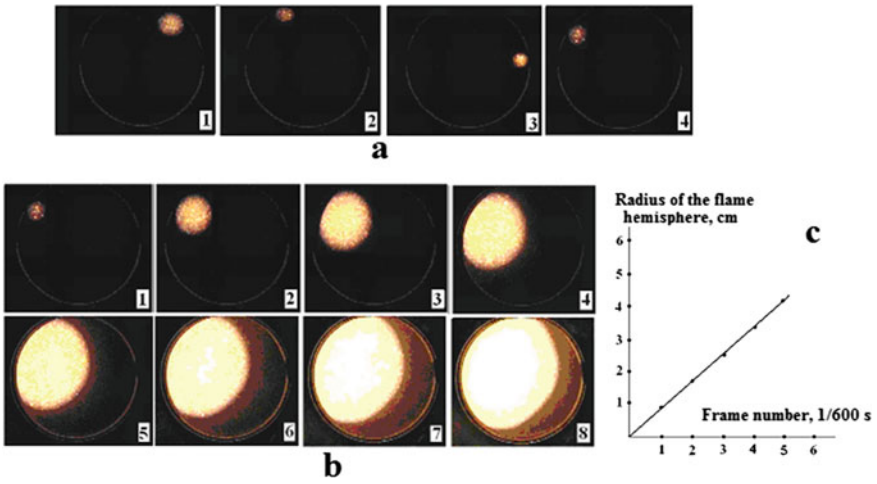

Fig. 1.2 **a** Video images of the initial centers of spontaneous ignition in stoichiometric n-pentane–air mixtures in four consecutive experiments at temperature of walls 1 650; 2 643; 3 645; 4 649 K. 600 shots/s, P = 1 atm. The numbers on each image correspond to the experiment serial number. **b** Sequences of video images of spatial development of ignition in stoichiometric n-pentane–air mixture at the temperature of the reactor walls 649 K, 600 shots/s. P = 1 atm. Numbers in the picture correspond to consecutive number of the video image. **c** The dependence of hemispherical flame visible radius of stoichiometric n-pentane–air mixture on time for (**b**)

A very important conclusion follows from the results obtained. It can be seen from Fig. 1.2a *that the process, called self-ignition (although in fact we are talking about thermal ignition), proceeds heterogeneously in space and its regularities are determined not only by the temperature of the reacting gas, but also by the material and the state of the surface (the presence of defects, which initiate primary active centers). This means that classical models that do not take into account surface heterogeneity and gas-dynamic features of the propagation of the reaction front, as, for example, the model discussed above, do not describe even qualitatively the emergence and development of the process of thermal ignition.*

One of the options for a new model that takes into account the inhomogeneity of the medium is proposed in Sect. 2.5, Chapter 2.

The sequences of video images of spatial development of ignition in stoichiometric n-pentane–air mixture at the temperature of the reactor walls 649 K corresponding to the development of one of the initial centers presented in Fig. 1.2a are shown in Fig. 1.2b.

As is seen in Fig. 1.2, hemispherical flame front develops from the initial center of ignition; then the front becomes asymmetric as new ignition centers occur. In these series of experiments the delay period of ignition made up not less than 7 s, therefore the uniform warming-up of a gas mixture in accordance with direct measurements [7, 64] was almost provided for, because the fast bleeding-in reduces the time of warming-up of a gas mixture. Therefore, combustion originates on the surface of

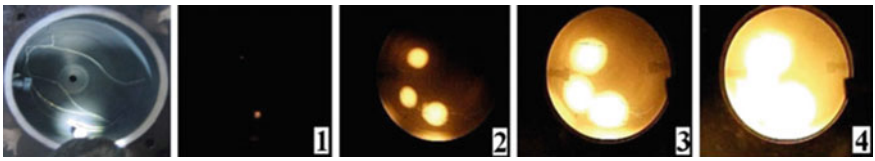

Fig. 1.3 The left frame: location of the platinum wire in the reactor; 1–4 consecutive frames of catalytic ignition of pentane–air stoichiometric mixture recorded at a frame speed of 600 frames/s. Initial conditions: a pentane–air stoichiometric mixture, $T_0 = 638$ K, $P_0 = 2$ atm

the steel reactor even under conditions of almost homogeneous warming-up of a gas mixture. As is seen from Fig. 1.2b, the flame front has a hemispherical form; the dependence of the flame radius on time can be easily estimated. The pressure during combustion was recorded by means of a pressure transducer.

From the time dependence of the visible radius of a spherical flame R(t) normal flame velocity $U_n = [dR(t)/dt]/\varepsilon_T$ was calculated. The value of ε_T was determined from the maximal pressure value of combustion Pb [7]: $P_b/P_0 = 1 - \gamma(\varepsilon_T - 1)$, P_0 -initial pressure, γ—ratio of specific heats ($\gamma = 1.2$ [7]) A typical result of the estimation by the example of Fig. 1.2b is shown in Fig. 1.2c. The experimental value of ε_T in the experiment makes up 3.35, then the normal flame velocity $Un = [dR(t)/dt]/\varepsilon_T$ determined from Fig. 1.2c from the change of visible radius of a spherical flame gives 150 cm/s in good agreement with [7].

We performed the following experiments to determine whether the surface produces a catalytic effect on the ignition of hydrocarbons. To do this, we introduced into the reactor a platinum wire of 0.5 mm in diameter and 0.5 m in length. Figure 1.3 displays a photograph showing the location of the wire in the reactor (the left frame), as well as frames showing the first moments of ignition of the pentane–air mixture in the presence of the catalytic surface. As can be seen from these frames (Fig. 1.3, shots 1–4), ignition kernels occur along the wire.

To find out the influence of the reactor coating material on the value of the third pressure limit P_3 the reactor surface was covered with a layer of potassium chloride (KCl) in some series of experiments. For this purpose, the reactor surface (except an optical window) was covered with saturated water solution of KCl (5 ml) and then water was pumped out. In other series of experiments, Pt foil 12×6 cm and 0.3 cm thick was placed in the reactor. Before each experiment, the reactor was pumped out to 10^{-1} Torr. Total pressure in the reactor was controlled with a vacuum gauge, the pressure in the buffer volume—with a manometer. Chemically pure gases and 99.99% Pt were used.

Experiments on thermal ignition of H_2–air mixtures over stainless steel and KCl have shown that in the immediate vicinity of P_3 the pressure in the reactor reaches the expected value (Fig. 1.1b), though the value of ignition delay period τ does not exceed 0.3 s, which is almost near certainty. So short values of τ can be explained by heterogeneous initiation occurring either on reactor surface or on the surface of artificial metal particles forming e.g. in motion of electromagnetic valve details. Note that in connection with the above, Fig. 1.1a is very conventional, since the limits

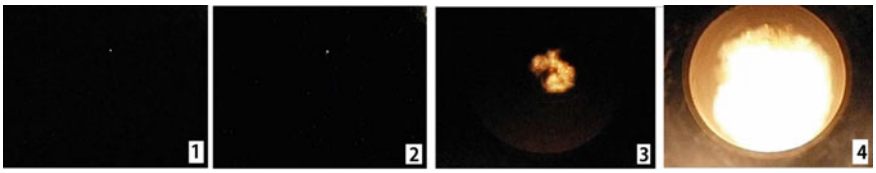

Fig. 1.4 Sequences of video images of spatial development of ignition on admission of H_2 to 1 atm of air at the temperature of reactor walls 680 K, 600 shots/s to total P = 2 atm. Material of the wall—stainless steel. As is seen, ignition is initiated on the particle heated in H_2 flow [76]

of thermal ignition depend on the state of the surface even for the same material. Luminescence of Ni and Fe particles in H_2 flow was detected in [76]. Ignition of H_2 at its admission into heated rector containing air really occurs on the surface of a radiating particle torn with airflow from the reactor surface (Fig. 1.4).

The increase in temperature leads to ignition at early stages of gas transfer inside the ignition area.

The data on the dependence of P_3 on pressure and on H_2 content in gas mixture are shown in the Fig. 1.5. We considered that ignition had occurred, if the pressure transducer recorded sharp growth of pressure after filling the reactor with gas mixture and the camera recorded gas luminescence. As is seen, the ignition temperature of H_2–air mixture in the stainless steel reactor increases as H_2 content in the mixture decreases. With an increase in pressure, the transition to ignition occurs in the narrow interval of temperatures being less than 1°. Temperature of ignition of H_2–air mixtures in the stainless steel reactor is ~ 20° more than in the reactor coated with potassium chloride and ~ 170° more than in the reactor containing Pt foil. This result means that P_3 depends on the material of reactor surface. It is also shown that as propene additive increases from 1 to 2% 40% H_2 + 60% air mixture does not ignite even at 733 K and pressure 1.9 atm, i.e. P_3 increases sharply. It means that H_2 combustion in the vicinity of P_3 is inhibited with small chemically active additive.

All experiments performed on high-speed registration of ignition have shown that the primary center of ignition occurs at the reactor surface, irrespective of the material of surface (Figs. 1.2, 1.3, 1.4 and 1.5); the place of occurrence of the center in a consecutive series of experiments changes from one experiment to another under the same initial conditions.

Therefore, chemical activity of various surface sites changes from one experiment to another as well as in [68]. We will notice that as distinct to initial stage of hydrocarbons combustion when the development of the primary single combustion center leads to propagation of flame front of hemispherical shape [68], propagation of H_2 flame from the primary surface center even in the presence of inhibitor has turbulent character (Figs. 1.4, 1.5). Therefore, it is possible to define only average speed of flame propagation from the experiment. The basic feature of processes observed implies that ignition occurs on separate surface sites at the same temperature of the reactor surface; these sites vary from one experiment to another (Fig. 1.5) that

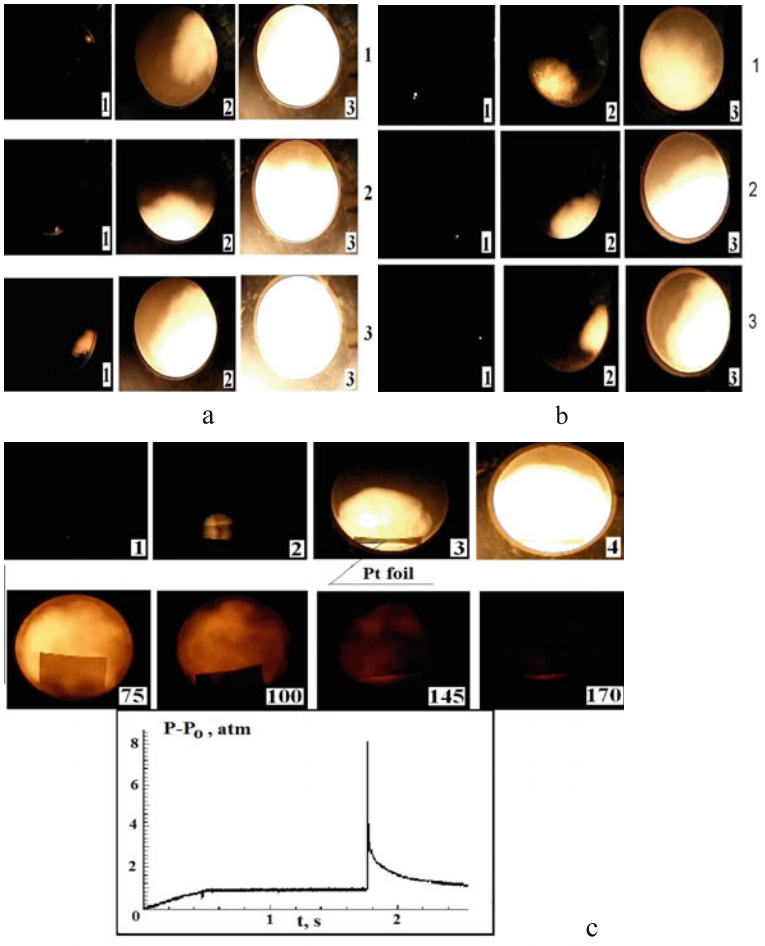

Fig. 1.5 **a** Sequences of video images of spatial development of ignition in 40% H_2 + air + 1% C_3H_6 + 1% CCl_4 at the temperature of reactor walls 698 K (1), 710 K (2), 725 K (3), 600 shots/s. P = 1 atm. Material of the wall—stainless steel. Numbers in each frame correspond to a consecutive number of the video image. **b** sequences of video images of spatial development of ignition in 40% H_2 + air + 1% C_3H_6 + 1% CCl_4 at the temperature of reactor walls 715 K (1), 725 K (2), 735 K (3), 600 shots/s. P = 1 atm. Material of the wall—KCl coating. Numbers in each frame correspond to consecutive number of the video image. **c** sequences of video images of spatial development of ignition in 40% H_2 + 60% air mixture at the temperature of reactor walls 523 K, 600 shots/s. P = 1 atm. Pt foil is placed in the stainless steel reactor. Its movement under explosion is clearly seen in shots 75,100. As is seen from shots 145–170, Pt foil becomes incandescent under gaseous reaction. Numbers in each frame correspond to consecutive number of the video image. Below is the time dependence of pressure change in the ignition

corresponds to a mode of ignition with heated surface [65–67], rather than a uniform ignition mode [77–80].

The data on the values of τ point to the same conclusion. Though over stainless steel and KCl τ does not exceed 0.3 s including the time of bleeding-in, the value of τ over Pt foil is 0.5 ÷ 1.2 s. This result means that over stainless steel and KCl the gas mixture does not warm up uniformly (a warming up period exceeds 0.3 s, see experimental above), but over Pt foil uniform heating takes place (Fig. 1.5c). We will notice that for lack of ignition (P_3 is not reached, see Fig. 1.1a) in immediate vicinity of P_3 the combustible gas in the reactor obviously warms up uniformly, i.e. we obtain reliable P_3 values by measurement "from below". In immediate vicinity of P_3, but above its value, ignition occurs locally over all surfaces investigated.

Let us compare P_3 values obtained in this work with the available literary data. In Fig. 1.6, the values of temperatures at $P_3 = 1$ atm are compared for mixtures of 40% H_2 + 60% air + 1% C_3H_6 + 1% CCl_4 (the present book) and mixtures $2H_2 + O_2$ [72]. The fact (Fig. 1.6) that the temperatures of ignition obtained with quick gas transfer method in this study are ~ 160° less than obtained in [72] has engaged our attention. It would appear reasonable that both without inhibitor and at replacement of air by oxygen the temperatures at $P_3 = 1$ atm for our experimental conditions should be even lower than those presented in Fig. 1.6.

Observable distinctions in the values of temperatures are obviously related to various experimental techniques used in the present work when the heated reactor was filled with preliminary prepared gas mixture, and [72], in which gas mixture was prepared in the heated reactor at temperatures close to the temperature of ignition. For this purpose in [72], the heated reactor was filled at first with H_2, and then with oxygen, which was allowed to bleed in through a thin capillary for 4 s, thus the values of τ reached 30 s. It can be assumed that with the use of the technique [72] oxygen could already react during bleeding-up in surface reactions, i.e. the composition of gas mixture at the moment of ignition essentially differed from the initial one. Therefore P_3 value obtained with the technique [72], can be concerned with the mixture of some other composition. Notice that in [72], the analysis of gas mixture composition during experiment was not performed.

The experimental results show that much as in hydrocarbons combustion [68] the process of H_2 combustion in the vicinity of P_3 is the ignition by chemically active heated surface which is accompanied by flame propagation into reactor volume. It means that in mathematical modeling of ignition of H_2–air mixtures in the vicinity of P_3 it is impossible to restrict the consideration to the analysis of a uniformly distributed problem. It is also necessary to consider the possibility of formation of the combustion centers on reactor surface along with gas phase combustion kinetics, i.e. to allow for heterogeneous processes.

Let us notice that within the framework of existing notions the changeover across a critical condition of ignition should be accompanied by substantial growth of an induction period τ. However this is observed only over Pt catalytic surface, probably because at comparably low temperatures (~ 520 K) the reaction of chain origination w_0 (determining the value of τ [60]) on Pt has the lowest activation energy as

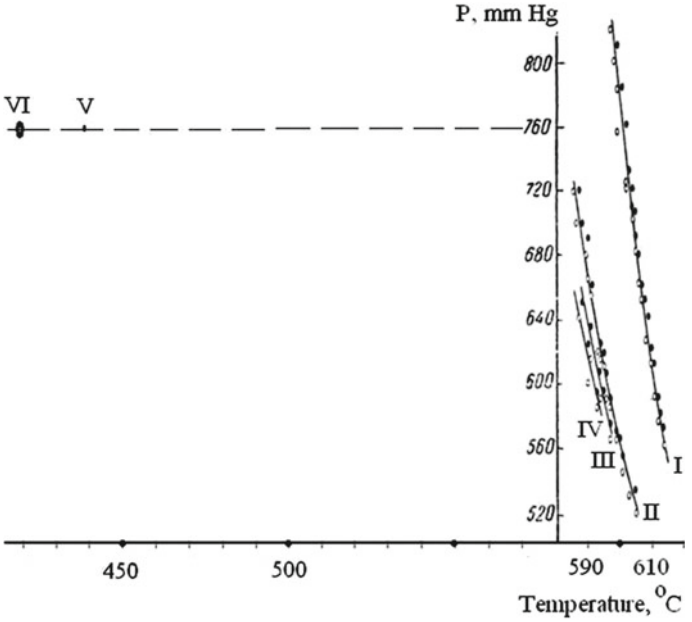

Fig. 1.6 Dependencies of P_3 of $2H_2 + O_2$ on temperature from [72] (I–IV)—(I) experiments in reactors with KCl coating, (II) experiments in pyrex glass reactors, (III) experiments in pyrex glass reactors $2H_2 + O_2 + 2\%$ H_2O, (IV) experiments with the mixture addition during the reaction, reactor diameter = 4 cm; (V), (VI) values of the third pressure limit obtained in the present work for 40% H_2 + air + 1% C_3H_6 + 1% CCl_4 for KCl coating and stainless steel, reactor diameter d = 12 cm

compared with stainless steel and KCl. As is seen from our experiments over stainless steel and KCl, reaction rate in the vicinity of the third pressure limit changes stepwise in a very narrow temperature interval ~ 1°, thus, ignition initiates at reactor surface. Really, the interval of 1° is too small for drastic change in reaction rate in the volume. One can assume that it is connected with the sharp change of reaction ability of certain elements (defects etc.) of reactor surface during the transition over a critical condition [77].

Summarizing, it is shown that the features of ignition of H_2 in air in the area of P_3 depend not only on the mixture composition, but also on the material of reactor surface and on the amount of chemically active additive. Comparably long delay times of 40% H_2 + air ignition at 1 atm were first observed over Pt surface. It is established that the process of ignition of H_2–air mixtures at atmospheric pressure begins with primary center occurrence on the most chemically active site of the surface, which initiates flame propagation into volume. These results will be useful to us in the course of further presentation of the material.

It should be noted that at the current state of experiment any comparison of the results of numerical calculations with experimental data is reliable only in a qualitative aspect, e.g. on the qualitative modeling of time dependence of velocity change

of movement of the boundary between initial and actively reacting components. The examination of the detailed kinetic mechanism introduces additional uncertainty into modeling. A large part of kinetic parameters is not accurate enough to draw reasonable conclusions using calculations. The issue of completeness of the used reaction set is always an open question, because an important reaction can be overlooked. Moreover, as there are no unicity theorems on reactive compressible Navier–Stokes equations, which are used very often for combustion modeling in low Mach approximation, the agreement between calculated quantities and experimental ones does not argue for accord between calculation and experiment, as there can be other sets of the governing parameters describing the same experimental dependencies [59].

As one can see, such difficulties arose even before the moment when we turned to the consideration of heterogeneous reactions on the catalyst surface. Indeed, all of the above about homogeneous reactions also applies to heterogeneous processes, especially as concerns both experimental determination of the rates of elementary reactions on the surface and the nature of these reactions themselves. In addition, since there are time dependent flows of reactants to the surface, the gas-dynamic features of the process should be taken into account along with a reaction mechanism that is, unfortunately, usually poorly known.

When the catalyst is introduced into the combustible mixture, new critical phenomena arise, namely the temperature and pressure limits of catalytic ignition, which are determined by the state and history of the catalyst surface. That is another phenomenon, which has not yet received enough attention: the dependence of the catalyst surface state on surface treatment by ignitions of a combustible gas mixture, manifested in the fact that the catalytic activity of the untreated surface is markedly different from that of the surface, above which ignitions were carried out. This phenomenon and its associated effects will be discussed in this book.

We will underline that extensive experimental and theoretical attention has been given to catalytic combustion in the past decade. The potential of heterogeneous processes in reducing emission of pollutants, improving ignition, and enhancing stability of flames has been recognized. The modeling and simulation of heterogeneous systems require the coupling of reactive flows with gas-surface interactions. The aim is to achieve a quantitative understanding of catalytic combustion. Catalytic ignition is an abrupt transition from a kinetically controlled system to one controlled by mass transport. Therefore, the complex interactions of chemical and transport processes in the gas phase as well as at the surface have to be included. Thus, the numerical simulation of catalytic ignition and the comparison of calculated and experimental results represents a suitable tool to validate qualitatively the models and the reaction mechanisms proposed.

The authors would also like to make the reader more familiar with virtually inaccessible works of Russian authors published up to 2022 in Russian.

Let us now highlight the main issues that have been addressed in this book.

Chapter 3 is focused on the establishment of the features of hydrogen and deuterium ignition over platinum, palladium, ruthenium and rhodium. The detection of instabilities of the spatial development of 40% H_2–air ignition as well as the establishment of the temperature dependence of delay times of ignition in the heated

reactor at 1 atm by means of a quick gas transfer in the presence of platinum foil or a Pt wire was carried out. Cellular combustion regime of the mixture in the presence of Pt wire over the interval 270–350 °C was observed for the first time. It was shown that the regime is caused by the catalytic action of Pt containing particles formed by decomposition of volatile platinum oxide in the gas phase. The experimental studies of low-pressure hydrogen combustion over Pd and Pt foils at total pressures from 10 to 180 Torr and initial temperatures of 20–288 °C were performed. We showed that the catalytic activity of the surface is higher than that over Pt foil. The activity of Pd foil reveals itself in both the occurrence of local ignition centers on the foil and the dark catalytic reaction of consumption of the flammable mixture. The comparative contribution of the mechanisms of both initiation by a surface reaction leading to active centers desorption and initiation of the ignition at the expense of only thermal heating with Pt surface, was established. It was determined that in the reaction of hydrogen combustion, metallic Pt acts as a heat source similar to (say) a tungsten wire heated by an external source. However, in the case under investigation, Pt is heated with an internal source, namely a surface catalytic reaction. It must be also taken into account that the composition of the surface layer changes during ignitions from Pt oxide (PtO_2) to another composition, exhibiting properties different from PtO_2. The experimental studies of low-pressure hydrogen and deuterium combustion over Rh, Ru, Pd and Pt wires at total pressures from 10 to 180 Torr and initial temperatures over the range 200 ÷ 500 °C were performed in order to establish the dependencies of catalytic ignition limits over noble metal surfaces on temperature and to indicate the governing factors of the problem of gas ignition by a catalytic surface as well. A macrokinetic study of the chemical properties of the two lighter hydrogen isotopes (protium and deuterium) dissolved in rhodium and palladium, namely the study of the influence of hydrides and deuterides of noble metals on hydrogen and deuterium combustion, was performed. It was revealed that Rh, Ru and Pd surfaces treated with $2H_2 + O_2$ ignitions show the defects in the form of openings, which are located on etching patterns; the etching substances are active intermediates of H_2 oxidation. It was found that before ignition catalytic wire is not heated up uniformly; initial centers of the ignition occur. It was shown that Rh is the most effective catalyst of $2H_2 + O_2$ ignition, the lowest ignition temperature over Rh coated Pd wire (Rh/Pd) was 210 °C, for Ru/Pd and Pd—300 °C, for Pt wire—410 °C at total pressures less than 200 Torr. The hysteresis phenomenon is observed over Ru/Pd, Pt and Pd wires; namely, the ignition limit value measured over the wire, which is not treated with ignitions (a procedure of increasing temperature from a state of no ignition), is higher than the value measured with a procedure of decreasing temperature from a state of a catalytic ignition. It was shown that Rh is the most effective catalyst of $2D_2 + O_2$ ignition, in this case the lowest ignition temperature over Rh coated Pd wire (Rh/Pd) was 100 °C. It is more accurate to speak about ignition over noble metals hydrides/deuterides; thus, the lowest ignition limit of $2D_2 + O_2$ over rhodium deuteride was 100 °C; thus, D_2 is more flammable than H_2 over Rh and Pd. The obtained results indicate the existence of a “kinetic inverse isotope effect”, which affects the reactivity of MeH and MeD, where Me = Rh, Pd.

Chapter 3 is focused on the establishment on the features of catalytic ignition of the mixtures of H_2 + C_1–C_6 hydrocarbons + O_2/air with platinum, palladium and rhodium. The tendencies in combustion of hydrogen and mixtures of hydrogen with methane over metallic Pd, including the use of an optoelectronic complex based on a hyperspectral sensor and high-speed color filming were revealed. It was shown experimentally that the ignition temperature of the 40% H_2 + air mixture over metallic Pd (70 °C, 1 atm) is lower than over the Pt surface. In addition, Pd wire initiates the ignition of the (30–60% H_2 + 70–40% $CH_4)_{stoich}$ + air mixtures, which cannot be initiated with Pt wire of the same size. This also means that Pd wire is more effective in initiation of ignition than Pt wire. The cellular structure of the flame front during ignition in the presence of Pd wire is missing in contrast to the results obtained on the Pt surface. It means that Pd is more suitable than Pt for hydrogen recombiners in nuclear power plants because the catalytic particles do not appear in the gas phase. The experimental value of the effective activation energy of the process over Pd was estimated at (3.5 ± 1) kcal/mol, which is characteristic of surface processes. This indicates the significant role of the dark reaction of H_2 and O_2 consumption on the Pd surface observed directly at low pressures. The presence of this reaction reduces the probability of accidental explosion compared to the Pt surface. It was found that in the presence of leucosapphire, there was no system of emission bands of H_2O* in the range 570–650 nm during H_2–O_2 ignition and a possible explanation of this effect was given. The appearance of an additional source of excited water molecules emitting in the range 900–970 nm was explained.

The combustion of hydrogen–hydrocarbon (C1–C6, namely CH_4, C_2H_6, C_3H_8, C_4H_{10}, C_5H_{12}, C_6H_{14})–air mixtures with θ = 0.6–1.2 over Pd at total pressures 1–2 atm was investigated. Both the features of a flame front propagation in the mixtures and the dependence of a flammability limit over Pd surface on temperature were established. The experiments were performed with gas mixtures of 30% C1–C6 hydrocarbon + 70% H_2 + air at θ = 0.6–1.2 and pressures 1–2 atm. It was experimentally shown that the temperature of the ignition limit over Pd at P = 1.75 atm, measured with a bottom-up approach by temperature, of the mixtures 30% methane + 70% hydrogen + air (θ = 0.9, T = 317 °C) and 30% propane + 70% H_2 + air (θ = 1, T = 106 °C) markedly drops after subsequent ignitions to T = 270 °C for H_2–CH_4 mix and to T = 32 °C for the H_2–C_3H_8 blend. The catalytic ignition limit returns to the initial value after treatment of the reactor with O_2 or air; i.e., a hysteresis phenomenon occurs. The ignition limit of the mixtures 30% (C2, C4, C5, C6) + 70% H_2 + air (θ = 0.6, 1.1, 1.2, 1.2, correspondingly) over Pd amounts to 25–35 °C at P = 1.75 atm; the hysteresis effect is missing. It was found that lean 30% C_2H_6 + 70% H_2 + air mix (θ = 0.6) shows the lowest temperature of the ignition limit: 24 °C at 1 atm. The estimate of the effective activation energy of the ignition of the mixes over Pd is ~ 2.4 ± 1 kcal/mol that is characteristic of a surface process. Thus, the usage of Pd catalyst allows igniting H_2–hydrocarbon mixtures at 1–2 atm at initial room temperature without external energy sources. The features of ignition of hydrogen–oxygen and hydrogen–methane–oxygen mixes at low pressure with hot Pd, Pt, Nichrome and Kanthal wires were revealed in order to establish whether there is a dependence of ignition temperature on fuel concentration and to estimate the

contribution of catalytic properties of the materials as well. It was found that the ignition temperatures of hydrogen–oxygen and hydrogen–methane–oxygen mixes at low pressure over heated Pd, Pt, Nichrome and Kanthal wires at 40 Torr increase with a decrease in H_2 concentration; only a heated Pd wire shows the pronounced catalytic action. Numerical calculations allowed elucidating the role of an additional branching step $H + HO_2 \rightarrow 2OH$. The peculiarities of ignition of premixed stoichiometric n-pentane-air mixtures were studied in a rapid mixture injection static reactor in the presence of metallic Pt and Pd in the region of negative temperature coefficient (NTC). It is shown that in the absence of noble metals thermoacoustic oscillations occur within NTC region. In the presence of Pt catalyst surface, which reacts with oxygen at the flame temperature and generates catalytic centers propagating into volume, thermoacoustic regimes of thermal ignition disappear; in other words, the catalytic Pt surface eliminates a certain inhibition stage of kinetic mechanism after the occurrence of the cool flame and NTC phenomenon vanishes. The stage may be e.g. the decomposition of some intermediate peroxide on Pt surface with the formation of a more reactive radical. In the presence of the catalytic surface (Pd), which does not react at the flame temperature and does not generate catalytic centers propagating into volume, NTC phenomenon occurs. Gas mixtures of (70–40%) hydrogen–(30–60%) propane–air mixtures ($\theta = 1$) over Pd at total pressures 1–2 atm. were investigated to establish both dependencies of the ignition delay period on time and the relationship of a flammability limit over Pd surface on temperature. It was found that at the combustion of (70–40%) hydrogen–(30–60%) propane–air mixtures ($\theta = 1$) over palladium at total pressures 1–2 atm the ignition delay periods first decrease with a decrease in temperature; then these increase until the catalytic ignition limit is achieved; i.e., NTC phenomenon occurs. The effective activation energy of the process is $E = 2.2 \pm 1$ kcal/mol that is characteristic of a surface process. Thus, NTC phenomenon is strongly associated with the state of Pd surface. It is found out that in the sample treated with ignitions, the defects in the form of openings, which are focused on etching patterns, arise. In the process, PdO particles originate in the process of oxidation of Pd surface; PdO particles decompose to Pd and O_2 at the temperature of flame products. This means that Pd is spent in the reaction of chemical etching with active intermediates of combustion. It should restrict the applicability of palladium in ignition devices. Low-pressure combustion of hydrogen–methane and hydrogen–isobutene mixtures over Rh and Pd surfaces at total pressures from 80 to 180 Torr and initial temperatures of 200–500 °C was studied in order to establish the regularities of temperature limits of flammability over noble metals and to reveal the possibility of synthesizing carbon nanotubes from these gaseous precursors. It was shown that, at total pressures up to 200 Torr, the catalytic ignition areas over the Rh and Pd surfaces are larger for $2H_2 + O_2$ mixtures than for $(H_2 + CH_4)_{stoich} + O_2$ and $(H_2 + C_4H_8)_{stoich} + O_2$ mixtures; the mixtures containing more than 50% hydrocarbons do not ignite. This behavior is directly related to the formation of a carbon-containing film on the noble metal surface while the fuel in the mixtures is consumed in a dark reaction. It has been shown that the dark reaction in the $(80\%\ H_2 + 20\%\ C_4H_8)_{stoich} + O_2$ mixture leads

to the formation of carbon nanotubes with a diameter within 10–100 nm; here noble metal acts both as a heater and catalyst.

Chapter 4 is aimed at the establishment of the regularities of catalytic ignition mainly of H_2–methane mixtures; in a series of experiments methane blends were replaced with ethane, ethylene and n-pentane.

Experimental determination of ignition temperatures and effective activation energies of ignition of mixes $(40 \div 70\%\ H_2 + 60 \div 30\%\ CH_4)_{stoich}$ + air over Rh was performed at $1 \div 2$ atm over temperature range $20 \div 300$ °C under static conditions in order both to establish catalytic effectiveness of Rh as a promising igniter, and to reveal factors, which determine the values of effective activation energies and to find out whether NTC phenomenon exists in the ignition.

It was shown that in the reactor, treated with ignitions, the ignition temperature of the mixture 70% H_2 + 30% methane with air over rhodium surface is 62 °C. The result indicates the potential of using rhodium catalyst to lower markedly the catalytic ignition temperature of the fuels based on hydrogen-methane mixtures. The critical condition for volume reaction is revealed: the volume process occurs at 45% H_2, but it is missing at $\leq$ 40% H_2. If $H_2 \leq 40\%$, only a slow surface reaction occurs; this phenomenon is qualitatively described by our calculations. It is revealed that the effective activation energies both of "upper" and "lower" limits of H_2 + methane oxidation over the range of linearity are roughly equal (2.5 ± 0.6) kcal/mol; it means that the key reactions, responsible for the occurrence of "upper" and "lower" ignition limits are almost certainly the same. It was shown that for Rh/Pd catalyst the chain development process has most likely heterogeneous nature because the effective activation energy is < 3 kcal/mol. Experimental determination of ignition temperatures and effective activation energies of ignition of mixtures $5\% \div 40\%\ H_2$–air over Rh and $(30 \div 70\%\ H_2 + 70 \div 30\%\ C_2H_6$ (and $C_2H_4))_{stoich}$ + air over Rh and Pd at 1 atm was performed over temperature range 20–300° under static conditions in order to compare catalytic effectiveness of Rh and Pd and to establish factors that determine the values of effective activation energies. It was shown that the obtained values of effective activation energy are in mutual agreement and are characteristic of the surface nature of Rh action; Rh is more catalytically active than Pd. The key features of catalytic ignition on metallic rhodium and palladium in a series of mixed fuels: namely hydrogen + synthesis gas and hydrogen + hydrocarbon (ethane, ethylene, propane, pentane) + air were identified to establish the boundaries of catalytic ignition regions, dependencies of effective ignition activation energies on the nature of a hydrocarbon, and the role of dark oxidation processes. It was shown that under conditions of our experiments not the chemical nature of the catalyst but that of C_2 hydrocarbon in the mix with H_2 is the determining factor of catalytic ignition. The catalytic ignition limits of synthesis gas over Rh/Pd are qualitatively different from the dependencies for combustible hydrogen-hydrocarbon: the "lower" catalytic limit dependence has a distinct maximum, which indicates a complex mechanism of the catalytic process; Arrhenius dependence of $\ln [H_2]_{lim}$ on $1/T$ could not be applied. Therefore, the interpretation of the "upper" and "lower" limits of catalytic ignition given in the literature should be refined. Long delay periods of catalytic ignition of hydrogen–n-pentane mixes (tens of seconds) and the absence of the dependence of

the periods on the initial temperature allow us to conclude that the catalytic ignition of hydrogen–n-pentane mixes is determined by the transfer of the molecules of the hydrocarbon blend to the surface of the catalytic wire. Experimental studies of low-pressure combustion of H_2–O_2 and H_2–CH_4–O_2 mixtures were carried out over Pt surface at total pressures from 20 to 180 Torr and initial temperatures of 400–600 °C. These were performed in order to establish the relationships of catalytic ignition limits over Pt on temperature and to reveal the features of ignition of hydrogen- methane mixes over Pt in a constant electric field in the absence of discharge. It was shown that the ignition limits of $2H_2 + O_2$ and $(80\%\ H_2 + 20\%\ CH_4)_{stoich} + O_2$ mixes over Pt wire do not depend on the applied voltage without discharge up to 1200 V. We showed that for $(80\%\ H_2 + 20\%\ CH_4)_{stoich} + O_2$ mixes the application of an electric field (1200 V) leads to the disappearance of Pt containing particles from the reaction volume formed by decomposition of volatile platinum oxide in gas phase, which indicates that these particles are charged. This may be due to the chemiionization phenomenon observed in the combustion of hydrocarbons and then adsorption of the charged particles onto the Pt containing particles. Is was shown that in combustion of $(80\%\ H_2 + 20\%\ CH_4)_{stoich} + O_2$ mix carbon nanotubes practically do not form as distinct from $(H_2 + C_4H_8)_{stoich} + O_2$ mix.

Chapter 5 is focused on the features of interaction of the surfaces of noble metals with a propagating flame front. The peculiarities of penetration of a flame front of the diluted methane-oxygen mixture in the volumes of complex geometry in the laboratory scale installation were established. It was shown that a flame propagation process in a conditional room containing an indoor space with two openings and a flammable material inside shows a wide variety of combustion modes depending on the geometry of this complex volume. The preliminary numerical calculation of the expected flame propagation patterns may not always be successful, a real experiment under laboratory conditions, assuming the possibility of scaling the process, seems to be the most informative one. The investigation into Pt behavior in the flame of methane combustion under conditions of turbulent flow was performed. We revealed that under certain conditions Pt catalyst can suppress combustion and thereby show the opposite effect due to the high efficiency of Pt surface coated with a Pt oxide layer in the reaction of chain termination. Therefore, kinetic factors could be the determining even under conditions of high turbulence. Specific features of oxidation of hydrogen and methane over platinum and palladium at low pressures (70–200 Torr) were established. The value of effective activation energy of the dark reaction over Pd is evaluated as $E = 4.1 \pm 1$ kcal/mol that is characteristic of a surface process. Under our conditions, no dark reaction on Pt wire was observed. It was shown that the rate of chain termination determines the value of the critical diameter for flame penetration through Pt or Pd cylinders; the efficiency of Pd surface in chain termination reaction is much greater than that of Pt.

References

1. H. Davy, Some new experiments and observations on the combustion of gaseous mixtures, with an account of a method of preserving a continuous light in mixtures of inflammable gases and air without flame. Phil. Trans. R. Soc. Lond. A **107**, 77 (1817)
2. P.M.D. Collins, The pivotal role of platinum in the discovery of catalysis. The pioneering work of Johann Wolfgang Döbereiner during the 1820s. Platinum Metal Review **30**(3), 141 (1986)
3. E. Davy, On some combinations of platinum. Phil. Trans. Roy. Soc. **110**, 108 (1820)
4. J.W Döbereiner, Über neu entdecke höchst merkwürdige Eigenschaften des Platins (Jena, 1823).
5. W. Prandtl, Deutscher Chemiker in der ersten Hälfte des neunzehnten Jahrhunderts (Weinheim, 1956), p. 49
6. J. W. Döbereiner, Zur Chemie des Platins (Stuttgart, 1836), p. 76.
7. B. Lewis, G. Von Elbe, *Combustion, Explosions and Flame in Gases* (Acad. Press, New York, 1987)
8. A.B. Welch, J.S. Wallace, Performance characteristics of a hydrogen-fueled diesel engine with ignition assist, SAE international fuels and libricants conference and exposition. Tulsa, OK (USA), SAE Paper 902070 (1990)
9. K. Persson, L.D. Pfefferle, W. Schwartz, A. Ersson, S.G. Jaras, Stability of palladium-based catalysts during catalytic combustion of methane: the influence of water. Appl. Catal. B **74**, 242 (2007)
10. A. Fernández, G.M. Arzac, U.F. Vogt, F. Hosoglu, A. Borgschulte, M.C.J. Jiménez de Haro, O. Montes, A. Züttel, Investigation of a Pt containing washcoat on SiC foam for hydrogen combustion applications. Appl. Catal. B **180**, 336 (2016)
11. A.W. Petrov, D. Ferri, M. Tarik, O. Kröcher, J.A. van Bokhoven, Deactivation aspects of methane oxidation catalysts based on palladium and ZSM-5. Top. Catal. **60**, 123 (2017)
12. N.M. Rubtsov, V.I. Chernysh, G.I. Tsvetkov, K.Y. Troshin, I.O. Shamshin, Ignition of hydrogen-methane-air mixtures over Pd foil at atmospheric pressure. Mendeleev Commun. **29**, 469 (2019)
13. N.M. Rubtsov, *Key Factors of Combustion, From Kinetics to Gas Dynamics* (Springer International Publishing, 2017).
14. N.M. Rubtsov, V.I. Chernysh, G.I. Tsvetkov, K.Y. Troshin, O.I. Shamshin, The features of hydrogen ignition over Pt and Pd foils at low pressures. Mendeleev Commun. **28**, 216 (2018)
15. W.R. Williams, C.M. Marks, L.D. Schmidt, Steps in the reaction $H_2 + O_2 = H_2O$ on Pt: OH desorption at high temperature. J. Phys. Chem. **96**, 5922 (1992)
16. J. Warnatz, M.D. Allendorf, R.J. Kee, M. Coltrin, A model of elementary chemistry and fluid mechanics in the combustion of hydrogen on platinum surfaces. Combust. Flame **96**, 393 (1994)
17. O. Deutschmann, R. Schmidt, F. Behrendt, J. Warnatz, Numerical modeling of catalytic ignition. Proc. Combust. Inst. **26**, 1747 (1996)
18. M. Rinnemo, M. Fassihi, B. Kasemo, Experimental and numerical investigation of the catalytic ignition of mixtures of hydrogen and oxygen on platinum. Combust. Flame **111**, 312 (1997)
19. V.V. Kalinchak, A.S. Chernenko, M.V. Sikorskyi, A.N. Sofronkov, A.V. Fedorenko, Cool air-gas mixtures with combustible gas admixtures steady flameless combustion delay time on platinum particle (wire). Physics and Chemistry of Solid State **19**, 53 (2018)
20. L. Jewell, B. Davis, Review of absorption and adsorption in the hydrogen–palladium system. Appl. Catal. A **310**, 1 (2006)
21. J.E. Worsham, M.K. Wilkinson, C.G. Shull, Neutron-diffraction observations on the palladium-hydrogen and palladium-deuterium systems. J. Phys. Chem. Solids **3**, 303 (1957)
22. M. Yussouff, B.K. Rao, P. Jena, Reverse isotope effect on the superconductivity of PdH, PdD, and PdT. Solid State Commun. **94**, 549 (1995)
23. M. Fleischmann, S. Pons, Electrochemically induced nuclear fusion of deuterium. J. Electroanal. Chem. Interfacial Electrochem. **261**, 301 (1989)
24. C.P. Berlinguette, Y.M. Chiang, J.N. Munday et al., Revisiting the cold case of cold fusion. Nature **570**, 45 (2019). https://doi.org/10.1038/s41586-019-1256-6

25. G. Karavalakis, T.D. Durbin, M. Villela, J.W. Miller, Air pollutant emissions of light-duty vehicles operating on various natural gas compositions. J Nat Gas Sci Eng **4**, 8 (2012)
26. U.S. Energy Information Administration. International energy outlook. https://www.eia.gov/todayinenergy/detail.php?idj32912
27. B. Durand, Petroleum, natural gas and coal: nature, formation mechanisms, future prospects in the energy transition. EDP Sciences 101 (2019)
28. Centre for Energy Economics Research and Policy. UK. BP Statistical review of world energy. https://www.bp.com/en/global/corporate/energy-economics/statistical-review-of-world-energy
29. C. Zou, Q. Zhao, G. Zhang, B. Xiong, Energy revolution: from a fossil energy era to a new energy era. Nat Gas Ind B **3**(1), 14 (2016)
30. A.W. Petrov, D. Ferri, F. Krumeich, M. Nachtegaal, J.A. van Bokhoven et al., Stable complete methane oxidation over palladium based zeolite catalysts. Nat Commun. **9**(1), 2545 (2018)
31. M. Mehrpooya, M. Khalili, M.M. Sharifzadeh, Model development and energy and exergy analysis of the biomass gasification process (based on the various biomass sources). Renew Sustain Energy Rev. **91**, 869 (2018)
32. F. Ahmad, E.L. Silva, M.B.A. Varesche, Hydrothermal processing of biomass for anaerobic digestion—a review. Renew Sustain Energy Rev. **98**, 108 (2018)
33. Y.S. Najjar, Gaseous pollutants formation and their harmful effects on health and environment. Innov Energy Policies **1**, 74 (2011)
34. P. Gelin, G.P.M. Primet, Complete oxidation of methane at low temperature over noble metal based catalysts: a review. Appl Catal B **39**(1), 60 (2002)
35. T.V. Choudhary, S. Banerjee, V.R. Choudhary, Catalysts for combustion of methane and lower alkanes review. Appl. Catal. A **234**, 82 (2002)
36. Z. Li, G.B. Hoflund, A review on complete oxidation of methane at low temperatures. J Nat Gas Chem. **12**(3), 153 (2003)
37. L.M. Quick, S. Kamitomai, Catalytic combustion reactor design and test results. Catal Today **26**(3–4), 303 (1995)
38. Z. Anxionnaz, M. Cabassud, C. Gourdon, P. Tochon, Heat exchanger/reactors (HEX reactors): concepts, technologies: state-of-the-art. Chem. Eng. Process. **47**(12), 2029 (2008)
39. G. Kolios, A. Gritsch, A. Morillo, U. Tuttlies, J. Bernnat et al., Heat-integrated reactor concepts for catalytic reforming and automotive exhaust purification. Appl Catal B **70**(1), 16 (2007)
40. H.A. Khan, J. Hao et al., Catalytic performance of Pd catalyst supported on Zr: Ce modified mesoporous silica for methane oxidation. Chem. Eng. J. **397**, 125489 (2020)
41. G.P.M. Primet, Complete oxidation of methane at low temperature over noble metal based catalysts: a review. Appl. Catal. B: Environ. **39**, 10 (2002)
42. T.G. Bond, B.A. Noguchi et al., Catalytic oxidation of natural gas over supported platinum: flow reactor experiments and detailed numberical modeling. Symp. (Int.) Combust. 1771 (1996)
43. C. Cullis, B. Willatt, Oxidation of methane over supported precious metal catalysts. J. Catal. **83**, 267 (1983)
44. G. Acres, A. Bird et al., The design and preparation of supported catalysts. Catalysis **4**, 91 (1981)
45. C. Cullis, T. Nevell et al., Role of the catalyst support in the oxidation of methane over palladium. J. Chem. Soc. Faraday Trans. 1: Phy. Chem. Cond. Ph. **68**, 1406 (1972)
46. A.T. Gremminger, H.W. Pereira de Carvalho et al., Influence of gas composition on activity and durability of bimetallic Pd-Pt/Al_2O_3 catalysts for total oxidation of methane. Catal. Today **258**, 470 (2015)
47. M. Adamowska, P. Da Costa, Structured Pd/γ-Al_2O_3 Prepared by washcoated deposition on a ceramic honeycomb for compressed natural gas applications. Journal of Nanoparticles **2015**, 121 (2015)
48. J.A. Federici, D.G. Vlachos, Experimental studies on syngas catalytic combustion on Pt/Al_2O_3 in a microreactor. Combust. Flame **158**, 2540 (2011)
49. B. Feng, Y. Zhai et al., Toward the mechanism study of Pd/γ-Al_2O_3-assisted bioalcohol combustion in a flow reactor. Energy Fuels **35**, 14954 (2021)

50. X.I. Pereira-Hernandez, A. DeLaRiva et al., Tuning Pt-CeO_2 interactions by high-temperature vapor-phase synthesis for improved reducibility of lattice oxygen. Nat Commun **10**, 1358 (2019)
51. L.-H. Xiao, K.-P. Sun et al., Low-temperature catalytic combustion of methane over Pd/CeO_2 prepared by deposition–precipitation method. Catal. Commun. **6**, 796 (2005)
52. G. Pecchi, P. Reyes et al., Methane combustion on Pd/SiO_2 sol gel catalysts. J. Catal. **179**, 309 (1998)
53. C.G. Silva, F.B. Passos et al., Effect of carburization conditions on the activity of molybdenum carbide-supported catalysts promoted by nickel for the dry reforming of methane. Energy Fuels **35**, 17833 (2021)
54. G.B. Park, T.N. Kitsopoulos et al., The kinetics of elementary thermal reactions in heterogeneous catalysis. Nat. Rev. Chem. **3**, 723 (2019)
55. K. Narui, K. Furuta et al., Catalytic activity of PdO/ZrO_2 catalyst for methane combustion. Catal. Today **45**, 173 (1998)
56. A.E. Shilov, G.B. Shul'pin, Activation and catalytic reactions of saturated hydrocarbons in the presence of metal complexes (Springer Science & Business Media, 2001)
57. N.M. Rubtsov, A.N. Vinogradov, A.P. Kalinin et al., The features of combustion of hydrogen and methane in oxygen and air in the presence of difluorodichloromethane additives. SN Appl. Sci. **1**, 1307 (2019)
58. V.S. Arutyunov, L.N. Strekova, The potential of hydrogen energy and possible consequences of its implementation. Oil & Gas Chemistry **1–2**, 8 (2021)
59. N.M. Rubtsov, The modes of gaseous combustion (Springer International Publishing Switzerland, 2016)
60. N.N. Semenov, *O nekotorykh problemakh khimicheskoi kinetiki I reaktsionnoi sposobnosti (On Some Problems of Chemical Kinetics and Reactivity)*, 2nd edn. (AN SSSR, Moscow, 1958)
61. C.N. Hinshelwood, H.W. Thompson, The kinetics of the combination of hydrogen and oxygen. Proc. Roy. Soc. London A **118**, 170 (1928)
62. V.V. Azatyan, A.G. Merzhanov, Branching chain nature of hydrogen combustion at atmospheric pressure. Rus. J. Phys. Chem. B **27**(11), 93 (2008)
63. N.M. Rubtsov, B.S. Seplyarskii, V.I. Chernysh, G.I. Tsvetkov, Investigation into self-ignition in chain oxidation of hydrogen, natural gas and isobutene by means of high-speed color cinematography. Mendeleev Commun. **19**, 366 (2009)
64. A.A. Borisov, V.G. Knorre, E.L. Kudrjashova, K.Y. Troshin, On temperature measurement in an induction period of the ignition of homogeneous gas mixtures in rapid mixture injection static setup. Russ. J. Phys. Chem. B **17**, 80 (1998)
65. Y.B. Zel'dovich, G.I. Barenblatt, V.B. Librovich, G.M. Machviladze, The mathematical theory of combustion and explosions (2011). https://doi.org/10.1007/978-1-4613-2349-5, Corpus ID 91204935
66. D.A. Frank-Kamenetsky, Diffusion and heat transfer in chemical kinetics (Plenum Press, 1969)
67. A.G. Merzhanov, B.I. Khaykin, Teoria Voln Gorenia v Gomogennych Sredach (Theory of Combustion Waves in Homogeneous Media), (ISMAN RAS, Chernogolovka, 1992)
68. N.M. Rubtsov, B.S. Seplyarsky, K.J. Troshin, G.I. Tsvetkov, V.I. Chernysh, High-speed colour cinematography of the spontaneous ignition of propane–air and n-pentane–air mixtures. Mendeleev Commun. **21**, 31 (2011)
69. V.V. Azatyan, Y.I. Pyatnitskii, N.A. Boldyreva, Detection of chemoluminescence during oxidation of hydrogen-containing compounds on the surface of platinum metals. Rus. J. Phys. Chem. A **67**, 235 (1988)
70. V.V. Azatyan, Heterophase development of chains in processes of combustion and pyrolysis. Rus. J. Phys. Chem. A **72**, 199 (1998)
71. J. Warnatz, U. Maas, R.W. Dibble, *Combustion: Physical and Chemical Fundamentals, Modeling and Simulation, Experiments, Pollutant Formation*, 3rd edn. (Springer, Berlin, 2001)
72. V.A. Poltorak, V.V. Voevodsky, Experimental investigation of the reaction of hydrogen oxidation and the third ignition limit. Russ. J. Phys. Chem. **24**, 299 (1950)

73. V.V. Azatyan, Chain nature of the third ignition limit of hydrogen-oxygen mixtures at atmospheric pressure. Russ. J. Phys. Chem. B **8**, 29 (2006)
74. N.M. Rubtsov, On the chain nature of the third ignition limit of $2H_2 + O_2$ mixture. Kinet. Catal. (Engl. Transl.) **51**, 206 (2010)
75. A. Macek, Effect of additives on formation of spherical detonation waves in hydrogen-oxygen-mixtures. AIAA J. **1**, 1915 (1963)
76. J.W. McBain, I. Clarence, Glassbrook, electrification and luminescence phenomena accompanying desorption of gases from metals. J. Am. Chem. Soc. **65**, 1908 (1943)
77. N.M. Rubtsov, A.N. Vinogradov, A.P. Kalinin, A.I. Rodionov, I.D. Rodionov, K.Y. Troshin, G.I. Tsvetkov, V.I. Chernysh, Study of combustion of hydrogen-air and hydrogen–methane–air mixtures over the palladium metal surface using a hyperspectral sensor and high-speed color filming. Russ. J. Phys. Chem. B **13**, 305 (2019)
78. C. Trevino, A. Linan, V. Kurdyumov, Catalytic ignition of hydrogen-air mixtures by a thin catalytic wire. Proc. Comb. Inst. **28**, 1359 (2000)
79. O. Deutschmann, Modeling of the interactions between catalytic surfaces and gas-phase. Catal Lett. **145**, 272 (2015)
80. N. Yedala, A.K. Raghu, N.S. Kaisare, A 3D CFD study of homogeneous-catalytic combustion of hydrogen in a spiral microreactor. Comb. Flame **206**, 441 (2019)

Chapter 2
The Features of Hydrogen and Deuterium Ignition Over Platinum, Palladium, Ruthenium and Rhodium

Abstract This chapter is focused on the establishment of the features of hydrogen and deuterium ignition over platinum, palladium, ruthenium and rhodium. The cellular combustion regime of the mixture in the presence of Pt wire over the interval 270–350 °C was observed for the first time. It was shown that the regime is caused by the catalytic action of Pt containing particles formed by decomposition of volatile platinum oxide in gas phase. We showed that the activity of Pd foil reveals itself in both the occurrence of local ignition centers on the foil and the dark catalytic reaction of consumption of the flammable mixture. A study of the chemical properties of the two lighter hydrogen isotopes (protium and deuterium) dissolved in rhodium and palladium, namely the study of the influence of hydrides and deuterides of noble metals on hydrogen and deuterium combustion, was performed. It was revealed that Rh, Ru and Pd surfaces treated with $2H_2 + O_2$ ignitions show the defects in the form of openings, which are located on etching patterns; the etching substances are active intermediates of H_2 oxidation. It was found that before ignition catalytic wire is not heated up uniformly; initial centers of the ignition occur. It was shown that Rh is the most effective catalyst of $2H_2 + O_2$ ignition. It was shown that Rh is the most effective catalyst of $2D_2 + O_2$ ignition, in this case the lowest ignition temperature over Rh coated Pd wire (Rh/Pd) was 100° lower than for $2H_2 + O_2$ ignition, thus, D_2 is more flammable than H_2 over Rh and Pd. The obtained results indicate the existence of a "kinetic inverse isotope effect", which affects the reactivity of MeH and MeD, where Me = Rh, Pd.

Keywords Ignition · Hydrogen · Deutherium · Air · Oxidation · Hydrides · Rhodium · Ruthenium · Palladium · Platinum · Catalytic limits · Dark reaction mode · Cellular · Reactive compressible Navier Stokes equations · Speed filming · Hyperspectrometer

This chapter presents to the reader mainly a description of the phenomenology of hydrogen oxidation with oxygen or air on noble metals.

In this regard, an important remark must be made here. Since the quantitative features of the ignition processes of the catalytic surface are investigated below, it becomes important to control the state of the surface. However, it is not possible to provide a micro-level control for a macro sample. In the present study, the same

N. M. Rubtsov et al., *Catalytic Ignition of Hydrogen and Hydrogen-Hydrocarbon Blends Over Noble Metals*, Heat and Mass Transfer,
https://doi.org/10.1007/978-3-031-28416-8_2

samples of wires and foils were made from the same Pt (and Pd) ingot, and Rh and Ru coatings were applied from the same samples of liquid reagents from the same jeweler. Because the heat losses at the ends of the sample where the contacts are attached play a prominent role, the samples were used of sufficient length and thickness so that the heat losses did not affect the results of the experiments. Thus, the length and diameter of the wires used below are those that increasing their length and decreasing the diameter did not affect the values of the measured limits of catalytic ignition.

In addition, in the course of the presentation, much attention will be paid to the treatment procedures of catalytic surfaces, which allowed the authors to achieve reproducibility of the results.

In this Chapter, the detection of instabilities of the spatial development of 40% H_2–air ignition as well as the establishment of the temperature dependence of delay times of ignition in the heated reactor at 1 atm by means of a quick gas transfer in the presence of platinum foil or a Pt wire was carried out. The cellular combustion regime of the mixture in the presence of Pt wire over the interval 270–350 °C was observed for the first time. It was shown that the regime is caused by the catalytic action of Pt containing particles formed by decomposition of volatile platinum oxide in the gas phase. Experimental studies of low-pressure hydrogen combustion over Pd and Pt foils at total pressures from 10 to 180 Torr and initial temperatures of 20–288 °C were performed. We showed that the catalytic activity of Pd surface is higher than that over Pt foil. The activity of Pd foil reveals itself in both the occurrence of local ignition centers on the foil and the dark catalytic reaction of consumption of the flammable mixture. The experimental studies of low-pressure hydrogen and deuterium combustion over Rh, Ru, Pd and Pt wires at total pressures from 10 to 180 Torr and initial temperatures over the the range 200 ÷ 500 °C were carried out. The aim was to establish the dependencies of catalytic ignition limits over noble metal surfaces on temperature and to indicate the governing factors of the problem of gas ignition by a catalytic surface as well. A macrokinetic study of the chemical properties of two lighter hydrogen isotopes (protium and deuterium) dissolved in rhodium and palladium, namely the study of the influence of hydrides and deuterides of noble metals on hydrogen and deuterium combustion, was performed. It was shown that Rh, Ru and Pd surfaces treated with $2H_2 + O_2$ ignitions show the defects in the form of openings, which are located on etching patterns; the etching substances are active intermediates of H_2 oxidation. It was found that before ignition catalytic wire is not heated up uniformly; initial centers of the ignition occur. It was shown that Rh is the most effective catalyst of $2H_2 + O_2$ ignition; the lowest ignition temperature over Rh coated Pd wire (Rh/Pd) is 210 °C. The hysteresis phenomenon is observed over Ru/Pd, Pt and Pd wires; namely, the ignition limit value measured over the wire, which is not treated with ignitions, is higher than the value measured with a procedure of decreasing temperature from a state of a catalytic ignition. It was shown that Rh is the most effective catalyst of $2D_2 + O_2$ ignition. It is more accurate to speak about ignition over noble metals hydrides/deuterides; thus, the lowest ignition limit of $2D_2 + O_2$ over rhodium deuteride was 100 °C; thus, D_2 is more flammable than H_2 over Rh and Pd. The obtained results indicate the existence of the "kinetic

inverse isotope effect", which affects the reactivity of MeH and MeD, where Me = Rh, Pd.

2.1 Cellular Combustion and Delay Periods of Ignition of Near Stoichiometric H_2–air Mixtures Over Pt Surface

A cellular mode of combustion of a 40% mixture of hydrogen with air in the presence of platinum wire and foil in the range of 270–350 °C at atmospheric pressure was found. Combustion cells caused by catalytic instability have been experimentally detected for the first time by using the methods of routine and 4D optical spectroscopy, which allows registering the intensity of the optical spectrum simultaneously depending on the wavelength and also by color speed filming. It was found that the cellular mode is determined by the catalytic combustion of hydrogen on Pt containing particles formed during the decomposition of unstable platinum oxide in gas phase. It is shown that the temperature dependence of the delays of hydrogen ignition above a platinum wire and foil in both stationary and rotating gases corresponds to an activation energy of 19 ± 3 kcal/mol, which is close to the activation energy of branching of the reaction chains of hydrogen oxidation.

The development of the technology of catalytically stabilized (CS) combustion requires the development of catalysts with increased activity (the temperature of reaching 50% conversion should be less than 450 °C) and thermal stability. This requires an understanding of the nature of catalytic surface processes, knowledge of the detailed low-temperature homogeneous kinetic mechanism and its relationship with the mechanism of heterogeneous chemical transformations. The homogeneous ignition in a catalytic reactor threatens the integrity of the catalyst and the reactor (and can cause their destruction), therefore the possibility of preventing such an event is of primary interest for the design of the CS reactor. Ignition in the gas phase is determined by the interrelation of heterogeneous and homogeneous factors (catalytic fuel consumption, adsorption/desorption reactions involving radicals). Therefore, reliable control of homogeneous ignition requires knowledge of the combustion mechanism in the presence of a catalyst. Turbines, in which natural gas is the main fuel, but natural gas combustion is stimulated by hydrogen in the presence of a CS catalyst are of particular interest [1]. The addition of small amounts of H_2 to natural gas increases the efficiency of the catalyst, stabilizes combustion and prevents flame pulsation. Therefore, knowledge of the features of catalytic combustion of hydrogen is an important step for understanding the stimulating effect of hydrogen in the combustion of hydrocarbons [1–6].

In [3], relatively long ignition delays were found in a 40% H_2–air mixture over a Pt foil at a total pressure of 1 atm. It was found that the ignition of H_2–air mixtures at atmospheric pressure begins with the appearance of a primary combustion center at the most chemically active surface area, which initiates the propagation of the

flame in the reactor. In addition, as shown in [7], the introduction of a platinum wire into the reactor eliminates the phenomenon of a negative temperature coefficient (the nature of which is still unclear) during combustion of a stoichiometric mixture of n-pentane with air, while platinum wire has no effect on the delay time of the thermal ignition of the mixture at lower temperatures. It follows from the above that in the understanding of combustion processes over catalytic surfaces now there are quite a lot of "white spots".

This paragraph is devoted to the detection and determining of the reasons for the instability of the spatial propagation of a mixture of 40% H_2–air in the presence of platinum foil or wire using high-speed color filming, routine optical and 4D spectroscopy. It discusses also the establishment of the temperature dependence of the ignition delay times of this mixture in a heated reactor at 1 atm in a static quick gas transfer installation.

2.1.1 Experimental

Two installations were used for the experiments. In the first setup (setup 1), hyperspectrometers and a high-speed color camera were used to register light emission. The presence of a hyperspectrometer made it possible to carry out 4D measurements (1-time, 2-wavelength, 3-spectrum intensity at a given wavelength, 4-coordinate of the emitting fragment of the light source are recorded). This setup was used to carry out experiments to analyze the optical spectra of cellular combustion of hydrogen over a platinum surface.

A STE-1 spectrometer with crossed dispersion was used in the second setup (setup 2) for the traditional registration of radiation, followed by recording the spectrum with a SONY DCR-SR200E video camera, sensitive in the wavelength range of 420–900 nm. It was processed then using Hesperus 3.0 program. This setup was used to carry out experiments to find out the nature of the 552 nm emission band, which is often recorded in combustion processes.

Installation 1 (Figs. 2.1 and 2.2) [8–11] consisted of a heated reactor (1), an electromagnetic valve (2), a buffer storage capacity (3), a cylinder with a gas mixture (4), a hyperspectrometer (5), a digital video camera (6), a rotating mirror (7), internal asbestos insulation (8), heater (9), external asbestos insulation (10), optical window (11), pressure sensor (12), ADC converter and computer for receiving and accumulating data (13), millivoltmeter for taking readings of thermocouple (14), aluminum ring to prevent gas circulation (15), spark ignition circuit (16). The strip in red, along which the 4D spectral survey is carried out, is shown in Fig. 2.2b. The width of this strip is about 1 mm. The blue circle marks the node for tangential gas injection into the reactor. The heated reactor 25 cm long and 12 cm in diameter was made of stainless steel and equipped with a tangential gas inlet (marked with a blue circle in Fig. 2.2a, b), collapsible covers, and an optical quartz window. An aluminum ring with an outer diameter of 11.2 cm and an inner diameter of 11 cm was introduced

into the reactor perpendicular to the gas flow in experiments where it was required to avoid gas circulation due to the presence of a tangential inlet (Fig. 2.2).

The temperature measurement accuracy was 0.3 K. An electromagnetic valve was used to open and close the gas pipelines. The reactor evacuated and heated to the required temperature was filled through the valve with a gas mixture from the high-pressure buffer storage capacity to the required pressure. Due to the sharp pressure drop in the buffer storage capacity and the reactor, a gas vortex arises after the solenoid valve is triggered in the reactor, leading to a reduction in the time required to establish a uniform temperature distribution [8]. As already mentioned, to prevent

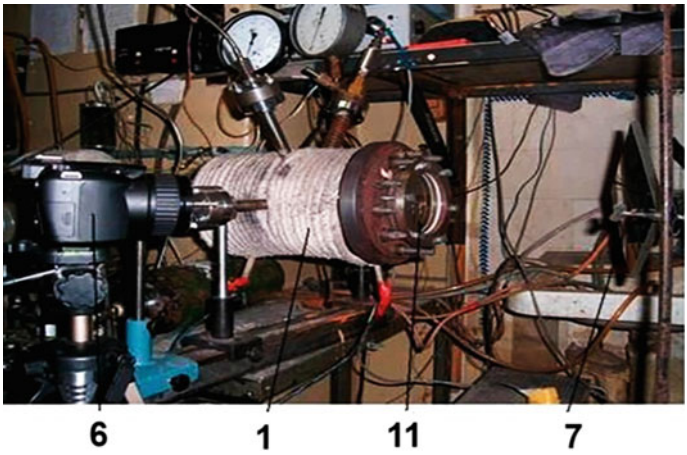

Fig. 2.1 Installation 1, photograph of the experimental installation

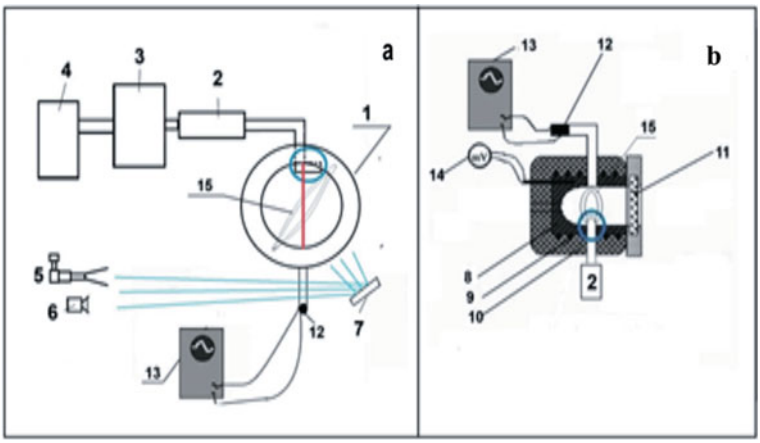

Fig. 2.2 Installation 1, **a** diagram of the experimental installation; **b** side diagram of the reactor

gas circulation, an aluminum ring was introduced into the reactor perpendicular to the gas flow.

It should be noted that direct measurements of the dynamics of temperature changes in the center of the reactor using thin thermocouples were performed under similar conditions as in [8]. In this work, it was experimentally shown that the heating time of the gas mixture did not exceed 0.3 s. The formula, which takes into account only the convective heating of the gas mixture, gives a heating time of the order of several tens of seconds [9].

In the present work, the pressure during admission and combustion was recorded using a "Karat-DI" tensoresistive sensor, the signal from which was fed through an ADC to a computer. At the moment of opening the solenoid valve, a light-emitting diode was switched on. The radiation was recorded by a movie camera. This moment was taken as the origin of the ignition delay, which made it possible independently of pressure measurements to determine its duration from a sequence of frames for each individual ignition. Flame velocities were determined from the change in the visible radius of the spherical flame, from which the apparent flame velocity was calculated. The magnitude of the degree of expansion of the combustion products was determined by the value of the maximum pressure developed during the combustion of the mixture P_b [6]:

$$P_b/\mathrm{Po} = 1 + \gamma(\varepsilon_T - 1)$$

The magnitude of a normal flame propagation velocity **Un** was determined from the relation $\mathbf{Un} = \boldsymbol{Vv}/\varepsilon_T$ [6]. Here ***Vv*** is the visible velocity of the flame.

Pt foil 12 × 6 cm and 0.3 cm thick or Pt wire 15 cm long and 0.3 cm in diameter was placed in the reactor of the installation 1. Before each experiment, the reactor was pumped down to 0.1 Torr. The pressure in the reactor was recorded with an exemplary vacuum gauge, and in the buffer storage capacity with an exemplary pressure gauge. Reagent grade gases (hydrogen, oxygen, methane) and 99.99% Pt were used.

The combustion process was recorded with a STE-1 spectrometer equipped with a SONY DCR_SR200E color video camera, or with a 4D spectrometer (hyperspectrometer) through an optical window in one of the removable covers (Fig. 2.1). Experiments on high-speed filming were carried out with gas mixtures of 40% H_2 + 60% air in the range of 270–350 °C without gas circulation. In this paragraph, both video recording of combustion was carried out with a color high-speed film camera Casio Exilim F1 Pro (frame rate—300–1200 s^{-1}) through an optical quartz window (the resulting video file was recorded in the computer memory and then processed frame-by-frame) and registration of combustion process with a hyperspectrometer (Fig. 2.2a). Then the obtained data were compared.

Various dispersing elements can be used in hyperspectrometers: a diffraction grating, a holographic grating, a prism, a combination of prisms, a combination of optical wedges and a diffraction grating, etc. A prism-based design was used in the case of VID—spectrometers (Fig. 2.3, to the left), a grating-based one—in BIK spectrometers (Fig. 2.3, to the right). The BIK hyperspectrometer contains an entrance objective lens 1, a diaphragm bundle 2, a collimator 3, consisting of

two sections 4 and 5. These sections are installed at an angle to each other, the optimal value of the rotation angle is 90°. A mirror 6 is placed between the collimator sections 4 and 5. A dispersing unit made in the form of a diffraction grating 7 is installed behind the collimator section 5. Further, along the path of the beams, the lens 8 and the photodetector array 9 are installed.

It the present paragraph, the measurements were performed using VID-IK3 hyperspectrometers [12–15] and their modified version (the photodetector array was rotated in it, and due to this, it became possible to programmatically control the angle of view and, accordingly, the frame rate). The appearance of both devices mounted on a rotary device is shown in Fig. 2.4, and the construction (the same for both devices) is presented in [13–15]. The optical layout of the hyperspectrometer is discussed in [14, 15]. The VID-IK3 hyperspectrometer has a better spectral resolution, and the modified VID-IK3 hyperspectrometer has a better spatial and temporal resolution. The use of two devices at once made it possible to reveal new features of the hydrogen combustion process over the platinum surface.

To demonstrate the capabilities of the VID-IK3 hyperspectrometer, we present the dependences of the intensity of the combustion spectra of 40% H_2–air mixture initiated by a Pt wire on the wavelength for different points (Fig. 2.5) on the position on the registration strip (red strip in Fig. 2.2a) and on time (Fig. 2.6).

As indicated above, since the time dependence for the combustion processes under study is quite smooth, and the spectral resolution of the VID-IK3 hyperspectrometer is two times better than that of the modified VID-IK3 hyperspectrometer then experiments on the study of the combustion of a mixture of 40% H_2–air, 320 °C, 1 atm initiated by Pt was measured with a VID-IK3 hyperspectrometer. To establish some spatial features, a modified VID-IK3 hyperspectrometer was used.

To diagnose dusty structures, particles emitted by a platinum wire when it was heated in atmospheric air were illuminated with a flat laser beam (“laser knife”), the shifting of which was no more than 200 μm.

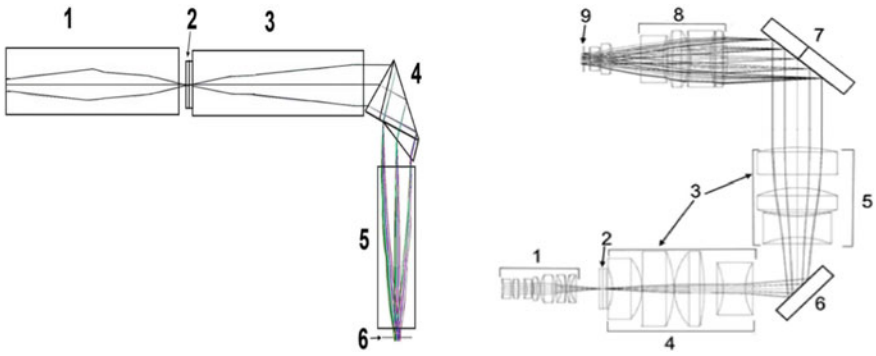

Fig. 2.3 To the left: Ray path in the VID-IK3 hyperspectral module (1) entrance lens, (2) diaphragm unit with a slit, (3) collimator, (4) dispersing element, (5) camera lens, (6) photodetector array. To the right: Optical system of the BIK1 hyperspectrometer

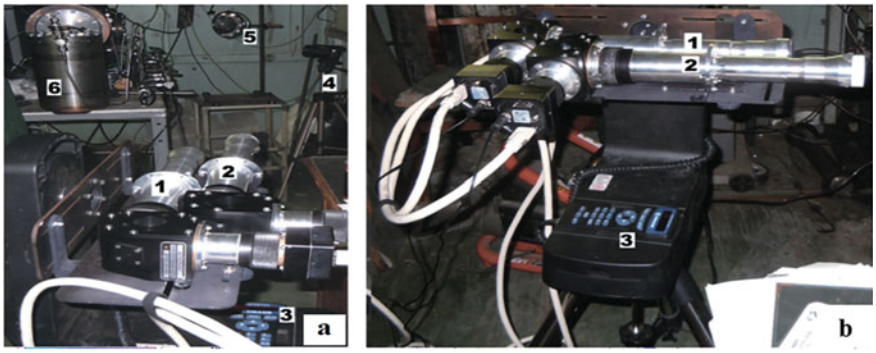

Fig. 2.4 Location of hyperspectrometers for studying flames: **a** (1) VID-IK3 hyperspectrometer, (2) VID-IK3 hyperspectrometer (modified), (3) rotary device, (4) Casio Exilim F1 Pro video camera on a tripod, (5) rotary mirror with an image of the optical window of the reactor, (6) bypass volume; **b** a block of hyperspectrometers on a rotating device

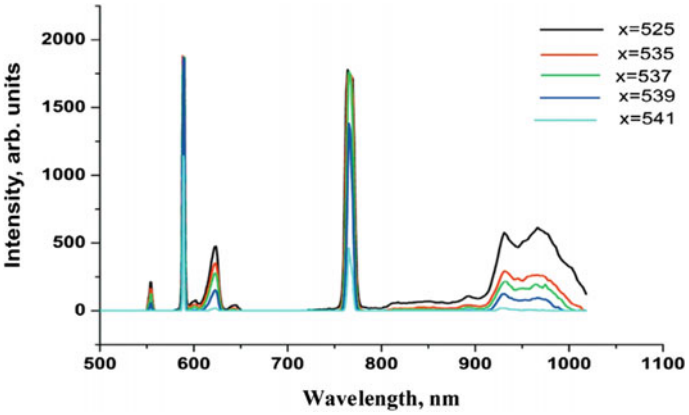

Fig. 2.5 Dependence of the emission spectra of combustion of 40% H_2–air mixture, initiated by a Pt wire, on the position on the red strip. The initial temperature is $T_0 = 320$ °C, $P_0 = 1$ atm

For visualization of solid particles, a semiconductor laser $\lambda = 532$ nm was used. The diagram and photographs of setup 2 are shown in Fig. 2.7. Here: (1) stainless steel reactor 15 cm long and 13 cm in diameter, equipped with an optical window 8, (2) rotary mirror, (3) collimator with holder, (4) spectrometer STE-1 with crossed dispersion, (5) spectrometer entrance slit, (6) SONY DCR_SR200E video camera, (7) spectrometer output window.

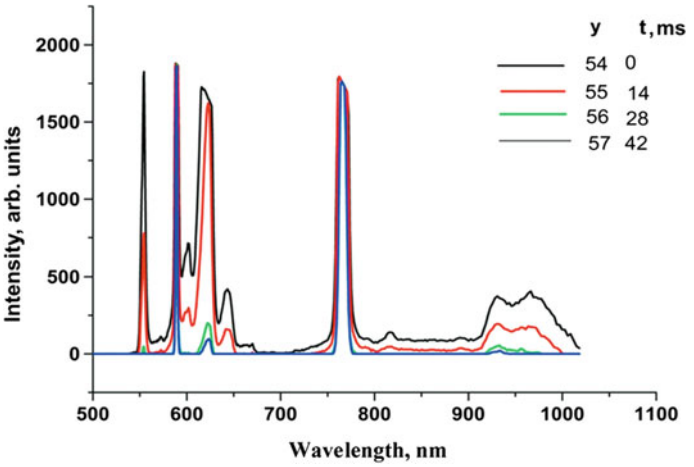

Fig. 2.6 Time dependence of the combustion spectra of 40% H_2–air mixture initiated by a Pt wire. $T_0 = 320$ °C, $P_0 = 1$ atm

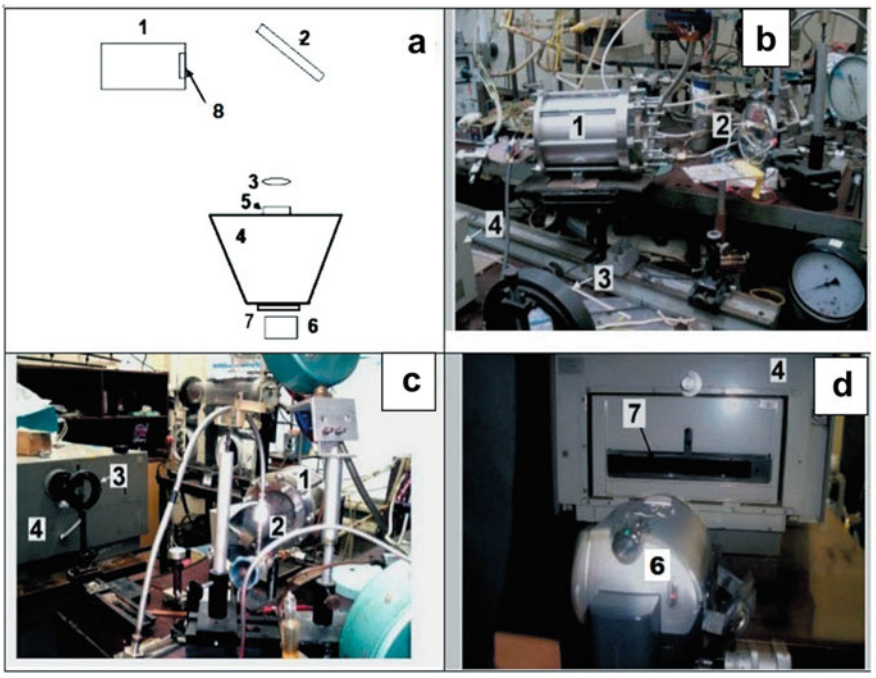

Fig. 2.7 Installation for registration of radiation spectra by optical spectroscopy. **a** block diagram of the installation; **b**, **c**, **d** photographs of the installation units

2.1.2 Results and Discussion

Installation 1 was used to study the spatial development of the ignition of mixtures of 40% H_2–air at a pressure of 1 atm. It should be noted that the ignition temperature of H_2–air mixtures at 1 atm in a reactor containing Pt foil [3] is ~ 170 °C lower than in a stainless steel reactor. It should be noted that the transition through the critical ignition condition is accompanied by a significant increase in the ignition delay period τ only over the catalytic Pt surface. When ignited over stainless steel, τ does not exceed 0.5 s and changes abruptly in a very narrow temperature range of ~ 1°. The delay periods in a 40% hydrogen–air mixture can reach tens of seconds both at temperatures less than 260 °C and above the "fresh" surface of the platinum foil. It is believed that the state of the "fresh" surface is realized in each initial (first) experiment, in which Pt is not pretreated with active centers of ignition.

A sequence of video images of the development of the ignition of the mixture of 40% hydrogen with air for various initiation conditions is shown in Fig. 2.8. As seen from Fig. 2.8a, a smooth homogeneous flame is observed during ignition initiated by a spark discharge at room temperature of the walls of the reactor, in the case of a stainless steel surface. As shown in Fig. 2.8b, if the Pt foil is placed in a stainless steel reactor, the flame front is also almost uniform. However, in the presence of a Pt wire (Fig. 2.8c), a cellular flame structure is observed. Before and after ignition, the Pt wire is heated due to catalytic reactions on the Pt surface. The addition of 15% CO_2 to the combustible mixture ensures complete suppression of the cellular combustion mode (Fig. 2.8d), while the 15% addition of helium practically does not affect the cellular combustion mode (Fig. 2.8e).

The results of the qualitative assessment of the flame velocities from the change in the visible radius of a spherical flame according to the equation given in the Experimental are shown in Fig. 2.9. It is seen in Fig. 2.9 that with spark initiation in a mixture diluted with carbon dioxide, a constant flame velocity is achieved after a certain time interval corresponding to the formation of a stable flame front (FF) [16, 17]. However, in the presence of a platinum catalyst, as can be seen in Fig. 2.9, a constant flame velocity (within the experimental error) is achieved almost immediately. In other words, the catalytic action of platinum leads to a sharp reduction in the time of formation of a stable FF. In addition, it can be seen from Fig. 2.9 that the normal flame velocity in the presence of a catalytic surface is noticeably higher ($\approx$ 2.6 m/s) than under conditions excluding the action of the catalyst (upon initiation by a spark discharge $\approx$ 1.9 m/s, in the presence of 15% CO_2 $\approx$ 1.8 m/s). The obtained values of normal velocities (without catalyst) agree within the error with the literature data [17]. On the other hand, it is known that the velocity of a laminar flame does not depend on the energy of the initiation source if the initiation energy is low (the so-called lean initiation [6]). Thus, the obtained experimental result requires an explanation.

Let us turn to the facts known from the literature. In [2] some experimental facts related to the reaction between platinum (the effective catalyst for the combustion of hydrogen and hydrocarbons) and oxygen at temperatures up to the melting point of

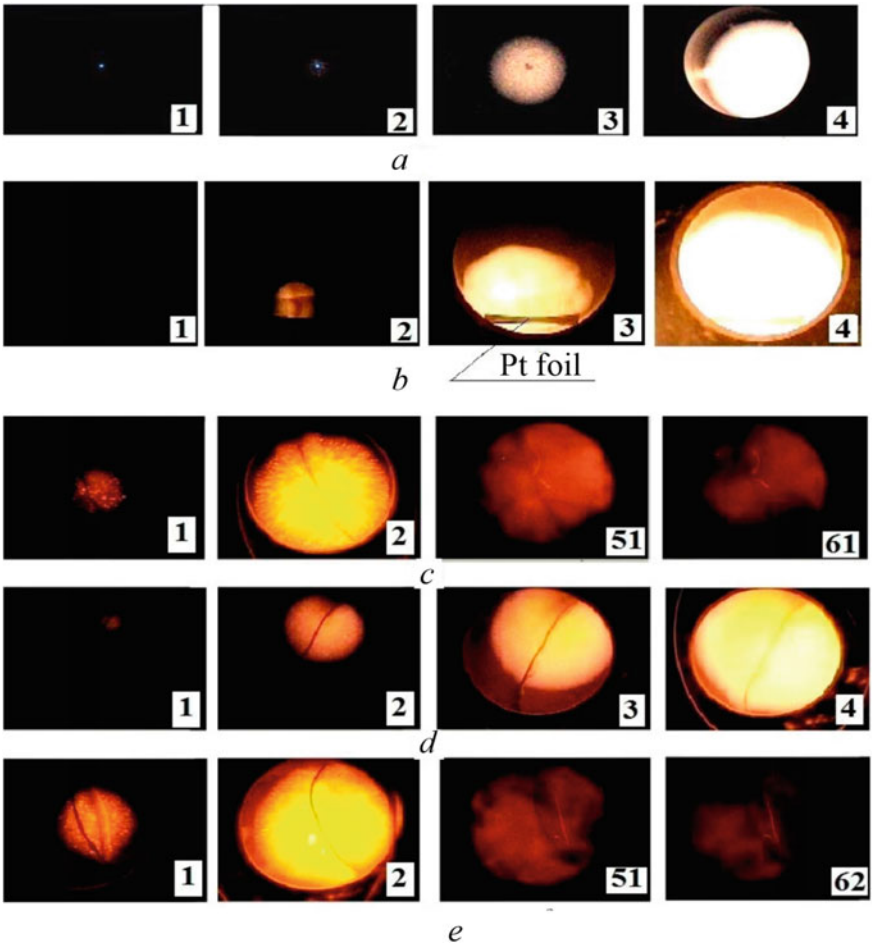

Fig. 2.8 Sequences of video images of the spatial development of the combustion process. The numbers on the frame correspond to the sequential number of the video image: **a** ignition of the mixture of 40% H_2 + 60% air at wall temperature of 200 °C, initiated by a spark; 600 frames/s; P = 1 atm; there is no platinum in the reactor; **b** ignition of the mixture of 40% H_2 + 60% air at wall temperature of 247 °C; Pt foil is placed in the reactor. **c** ignition of the mixture of 40% H_2 + 60% air at wall temperature of 316 °C; The Pt wire is placed in the reactor. It can be clearly seen in frames 1, 61. It is also seen from these frames that the Pt wire is heated before and after the explosion due to catalytic reactions on the Pt surface; **d** ignition of the mixture of 85% (40% H_2 + 60% air) + 15% CO_2 at wall temperature of 320 °C in the presence of a Pt wire; **e** ignition of the mixture of 85% (40% H_2 + 60% air) + 15% He at wall temperature of 309 °C in the presence of Pt wire

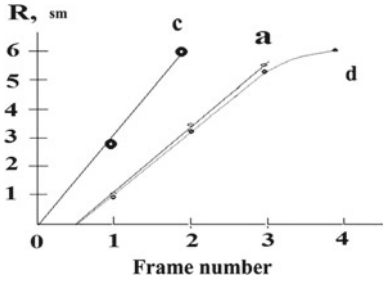

Fig. 2.9 The dynamics of an increase in the radius R of the front of the laminar flame, calculated from an increase in the visible radius of the flame front from the data in Fig. 2.8: experiments **a**; **b**; **c**; $P_0 = 1$ atm, 600 frames/s

platinum are considered. In [2], it was found that a thin film of thermally unstable solid platinum oxide (more likely, platinum dioxide PtO_2, or PtO [3]) is formed in air or oxygen at room temperature [4] on the surfaces of a Pt wire or thin foil and it thickens with an increase in temperature to about 500 °C.

However, when this temperature is exceeded, the oxide disproportionates with the formation of metal [5]. Therefore, the weight loss of platinum in an oxidizing environment at elevated temperatures (470–540 °C) is explained by the formation of volatile platinum oxides, followed by the deposition of platinum on colder surfaces as a result of the decomposition of oxides. This is shown in the illustration (Fig. 1) given in [2]. It shows a platinum-containing layer on a lining brick of a CS reactor, recovered after long-term operation. It can be seen from the illustration that a black oxide film is deposited at cooler edges, and crystalline platinum is deposited at a hotter surface.

This means that molecules or clusters of both platinum oxides and platinum metal exist in the gas phase at temperatures above 500 °C. Therefore, Pt-containing particles diffusing into a medium containing a combustible gas (for example, into a hydrogen–air mixture), for example, during the heating of a Pt wire, are catalytic centers, on which hydrogen can be ignited directly during the propagation of the flame front.

Consequently, one can expect the appearance of an unstable flame front (FF) caused by catalytic centers distributed in the gas phase during the combustion of hydrogen initiated by a Pt wire. This instability should be observed under the conditions, under which there is no thermal diffusion instability (the composition of the combustible mixture is close to stoichiometric one [6]). Let us recall that the thermal diffusion instability is observed in flames, in which the rates of heat transfer and diffusion are different, i.e. $Le \neq 1$ (Lewis number $Le = D/\alpha$, where D is the diffusivity of the component that determines the combustion process, α is the thermal diffusivity). Such instability leads, for example, to the cellular nature of the propagation of flames in lean hydrogen–air and hydrogen–oxygen mixtures. In this work, a cellular regime is discovered and investigated, which is not associated with thermal diffusion instability.

The experimental data presented are in agreement with the experimental fact [2, 4, 5], indicating that the oxide layer on a bulk Pt sample with a lower surface-to-volume ratio is thinner than on a Pt wire, for which the surface-to-volume ratio, obviously,

is larger. Therefore, the number of Pt particles in the volume during heating of a massive sample is not high enough to affect the structure of the flame front.

We investigated the behavior of a heated platinum wire in an oxidizing atmosphere (air) under various conditions (Fig. 2.10) for a clearer illustration of the above in the next series of experiments. The results of visualizing the process of heating a Pt wire with a current of 2 A is demonstrated in Fig. 2.10a. For this purpose, the wire was illuminated with a vertical flat "laser knife" (see Experimental). It can be seen from Fig. 2.10a that ultradispersed particles evaporate from a platinum wire when heated, which are platinum oxides, according to [2–5].

It is obvious that in the experiment on the initiation of the ignition of hydrogen with Pt wire in a heated reactor during a delay period of $3 \div 70$ s under our conditions, ultradispersed platinum oxide can spread up to ignition throughout the entire volume of the reactor because the registration of the evaporation of platinum oxide from the wire is carried out at a rate of 60 frames per second.

In a "cold" reactor (Fig. 2.10b), i.e. when the ignition of a mixture 40% H_2 + 60% air is initiated by heating Pt wire at wall temperature of 200 °C, platinum oxide

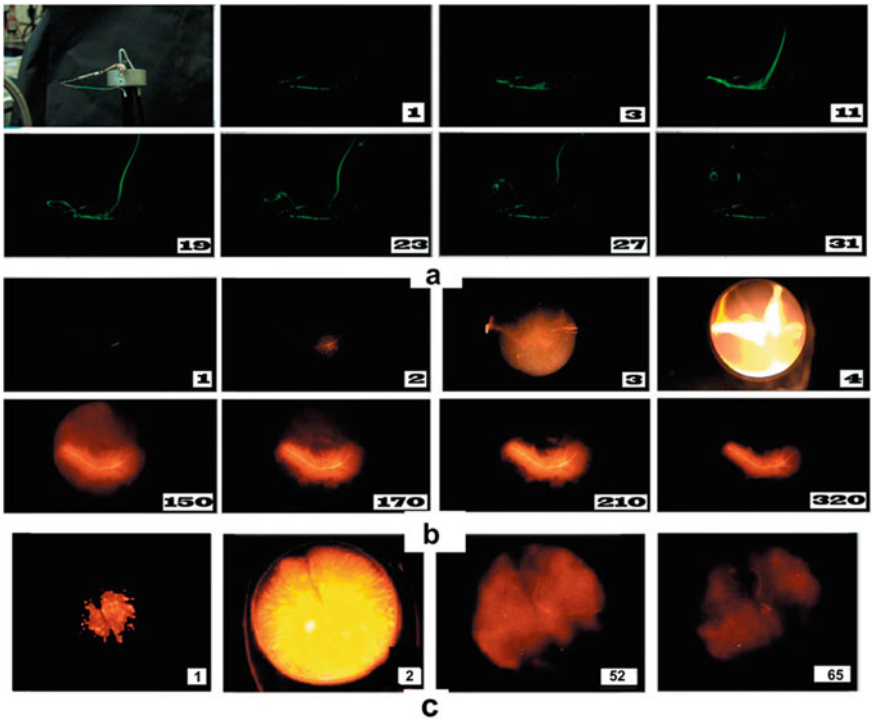

Fig. 2.10 Behavior of heated platinum wire under various conditions: **a** heating the Pt wire (current is 2 A). The wire is illuminated with a vertical flat "laser knife". 60 frames/s; **b** ignition of the mixture of 40% H_2 + 60% air initiated by heated Pt wire at wall temperature of 200 °C; **c** ignition of the mixture of 40% H_2 + 60% air at wall temperature of 316 °C in the presence of a Pt wire

does not have time to spread evenly throughout the reactor before ignition, since the delay time of thermal ignition is already hundredths of a second. In this regard, under these conditions, the cellular combustion mode is practically not manifested, to the same extent as in a heated reactor (compare Fig. 2.10b and c).

The issue of the mechanism of the participation of ultradispersed Pt particles in combustion, as well as the determination of the features of hydrogen combustion in the presence of platinum, was solved experimentally using 4D spectroscopy. Thanks to this method, it is possible to record optical spectra of radiation from a given point in space at facility (1), as well as routine optical spectroscopy at facility (2). Initial RGB of hyperspectral images (which further are analyzed with a special program package) of investigated combustible mixtures: 40% hydrogen + air upon initiation by a spark discharge [15], 40% hydrogen + air upon initiation with a platinum wire are shown in Fig. 2.11a, b.

In Fig. 2.11a, b, the window axis (x-axis) corresponds to the red strip in Fig. 2.2a, and the y-axis corresponds to the dependence of the combustion process on time. Each strip along the y-axis in Fig. 2.11 corresponds to one frame of information accumulation on the photodetector matrix of the hyperspectrometer (300 frames/s).

A comparison of the optical emission spectra of a hydrogen flame initiated by a platinum wire and recorded along a vertical strip along the diameter of the optical window (red strip, Fig. 2.2a), and a spark discharge is demonstrated in Fig. 2.12a. Let us preliminarily point out that the hydrogen flame at low pressures is practically invisible. The reason to this is that its radiation is mainly due to the radiation of hydroxyl radicals OH $A^2\Sigma - X^2\Pi$ in the ultraviolet region at 306 nm [18]. Attention is drawn to the features of the flame spectrum (Fig. 2.12a, b) in the visible region, namely the system of emission bands in the range of 570–650 nm, which makes the hydrogen flame visible at elevated pressures, along with the lines of sodium atoms (581 nm) and potassium (755 nm), inherent in all hot flames [18] and in this case emitted from the region filled with combustion products. In [15], we showed that the bands in the region of 600 nm in a hydrogen flame, according to the data of [19], relate to the radiation of water vapor. In Table 4 from [19], cited in [15], the assignment of the bands in Fig. 2.12a (black curve, see also Fig. 2.4d) to water vapor,

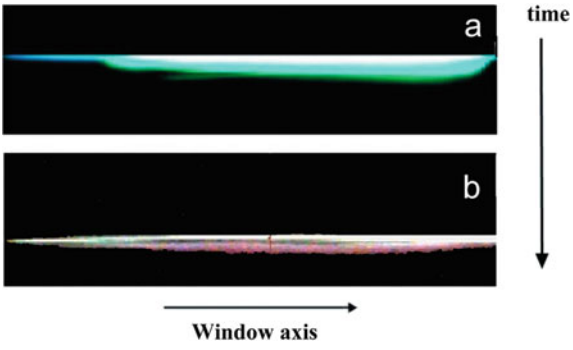

Fig. 2.11 RGB hyperspectral images: **a** combustion of 40% hydrogen in air, initiated by a platinum wire, **b** combustion of 40% hydrogen in air, initiated by a spark discharge

which is a product of the hydrogen oxidation reaction is given. Thus, the observed spectral lines belong only to the reaction products.

It can be seen in Fig. 2.12b and c, which show the combustion spectra of the mixture of 40% H_2–air, (T_0 = 320 °C, P_0 = 1 atm) in the range of 550–650 nm, recorded after initiation with platinum wire, deployed along the vertical x axis of the reactor, and the dependence of the maximum values of the spectrum intensity for a wavelength of 622 nm from the x coordinate along the vertical axis of the reactor, that at the selected time two maxima are recorded at x = 488 and x = 503

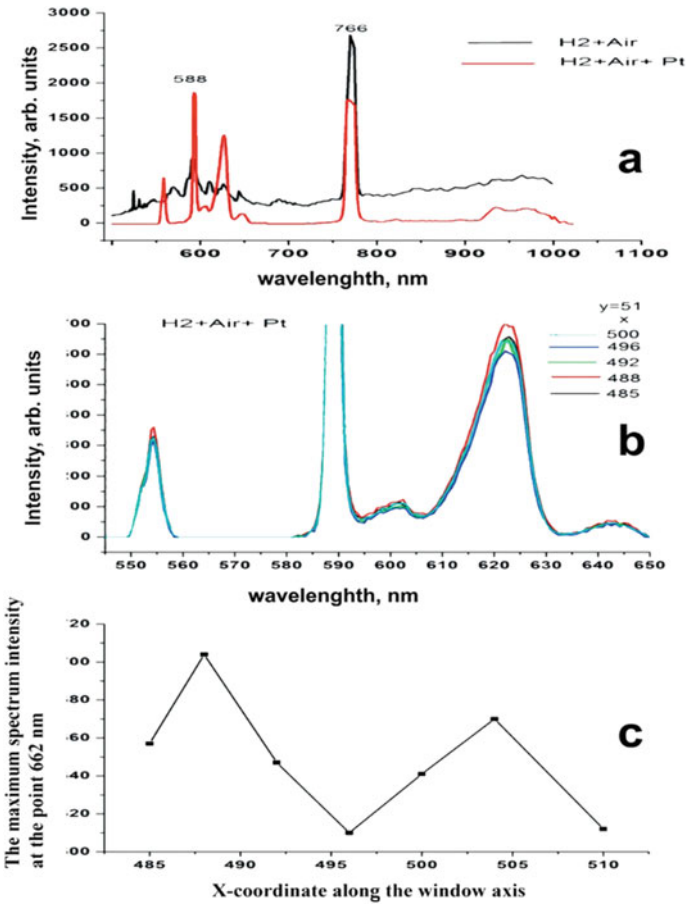

Fig. 2.12 **a** comparison of the spectra of hydrogen combustion initiated by a spark discharge. 40% H_2–air, 20 °C, 1 atm (black curve) and initiated by a platinum wire. 40% H_2–air, 320 °C, 1 atm (red curve) **b** combustion spectra of a mixture of 40% H_2–air, 320 °C, 1 atm in the range 550–650 nm, recorded after initiation with a platinum wire, deployed at the moment corresponding to frame 2 in Fig. 2.5c, along the vertical x-axis of the reactor (red strip in Fig. 2.2a). **c** dependence of the maximum value of the spectrum intensity for a wavelength of 622 nm on the x coordinate along the vertical axis of the reactor

along the x axis, located between the spatial coordinates with relative values of 485 and 510. This means that combustion in space is inhomogeneous, otherwise the intensities of the spectral lines would change smoothly in the direction of decreasing or increasing coordinates. In other words, 4D spectroscopy makes it possible to register combustion cells, as was done above by high-speed filming (Fig. 2.8c, f; Fig. 2.10c). The experimenter may be questioned whether the observed maxima in Fig. 2.12c are concerned with various noises, namely read noise, dark noise, quantization error or shot effect.

Among these problems, the most important is the shot effect, since in our case it exceeds the other noises in intensity by orders of magnitude. However, special experiments have shown that the shot effect does not affect the features of the behavior of the spectra shown in Fig. 2.12c. Primary data are shown in Fig. 2.13.

The foregoing is confirmed by the fact that the luminescence inhomogeneities caused by the catalytic instability of the phase transition are recorded not only by the high-speed filming method (Fig. 2.8c), but also by a hyperspectrometer (the same experiment, Fig. 2.14) directly on the hypercube. Indeed, it can be seen from Fig. 2.14 that when measured with a modified VID-IK3 hyperspectrometer on a combustion hypercube of a 40% H_2–air mixture ($T_0 = 320$ °C, $P_0 = 1$ atm), bright spots (hot spots) are recorded corresponding to the combustion cells observed in Figs. 2.8c, d and Fig. 2.10c.

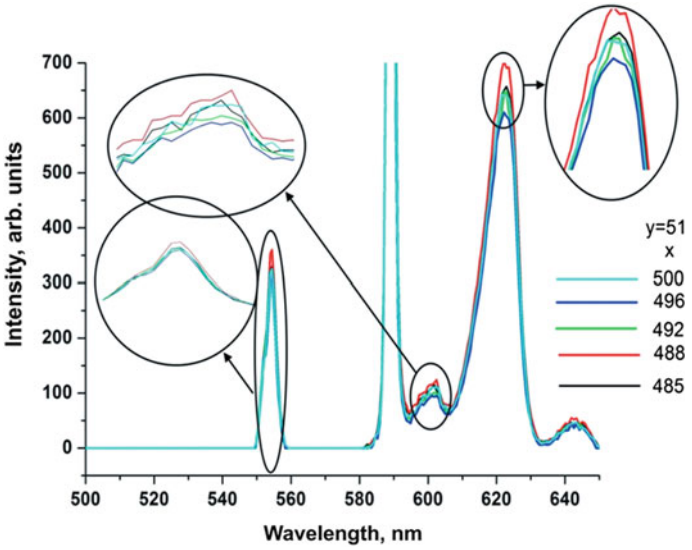

Fig. 2.13 Dependences of the light emission intensity of the combustion of a mixture of 40% H_2–60% air in the range 550–650 nm, recorded after initiation with a platinum wire, $T_0 = 320$ °C, $P_0 = 1$ atm

Fig. 2.14 RGB hyperspectral image of the combustion of a mixture of 40% H_2–air, initiated by a platinum wire, obtained using a modified VID-IK3 hyperspectrometer, $T_0 = 320$ °C, $P_0 = 1$ atm, spectral interval 550–650 nm

The main feature of these "hot spots" is that the emission spectra of combustion along and across these points, depending on both the y coordinate and x (time), behave not symbiotically and have a maximum inside this point.

The spectra along one of these points (point 1 in Fig. 2.14) for different values of x (along the red strip in Fig. 2.2a) are shown in Fig. 2.15. The dependence of the position of the spectrum maximum for a wavelength of 972 nm on the x coordinate for point 1 (Fig. 2.14) is demonstrated in Fig. 2.16.

The spectra across point 1 for different values of y (time) are indicated in Fig. 2.17.

The dependence of the intensity maximum for the 972 nm line (Fig. 2.18) of point 1 (Fig. 2.14) on y (time) is shown in Fig. 2.18.

As is seen in Figs. 2.16 and 2.18, the spectral intensities for these points do not behave symbatically. It is interesting to note that these points are displaced along the x-axis depending on the recording time, that is, as cells that change their position in

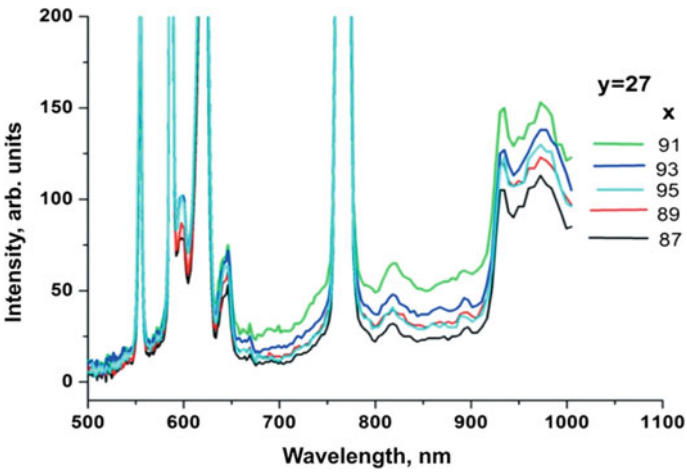

Fig. 2.15 Dependence of the intensity of combustion emission spectra for different values of x (along the red strip in Fig. 2.2a) for point 1 (Fig. 2.14)

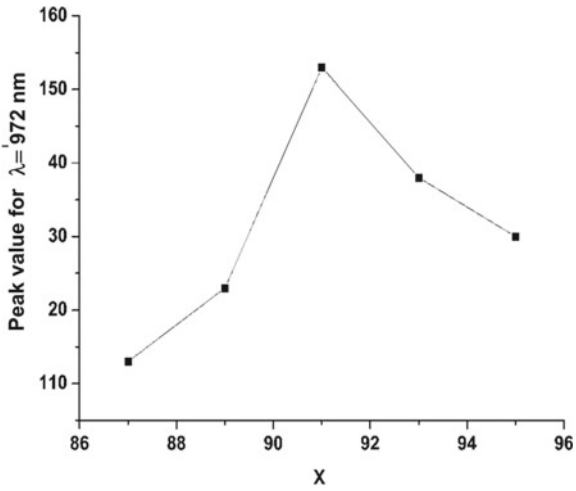

Fig. 2.16 Dependence of the position of the spectrum maximum for a wavelength of 972 nm on the x coordinate for point 1 (Fig. 2.14)

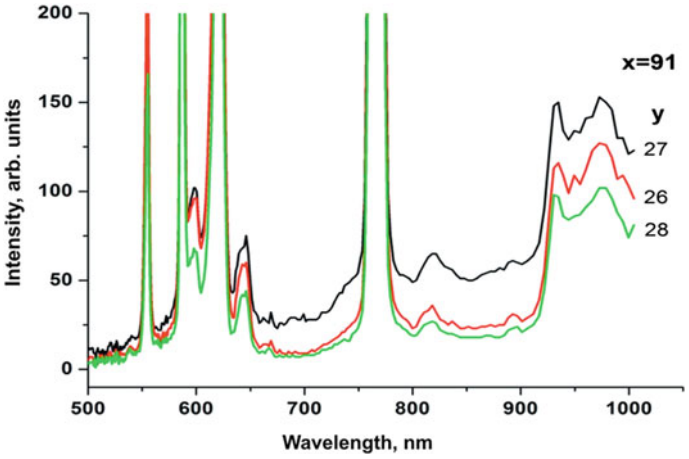

Fig. 2.17 Dependence of the emission spectra of combustion on y (time) for point 1 (Fig. 2.14)

the video frames in Figs. 2.8c, d and 2.10c. An important conclusion also follows from the data obtained that the emission spectrum of the cells is close to the emission spectrum of a gray body (intensity maxima in space are observed simultaneously in different parts of the investigated spectral interval), that is, the emission of points (cells) really corresponds to the emission of incandescent catalyst particles.

Let us focus on the features of the emission spectrum of hydrogen combustion in a heated reactor in the presence of a platinum wire. It can be seen from Fig. 2.12a (compare also with Figs. 2.4d and 2.12b) that in this case an additional band at 552 nm appears in the emission spectrum of the hydrogen flame. According to the literature, the nature of the appearance of radiation at this wavelength has not yet been

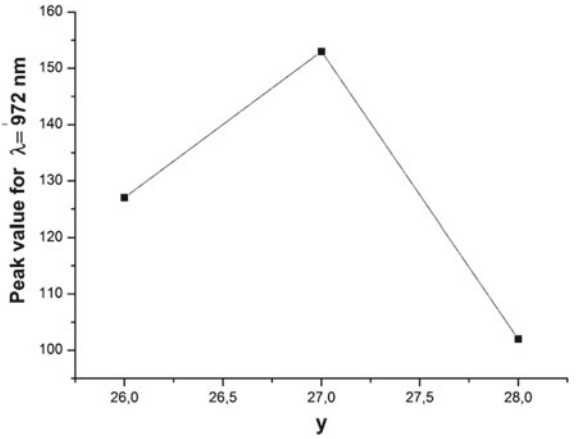

Fig. 2.18 Dependence of the maximum intensity for the line 972 nm (Fig. 2.16) point 1 (Fig. 2.14) on y (time)

established. The indicated band in the emission spectrum (Fig. 2.13a) is observed during intense combustion of rich mixtures of industrial hydrocarbons, i.e. in the presence of soot particles [20], as well as in the combustion of methane in the presence of heated coal dust. Obviously, in both of these cases, neither hydrogen nor platinum is involved in the combustion process. Therefore, for this study, to find out whether the radiation source at a wavelength of 552 nm is associated with the evaporation of platinum oxide from a heated platinum surface was of fundamental importance.

For this purpose, a cylindrical furnace 6 cm in diameter and 3 cm long was placed in reactor 1. A compressed coal tablet (anthracite, trade mark GOST 25,543- 88b, particles with an average diameter of 55 μm) was placed in its internal hole, heated for 3 min to 400 °C and a stoichiometric mixture of natural gas with oxygen up to 150 mm Hg and admitted into installation 2 (Fig. 2.2). Ignition was initiated by a spark discharge. The emission spectrum recorded using optical spectroscopy is shown in Fig. 2.19a. As seen from Fig. 2.19a, the 552 nm band is clearly observed in this spectrum. However, as indicated above, to observe this band, hydrocarbon is needed as a combustible, as well as heated coal powder. In the next experiment, the conditions remained the same, only methane was replaced by hydrogen. At the same time, the 552 nm band remained in the spectrum. In the absence of carbon dust in a clean (washed with ethanol) reactor, this band was no longer observed (cf. Figs. 2.4d and 2.12b) both upon initiation of ignition by a spark discharge or by a heated platinum wire. Thus, the method of initiating the ignition is not associated with the occurrence of this emission band.

This led us to the conclusion that experiments at room temperature and in a heated reactor differ methodically by the presence of an aluminum ring to prevent gas circulation in the heated reactor (see Sect. 2.1.1).

Therefore, a thin aluminum foil was introduced into the “cold” reactor, which was used to cover the inner walls of the reactor. The initiation was carried out with a heated platinum wire. The result of the experiment is shown in Fig. 2.19b, and the

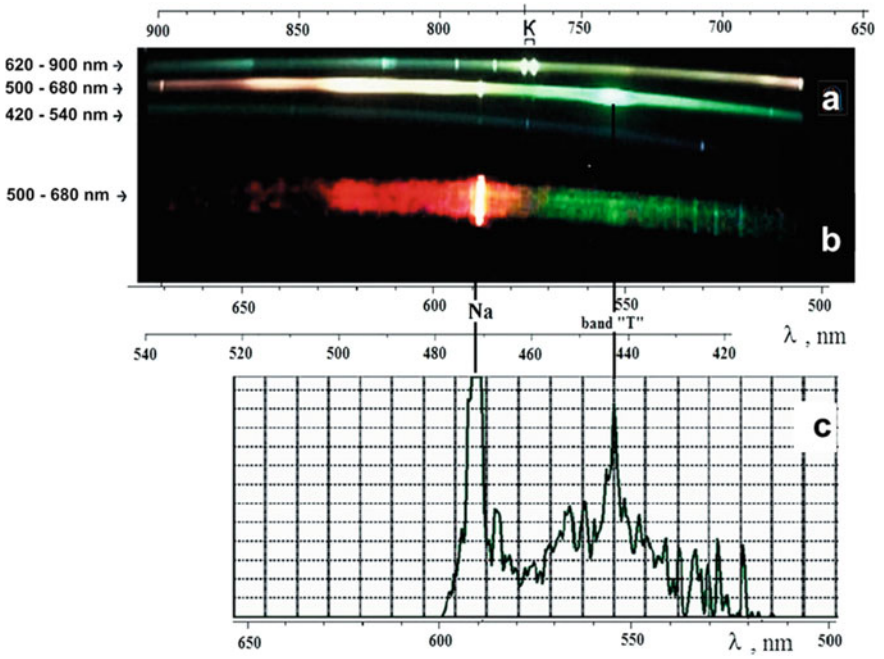

Fig. 2.19 **a** optical spectrum of radiation during combustion of a stoichiometric mixture of methane in oxygen in the presence of carbon dust heated to 400 °C. P = 150 mm Hg; **b** optical spectrum of hydrogen combustion in air upon initiation by a heated platinum wire in the presence of a thin (0.1 mm) aluminum foil covering the reactor walls. P = 1 atm, initial temperature 20 °C. **c** spectrum b after processing using the Hesperus 3.0 software package

result of its digital processing using the Hesperus 3.0 program is shown in Fig. 2.19c. It can be seen from Fig. 2.19b that when a mixture of 40% H_2–air is ignited, it is possible to observe a band at 552 nm. It should be noted that the appearance of copper lines (515, 521, 529, 532 nm [21]) is because the platinum wire was attached to copper electrodes, which were heated at the attachment points.

Thus, the occurrence of emission at a wavelength of 552 nm is most likely due to the radiation of metal impurities contained in aluminum. Excitation of metal atoms is carried out during the recombination of atoms and radicals arising during combustion on the hot surface of aluminum (the flame temperature of a mixture of 40% H_2–air is ~ 2200 °C [22]) with the release of a significant amount of energy.

For example, it is known that a platinum wire placed at a distance of 7 cm from the RF discharge can even melt due to the energy released during the recombination of oxygen atoms on the surface ($2O \rightarrow O_2 + 116.4$ kcal/mol) [23]. This energy corresponds to ultraviolet radiation at a wavelength of about 270 nm. The sources of radiation at a wavelength of 552 nm can be impurities of atoms of alkaline earth metals in industrial aluminum, which contains Fe, Cu, Mn, Mg, Cr, Ni [24] and trace amounts of alkali and alkaline earth metals, in particular, Ca [25]. As shown in

[26], excited CaOH and CuOH (calcium monohydroxide, copper monohydroxide) molecules can provide radiation at 552 nm. Since carbon powders contain a large amount of inorganic impurities, including metals and their salts [27], the 552 nm band during coal combustion is obviously of the same origin.

This result also means that the introduction of platinum into the hydrogen oxidation flame does not lead to changes in the visible emission spectrum of this flame as compared to initiation by an electric discharge. Thus, the processes of evaporation and decomposition of Pt oxide, which has catalytic properties, like platinum itself, determine the role of platinum. Directly related to these processes is the cellular mode discovered in this work for the Pt-initiated combustion of a mixture of 40% H_2 with air—a composition close to stoichiometric one. Thus, in accordance with the above, during the ignition delay period in the gas phase, the molecules or clusters of Pt and platinum oxide are formed at the temperature of the platinum wire in the combustible gas above 500 °C. Pt-containing ultrafine particles diffusing into the reaction volume act as catalytic centers, on which hydrogen is oxidized, which leads to strong heating of these particles. These incandescent particles are perceived as flame cells on video filming and when recording by the 4D spectroscopy method. In fact, they are such cells, in the area of which combustion occurs most intensely. We point out that the rate of diffusion of catalytic particles in the gas should determine the possibility of implementing cellular combustion. This is indeed the case. For example, the diffusion rate of catalytic particles decreases in the presence of 15% CO_2. These particles "do not keep up" behind the propagating combustion front (Fig. 2.8d), and the cellular combustion mode is not recorded. On the other hand, the addition of 15% light He (Fig. 2.8e) does not lead to the disappearance of the cellular combustion regime.

Let us turn to the analysis of the temperature dependences of the ignition delay times during the combustion of hydrogen in the presence of a platinum surface in a heated reactor. The ignition delay time τ is one of the most important macrokinetic characteristics of thermal ignition, which can be measured in relatively simple ways.

In this case, an important experimental fact is that, according to data [26, 28] in a shock tube and in a rapid compression machine, thermal ignition has a cellular nature. We have also recently shown [3, 7] that the ignition of mixtures of hydrogen and n-pentane with air in a bypass plant at a total pressure of 0.6–2 atm begins with the appearance of a primary ignition center on the most chemically active area of the surface. Thus, thermal ignition includes the stages of warm-up, local ignition and flame propagation. This means that cellular ignition is the rule, not the exception, i.e. "self-ignition" as a process that occurs simultaneously in the entire volume of the reactor, apparently, is not provided in principle.

The temperature dependence of the ignition delay times for a mixture of 40% H_2 and air in the reactor in the presence and in the absence of a gas flow (Fig. 2.19) above the catalytic surface (Pt foil or Pt wire) in Arrhenius coordinates is shown in Fig. 2.20. As is seen from Fig. 2.20, the effective activation energy E is practically the same for both the Pt foil and the Pt wire, both in the presence and in the absence of a gas flow. The experimental value of E is 19 ± 3 kcal/mol and is close to that of the hydrogen combustion branching reaction $H + O_2 \rightarrow OH + O$ (16.7 kcal/mol

[22, 29, 30]). This means that the ignition delay in the initiation of hydrogen combustion by the platinum surface is determined by the slowest stage of the kinetic mechanism, namely, the branching reaction, the slowest stage in the sequence of reactions leading to flame propagation. Indeed, the value of the delay period for the initial stage of the combustion process is $\tau \approx 1/\varphi$, where φ is the so-called branching factor, which includes the value of the rate constant of the activated branching reaction in the case of a hydrogen oxidation reaction (see Chap. 1).

As is known [22], the coordinate of the point of intersection of straight lines with the ordinate axis in Fig. 2.20 is approximately inversely proportional to the frequency of active collisions. Since the surface area of the Pt wire is less than that of the Pt foil, the frequency of collisions with the surface is lower for the Pt wire. In addition, the collision frequency for a Pt foil in a stationary gas is less than for the same foil in a circulating gas. This is illustrated in Fig. 2.20.

We briefly summarize the results obtained in this paragraph. A cellular mode of combustion of 40% hydrogen–air mixture in the presence of platinum wire and foil in the range of 270–350 °C at atmospheric pressure was discovered. Combustion cells caused by catalytic instability have been experimentally detected for the first time using the 4D optical spectroscopy method, which allows recording the intensity of the optical spectrum simultaneously depending on the wavelength, time and coordinate.

It was found that the cellular mode is determined by the catalytic combustion of hydrogen on Pt-containing particles formed during the decomposition of unstable platinum oxide in the gas phase. During the ignition delay period at the temperature of the platinum wire in the combustible gas above 500 °C, molecules or clusters of Pt oxide and platinum are formed in the gas phase. Pt-containing ultrafine particles diffusing into the reaction volume act as catalytic centers, on which hydrogen is oxidized, which leads to strong heating of these particles. These incandescent particles are perceived as flame cells on video filming and, in fact, are such cells, in the

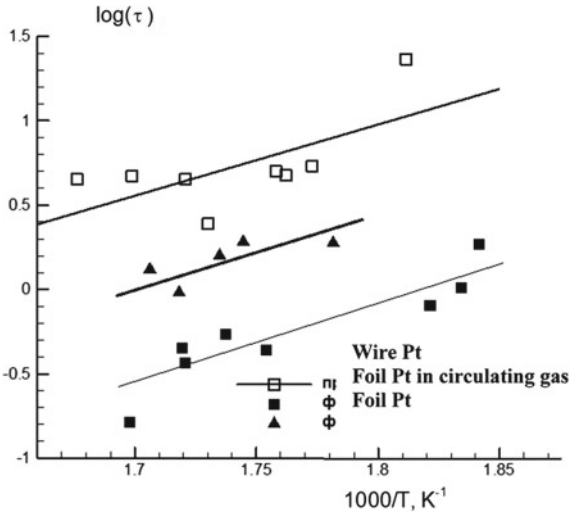

Fig. 2.20 Temperature dependence of the delay times of thermal ignition for a mixture of 40% H_2 with air in the reactor of the bypass installation in the presence and in the absence of a gas flow at a pressure of 1 atm. Black triangles—ignition initiated by platinum foil, gas at rest; black squares—platinum foil initiated ignition, circulating gas; empty squares—ignition initiated by platinum wire, the gas is at rest

area of which combustion is most intense. It is shown that the temperature dependence of the hydrogen ignition delays on a platinum wire and foil in both stationary and rotating gases corresponds to activation energy of 19 ± 3 kcal/mol, which is close to the activation energy of branching of hydrogen oxidation reaction chains. The impurity origin of the 552 nm emitting band, which is often recorded during combustion of gas and dust-gas mixtures, has been determined.

The results obtained are of immediate importance for the development of Catalytic Stabilization (CS) technology and the development of catalysts with increased activity. The results are also important for verification of theoretical concepts of the propagation of dust and gas flames.

2.2 Hydrogen Ignition Over Pt and Pd Foils at Low Pressures

In the previous paragraph, a cellular mode of hydrogen combustion above Pt surface was detected. It was found that the cellular mode is determined by the catalytic combustion of hydrogen on Pt-containing particles formed during the decomposition of platinum oxide in gas. During the ignition delay period at the temperature of the platinum wire in the combustible gas above 500 °C, molecules or clusters of Pt oxide and platinum are formed in the gas phase. Pt-containing ultrafine particles diffusing into the reaction volume act as catalytic centers, on which hydrogen is oxidized, which leads to strong heating of these particles.

This paragraph addresses the phenomenological features of hydrogen combustion over platinum and palladium.

It is known that catalytic hydrogen combustion boilers operate at relatively low temperatures and can generate heat for household applications without CO_2 and NO_x emissions [31, 32]. Thus, the design of catalysts for hydrogen combustion becomes important. Catalysts for hydrogen combustion should possess properties such as capacity for oxygen storage, thermal stability and should provide hydrogen and oxygen activation, which can be attained with noble metals in support. Noble metals have strong capability of adsorbing hydrogen and oxygen at low temperatures [33, 34]. Recently, Borguet et al. [33] reported high hydrogen adsorption capacity and low H_2 dissociation temperature on palladium. Moreover, understanding H_2 and O_2 behavior on the catalyst surface is crucial to focus on the mechanisms of commercialized processes such as preferential oxidation and H_2 combustion. In addition, the airship fabric bag emissions of dilute hydrogen can be used in a power generation system by low temperature catalytic combustion technology. Due to the low pressure in the stratosphere, the application of catalytic combustion in stratospheric airship power generation systems provides advantages over the conventional technology of low ignition temperature under lean combustion conditions, low pollution emissions, high combustion efficiency and stability [35, 36]. Exothermic energy obtained from the hydrogen catalytic combustion reaction can be provided to the power generation

system as a heat source, which avoids carrying additional fuels into the stratosphere. For the low temperature catalytic combustion of hydrogen, noble metal catalysts such as palladium and platinum drew significant attention because of their high catalytic combustion activity and a relatively simple preparation method [37]. In the stratosphere, the pressure is between 5.5 and 1.2 kPa [38]. The H_2 reaction kinetics at low and atmospheric pressures differs from each other. Consequently, it is important to find out the difference.

Note that noble metals form oxides, which depending on the reactivity, determine both the speed and the mechanism of catalytic process; it markedly complicates the optimization of catalysis conditions. For instance, Pd transforms to PdO at temperatures lower than 820 °C, and very unstable PtO_2 can hardly be generated below 500 °C. Because of greater stability of PdO in comparison with PtO_2, in the case of Pd catalyst, the active phase is PdO, whereas in the case of Pt, the active phase is metallic Pt. In methane combustion, the activity of PdO is greater than that of Pt, which results in higher conversions for PdO [39]. We have shown recently that, in the reaction of hydrogen combustion, metallic Pt acts as a heat source similar to a tungsten wire heated by an external source. Obviously, Pt is heated with an internal source, namely, a surface catalytic reaction. The composition of the surface layer changes during ignitions from PtO_2 to another composition, exhibiting properties different from those of PtO_2 [40]. We also observed cellular combustion regimes of 40% H_2–air mixture in the presence of Pt wire at 270–350 °C [41], which were caused by the catalytic action of Pt-containing particles formed upon decomposition of volatile platinum oxide in the gas phase.

Even against that background, the peculiarities of ignition of H_2 over Pt and Pd at low pressures remain not clear enough. This work was focused on experimental studies of low-pressure hydrogen combustion over Pd and Pt foils at total pressures from 10 to 180 Torr and initial temperatures of 20–288 °C.

2.2.1 Experimental

The experiments were performed with stoichiometric gas mixtures $2H_2 + O_2$. Two reactors were used. Reactor I was a quartz cylinder 12 cm high and 8 cm in diameter with a removable CsI window at the butt-end of the cylinder, inlets for gas blousing, pumping out and ignition of gas mixture (Fig. 2.21a). The CsI optical window (35 mm in diameter and 5 mm thick) withstands only five impacts of ignitions at 40 Torr; it was then replaced. Reactor II was a quartz one 4 cm in diameter and 30 cm long heated up with an electric furnace, and the temperature was controlled by a thermocouple. The reactor was supplied with a removable quartz window on its butt-end (Fig. 2.21b). Reactor I was used for studying the initiated ignition, which was provided by heating Pd or Pt foils (0.06 mm thick 80 mm long and 1 mm wide).

Thermal ignition over these foils was studied in reactor II. High-speed recording of ignition dynamics was carried out from the butt-end of reactor II with a video camera (frame frequency, 600 frames s^{-1}), sensitive in the spectral range of 420–740 nm. An

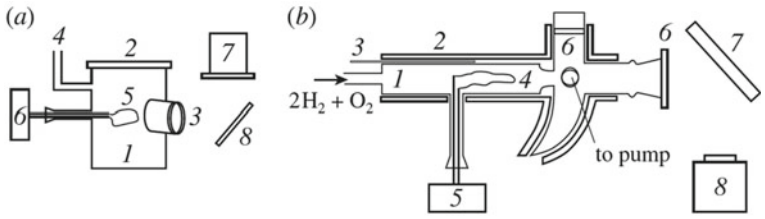

Fig. 2.21 Experimental installations: **a** for the study of initiated ignition, (1) quartz cylinder 12 cm high and 8 cm in diameter, (2) quartz vacuum cover, (3) CsI window, (4) to the pump, (5) Pt/Pd foil, (6) foil heater, (7) infrared Flir 60 IR camera, and (8) rotating mirror; **b** for the study of thermal ignition, (1) quartz reactor of 4 cm in diameter and 30 cm long heated up in the electric furnace, (2) heater, (3) thermocouple, (4) Pt/Pd foil, (5) ADC computer based system, (6) optical window, (7) rotating mirror, and (8) Casio F1 Exilim Pro high-speed digital camera

infrared camera Flir 60 (frame frequency 60 frames s^{-1}, 320 × 240 pix, sensitivity interval 8–14 μm) was used to determine the dynamics of change in temperature of Pt and Pd foils before ignition. A video recording was turned on at an arbitrary moment before initiation. A video file was stored in computer memory and its time-lapse processing was performed. The pumped and heated reactor II was filled with the gas mixture from a high-pressure buffer volume to necessary pressure. In reactor I, the foils were quickly heated to ignite the flammable mixture; in reactor II, the resistance of the foils during thermal ignition was measured. The temperature of the foil during ignition was estimated by an ADC based acquisition system taking into account the temperature dependence of metal resistivity in the computer program. Before each experiment, the reactor was pumped down to 10^{-2} Torr. Total pressure in the reactor was monitored with a vacuum gauge, and the pressure in the buffer volume was monitored with a manometer. Chemically pure gases, 99.99% Pt and 99.85% Pd were used.

2.2.2 Results and Discussion

Temperatures of ignition of $2H_2 + O_2$ mixture over heated foils of both Pt and Pd were determined. Typical experiments at a total pressure of 40 Torr are shown in Fig. 2.22. It is essential that, after previous ignition, the water vapor should be completely pumped out from the reactor prior to the next run; otherwise, the ignition may not happen. In this case, when heating the foil, the total pressure in the reactor decreases by one third without explosion; i.e., the reaction proceeds completely. Note that, for Flir 60, the temperature indicator is slightly delayed as compared with filming; therefore, the maximum temperature $T_{exp} = 194$ °C (shown on the top left of each frame) in the third frame of Fig. 2.22a corresponds to that of the foil immediately before ignition; the temperature in the fifth frame ($T_{exp} = 241$ °C) corresponds to that of the foil heated with the flame. Analogously, in Fig. 2.22b: the

maximum temperature in the third frame ($T_{exp} = 248$ °C) corresponds to that of the foil immediately before ignition; the temperature in the fifth frame ($T_{exp} = 339$ °C) corresponds to that of the foil heated with the flame.

An emissivity factor in these experiments was 0.95 (close to blackbody one). In this case, the colors of the Flir 60 display are most comfortable for the experimenter. However, the recommended emissivity factor over the range 8–14 μm for Pd foil is ~ 0.05 (http://www.zaoeuromix.ru/) or 0.05–0.1 (http://www.thermalinfo.ru/) for Pt foil. We took an estimated value of 0.07 for both foils. Thus, the actual temperature before ignition of $2H_2 + O_2$ mixture at 40 Torr can be estimated from Stefan–Boltzmann law: $0.95T_{exp}^4 \approx 0.07T_{act}^4$ for both foils.

We get an ignition temperature of 623 °C and heated foil temperature of 714 °C for Pd foil; the values for Pt foil are 727 and 903 °C, respectively. The obtained ignition temperature of Pt foil is larger than that measured at 1 atm by other means [40] (584 °C). It is related to different conditions of heat losses and heterogeneous chain termination (see below). Even the minimum temperature value (584 °C) is already enough to ignite a 40% H_2 + air mixture [42] i.e., the influence of the catalytic $H_2 + O_2$ reaction over noble metals is essentially negligible in case of initiated ignition. It was found that the thermal ignition of 2 $H_2 + O_2$ over both foils is missing up

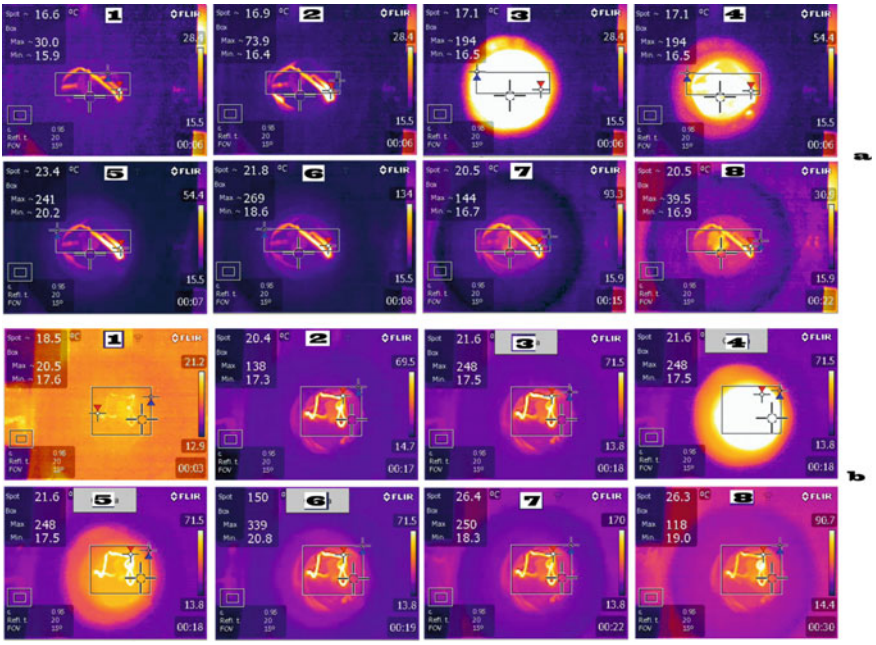

Fig. 2.22 Investigation of initiated ignition by means of the IR camera: **a** Over heated Pd foil (60 frames s^{-1}, $T_0 = 20$ °C, $P_0 = 40$ Torr). Time in seconds is given at the bottom-right of each frame. Red and blue triangles show the maximum and minimum temperatures in the rectangle, cross indicates the temperature at the point. The emissivity factor is set equal 0.95. **b** Over heated Pt foil (60 frames s^{-1}, $T_0 = 20$ °C, $P_0 = 40$ Torr)

to 100 Torr. Thus, the usage of a CsI optical window and the IR camera does not make any sense because of the risk of the device damage with CsI splinters in case of ignition.

However, in the experiments without ignition, we observed that, at 100 Torr of 2 $H_2 + O_2$, Pd foil gets heated by ~ 60 °C using the ADC based acquisition system accounting for the temperature dependence of metal resistivity (Fig. 2.21b). At the same time, the total pressure in the reactor decreases by one third for ~ 3 s, indicating that the hydrogen oxidation is fully completed. Pt foil heats up only by ~ 10 °C and no consumption of the initial flammable mixture is observed. It means that, at pressures < 100 Torr and T_0 < 300 °C, Pt foil shows no prominent catalytic properties in contrast to Pd foil.

For the spatial development of ignition of $2H_2 + O_2$ mixture at pressures up to 180 Torr and 290 °C over both foils, it was shown that the thermal ignition over Pt foil is missing at 180 Torr and 288 °C. We reported earlier [40, 41] that the thermal ignition of 40% H_2 + air mixture at 1 atm already occurs at 260 °C in the reactor 140 mm in diameter. Thus, at lower pressures the heterogeneous chain termination on the reactor walls as well as heat losses are markedly pronounced despite the catalytic activity of the surface. Indeed, using the Einstein–Smoluchowski equation $x^2 = 2D$t (x is a mean diffusion path of a probe particle for a time t, and D is diffusivity close to thermal conductivity), we get $t_1/t_2 = {x_1}^2/{x_2}^2$, where the subscripts 1 and 2 refer to the reactors of different diameters. The computation of wall termination effects in gas-phase radical reactions was described in detail [42]. We give only estimates. In this work $x_1 = 2$ cm, in Ref. [10] $x^2 = 7$ cm, then $t_1/t_2 = 4/49$. This value is still less for atmospheric pressure [30, 40].

Therefore, the mean time for a particle to reach the wall in the reactor with a smaller radius at a total pressure of 180 Torr is much less than that for the reactor with a radius of 7 cm at 1 atm. The same applies to heat losses.

The typical sequence of frames of the thermal ignition over Pd foil at 180 Torr and 288 °C is shown in Fig. 2.23. In accordance with published data [40, 41] Pd foil becomes red-hot before and after ignition due to catalytic reactions on Pd surface, the delay period of ignition makes 4 ± 0.3 s. Since Pd foil is not heated up uniformly (see frames 21–58 in Fig. 2.23), the temperature measured by means of Pd foil is a lower boundary of the real temperature of the ignition center, which ignites the combustible mixture. Indeed, it takes a certain time to warm up an entire wire; therefore, the temperature values obtained are underestimated.

At 288 °C and pressures < 180 Torr, the ignition is missing. However, total pressure in the reactor decreases by one third for ~ 3 s, indicating that hydrogen oxidation is fully completed. It means that, at pressures of > 100 Torr, the catalytic activity of the Pd surface is high as compared to Pt foil. The monitoring of warming-up kinetics using the temperature dependence of resistance in 2 $H_2 + O_2$ by means of ADC computer based acquisition system is shown in Fig. 2.24. According to Figs. 2.23, 2.24, the activity of Pd foil expresses itself in both the occurrence of local ignition centers on the foil, from which combustion wave propagates (see also Fig. 2 [40]), and the dark catalytic consumption of the flammable mixture, which complicates catalytic reaction proceeding owing to consumption of initial flammable gas. The

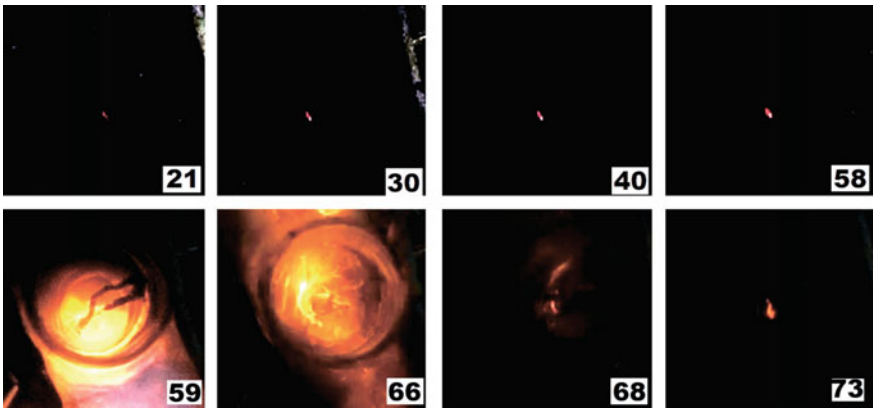

Fig. 2.23 High-speed filming of the thermal ignition of a $2H_2 + O_2$ mixture, 600 frames s^{-1}, T_0 = 288 °C, P_0 = 180 Torr

preheating catalytic process is observed over both foils. At 180 Torr over Pd foil (Fig. 2.24, curve *1*), the catalytic process provides thermal ignition; the warming-up is enough to ignite the mixture [22]. Obviously, the value of the warming-up is underestimated because the foil is unevenly heated during ignition (Fig. 2.23). At 150 Torr over Pd foil (Fig. 2.24, curve 2) and at 180 Torr over Pt foil, the warming-up during preheating is much lower, and it is not enough to provide the ignition of $2H_2 + O_2$ mixture [22].

The measured warming-up at ignition of this mixture (~ 1900 °C) agrees well with the literature data accounting for both heterogeneous chain termination and heat losses in the reactor of comparatively small diameter (4 cm) [12].

Summarizing, in the experiments on $2H_2 + O_2$ ignition over Pd and Pt foils at total pressures of 40–180 Torr and T_0 = 20–288 °C, the temperature of the foils during

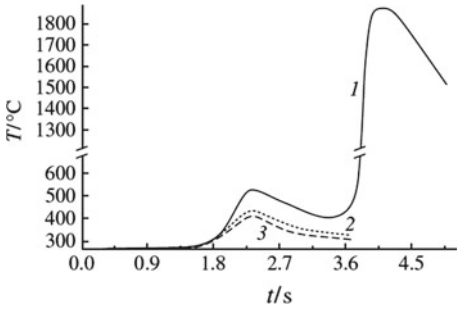

Fig. 2.24 Measurement of warming-up by the dependence of resistance on temperature in $2H_2 + O_2$ using ADC computer based acquisition system. (1) Pd foil, T_0 = 288 °C, P_0 = 180 Torr, ignition occurred; (2) Pd foil, T_0 = 288 °C, P_0 = 150 Torr, no ignition; (3) Pt foil, T_0 = 288 °C, P_0 = 180 Torr, no ignition

ignition was measured by both an infrared camera and an ADC based acquisition system accounting for the temperature dependence of the metal resistivity. It was shown that the temperature of the initiated ignition at 40 Torr over heated Pd foil is ~ 100 °C lower than over Pt foil. Even the minimum temperature value (623 °C) is sufficient to ignite $2H_2 + O_2$ mixture; i.e., the influence of a catalytic $H_2 + O_2$ reaction over the noble metals is negligible in case of initiated ignition. The presence of water vapor prevents ignition. For thermal ignition at 180 Torr and 288 °C over Pd foil the catalytic activity of the surface is higher than that over Pt foil. The activity of Pd foil reveals itself in both the occurrence of local ignition centers on the foil, from which combustion wave propagates, and the dark catalytic reaction of consumption of the flammable mixture.

2.3 Ignition of Hydrogen–Air Mixtures Over Pt at Atmospheric Pressure

In the previous paragraph, it was shown that at subatmospheric pressures the temperature of the initiated ignition at 40 Torr over heated Pd foil is ~ 100 °C lower than over Pt foil. This paragraph focuses on the features of catalytic ignition over Pt at atmospheric pressure.

Catalytic chemistry of hydrogen oxidation over noble metals has been investigated in a number of studies [e.g., 43, 44]. For coupled heterogeneous and homogeneous combustion systems, however, there are only a few investigations (especially at elevated pressures) for hydrogen and hydrogen-containing fuels. The homogeneous ignition of fuel-lean and fuel-rich H_2/air mixtures over Pt-coated stagnation flow surfaces has been investigated at atmospheric pressure by Bui et al. [45], establishing the impact of equivalence ratio on the ignition temperature. It is essential to ascertain the operating conditions (pressure, mixture preheat, catalytic wall temperature, reactor geometrical confinement and residence time), under which gas-phase chemistry plays a substantial role, given the growing interest in catalytic combustion systems using either hydrogen or hydrogen-enriched fuels [46, 47].

We have recently observed [55] cellular combustion regime of 40% H_2–air mixture in the presence of Pt wire over the interval 270–350 °C (see previous paragraph). It was found out that the regime is caused by the catalytic action of Pt containing particles formed by decomposition of volatile platinum oxide in the gas phase. As is known [2Catalytic ignition, and the related extinction and instability phenomena are of practical importance, e.g., in car exhaust catalysis [48], in catalytic afterburning [49], in chemical reactors and in catalytic combustion [50]. Catalytic ignition is also of purely scientific interest as an incompletely understood critical phenomenon, where the system undergoes a transition from one steady-state, essentially controlled by surface reaction kinetics, to another steady-state, primarily controlled by mass transport [51]. Due to the nonlinear coupling of kinetics, mass and heat transport, the same system not only exhibits ignition, but also oscillatory and chaotic behavior [52]. In addition, the ignition can yield information about rate constants. Two experimental techniques are commonly employed, namely the heated wire technique and the heated

gas technique [53]. As is stated in [54], ignition is determined by a coupling of the preignition surface reaction kinetics and the heat losses. The heated wire technique was used in [54].

We have recently observed [55] cellular combustion regime of 40% H_2–air mixture in the presence of Pt wire over the interval 270–350 °C (see previous paragraph). It was found out that the regime is caused by the catalytic action of Pt containing particles formed by decomposition of volatile platinum oxide in the gas phase. As is known [2], thin film of feebly stable, solid platinum forms on platinum surfaces in air or oxygen at room temperature and thickens as the temperature is raised to about 500 °C, when it decomposes. The loss of weight of platinum at higher temperatures is attributed to the formation of gaseous platinum oxide, and deposition of platinum on cooler surfaces (above about 500 °C) to its disproportionation. It means that the molecules or clusters of both platinum oxide and platinum metal exist in gaseous phase at temperatures over 500 °C.

Even against that background, the nature of the source of ignition of H_2 over Pt remains unclear.

Thus, the description of ignition of H_2 over Pt surface must take into account both the heating of the Pt surface due to the catalytic reaction of H_2 oxidation, probably to the temperature of thermal ignition and desorption of the chain carriers from the surface as a result of the same surface reaction. It is possible that the contribution of one of these processes could be much less than that from another one. Really, the ignition is observed only if Pt surface becomes red-hot [3].

The paragraph is focused on the establishment of the comparative contribution of the mechanisms of (a) initiation by a surface reaction leading to active centers desorption and (b) initiation of the ignition at the expense of only thermal heating with Pt surface.

2.3.1 Experimental

The experiments were performed with gas mixtures of 40% H_2 + 60% air at 270 ÷ 350 °C. A heated cylindrical stainless steel reactor 25 cm in length and 12 cm in diameter equipped with demountable covers and an optical quartz window in one of the covers (Fig. 2.25) [6, 7, 9].

The accuracy of temperature measurements was 0.3 K. Registration of ignition and flame propagation was performed by means of a color high-speed camera Casio Exilim F1 Pro (the frequency of shots—600 s^{-1}). A video file was stored in computer memory and its time-lapse processing was performed [12–14]. The pumped and heated reactor was quickly filled with the gas mixture from a high-pressure buffer volume to a necessary pressure. An electromagnetic valve was used to open and close gas communications. A pressure transducer recorded pressure in the course of bleeding-in and combustion. Either Pt foil 12 × 6 cm and 0.3 cm thick or a Pt wire 8 cm long and 0.3 cm in diameter were placed in the reactor. The Pt wire was used both to ignite the flammable mix and to measure the temperature of the wire as a bridge arm. The temperature of the Pt foil during ignition was estimated by means of

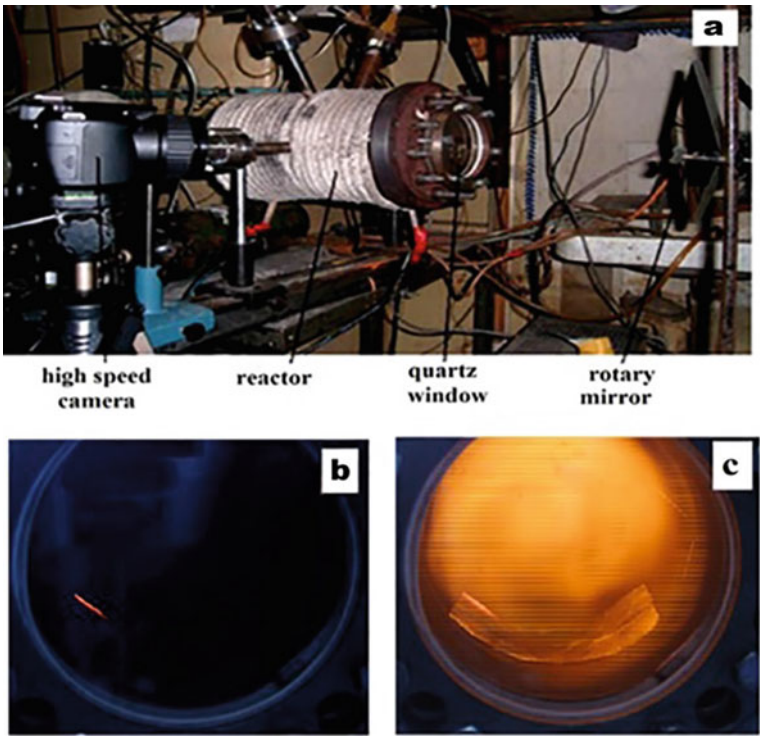

Fig. 2.25 **a** experimental installation; **b** Pt foil in the reactor before ignition; **c** Pt foil in the reactor after ignition (the foil is illuminated with 40% H_2 + air flame)

a double-beam color pyrometer (Figs. 2.22 and 2.23). Before each experiment, the reactor was pumped down to 0.1 Torr. Total pressure in the reactor was monitored with a vacuum gauge, and the pressure in the buffer volume—with a manometer. Chemically pure gases and 99.99% Pt were used.

2.3.2 Results and Discussion

Spatial development of ignition of preliminary prepared 40% H_2–air mixtures at 1 atm pressure was investigated both over Pt foil and over a Pt wire. We remind that the temperature of thermal ignition of H_2–air mixtures at 1 atm in the reactor containing Pt foil [3] is ~ 170 K less than that in the stainless steel reactor without the foil. However, Pt foil in the H_2–O_2 mix can be heated up to the temperature value, which could be higher than that of ignition in a stainless steel reactor i.e. the temperature of the reactor walls is not the governing parameter of a thermal ignition.

Delay times of ignition in the mixtures over Pt foil can reach tens of seconds at the temperature less than 260 °C in the case of the very first experiment, in which the Pt surface has not been treated with active centers of ignition yet.

In the following series of experiments the temperature of Pt foil during ignition was estimated using a two-beam color pyrometer (Fig. 2.26). Because Pt foil is not heated up uniformly (see also Fig. 2.25b), in the first experiment the red-hot site of the Pt foil was identified; in the second one both beams were directed at that site to estimate the temperature.

As is seen in Fig. 2.26, only a discrete ignition center is brought to red heat (shown with a white circle in the frames 25, 40). Because a double-beam color pyrometer takes a temperature value between the beams on the surface under investigation, the mean temperature value of the region between the beams is measured.

The temperature is 584 °C at the moment preceding ignition (the ignition occurs in the 41st frame). This value is evidently a lower boundary of the actual temperature of the ignition center. Really, using a color table of metals (e.g. www.ecolain39.ru) the temperature of the active center for the 40th frame of Fig. 2.26 could be roughly estimated as ~ 800 °C, the temperature of the red hot part of the foil from Fig. 2.25.b is ~ 730 ÷ 800 °C. All the values are in good agreement with each other. In addition, the minimum temperature value (584 °C) is already enough to ignite 40% H_2 + air mix [22].

Thus, based on the results obtained one can come to a conclusion that Pt acts as a heat source similar to the wire heated by an external source. However, in the case under investigation Pt is heated with an internal source, namely a surface catalytic reaction.

Fig. 2.26 Registration of the initiation of ignition of 40% H_2 + air with Pt foil with a two-beam color pyrometer indicating temperature values in °C. An ignition center on the foil is shown with a white circle in the frames 25, 40. $P_0 = 1$ atm. $T_0 = 305$ °C

To make a closer examination of the role of the surface reaction in the following series of experiments, a Pt wire was used both to ignite the flammable mix and to measure the temperature of the wire as a bridge arm (Fig. 2.27b). At the same time color speed filming was performed. Typical sequences of frames of high-speed filming of FF propagation in the gas mixture initiated with a Pt wire are shown in Fig. 2.27a. As is seen in the 3rd frame of Fig. 2.27a, in the presence of the Pt wire a cellular structure of FF is observed according to published data [34]; the Pt wire is red-hot before and after ignition due to catalytic reactions on the Pt surface.

In Fig. 2.28, the oscillogram of simultaneous registration of the signals from the pressure transducer and the Pt wire as a bridge arm are presented. As is seen in Fig. 2.28, total pressure in the reactor reaches 1 atm to the moment of the ignition.

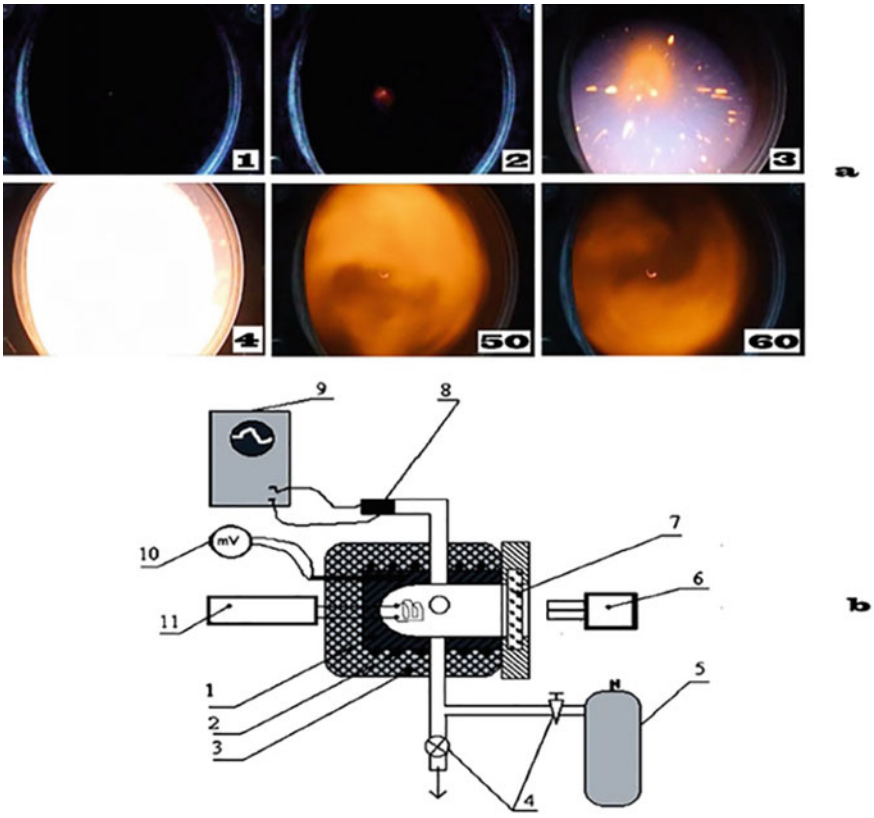

Fig. 2.27 **a** High speed color registration of the initiation and flame propagation in 40% H_2 + air mix with a platinum wire, 600 frames/s. Numbers in each frame correspond to consecutive number of the video image; the first frame is when Pt wire becomes red-hot; **b** schematic diagram of the experimental setup: (1) reactor, (2) electric heater, (3) thermal insulation, (4) valves, (5) mixer, (6) digital video camera (or pyrometer in the case of Pt foil, Fig. 2.25), (7) optical window, (8) pressure transducer, (9) ADC–computer based data acquisition system, (10) digital voltmeter, and (11) measurement bridge, Pt wire is a bridge arm

Because (see Fig. 2.27a, frames 1, 2; see also Sect. 2.1) the Pt wire similar to the Pt foil is not heated up uniformly, the temperature value measured by means of the Pt wire is a lower boundary of the real temperature of the ignition center, which ignites the combustible mix. Really, it takes a certain time to warm up the wire, therefore the values of the temperature obtained by the method are underestimated.

Let us estimate the lower boundary value of temperature, which is enough to ignite the combustible mixture. One can see from the presented dependencies of the temperature on time at Pt initiated ignition (Fig. 2.29) that the difference between initial temperatures for e.g. 300 °C (green curve) and 320 °C (blue curve) makes 0.01 arbitrary units, the difference between initial temperature and the temperature of ignition at 5900 ms makes ~ 0.1 arbitrary units. Therefore, the lower boundary value of temperature could be estimated as 20 °C (0.1/0.01) ~ 200 °C i.e. the lower limit of the temperature of ignition is 500 °C. This value compares well with previously obtained ones; it is also consistent with the conclusion made above that Pt acts as a heat source similar to the wire heated by an external source.

It should be noted, however, that ignition delays τ for the experiments presented in Fig. 2.29 markedly differ: τ (280 °C) = 35 s, τ (300 °C) = 10 s, τ (320 °C) = 7.5 s. Thus, as it was already stated above, τ reaches its highest value in the case of the first experiment at 280 °C over "fresh" Pt surface, the temperature of ignition is 20° lower (red curve) as well. It means that the state of surface of untreated Pt provides the lowest ignition temperature.

In the following experiments the dependence of the surface state of the Pt wire (starting from the "fresh" one) on the number of ignitions was studied.

As is seen in Fig. 2.30, the highest value of a delay period of ignition is observed in the first experiment; τ values for Pt surface treated with ignitions are markedly far from this value. It is also seen that over "fresh" Pt surface at the moment 4.5 s the 40% H_2–air mix is about to ignite; approximately by that moment, the ignition over the treated Pt surface occurs. Over the fresh surface in the time interval between 4.5 and

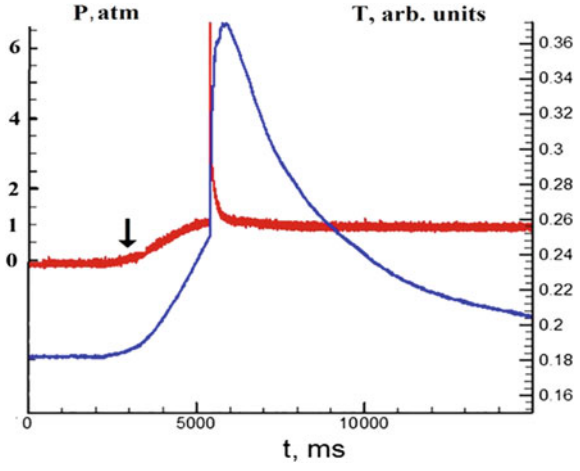

Fig. 2.28 Simultaneous recording of the pressure (red) and the temperature with the Pt wire (blue), T_0 = 320 °C P_0 = 1 atm. The arrow shows the beginning of gas admission

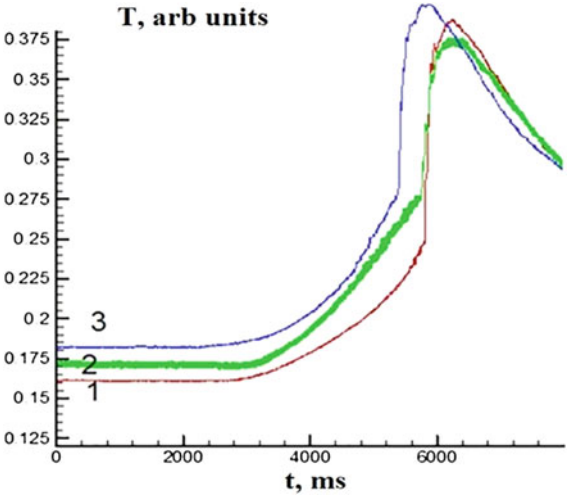

Fig. 2.29 The dependence of the temperature on time at initiated ignition of 40% H_2 + air mix with Pt wire. (1) $T_0 = 280$ °C, (2) $T_0 = 300$ °C, (3) $T_0 = 320$ °C. $P_0 = 1$ atm. The curves are brought into coincidence for the delay times of ignition differ from each other

14 s the surface somehow reconstructs itself; then ignition takes place. Moreover, the curve 1 is placed lower than the others. It means that the dependence of the resistance on temperature discerns between "fresh" Pt and treated Pt, i.e. the materials of the "fresh" Pt wire and the treated one differ markedly. As is shown in Sect. 2.1, before the ignition, Pt surface is coated with a layer of platinum oxide; after ignition, a fraction of the layer in the form of ultra-disperse particles of Pt oxide is emitted under heating and spreads over the reactor volume. This suggests that after the first ignition the platinum oxide layer becomes so thin that it does not have time to be recovered. Thus, the first ignition occurs over a thick layer of Pt oxide, the following ignitions take place over the surface of another composition, which needs further investigation with Auger or XPS methods.

Summarizing, the results obtained in the paragraph allow one concluding that in the reaction of hydrogen combustion, metallic Pt acts as a heat source similar to (say) a tungsten wire heated by an external source. However, in the case under investigation, Pt is heated with an internal source, namely a surface catalytic reaction. It must be also taken into account that the composition of the surface layer changes during ignitions from Pt oxide (PtO_2) to another composition, exhibiting properties different from PtO_2.

2.4 Surface Modes of Catalytic Ignition of Flammable Gases Over Noble Metals

In the previous paragraph, we showed that the chemical composition of the surface changes during ignitions from Pt oxide to another one, which implies the possibility

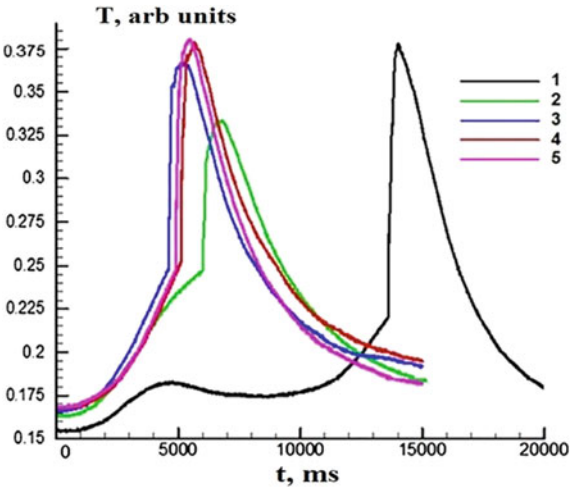

Fig. 2.30 Dependence of the ignition delay of 40% H_2–air mix over the Pt wire on the number of ignitions (1–5). $P_0 = 1$ atm. $T_0 =$ 304 °C

of occurrence of different surface modes of catalytic ignition depending on the degree of surface treatment with ignitions.

The challenges in the safety of producing, transporting and storing hydrogen supplies need to be fixed before extensive use of hydrogen as a common fuel. One of the main hazards is accidental ignition, since hydrogen has much wider flammability limits than most conventional fuels [56]. One of the possible sources of ignition is a hot surface. Thus, it is important to be able to establish and avert conditions, under which the ignition can take place when a hydrogen-oxidizer mixture is exposed to a hot surface when entering a tube or a storage chamber. However, hydrogen is difficult to be ignited by compression and some additional igniter, for instance a glow plug, is used [57]. Therefore, the design of combustion devices requires information about a hot surface ignition.

The catalytic combustion of hydrogen is of interest because catalytic hydrogen combustion devices operate at comparatively low temperatures and can work without CO_2 and NO_x emissions [58]. For H_2 combustion reaction, the catalysts should possess thermal stability; these should be able to ensure that H_2 oxidation occurs without incidental explosion. That fully applies to noble metals as catalysts. In addition, information on H_2 and O_2 reactions on the catalyst surface is important for understanding the mechanisms of many commercialized processes such as preferential oxidation and H_2 combustion.

Catalytic converters are the main exhaust gas treatment system in automobiles and other devices; these utilize an oxidation reduction process to reduce toxic emissions. In order to stimulate the reaction, noble metals are used as catalyst materials. However, Pt based catalysts are not effective enough with methane; Pd catalyst can provide higher methane conversion [59]. Pd seems to be more usable for hydrogen recombiners in NPP, because catalytic particles as ignition centers formed by decomposition of volatile oxide do not appear in gas phase as compared to Pt [16]. The

experimental value of the effective activation energy of the process is estimated by different methods as ~ (3.5 ± 1.5) kcal/mol that is characteristic of surface processes [60]. It indicates the noticeable role of the dark reaction of consumption of H_2 and O_2 observed directly at low pressures [60]. The occurrence of that reaction reduces the probability of accidental explosion.

The interest is renewed recently to localized hydrogen generation with a focus on hydrocarbon reforming process [61], where methane is one of the prime sources and Rh or Pt are main catalysts of hydrocarbon to hydrogen conversion [62]. Autothermal reforming as a means of hydrogen production has been gaining academic and research interest due to its thermodynamically neutral nature and feasible operating conditions [63]. A number of experimental studies have been performed to investigate ignition of hydrogen by a hot surface. We will focus on the main ones, in our opinion. As we mentioned above, Warnatz and coworkers [64] studied catalytic combustion and ignition of hydrogen using detailed kinetic mechanisms for both surface and gas-phase reactions. Deutschmann et al. [65] studied catalytic ignition of different fuels on different catalyst materials. In their numerical simulations, they showed that one or the other reactant almost covers the surface before ignition. In a series of experiments with very thin catalytic wires, Rinnemo et al. [54] determined the critical ignition temperature of hydrogen mixtures as a function mainly of the mixture composition. Kalinchak et al. [66] presented the analysis for the catalytic ignition using a simplified model for the heterogeneous chemistry. The results reveal a lack of universality of the ignition temperature concept and the need of a more profound understanding of the problem for example, homogeneous heating of the catalyst is postulated, which, as can be seen from our experiments, does not correspond to reality. Therefore, the peculiarities of ignition of H_2 over noble metals remain not clear enough.

This paragraph focuses on experimental studies of hydrogen and hydrogen-propane ignition over Pd wire and Pd foil at total pressures 1 ÷ 2 atm and initial temperatures of 60 ÷ 270 °C using high speed cinematography to establish the peculiarities of ignition on the noble metal surface.

2.4.1 Experimental

The experiments were performed with stoichiometric gas mixtures (H_2 + 30 ÷ 70% $C_3H_8)_{stoich}$ + air and 40% H_2 + air. The reactor used in experiments was a heated stainless steel cylinder 25 cm in length and 14 cm in diameter, equipped with demountable covers and an optical sapphire window in one of the covers (Fig. 1 [67]). The pumped and heated reactor was filled with a gas mixture from a high-pressure buffer volume to 1 atm. Catalytic ignition was provided by Pd wire (0.3 mm thick and 80 mm long) or Pd foil (0.07 mm thick, 30 mm in width and 80 mm in length, half rolled-up into a tube, see Fig. 2.31). The experiments on the detection of initial ignition centers on the catalytic wire using speed cinematography were performed at total pressure 1 atm by means of a color high-speed camera Casio Exilim F1 Pro (frame frequency ÷ 600 s^{-1}) and a high-speed PHANTOM camera

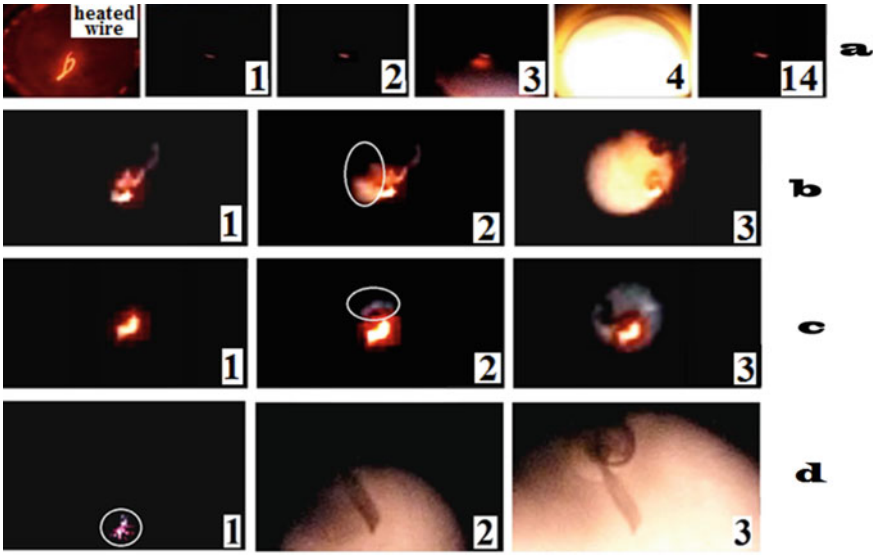

Fig. 2.31 **a** High-speed filming of the catalytic ignition of a 40% H_2 + air mixture over Pd wire, the frame to the left is the appearance of the wire heated at 1 Torr by an external source. 600 frames s^{-1}, $T_0 = 60$ °C, $P_0 = 1$ atm. **b** High-speed filming of the catalytic ignition of a mixture (70% H_2 + 30% $C_3H_8)_{stoich}$ + air over Pd wire. 600 s^{-1}, $T_0 = 61.5$ °C, $P_0 = 1$ atm. **c** High-speed filming of the catalytic ignition of a mixture (70% H_2 + 30% $C_3H_8)_{stoich}$ + air over Pd wire, 600 s^{-1}, $T_0 = 61.5$ °C, $P_0 = 1$ atm, **d** High-speed filming of the catalytic ignition of a mixture 40% H_2 + air over Pd wire, 1200 s^{-1}, $T_0 = 154$ °C, $P_0 = 1$ atm. White circles highlight primary ignition centers. The first frame corresponds to the moment of the occurrence of a primary ignition center

with a speed up to 10,000 s^{-1} sensitive in the spectral range of 420 ÷ 740 nm. The accuracy of temperature measurements was ± 0.3 K. Before each experiment, the reactor was pumped down to 10^{-2} Torr. Total pressure in the reactor was monitored with a vacuum gauge, and the pressure in the buffer volume was monitored with a manometer. Chemically pure gases and 99.85% Pd were used.

2.4.2 Results and Discussion

Typical frame sequences of the catalytic ignition at 1 atm of (a) 40% H_2 + air mixture over Pd wire, (b, c) (70% H_2 + 30% $C_3H_8)_{stoich}$ + air at 61.5 °C over Pd wire, and (d) 40% H_2 + air over Pd foil at 154 °C are shown in Fig. 2.31. In accordance with published data [16, 67], Pd wire/foil becomes red-hot before and after ignition due to catalytic reactions on Pd surface. Ignition temperature over Pd wire is lower for (70% H_2 + 30% $C_3H_8)_{stoich}$ + air mixture than over Pd foil for more flammable 40% H_2 + air due to due to the higher rate of heat removal from the hot primary ignition center, determined by the section of the heat conductor, which is noticeably higher for the

foil. As is seen in Fig. 2.31, the wire is not heated up uniformly (compare frames 1–3 with the left frame in Fig. 2.31a; localized initial centers of ignition can be clearly seen in corresponding frames in Fig. 2.31b–d. As is seen, the location of a primary ignition center changes from ignition to ignition (Fig. 2.31b, c frame 2). The result is consistent with that we obtained in [5]: the gaseous process of ignition of H_2–air and hydrocarbon–air mixtures at atmospheric pressure begins with the occurrence of an initial center at the most chemically active site of the surface.

All experiments on high-speed registration of catalytic ignition of the mixture 40% H_2 + air over Pd foil with Phantom camera have shown that the initial center of ignition originates on the reactor surface (Fig. 2.32a, 4000 s^{-1}); in subsequent experiments under the same conditions, the site of origin of the initial center varies (Fig. 2.32b). It should be noted that the high-speed filming of the developing catalytic ignition of the mixture 40% H_2 + air over Pd foil (10,000 s^{-1}) shows the movement of gas to the center of the reactor after touching the reactor walls. Pay attention to the movement of dust particles torn from the walls towards the center (frames 32, 36) and subsequent strong heating of the reaction products due to compression (Mahe effect [68]).

This means that the initiation of the thermal ignition process is always determined by the presence of active centers on the surface, the properties of which are determined by both surface defects having an excess of free energy and their catalytic properties; the ignition process includes stages of warming-up, local ignition, and flame propagation. The chemical activity of various sites of the surface changes from one ignition to another. The basic feature of ignition process lies in the fact that ignition occurs at separate sites of surface at a uniform temperature of the reactor

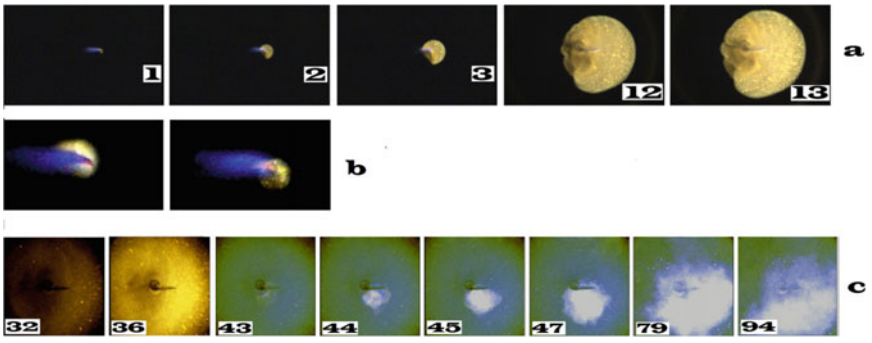

Fig. 2.32 **a** High-speed filming of the catalytic ignition of the mixture 40% H_2 + air over Pd foil, 4000 s^{-1}, $T_0 = 150$ °C, $P_0 = 1$ atm. The first number of the frame corresponds to the moment of the occurrence of the primary ignition center. **b** Photos of the flame initiation with catalyst for two subsequent experiments taken from high-speed filming of the catalytic ignition of the mixture 40% H_2 + air over Pd foil, 10,000 s^{-1}, $T_0 = 150$ °C, $P_0 = 1$ atm. High-speed filming of the developing catalytic ignition of the mixture 40% H_2 + air over Pd foil, 10,000 s^{-1}, $T_0 = 150$ °C, $P_0 = 1$ atm. **c** High-speed filming of the developing catalytic ignition of the mixture 40% H_2 + air over Pd foil, 10,000 s^{-1}, $T_0 = 150$ °C, $P_0 = 1$ atm. The first number of the frame corresponds to the moment of the occurrence of a the primary ignition center

surface. Therefore, combustion originates on the surface of uniformly heated reactor even under conditions of almost homogeneous warming up of a gas mixture.

It should be noted in this connection that the ignition of the combustible mix in the heated reactor in swirling flow is on the contrary homogeneous [8]. If the swirling flow is missing in the installation, as it takes place under conditions of this work, the ignition is heterogeneous, i.e. the regimes of thermal ignition differ qualitatively. These regimes are not evidently determined with reaction kinetics, which remains the same; these are governed in fact with only gas dynamics. *It means that if the researcher applies e.g., a by-pass method, he has to make certain estimations of the geometry of the flow in the installation to exclude the factors, which should hinder obtaining the results required. The factors cannot be reduced to the comparison of characteristic times of homogeneous chemical and gas dynamic processes; in this case, heterogeneous reactions must be taken into account.*

2.5 Hydrogen and Deuterium Ignition Over Noble Metals at Low Pressures

Based on the results obtained in previous paragraphs, it can be concluded that the information obtained is now sufficient to give a qualitative description of the ignition mechanism of the catalytic surface. This paragraph also establishes the features of deuterium combustion over noble metals.

As we stated above, the development of the technology of catalytically stabilized combustion requires the development of catalysts with increased activity and thermal stability. This requires an understanding of the nature of catalytic surface processes, knowledge of the detailed low-temperature homogeneous kinetic mechanism and its relationship with the mechanism of heterogeneous chemical transformations. The homogeneous ignition in a catalytic reactor threatens the integrity of the reactor and the working space, therefore the possibility of preventing such an event is of primary interest for the design of the reactor. Ignition in the gas phase is determined by the interrelation of heterogeneous and homogeneous factors (catalytic fuel consumption, adsorption/desorption reactions involving radicals). Therefore, reliable control of homogeneous ignition requires knowledge of the combustion mechanism in the presence of catalyst. In order to stimulate the reaction, noble metals such as Pt, Rh, Ru and Pd are used as catalyst materials. Pt based catalysts are not effective enough with methane; however, Pd catalyst can provide higher methane conversion [59]. The peculiarities of catalytic action of noble metals have been under discussion. Noble metals influence the flammability of hydrogen–methane blends differently. It was shown that the ignition temperature of the mixture 40% H_2–air over Pd metal (70 °C, 1 atm) is ~ 200° less than over the Pt surface (260 °C, 1 atm) [69]. Furthermore, Pd ignites stoichiometric mixes (30 ÷ 60% H_2 + 70 ÷ 40% CH_4) + air [$\theta = 1$, equivalence ratio θ is a fraction of fuel in the mix with air: $\theta\ H_2 + 0.5\ (O_2 + 3.76\ N_2)$]; metallic Pt cannot ignite these up to 450 °C, i.e. Pd is more effective than Pt.

It was also shown that the cellular structure of a flame front at hydrogen ignition with Pd is not observed in contrast to Pt surface. Thus, Pd seems to be more usable for hydrogen recombiners in NPP, because no catalytic particles as ignition centers formed by decomposition of volatile oxide can appear in gas phase in contrast to Pt [16]. The experimental value of the effective activation energy of catalytic ignition over Pt is ~ 18 kcal/mol and is close to one of $H + O_2$ branching step [22]; the value over Pd is ~ 3.5 kcal/mol that is characteristic of surface processes [69]. It indicates the noticeable role of the dark reaction of consumption of H_2 and O_2, also referred to as "flameless combustion", which is observed at low pressures [70]. The occurrence of that reaction evidently reduces the probability of an accidental explosion.

A number of experimental studies has been performed to investigate the hydrogen ignition by a hot surface. Williams et al. [71] proposed a model for the catalytic combustion of hydrogen at high temperatures. Warnatz and coworkers [64] studied the catalytic combustion and ignition of hydrogen using detailed kinetic mechanisms for both surface and gas-phase reactions. Deutschmann et al. [65] studied the catalytic ignition of different fuels on different catalyst materials. In their numerical simulations, they showed by numerical calculations that one or the other reactant almost covers the surface before ignition. In a series of experiments with very thin catalytic wires, Rinnemo et al. [54] determined the critical ignition temperature of hydrogen mixtures as a function mainly of the mixture ratio. Kalinchak et al. [66] presented an analysis for the catalytic ignition using a simplified model for the heterogeneous chemistry. It should be noted that most of the rate constants for detailed mechanisms have obviously not been determined experimentally, so one should not expect predictive properties from such a calculation. In all works, the heating of the catalytic wire in the reaction is considered homogeneous, which does not agree with our experimental data. The results obtained indicate the need for a deeper understanding of the problem, since the available calculated data do not even describe the experiment qualitatively.

It is known that hydrogen and deuterium form binary intermetallic hydrides/deuterides with palladium, thus, the features of ignition over the surfaces of hydrides of noble metals have been a subject of investigation in this work. Unlike many known metallic hydrides, very little macroscopic deformation of the palladium lattice occurs, and the mechanical properties of the hydride are very similar to those of pure metal. There have been almost 150 years of active research into the palladium hydride/deuteride system up to now. Numerous literature reviews have been published on the system [72]. In 1957, the first diffraction patterns of β-PdH and β-PdD were recorded [73]. There is the "inverse isotope effect" observed [74] whereby heavier hydrogen isotopes have a higher critical temperature at similar H/D/T loading. Similar "inverse isotope effects" can also be found in the rate of diffusion of hydrogen isotopes through the palladium lattice. At low temperatures, hydrogen isotopes exhibit an "inverse isotope effect" (where heavier isotopes diffuse faster than their lighter counterparts do).

The current paragraph focuses on experimental studies of low-pressure hydrogen and deuterium combustion over Rh, Ru, Pd and Pt wires at total pressures from 10 to 180 Torr and initial temperatures over the range 200 ÷ 500 °C in order to establish the

dependencies of catalytic ignition limits over noble metal surfaces on temperature and to indicate the governing factors of the problem of gas ignition by a catalytic surface. A macrokinetic study of the chemical properties of the two lighter hydrogen isotopes (protium and deuterium) dissolved in rhodium and palladium, namely the study of the influence of hydrides and deuterides of noble metals on hydrogen and deuterium combustion, is performed.

2.5.1 Experimental

The experiments were performed with stoichiometric gas mixtures $2H_2/D_2 + O_2$. The reactor was a quartz one 4 cm in diameter and 30 cm long heated up with an electric furnace (Fig. 2.33); the temperature was controlled by a thermocouple. The reactor was supplied with an optical quartz window on its butt-end. The reactor was used for studying thermal/catalytic ignition provided by Pd and Pt wires (0.3 mm thick 80 mm long) as well as Rh and Ru samples, which were made by electrochemical deposition of Rh or Ru layers 15 μm thick on Pd wire (0.3 mm thick 80 mm long). Pd was chosen because its coefficient of thermal expansion is the closest to those of Rh and Ru [75], since Ru metal is fragile and one cannot stretch it into wire; Rh wire is relatively expensive. The accuracy of temperature measurements was ± 0.3 K. Registration of ignition and flame propagation was performed by means of a color high-speed camera Casio Exilim F1 Pro (frame frequency –600 s^{-1}) sensitive in the spectral range of 420–740 nm.

The overall intensity of chemiluminescence in the reactor was recorded with a FD—24 photodiode (Fig. 2.33, 12). A video recording was turned on at an arbitrary moment before the mixture was injected into reactor. A video file was stored in computer memory; a Nikon 1J2 digital camera was used for video recording (Fig. 2.33, 7). The pumped and heated reactor was filled with a gas mixture from a high-pressure buffer volume to necessary pressure, the resistance of the wires

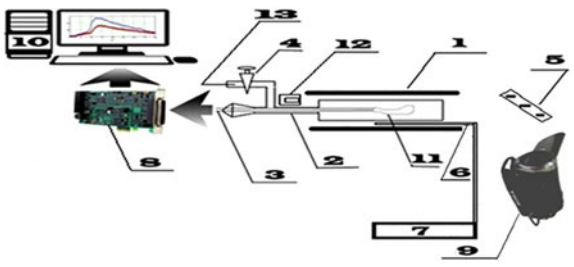

Fig. 2.33 Schematic of the experimental installation for the study of thermal/catalytic ignition over the wire. (1) electric furnace, (2) quartz reactor of 4 cm in diameter and 30 cm long, (3) vacuum feed-through, (4) vacuum valve, (5) rotating mirror, (6) thermocouple, (7) millivoltmeter for thermocouple, (8) ADC computer based system, (9) Nikon 1J2 digital camera, (10) computer, (11) noble metal wire, (12) FD-24a photodiode, (13) gas inlet, to pressure gauge, to the pump

during ignition was measured. The ignition limit pressure was considered as a mean pressure P Torr, at P + 0.02 P the ignition occurs, at P − 0.02 P it does not occur, all other things being equal. The pump-down time between experiments was 30 min. The ignition limit was measured at increasing pressure with a step 2 Torr until the ignition occurred (when increasing temperature from a state of no ignition) and at decreasing pressure with a same step until the ignition was no longer observed (when decreasing temperature from a state of a catalytic ignition).

The microstructure of Pd foils was examined using field emission, ultra-high resolution scanning electron microscope (SEM) Zeiss Ultra Plus (Germany) equipped with X-ray Microanalysis console INCA 350 Oxford Instruments.

The mean temperature of the wire during ignition was recorded by an ADC based acquisition system, taking into account the temperature dependence of metal resistivity during computer analysis of the signal. Before each experiment, the reactor was pumped down to 10^{-2} Torr. Total pressure in the reactor was monitored with a vacuum gauge (Fig. 2.33, 10), and the pressure in the buffer volume was monitored with a manometer. Chemically pure gases, 99.99% Pt and 99.85% Pd were used.

2.5.1.1 Hydrogen Ignition Over Rhodium, Ruthenium, Palladium and Platinum

Ignition limits in conventional P–T coordinates [22] of thermal/catalytic ignition of $2H_2 + O_2$ mixture over Pt, Pd, Ru/Pd and Rh/Pd were determined. The experiments showed that in the absence of ignition in the vicinity of the explosion limit, total pressure in the reactor decreases by one third without explosion; i.e., the reaction proceeds to completion. It is essential to note that, after previous ignition, the water vapor should be completely pumped out of the reactor prior to the next experiment; otherwise, the ignition may not occur.

As is shown in Sect. 2.4 (Fig. 2.31) and in accordance with published data [16, 70], Rh/Pd wire becomes red-hot before and after ignition due to catalytic reactions on catalytic surface. As is seen in Fig. 2.31, the wire is not heated up uniformly (compare frames 1–3 with the left frame in Fig. 2.31a); initial centers of the ignition can be clearly seen in frame 3 in Fig. 2.32b, c. As is seen, the location of a primary catalytic center changes from ignition to ignition. Hence, because it takes a certain time to warm up an entire wire, the temperature values obtained from the change of resistance are underestimated and correspond to the average temperature of the wire. The difference in the temperature of the noble metal surface at the moment preceding ignition and the temperature of the primary ignition center on the surface when ignited, is estimated in [16, 70] and it can reach $\geq 200°$ at 1 atm [70]; at lower pressures it should be less due to chain termination and heat losses (see below).

We showed earlier that the ignition of $2H_2 + O_2$ mixture over Pt wire in the reactor similar to described in this work, does not occur at total pressures lower than 180 Torr at 288 °C [70]. We reported also [16, 76] that the thermal/catalytic ignition of 40% H_2 + air mixture at 1 atm over Pt already occurs at 260 °C in the reactor 140 mm in diameter. Thus, at lower pressures the heterogeneous chain termination

on the reactor walls as well as heat losses should be taken into account along with catalytic activity and the state of the surface. It was shown in [70], that at a total pressure of 180 Torr the mean time for a particle to reach the wall in the reactor with a smaller radius is much less than that for the reactor with a radius of 7 cm at 1 atm. Thus, the role of chain termination increases with a decrease in a reactor diameter. The same applies to heat losses.

The monitoring of ignition dynamics $2H_2 + O_2$ using the temperature dependence of resistance by means of ADC computer based acquisition system of Rh/Pd and Ru/Pd wires is shown in Fig. 2.34a, b correspondingly. According to our experiments, the activity of catalytic wire is expressed in the occurrence of local ignition centers on the wire (see Sect. 2.3 and Fig. 2 [19], where local ignition centers on the Pt foil are clearly observed in the frames, (Fig. 2.22), from which combustion wave propagates. It is expressed as well in the dark catalytic reaction of the consumption of $2H_2 + O_2$ mixture. The preheating catalytic process provides the warming-up, which is enough to ignite the mixture [16, 40, 77]. As is outlined above, the value of the warming-up temperature is underestimated because the wire is nonuniformly heated during ignition (Fig. 2.31).

Auto–ignition areas of $2H_2 + O_2$ mixes over the catalytic wires are presented in Fig. 2.35 in P–T coordinates. As is seen in Fig. 2.35, Rh is the most active surface, Ru and Pd surfaces are less active; their catalytic activity is approximately the same.

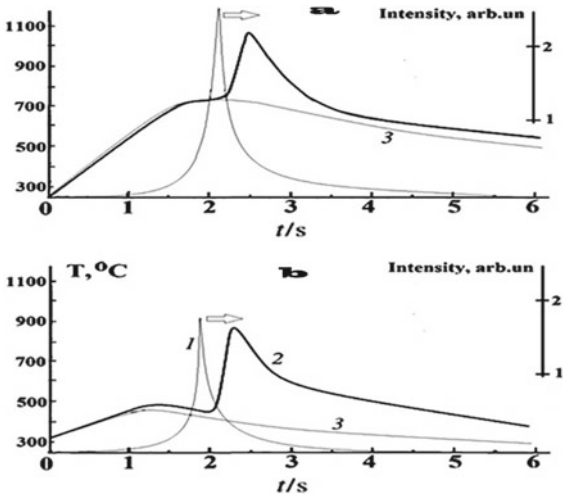

Fig. 2.34 Measurement of chemiluminescence by the photodiode and average value of the warming-up by the dependence of resistance on temperature in $2H_2 + O_2$ using ADC computer based acquisition system, **a** over Rh/Pd wire, (1) ignition recorded with FD-24a photodiode, $T_0 =$ 233 °C, $P_0 =$ 139 Torr; (2) mean temperature of the wire, $T_0 =$ 233 °C, $P_0 =$ 139 Torr, ignition occurred; (3) mean temperature of the wire, $T_0 =$ 231 °C, $P_0 =$ 135 Torr, no ignition. **b** over Ru/Pd wire, (1) ignition recorded with FD—24 a photodiode, $T_0 = 310$ °C, $P_0 = 99$ Torr; (2) mean temperature of the wire, $T_0 = 310$ °C, $P_0 = 99$ Torr, ignition occurred; (3) mean temperature of the wire, $T_0 = 310$ °C, $P_0 = 95$ Torr, no ignition

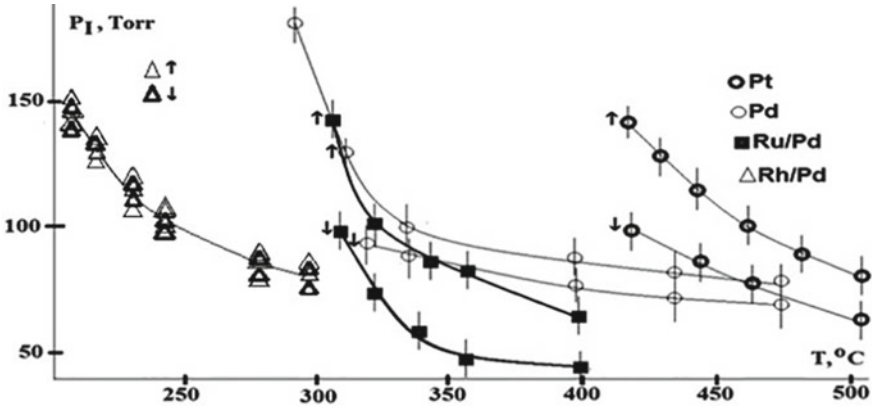

Fig. 2.35 Thermal/catalytic ignition areas of $2H_2 + O_2$ mixes over noble metal wires in pressure–temperature coordinates. The arrow oriented upwards corresponds to a procedure of increasing temperature from a state of no ignition (bottom-up approach) and the arrow oriented downwards corresponds to decreasing temperature from a state of catalytic ignition (top-down approach). To the right of each curve the ignition occurs, to the left—the ignition does not occur

Notice that the hysteresis phenomenon is observed over Ru, Pt and Pd wires. The ignition limit value measured over the wire, which is not treated with ignitions (when increasing temperature from a state of no ignition), is higher than the value measured when decreasing temperature from a state of catalytic ignition; the same applies to the delay periods of ignition. The delay periods measured when decreasing temperature from a state of catalytic ignition do not exceed a few seconds; though these measured when increasing temperature from a state of no ignition reach 120 s. The higher ignition limit obtained by increasing temperature from a state of no ignition is reversible and may be attained again after several ignitions or by reactor treatment with air or O_2. This means that the surface state and probably its composition (see below) of noble metal changes in the course of ignitions. Because the ignition limit returns to its original value after a certain treatment, the surface state is restorable. Thus, the ignition limit permanently decreases after first ignition until it reaches the lowest value, which can be measured when decreasing temperature from a state of the first catalytic ignition; the treatment with air or O_2 restores the ignition limit to its original value. The nature of this phenomenon needs further investigation.

The hysteresis phenomenon observed means that the catalytic surface changes its state after ignition in agreement with [16, 40, 77, 78]. Meanwhile, as is seen in the Figure, Rh surface does not exhibit the phenomenon; the ignition limit values measured by both procedures are practically equal. There can probably be a difference in the values for upwards and downwards temperature change, but we cannot resolve it with our experimental procedure. As outlined below, this may be due to the fact that though at 600 ÷ 800 °C, an oxide Rh_2O_3 film forms on Rh surface, but when the temperature rises to 1000 °C, the oxide film on Rh surface decomposes to metal again; thus, the surface does not change its composition.

The morphology of Rh, Ru and Pd wires before and after 50 ignitions (at initial pressure 100 Torr) was studied. We did not examine Pt wire, because after ignition it is quickly covered with PtO_2 oxide [16]; thus, the change in surface appearance cannot be reliably visualized. The results of electron spectroscopy investigation are presented in Fig. 2.36.

As is seen, untreated samples represent the surface with rolling marks (Fig. 2.36, first micrographs on the left, no ignition). In the samples treated with ignitions, the defects in the form of openings develop (Fig. 2.36, after ignitions). Their depth reaches < 1 μm in the case of Pd and Rh/Pd wires. These defects seemingly focus on etching patterns; the etching substances are evidently active intermediates of H_2 oxidation. As is seen in Fig. 2.36, the interaction of $2H_2 + O_2$ reaction with Pd and Ru is most pronounced as compared to Rh surface, this may be the reason for the lack of hysteresis phenomenon; this is evidently due to the chemistry of the noble metals.

In [77], PdO particles were observed by means of speed color cinematography. The particles originate in the process of oxidation of Pd surface; these partially decompose to Pd and O_2 at the temperature of flame products. This means that the

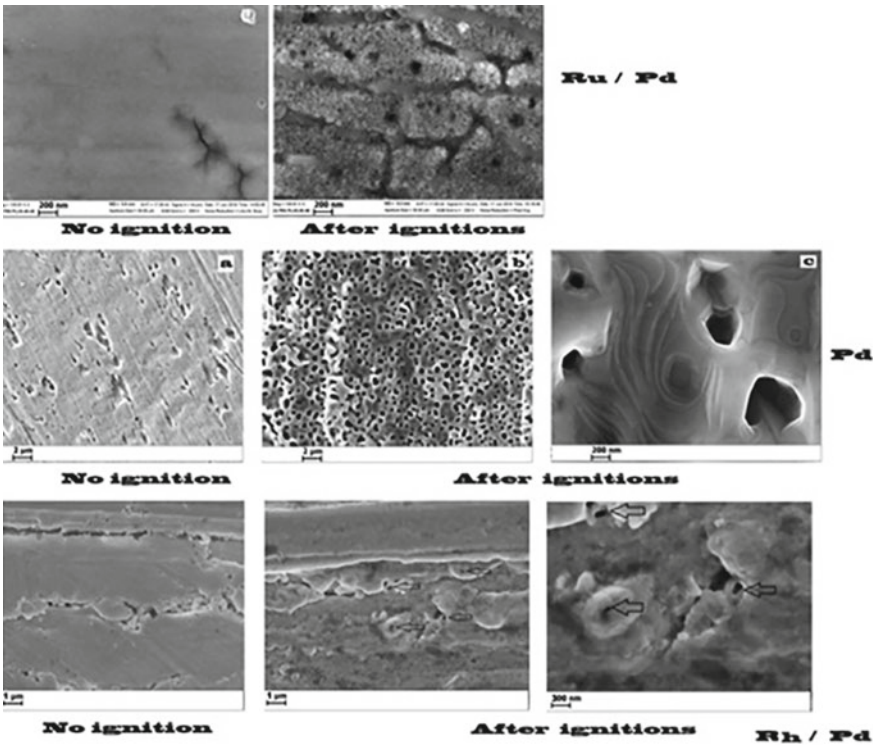

Fig. 2.36 SEM micrographs of the wire surface: of initial wire, of treated wire by 50 ignitions. Arrows indicate the etching patterns

catalyst (Pd) is consumed in the reaction of chemical etching with (most likely) active intermediates of the flame; however, the rate of this consumption is markedly smaller than in the case of Pt. As is known [78], freshly recovered ruthenium in a finely fragmented state reacts with oxygen quite intensively, warming up to the red crippling temperature. Heating the metal ruthenium under an oxygen atmosphere to a temperature of 1000 °C results in the formation of a solid RuO_2 oxide on the surface. At temperatures above 700 °C, weight losses are observed due to the formation of volatile RuO_4 oxide; thus, Ru is also consumed in the course of combustion.

As is shown in [79], rhodium, when heated in the air, has a peculiar behavior. At a temperature of 600–800 °C, an oxide Rh_2O_3 film forms on its surface. When the temperature rises from 800 to 1000 °C, the oxide film on the rhodium surface decomposes to metal and oxygen again. It means that Rh is consumed in the least degree in reaction with the intermediates of the combustion process; it agrees with the experiment presented in Fig. 2.36.

We mentioned above that there are some discrepancies in the analysis of the problem on ignition of flammable gas mixtures with a catalytic wire. In the work [65], in the experiments for determination of the catalytic ignition temperature, the flammable mixture flew slowly at atmospheric pressure around a catalytic wire or there was a stagnation flow toward a catalytic foil. The temperature of the catalyst was increased by a stepwise increase of the current applied to the catalyst, i.e. the catalyst was heated by an external source. However, in [80], the calculations of catalytic ignition temperature were compared with the data [65], which is not correct. In addition, under flow conditions the ignition temperature of H_2–O_2 mixes over Pd foil decreases for leaner mixtures [65]; this feature is in agreement with calculations [65, 80]. On the contrary, under static conditions in a heated chemical reactor with a Pd wire inside, the catalytic ignition temperature of H_2–O_2 mix increases with an increase in H_2 concentration in a flammable mixture [76]. In ref. [65], the detailed mechanism of adsorption–desorption and surface oxidation of hydrogen on platinum is considered, elementary constants of 23 elementary reactions are given. It is obvious that these constants are estimates obtained from general considerations rather than experimental values; therefore, the reliability of the calculations is somewhat doubtful. In all the works considered above, as well in [54, 66] it is assumed that the temperature of the wire is uniform; this is contrary to the experiment shown in Fig. 2.31. These facts must be taken into account in the further consideration.

2.5.1.2 Observation of a Kinetic Inverse Isotope Effect in Chain Branched Ignition of $2H_2 + O_2$ and $2D_2 + O_2$ Over Rh and Pd

As it was stated above, there is the "inverse isotope effect" observed in [74] whereby heavier hydrogen isotopes have a higher critical temperature at similar H/D/T loading, in addition, heavier isotopes diffuse faster than their lighter counterparts. Below is described the detection of "kinetic inverse isotope effect", which is that $2D_2 + O_2$ mix over both, Rh and Pd deuterides, is more flammable than $2H_2 + O_2$ mix. In addition, Rh and Pd hydrides have proven to be less reactive than appropriate deuterides.

We have shown above that Rh is the most effective catalyst of $2H_2 + O_2$ ignition, the lowest limit of catalytic ignition occurs over Rh wire, the minimum temperatures of catalytic ignition limits over Ru and Pd are ~ 100° higher, their catalytic activity is approximately the same. Notice that the hysteresis phenomenon is observed over Ru, Pt and Pd wires, namely the ignition limit value measured over the wire, which is not treated with ignitions (a procedure of increasing temperature from a state of no ignition) is higher than the value measured with a procedure of decreasing temperature from a state of catalytic ignition. The ignition limit is reversible: after reactor treatment with air or O_2, the ignition limit returns to the value corresponding to a procedure of increasing temperature from a state of no ignition. It means that the catalytic surface changes its state after ignition in agreement with [16, 69, 77]. Meanwhile, as is seen in Fig. 2.35, Rh surface does not exhibit the phenomenon; the ignition limit values measured by both procedures are equal within the limits of experimental procedure error. Below are presented experimental studies of low-pressure hydrogen and deuterium combustion over Rh and Pd wires at total pressures from 10 to 180 Torr and initial temperatures of 90 ÷ 500 °C, particularly in order to compare the dependencies of flammability limits over surfaces of noble metal hydrides/deuterides on temperature.

Catalytic ignition limits in P–T coordinates [22] of catalytic ignition of $2D_2 + O_2$ mixtures in comparison with $2H_2 + O_2$ ones over Pd and Rh/Pd were determined. The dependencies are shown in Fig. 2.38. As is seen in Figs. 2.37 and 2.38, the certain procedure is needed to achieve catalytic ignition on untreated Rh/Pd wire. First, the wire was kept in the reactor filled with 500 Torr of D_2 for 2 h at 200 °C. Then the reactor was filled with the mix $2D_2 + O_2$ at given pressure and temperature (points 1, 2) and then in 10 min after gas input the reactor was pumped out. Then at the point 3 catalytic ignition occurred. Further, the pressure and temperature of each following ignition markedly decreased. It means that the material of the wire absorbed deuterium enough for ignition to occur; in this case, rhodium deuteride was evidently formed. Notice that Rh deuteride is comparably stable.

Rhodium deuteride maintains its properties after $2H_2 + O_2$ ignitions treatment. We did not observe any noticeable substitution of D by H with hydride formation, because the ignition limit of either mixture ($2H_2 + O_2$ and $2D_2 + O_2$) after $2H_2 + O_2$ ignitions kept its value for days for any given temperature from the interval investigated. As is seen in Fig. 2.37, Rh deuteride is the most active surface for both $2H_2 + O_2$ and $2D_2 + O_2$ ignitions; for the latter mix one can obtain the catalytic ignition at ~ 100 °C; $2H_2 + O_2$ mixture over Rh deuteride ignites at higher temperatures, thus, D_2 is more flammable than H_2 over Rh deuteride ("kinetic inverse isotope effect"). Notice that the hysteresis phenomenon is not observed over Rh/Pd wire. It means that the catalytic surface does not noticeably change its state and composition after ignition.

The dependencies of catalytic ignition limits of thermal/catalytic ignition of $2D_2 + O_2$ mixtures in comparison with $2H_2 + O_2$ ones over Pd are shown in Fig. 2.38.

As is seen in Fig. 2.38, a similar procedure as for Rh/Pd wire (see Fig. 2.37) must be performed to obtain catalytic ignition on untreated Pd wire. The end of the procedure means that Pd has absorbed deuterium in an amount sufficient to ignite

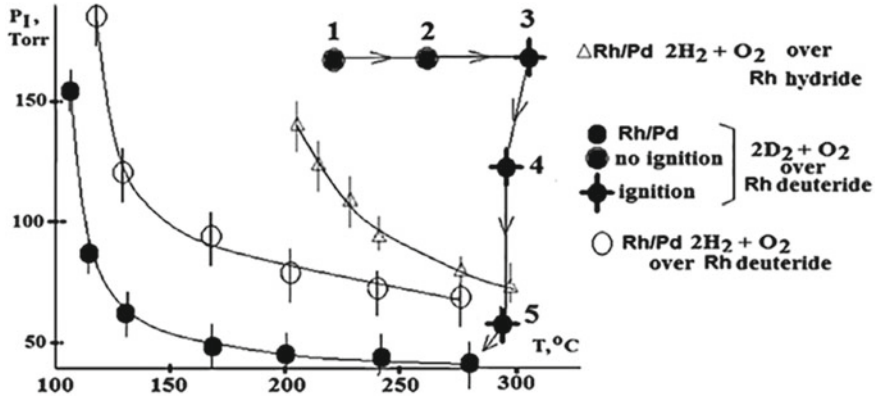

Fig. 2.37 Catalytic ignition areas of $2H_2 + O_2$ and $2D_2 + O_2$ mixes over Rh/Pd wire in pressure–temperature coordinates. To the right of each curve the ignition occurs, to the left—the ignition does not occur. Points 1–5 mean the order of processing of "fresh" Rh/Pd wire to obtain ignition. Before point 1, the wire was kept in the reactor filled with 500 Torr D_2 for 2 h at 200 °C

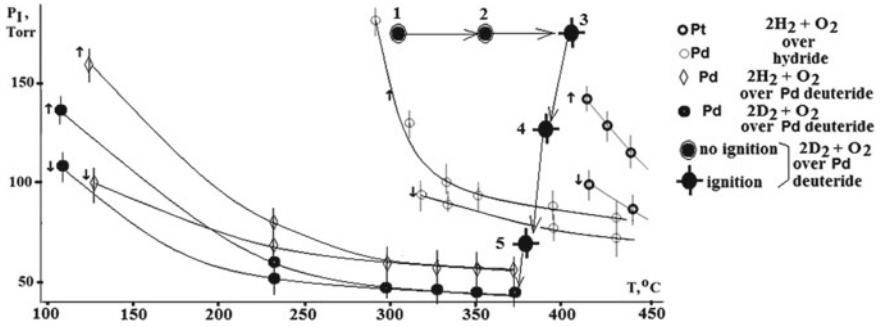

Fig. 2.38 Catalytic ignition areas of $2H_2 + O_2$ and $2D_2 + O_2$ mixes over Pd wire in pressure–temperature coordinates. To the right of each curve the ignition occurs, to the left—the ignition does not occur. Points 1–5 mean the order of processing of "fresh" Pd wire to obtain ignition. Before point 1, the wire was kept in the reactor filled with 500 Torr D_2 for 2 h at 200 °C

a flammable mixture; in this case, palladium deuteride was formed. Pd deuteride is also comparably stable. It maintains its properties after treatment with tens $2H_2 + O_2$ ignitions. Any substitution of D atoms by H ones with hydride formation was not observed; pressure ignition limit of either mixture ($2H_2 + O_2$ and $2D_2 + O_2$) after $2H_2 + O_2$ ignitions kept its value for days for any given temperature from the interval investigated.

As is seen in Fig. 2.38, Pd deuteride is also the most effective catalyst of $2H_2 + O_2$ ignition, whereas the lowest ignition temperature of $2D_2 + O_2$ over Pd deuteride is 110 °C for total pressures < 200 Torr. As in the case of Rh deuteride, $2H_2 + O_2$ mixture over Pd deuteride ignites at higher temperature. Notice that the hysteresis

phenomenon is now observed over Pd deuteride; the limit values of both $2H_2 + O_2$ and $2D_2 + O_2$ ignition measured with a procedure of increasing temperature from a state of no ignition are higher than the value measured with a procedure of decreasing temperature from a state of catalytic ignition. The ignition limit is reversible: after reactor treatment with O_2, the ignition limit returns to the highest value corresponding to a procedure of increasing temperature from a state of no ignition, i.e. the catalytic surface changes its state after ignition. However, hysteresis phenomenon is weakly expressed: at 300 °C the values of ignition limits determined with a procedure of increasing temperature from a state of no ignition and with a procedure of decreasing temperature from a state of catalytic ignition are almost equal.

The most interesting result is that $2D_2 + O_2$ mix over both, Rh and Pd deuterides, is more flammable than $2H_2 + O_2$ mix. In addition, Rh and Pd hydrides have proven to be less active than appropriate deuterides. The results obtained indicate the existence of a "kinetic inverse isotope effect", which affects the reactivity of MeH and MeD, where Me = Rh, Pd. Nevertheless, the revealed feature is not due to gas ignition, because the rate constant of chain branching in $D_2 + O_2$ процесce ignition ($D + O_2 \rightarrow OD + O$; $k = 9.10^{13} \exp(-7500/T)$ cm^3/ molecule s) is smaller than in $H_2 + O_2$ ignition ($H + O_2 \rightarrow OH + O$; $k = 2.10^{14} \exp(-8450/T)$ cm^3/molecule s) [81].

It is worthwhile to indicate experimental patterns, specific to static conditions, which should be considered in the course of the calculations. First, as is shown above, the heterogeneous chain termination on the reactor walls should be taken into account, therefore, the branching chain ignition mechanism in gaseous phase [22] should be considered. Second, a reversible change in the state of the catalytic surface after ignitions should be accounted for, because this causes the changes in the values of ignition limits and delay periods of ignition. In addition, the observed occurrence of local ignition centers on the catalytic wire, which initiate propagation of the gaseous reaction front, allows use of the analytical solution of the problem on the local ignition based on a thermal explosion of the flat P-shaped center of a warming up (hot spot) in a chain-branched gas reaction [82].

It should be also noted that the catalytic ignition limit is very sensitive to the nature of the atoms (H or D), which are embedded in a crystal lattice of the noble metal, and, accordingly, these must be present on the catalytic surface, which initiates the reaction. Such a feature is characteristic of the chain process, so the reaction on the surface was modeled below as a chain one. In addition, we specially checked that the modeling using the only simple exothermic Arrhenius reaction on the surface could not provide the results obtained below in the numerical simulation. Furthermore, the occurrence of local ignition centers on the wire, and the dark catalytic reaction of the consumption of $2H_2 + O_2$ mixture should be accounted for.

It should be noted that at the current state of experiment any comparison of the results of numerical calculations with experimental data is reliable only in qualitative aspect, e.g. on the qualitative modeling of time dependencies of experimentally measured velocities, concentrations etc. The examination of the detailed kinetic mechanism introduces additional uncertainty into modeling. A large part of kinetic parameters is not accurate enough to draw reasonable conclusions using calculations. The issue of completeness of the used reaction set is always an open question, i.e.

an important reaction can be overlooked. Moreover, as there are no unicity theorems on reactive compressible Navier–Stokes equations, which are used very often for combustion modeling in low Mach approximation, the agreement between calculated quantities and experimental ones does not argue for accord between calculation and experiment, as there can be other sets of the governing parameters describing the same dependencies [16].

We attempted to illustrate qualitatively some above-mentioned factors in consideration of the catalytic ignition with catalytically heated wire by means of numerical modeling using the system of compressible dimensionless reactive Navier–Stokes equations in low Mach number approximation. The aim was to interpret the occurrence of the dark reaction and ignition modes as well as the occurrence of local ignition centers on the catalytic wire in the case of the catalytic ignition (see Appendix). The catalytic wire was simulated by a rectangular region in the middle of the reactor as represented in Fig. 2.39. The parameters, initial and boundary conditions are given in the Appendix. The results of the calculation with the package FlexPDE 6.08, 1996–2008 PDE Solutions Inc. [83] of the reaction sets (1, 2 see Appendix) are shown in Fig. 2.39.

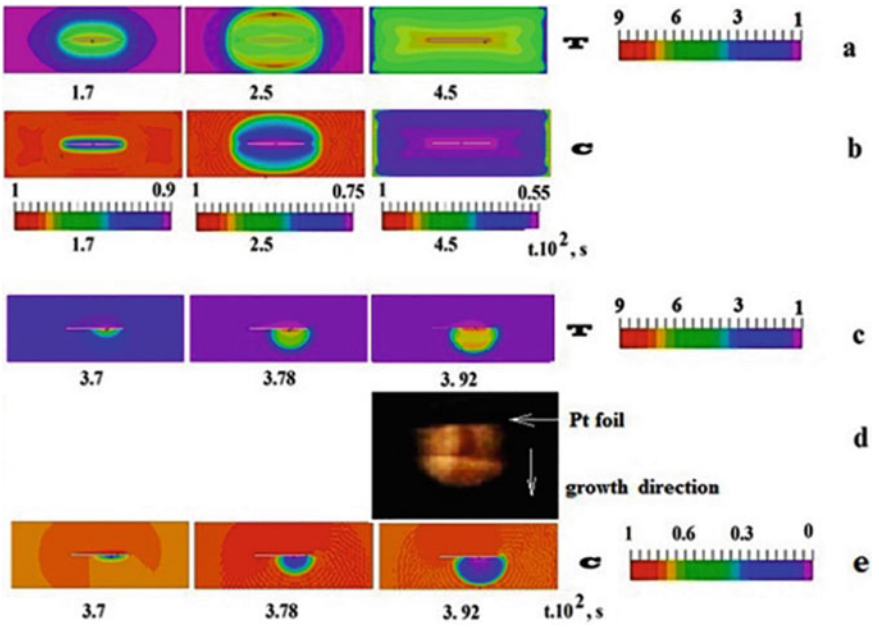

Fig. 2.39 Numerical simulation of ignition on catalytic wire. **a** change of dimensionless temperature for dark reaction, **b** change of dimensionless concentration of the initial reagent C for dark reaction $T_0 = 1$; **c** change of dimensionless temperature T for ignition, **d** photo of the growing ignition center on the Pt foil ([16], Fig. 11.3); other parameters are given in the text, **e** change of dimensionless concentration C for dark reaction $T_0 = 2$. Scales of dimensionless temperature and concentration are shown on the right; for the dark reaction scales of dimensionless concentration are shown below Fig. 2.39b)

As is seen in Fig. 2.39, the main observed features of the catalytic ignition are qualitatively illustrated: in the dark reaction, the rate of consumption of initial reagent is slower than during the ignition; the occurrence of local ignition centers on the catalytic wire in the case of the ignition is modeled. The dynamics of the growing of the ignition center is perfectly consistent with the experiment, cp. the experimental frame from [16] and the computed T front at 0.0392 s. Thus, the qualitative model allows obtaining both, the mode of the emergence of the primary ignition centers on the wire followed by a local ignition, and the mode of a dark catalytic reaction of the consumption of the initial reagent C.

Let's briefly summarize the obtained results. Hydrogen and deuterium combustion over Rh, Ru, Pd and Pt wires at total pressures up to 200 Torr and initial temperatures up to 500 °C was investigated in order both to establish the dependencies of catalytic ignition limits over noble metal surfaces on temperature and to indicate the governing factors of the problem of gas ignition by a catalytic surface. It was revealed that Rh, Ru and Pd surfaces treated with $2H_2 + O_2$ ignitions show the defects in the form of openings, which are located on etching patterns; the etching substances are active intermediates of H_2 oxidation. It was found that before ignition catalytic wire is not heated up uniformly; initial local centers of the ignition occur. It was shown that Rh is the most effective catalyst of $2H_2 + O_2$ ignition, the lowest ignition temperature over Rh coated Pd wire (Rh/Pd) was 210° C, for Ru/Pd and Pd—300 °C, for Pt wire—410 °C at total pressures less than 200 Torr. The hysteresis phenomenon is observed over Ru/Pd, Pt and Pd wires; namely the ignition limit value measured over the wire, which is not treated with ignitions (a procedure of increasing temperature from a state of no ignition), is higher than the value measured with a procedure of decreasing temperature from a state of catalytic ignition. It was shown that Rh is the most effective catalyst of $2D_2 + O_2$ ignition, in this case the lowest ignition temperature over Rh coated Pd wire (Rh/Pd) was 100 °C. It is more accurate to speak about ignition over noble metals hydrides/deuterides; thus, the lower ignition limit of $2D_2 + O_2$ over rhodium deuteride was 100° C; thus, D_2 is more flammable than H_2 over Rh and Pd. The obtained results indicate the existence of a "kinetic inverse isotope effect", which affects the reactivity of MeH and MeD, where Me = Rh, Pd.

2.6 Conclusions

A cellular combustion regime of 40% H_2–air mixture in the presence of Pt wire over the interval 270–350 °C was observed for the first time. It is shown that the regime is caused by the catalytic action of Pt containing particles formed by decomposition of volatile platinum oxide in the gas phase.

It was shown that the temperature of the initiated ignition at 40 Torr over heated Pd foil is ~ 100 °C lower than over Pt foil. Even the minimum temperature value of the foil (623 °C) is sufficient to ignite $2H_2 + O_2$ mixture; i.e., the influence of a catalytic $H_2 + O_2$ reaction with desorption of active intermediates from the surface of noble metals is negligible in case of initiated ignition. The presence of water

vapor prevents ignition. For thermal ignition at 180 Torr and 288 °C over Pd foil the catalytic activity of the surface is higher than that over Pt foil. The activity of Pd foil reveals itself in both the occurrence of local ignition centers on the foil, from which combustion wave propagates; and the dark catalytic reaction of consumption of the flammable mixture.

It was shown that in the reaction of hydrogen combustion metallic Pt acts as a heat source similar to e.g. a tungsten wire heated by an external source. However, in the case under investigation, Pt is heated with an internal source, namely a surface catalytic reaction. It must be also taken into account that the composition of the surface layer changes during ignitions from Pt oxide (PtO_2) to another composition, exhibiting properties different from PtO_2.

Hydrogen and deuterium combustion over Rh, Ru, Pd and Pt wires at total pressures up to 200 Torr and initial temperatures up to 500 °C was investigated in order both to establish the dependencies of catalytic ignition limits over noble metal surfaces on temperature and to indicate the governing factors of the problem of gas ignition by a catalytic surface. It was revealed that Rh, Ru and Pd surfaces treated with $2H_2 + O_2$ ignitions show the defects in the form of openings, which are located on etching patterns; the etching substances are active intermediates of H_2 oxidation. It was found that before ignition, catalytic wire is not heated up uniformly; initial centers of the ignition occur. It was shown that Rh is the most effective catalyst of $2H_2 + O_2$ ignition, the lowest ignition temperature over Rh coated Pd wire (Rh/Pd) was 210 °C, for Ru/Pd and Pd—300 °C, for Pt wire—410 °C at total pressures less than 200 Torr. The hysteresis phenomenon is observed over Ru/Pd, Pt and Pd wires; namely the ignition limit value measured over the wire, which is not treated with ignitions (a procedure of increasing temperature from a state of no ignition), is higher than the value measured with a procedure of decreasing temperature from a state of catalytic ignition. It was shown that Rh is the most effective catalyst of $2D_2 + O_2$ ignition, in this case the lowest ignition temperature over Rh coated Pd wire (Rh/Pd) was 100 °C. It is more accurate to speak about ignition over noble metals hydrides/deuterides; thus, the lowest ignition limit of $2D_2 + O_2$ over rhodium deuteride was 100 °C; thus, D_2 is more flammable than H_2 over Rh and Pd. The obtained results indicate the existence of a "kinetic inverse isotope effect", which affects the reactivity of MeH and MeD, where Me = Rh, Pd.

It was shown that the initiation of the thermal ignition process is always determined by the presence of reactive centers on the surface, the properties of which are determined by both, surface defects having an excess of free energy, and their catalytic properties; the ignition process includes the stages of warming-up, local ignition, and flame propagation. The chemical activity of various sites of the surface changes from one ignition to another. The basic feature of ignition process lies in the fact that ignition occurs at separate sites of the surface at uniform temperature of the reactor surface. Therefore, combustion originates on the surface of the reactor even under conditions of almost homogeneous warming up of a flammable gas mixture. It was found that the qualitative model based on the reactive compressible Navier–Stokes equations allows obtaining both the mode of the emergence of primary ignition

centers on the wire followed by a local ignition, and the mode of a dark catalytic reaction of the consumption of the initial reagent.

Appendix

We approximately illustrated the observed regularities by means of numerical modelling using 2D compressible dimensionless reactive Navier–Stokes equations in low Mach number approximation [84] suggested in [84–88]. The equations showed a qualitative agreement with experiments [16, 86].

The approximation of a small Mach number is obtained from the Navier–Stokes equations for a compressible medium by expanding each variable in a series in powers of γM^2, where is the γ adiabatic exponent and M is the Mach number. For each variable, the lowest order term is retained, with the exception of pressure P, which is divided into two components: thermodynamic pressure $P_0(t)$, homogeneous in space, and the hydrodynamic pressure $p_2(x, y, t)$: $P = P_0(t) + \gamma M^2 p_2(x, y, t) + O(M^3)$, where P_0 is calculated as in [88]. Density ρ, temperature T, pressure P and concentration C were nondimentionalized according to their initial values: ρ_0, T_0, $P_0 = \rho_0 R T_0$, C_0. This system is presented below and describes the propagation of a flame in a two-dimensional area. Compressible dimensionless reactive Navier–Stokes equations in low Mach number approximation take the following form. Indexes t, x, y mean differentiation on t, x, y.

$$
\begin{aligned}
&\rho \mathrm{T} = P && \text{(a)}\\
&\rho_{\mathrm{t}} + (\rho \mathrm{v})_{\mathrm{y}} + (\mathrm{pu})_{\mathrm{x}} = 0 && \text{(b)}\\
&\rho\left(\mathrm{u}_t + \mathrm{v}\mathrm{u}_{\mathrm{y}} + \mathrm{u}\mathrm{v}_{\mathrm{x}}\right) + P_y/\gamma M^2 = 1/\mathrm{Fr} + \mathrm{Sc}\left(\nabla^2 \mathrm{v} + 1/3\, K_y\right) && \text{(c)}\\
&\rho\left(\mathrm{v}_t + \mathrm{v}\mathrm{u}_{\mathrm{y}} + \mathrm{u}\mathrm{u}_{\mathrm{x}}\right) + P_x/\gamma M^2 = 1/\mathrm{Fr} + \mathrm{Sc}\left(\nabla^2 \mathrm{u} + 1/3\, K_x\right) && \text{(d)}\\
&\rho\left[T_t + \mathrm{v}T_y + \mathrm{u}\,\mathrm{T}_{\mathrm{x}}\right] - (\gamma - 1)/\gamma P_t - (\gamma - 1)/\gamma M^2\left[P_t + \mathrm{u}P_x + \mathrm{v}P_y\right] = \nabla^2 T + \beta_1 \mathrm{W} && \text{(e)}\\
&\rho\left[\mathrm{C}_t + \mathrm{v}C_y + \mathrm{u}C_{\mathrm{x}}\right] = \nabla^2 \mathrm{C} - \beta \mathrm{W} && \text{(f)}\\
&\mathrm{W} = (1 - \mathrm{C}) \exp(\zeta - \zeta/\mathrm{T}) && \text{(g)}\\
&\mathrm{P}_{\mathrm{tt}} - 1/\mathrm{M}^2 \nabla^2 P = \mathrm{q}(C_P - 1)\beta_1 \mathrm{W}_{\mathrm{t}} && \text{(h)}
\end{aligned}
\tag{2.1}
$$

where $\nabla^2 = (\ldots)_{yy} + (\ldots)_{xx}$ is the two-dimensional Laplace operator, $K^v = v_y + u_x$ is the viscous dissipation $P_{tt} = \mathrm{d}^2 P/\mathrm{d}t^2$, $\mathrm{d}(\ldots)/\mathrm{d}t$ is a material derivative, u and v are the velocity components in the directions x, y, respectively, ρ is the density and T is the temperature.

The chemical reaction is presented in the set (2.1) by a single first order Arrhenius reaction. C—reagent concentration, 1-C—extent of transformation, ζ—dimensionless coefficient proportional to E/R. Dimensionless parameters—Schmidt's criterion $\mathrm{Sc} = \nu/\mathrm{D}$, D—diffusivity (0.3 cm^2/s at 1 atm [89]), ν—gas kinematical viscosity (10^{-5} cm^2/s [89]),γ—adiabatic exponent—relation of constant pressure and constant volume thermal capacities; β_1 the nondimensional amount of heat released in the reaction, β is a kinetic coefficient proportional to Damköhler number. The initial values

are the following: $\rho_0 = 0.001$ g/cm^3 [89], $T_0 = 1$, $P_0 = \rho_0 T_0$, $\zeta = 10.5$, $\gamma = 1.4$, $\beta = 0.2$, $\beta_1 = 0.3$, Cp = 0.3 kal/g grad [89] and $C_0 = 0$, respectively. These values were used for calculations in Fig. 2.39. Lewis number is equal to Le = 1 that assumes equality of Sc = Pr where Pr = ρ_0Cp ν/λ, λ—heat conductivity and Cp—thermal capacity at constant pressure. Scales of length and speed are determined as $l_d^2 = Dt_d$, and $U_d = l_d/t_d$, respectively. Then Reynolds number is $l_d U_d/\nu = 1/Sc$. Froude number $Fr = U_d^2/gl_d$ where g—acceleration of a free fall, is accepted equal zero. Mach number is $M = U_d/c_0$; it is accepted equal 0.025, where c_0—the speed of sound. It is obvious that if M = 0, fluctuations of pressure are missing. At $M \to 0$ the reference value of average pressure of P_0 becomes much higher, than the average value $\rho_0 U_d^2$ for pressure fluctuations at the average pressure P_0. The velocity field is determined by these fluctuations. If the standard representation of pressure is used, then usual replacement of variables $P = P_0 p$ leads to occurrence of a factor $1/M^2$ in the term *grad p* in the impulse equation [88]. It is accepted that pressure values satisfy wave equation [the last equation (h) of the set (2.1)], which can be obtained from the continuity and impulse equations taking into account internal power sources and neglecting terms of order $1/M^4$ [90]. The equation (h) of the set (2.1), describing waves in the moving non-uniform media with a heat source, follows from continuity and impulse equations ($q = l_d^2 / (U_d^4 \rho_0) \sim 1$—the parameter arising at the reduction to a dimensionless form). In order that the quantity of the equations corresponds to the number of unknowns, eq (b) is excluded from the set (2.1) in the further analysis.

Due to the surface chemical reaction, a natural convective flow occurs around the wire, which is accounted for with Navier–Stokes equations. Thus, the following reaction set rather than simple Arrhenius reaction was analyzed. The reaction velocity in the volume was presented by an elementary chain mechanism: $C \to 2n$ (w0) and $n + C \to 3n +$ products. w0 can be neglected [91]. In this case, the equations f, g (see set (2.1) Appendix) were replaced with the following ones: (initial condition for concentration changes to $C_0 = 1$).

$$\rho\left[C_t + vC_y + uC_x\right] = \Delta^2 C - \beta_0 nW$$
$$\rho\left[n_t + v\,n_y + u\,n_x\right] = \Delta^2 n + 2\beta_0 nW$$

$W = C \exp(\zeta\text{-}\zeta/T)$—volume reaction.

$W_1 = C \exp(\zeta_1\text{-}\zeta_1/T)$—surface reaction

The catalytic wire was simulated by a rectangular region in the middle of the reactor as is shown in Fig. 2.39. Chemical exothermic branching reaction occurred on the boundaries of the "wire", boundary conditions on the "wire" took the form $T_t = \delta\beta_1 W_1$ (heat release), $n_t = \delta\beta W_1$ (surface propagation, not necessarily branching), $C_t = 0.2C$ (adsorption of the initial reagent); δ- the scale coefficient, which determined only the duration of the calculations. n = 0 (heterogeneous chain termination) was set on the reactor walls, $C_t = 0$, $T_t = T_0$. The parameters were assumed to be $\zeta = 7.5$ (close to activation energies of the branching reactions of H_2 and D_2 volume

oxidation), $\zeta_1 = 1.5$ (the estimate of the value was obtained in Refs. [16, 76]), $\beta = 0.15$, $\beta_1 = 0.22$, diffusivity $D_n = 0.9$. The initial temperature of the gas was given with initial conditions: $T_0 = 1$ for dark reaction, $T_0 = 2$ for ignition.

The solution of the problem was carried out by finite element analysis using software package (FlexPDE 6.08, 1996-2008 PDE Solutions Inc. [83]).

References

1. C. Appel, J. Mantzaras, R.Schaeren R. Bombach, A. Inauen, Catalytic combustion of hydrogen–air mixtures over platinum: validation of hetero-homogeneous reaction schemes. Clean Air. **5**(1), 21 (2004). https://doi.org/10.1615/InterJEnerCleanEnv.v5.N1.20
2. J.C. Chaston, Reaction of oxygen with the platinum metals. The oxidation of platinum. Platinum Metals Rev. **8**(2), 50 (1964)
3. N.M. Rubtsov, B.S. Seplyarskii, K. Ya Troshin, V.I. Chernysh, G.I. Tsvetkov, Investigation into spontaneous ignition of hydrogen–air mixtures in a heated reactor at atmospheric pressure by high-speed cinematography. Mendeleev Commun. **22**(4), 222 (2012). https://doi.org/10.1016/j.mencom.2012.07.001
4. D.L. Perry, S. Phillips, Handbook of inorganic compounds (CRC Press, 1995), p. 296
5. *Chemistry Foundations and Applications*, 3, ed. by J.J. Lagowski (Thomson Gale, 2004), p. 267
6. Y.B. Zel'dovich, G.I. Barenblatt, V.B. Librovich, G.M. Machviladze, The mathematical theory of combustion and explosions (2011). https://doi.org/10.1007/978-1-4613-2349-5, Corpus ID 91204935
7. A.A. Borisov, N.M. Rubtsov., G.I. Skachkov, K.Y. Troshin. Gas phase spontaneous ignition of hydrocarbons. Russ. J. Phys. Chem. B. **6**(4), 517 (2012). https://doi.org/10.1134/S1990793112080040
8. K.Y. Troshin, I.O. Shamshin, V.A. Smetanuik, A.A. Borisov, Self-ignition and combustion of gas mixtures in the volume with vortex flow. Russ. J. Phys. Chem. B **11**, 952 (2017)
9. N.M. Rubtsov, B.S. Seplyarskii, K.Y. Troshin, G.I. Tsvetkov, V.I. Chernysh, High-speed color cinematography of the spontaneous ignition of propane–air and n-pentane–air mixtures. Mendeleev Commun. **21**(1), 31 (2011). https://doi.org/10.1016/j.mencom. 2011. 01. 013
10. A. Khalil, A.K. Gupta, Dual injection distributed combustion for gas turbine application. J. Energy Resources and Technology, **136**(1), 0116012014. https://doi.org/10.1115/1.4025020
11. A. Khalil, A.K. Gupta, K.M. Bryden, S.C. Lee mixture preparation effects on distributed combustion for gas turbine application. J. Energy Resources and Technology **134**(3), 032201 (2012). https://doi.org/10.1115/1.4006481
12. I.D. Rodionov, A.I. Rodionov, L.A. Vedeshin, V.V. Egorov, A.P. Kalinin, Airborne hyperspectral systems for solving remote sensing problems. Izvestiya Atmospheric and Oceanic Physics **50**(9), 989 (2014). https://doi.org/10.1134/S0001433814090175
13. A.P. Kalinin, A.G. Orlov, A.I. Rodionov, K.Y. Troshin, Demonstration of the possibilities to study combustion and explosion processes on the base of hyperspectral remote sensing. Physical-Chemical Kinetics in Gas Dynamics **8** (2009). http://chemphys.edu.ru/issues/2009-8/articles/202/
14. Vision system overview, C&PS Flight Technical Services (2013). https://www.mygdc.com/assets/public_files/gdc_services/pilot_services/presentations/Vision_Systems_Overview.pdf
15. N.M. Rubtsov, B.S. Seplyarskii, K.Y. Troshin, G.I. Tsvetkov, V.I. Chernysh, High-speed colour cinematography of the spontaneous ignition of propane–air and n-pentane–air mixtures. Mendeleev Commun. **21**, 31 (2011)
16. N.M. Rubtsov, The modes of gaseous combustion (Springer International Publishing, 2015). https://doi.org/10.1007/978-3-319-25933-8

17. N.M. Rubtsov, B.S. Seplyarskii, K.Y. Troshin, G.I. Tsvetkov, V.I. Chernysh, Initiation and propagation of laminar spherical flames at atmospheric pressure. Mendeleev Commun. **21**(4), 218 (2011). https://doi.org/10.1016/j.mencom.2011.07.016
18. R. Pierse, A. Gaydon, The identification of molecular spectra (Academic Press, London, 1941)
19. T. Icitaga, Emission spectrum of the oxy-hydrogen flame and its reaction mechanism. Formation of the activated water molecule in higher vibrational states. The Review of Physical Chemistry of Japan **13f**(2), 96 (1939)
20. P. Stamatoglou, Master Thesis, Lund University (2014)
21. NIST Atomic Spectra Database. http://physics.nist.gov/PhysRefData/ASD/lines_form
22. B. Lewis, G. Von Elbe, Combustion, explosions and flame in gases (Academic Press, London, 1987)
23. V.M Maltsev, M.I. Maltsev, L.Y Kashporov, Osnovnyye kharakteristiki goreniya (Basic combustion characteristics) (Moscow: Chemistry, 1977)
24. H.L. Thomas, Trace elements in Al-Si foundry alloys. Dissertation, Norwegian University of Science and Technology (2013)
25. W. Meyerriecks, K.L. Kosanke, Color values and spectra of the principal emitters in colored flames. Journal of Pyrotechnics **18**, 720 (2003)
26. S.G. Saytzev, R.I. Soloukhin, Study of combustion of adiabatically heated gas mixture, in *Proceedings of 8th Symposium (Int.) on Combustion* (The Combust. Inst., Pittsburgh, 1962), p. 2771
27. R.K. Eckhoff, *Dust Explosions in the Process Industries*, 3rd edn. (Gulf Professional Publishing/Elsevier, Boston, 2003)
28. J.C. Livengood, W.A. Leary, Catalytic ignition by rapid compression. Ind. Eng. Chem. **43**(12), 2797 (1951)
29. T.C. Germann, W.H. Miller, Quantum mechanical pressure dependent reaction and recombination rates for OH + O →O_2 + H. J. Phys. Chem. A **101**, 6358 (1997)
30. D.A. Frank-Kamenetsky, *Diffusion and Heat Transfer in Chemical Kinetics* (Plenum Press, 1969)
31. S. Chu, A. Majumdar, Opportunities and challenges for sustainable energy feature. Nature **488**, 294 (2012)
32. P.E. Dodds, I. Staffell, A.D. Hawkes, F. Li, P. Grünewald, W. McDowall, P. Ekins, Hydrogen and fuel cell technologies for heating. A review. Int. J. Hydrogen Energy **40**, 2065 (2015)
33. D. Sil, J. Hines, U. Udeoyo, E. Borguet, Palladium nanoparticle-based surfaceacoustic wave hydrogen sensor. ACS Appl. Mater. Interfaces **7**, 5709 (2015)
34. A. Fernández, G.M. Arzac, U.F. Vogt, F. Hosoglu, A. Borgschulte, M.C. Jiménez de Haro, O. Montes, A. Züttel, Investigation of a Pt containing washcoat on SiC foam for hydrogen combustion applications. Appl. Catal B **180**, 336 (2016)
35. X. Wang, Y. Shi, N. Cai, X. Lu, W. Yao, Low pressure catalytic combustion of hydrogen on palladium. J. Power Energy Eng. **3**, 49 (2015)
36. S. Marco, M. John, Hetero-/homogeneous combustion of hydrogen/air mixtures over platinum: fuel-lean versus fuel-rich combustion modes. Int. J. Hydrogen Energy **38**, 10654 (2013)
37. J.F. Kramer, S.-A.S. Reihani, G.S. Jackson, Low-temperature combustion of hydrogen on supported Pd catalysts. Proc. Combust. Inst. **29**, 989 (2002)
38. J.M. Zhang, Y.P. Lu, Research on equilibrium point estimation of stratospheric balloon trajectory control system. Aerospace Control **25**, 4 (2007)
39. R.E. Hayes, S.T. Kolaczkowski, P.K.C. Li, S. Awdry, The palladium catalysed oxidation of methane: reaction kinetics and the effect of diffusion barriers. Chem. Eng. Sci. **56**, 4815 (2001)
40. N.M. Rubtsov, V.I. Chernysh, G.I. Tsvetkov, K.Y Troshin, I.O. Shamshin, Ignition of hydrogen–air mixtures over Pt at atmospheric pressure. Mendeleev Commun. **27**, 307 (2017)
41. N.M. Rubtsov, A.N. Vinogradov, A.P. Kalinin, A.I. Rodionov, K.Y. Troshin, G.I. Tsvetkov, V.I. Chernysh, Cellular combustion and delay periods of ignition of a nearly stoichiometric H_2–air mixture over a platinum surface. Mendeleev Commun. **26**, 160 (2016)
42. R.M. Marshall, C.P. Quinn, Computation of wall termination effects in gas-phase radical reactions. Trans. Faraday Soc. **61**, 2671 (1965)

43. Y. Ghermay, J. Mantzaras, R. Bombach, K. Boulouchos, Homogeneous combustion of fuel-lean $H_2/O_2/N_2$ mixtures over platinum at elevated pressures and preheats. Comb. Flame **158**, 1491 (2011)
44. M. Maestri, A. Beretta, T. Faravelli, G. Groppi, E. Tronconi, D.G. Vlachos, Two-dimensional detailed modeling of fuel-rich H_2 combustion over Rh/Al_2O_3 catalyst. Chem. Eng. Sci. **63**, 2657 (2008)
45. P.A. Bui, D.G. Vlachos, P.R. Westmoreland, Homogeneous ignition of hydrogen/air mixtures over platinum. Proc. Combust. Inst. **26**, 1763 (1996)
46. V. Seshadri, N.S. Kaisare, Simulation of hydrogen and hydrogen-assisted propane ignition in Pt catalyzed microchannel. Comb. Flame **157**, 2051 (2010)
47. A. Scarpa, P.S. Barbato, G. Landi, R. Pirone, G. Russo, Combustion of methane-hydrogen mixtures on catalytic tablets. Chem. Eng. J. **154**, 315 (2009)
48. D. Schweich, J.P. Leclerc, in *Catalysis and Automotire Pollution Control*, vol 2, ed. by A. Crucq (Elsevier, Brussels, 1990), p. 437
49. T. Schmidt in *Catalysis and Automotire Pollution Control*, vol 2, ed. by A. Crucq (Elsevier, Brussels, 1990), p 55
50. D.L. Trimm, Catalytic combustion (review). Appl. Catal. **7**(3), 249 (1983)
51. A. Schwartz, L.L. Holbrook, H. Wise, Catalytic oxidation studies with platinum and palladium. J. Catal. **21**, 199 (1971)
52. M.M. Slin'ko, N.I. Jaeger, *Oscillating Heterogeneous Catalytic Systems* (Elsevier, Amsterdam, 1994)
53. S.W. Weller, C.G. Rader, Ignition on catalytic wires: kinetic parameter determination by the heated-wire technique. AIChE J. **21**, 176 (1975)
54. M. Rinnemo, O. Deutschmann, F. Behrendt, B. Kasemo, Experimental and numerical investigation of the catalytic ignition of mixtures of hydrogen and oxygen on platinum. Comb. Flame **111**, 312 (1997)
55. N.M. Rubtsov, A.N. Vinogradov, A.P. Kalinin, A.I. Rodionov, I.D. Rodionov, K.Y. Troshin, G.I. Tsvetkov, V.I. Chernysh, High speed multidimensional optical complex in research of ignition and combustion features of 40% H_2–air mix in the presence of platinum. Physical-Chemical Kinetics in Gas Dynamics **17**(1) (2016). http://chemphys.edu.ru/issues/2016-17-1/articles/615
56. M. Fisher, Safety aspects of hydrogen combustion in hydrogen energy-systems. Int. J. Hydrogen Energy **11**, 593 (1986)
57. T. Ozgur, E. Tosun, C. Ozgur, G. Tuccari, K. Aydin, Numerical studies of engine performance, emission and combustion characteristics of a diesel engine fuelled with hydrogen blends. Adv. Mat. Research **1016**, 582 (2014)
58. K. Persson, L.D. Pfefferle, W. Schwartz, A. Ersson, S.G. Jaras, Stability of palladium-based catalysts during catalytic combustion of methane: the influence of water. Applied Catal. B: Environmental **74**, 242 (2007)
59. A.W. Petrov, D. Ferri, M. Tarik, O. Kröcher, J.A. van Bokhoven, Deactivation aspects of methane oxidation catalysts based on palladium and ZSM-5. Top. Catal. **60**, 123 (2017)
60. N.M. Rubtsov, B.S. Seplyarskii, M.I. Alymov. Initiation and flame propagation in combustion of gases and pyrophoric metal nanostructures (Springer International Publishing, 2021)
61. R. Chaubey, S. Sahu, O.O. James, S. Maity, A review on development of industrial processes and emerging techniques for production of hydrogen from renewable and sustainable sources. Renew. Sustain. Energy Rev. **23**, 443 (2013)
62. R. Horn, K. Williams, N. Degenstein, A. Bitschlarsen, D. Dallenogare, S. Tupy et al., Methane catalytic partial oxidation on autothermal Rh and Pt foam catalysts: oxidation and reforming zones, transport effects, and approach to thermodynamic equilibrium. J. Catal. **249**, 380 (2007)
63. J. Chen, B. Liu, X. Gao, D. Xu, Production of hydrogen by methane steam reforming coupled with catalytic combustion in integrated microchannel reactors. Energies **11**, 2045 (2018)
64. J. Warnatz, M.D. Allendorf, R.J. Kee, M. Coltrin, A model of elementary chemistry and fluid mechanics in the combustion of hydrogen on platinum surfaces. Comb. Flame **96**, 393 (1994)
65. O. Deutschmann, R. Schmidt, F. Behrendt, J. Warnatz, Numerical modeling of catalytic ignition. Proc. Combust. Inst. **26**, 1747 (1996)

66. V.V. Kalinchak, A.S. Chernenko, M.V. Sikorskyi, A.N. Sofronkov, A.V. Fedorenko, Cool air-gas mixtures with combustible gas admixtures steady flameless combustion delay time on platinum particle (wire). Physics and Chemistry of Solid State **19**, 53 (2018)
67. A.P. Kalinin, N.M. Rubtsov, A.N. Vinogradov, V.V. Egorov, N.A. Matveeva, A.I. Rodionov, A.Y. Sazonov, K.Y. Troshin, G.I. Tsvetkov, V.I. Chernysh, Ignition of hydrogen-hydrocarbon (C1–C6)–air mixtures over the palladium surface at 1–2 atm. Russ. J. of Phys. Chem. B **14**, 413 (2020)
68. D. Chalet, A. Mahe, J. Migaud, J.-F. Hetet, A frequency modelling of the pressure waves in the inlet manifold of internal combustion engine. Appl. Energy **88**, 2988 (2011)
69. N.M. Rubtsov, V.I. Chernysh, G.I. Tsvetkov, K.Y. Troshin, O.I. Shamshin, Ignition of hydrogen-methane-air mixtures over Pd foil at atmospheric pressure. Mendeleev Commun. **29**, 469 (2019)
70. N.M. Rubtsov, V.I. Chernysh, G.I. Tsvetkov, K.Y. Troshin, O.I. Shamshin, The features of hydrogen ignition over Pt and Pd foils at low pressures. Mendeleev Commun. **28**, 216 (2018)
71. W.R. Williams, C.M. Marks, L.D. Schmidt, Steps in the reaction $H_2 + O_2 = H_2O$ on Pt: OH desorption at high temperature. J. Phys. Chem. **96**, 5922 (1992)
72. L. Jewell, B. Davis, Review of absorption and adsorption in the hydrogen–palladium system. Appl. Catal. A **310**, 11 (2006)
73. J.E. Worsham, M.K. Wilkinson, C.G. Shull, Neutron-diffraction observations on the palladium-hydrogen and palladium-deuterium systems. J. Phys. Chem. Solids **3**, 303 (1957)
74. M. Yussouff, B.K. Rao, P. Jena, Reverse isotope effect on the superconductivity of PdH, PdD, and PdT. Solid State Commun. **94**, 549 (1995)
75. Engineering ToolBox, Coefficients of Linear Thermal Expansion (2003). [online] Available at: https://www.engineeringtoolbox.com/linear-expansion-coefficients-d_95.html
76. N.M. Rubtsov, A.N. Vinogradov, A.P. Kalinin, A.I. Rodionov, I.D. Rodionov, K.Y. Troshin, G.I. Tsvetkov, V.I. Chernysh, Study of combustion of hydrogen–air and hydrogen–methane–air mixtures over the palladium metal surface using a hyperspectral sensor and high-speed color filming. Russ. J. Phys. Chem. B **13**, 305 (2019)
77. N.M. Rubtsov, M.I. Alymov, A.P. Kalinin, A.N. Vinogradov, A.N. Rodionov, K.Y. Troshin, Distancionnoe issledovanie processov gorenia i vzryva na osnove optoelektronnych metodov (Remote investigation of combustion and explosion processes based on optoelectronic methods) (KuBiK pulishing, Saratov, 2019)
78. C. Mun, L. Cantrel, C .Madic, A literature review on ruthenium behaviour in nuclear power plant severe accidents, irsn-00177621 (2007) https://hal-irsn.archives-ouvertes.fr/irsn-00177621
79. A. Carol, G.S. Mann, High-temperature oxidation of rhodium. Oxid. Met. **34**, 110 (1990)
80. C. Trevino, A. Linan, V. Kurdyumov, Catalytic ignition of hydrogen-air mixtures by a thin catalytic wire. Proc. Comb. Inst. **28**, 1359 (2000)
81. F. Wesley, Table of recommended rate constants occurring in combustion (Chemical kinetics information Centre, National bureau of standards (Washington DC, 1980)
82. N.M. Rubtsov, B.S. Seplyarski, M.I. Alymov, *Ignition and Wave Processes in Combustion of Solids* (Springer International Publishing, 2017)
83. G. Backstrom, *Simple Fields of Physics by Finite Element Analysis* (GB Publishing, 2005)
84. T. Alasard, Low Mach number limit of the full Navier-Stokes equations. Arch. Ration. Mech. Anal. **180**, 1 (2006)
85. A. Majda, *Equations for Low Mach Number Combustion* (Center of Pure and Applied Mathematics, University of California, Berkeley, PAM-112, 1982)
86. N.M. Rubtsov, I.M. Naboko, B.S. Seplyarskii, V.I. Chernysh, G.I. Tsvetkov, Non-steady propagation of single and counter hydrogen and methane flames in initially motionless gas. Mendeleev Commun. **24**, 308 (2014)
87. V. Akkerman, V. Bychkov, A. Petchenko, L.-E. Eriksson, Accelerating flames in cylindrical tubes with nonslip at the walls. Comb. Flame **145**, 206 (2006)
88. F. Nicoud, Conservative high-order finite-difference schemes for low-Mach number flows. J. of Computational Physics **158**, 71 (2000)
89. Tablitsy fizicheskich velichin (Tables of Physical Values), ed. by I.K. Kikoin (Atomizdat, Moscow, 1976)

90. M.J. Lighthill, On sound generated aerodynamically. II. Turbulence as a source of sound. Proc. R. Soc. Lond. A **222**, 11 (1954)
91. V.S. Posvyanskii, Skorost I predely rasprostranenia izotermicheskich plamen (Velocity and Propagation Limits of Isothermal Flames), Dissertation, Moscow: Inst. of Chemical Physics USSR (1976)

Chapter 3
Regularities of Combustion of Hydrogen–Hydrocarbon (C1–C6)–Air and Hydrocarbon–Air Mixtures Over Surfaces of Noble Metals

Abstract This chapter is focused on the establishment on the features of catalytic ignition of the mixtures of H_2 + C_1–C_6 hydrocarbons + O_2/air with platinum, palladium and rhodium. The tendencies in combustion of hydrogen and mixtures of hydrogen with methane over metallic Pd, including the use of an optoelectronic complex based on a hyperspectral sensor and high-speed color filming were revealed. We showed that the cellular structure of the flame front during ignition in the presence of Pd wire is missing in contrast to the results obtained for the Pt surface. It means that Pd is more suitable than Pt for hydrogen recombiners in nuclear power plants because the catalytic particles do not appear in the gas phase. The experimental value of the effective activation energy of the process over Pd was estimated as (3.5 ± 1) kcal/mol, which is characteristic of surface processes. This indicates the significant role of the dark reaction of H_2 and O_2 consumption on the Pd surface observed directly at low pressures. The combustion of hydrogen–hydrocarbon (C1–C6, namely CH_4, C_2H_6, C_3H_8, C_4H_{10}, C_5H_{12}, C_6H_{14})–air mixtures with $\theta = 0.6$–1.2 over Pd at total pressures 1–2 atm was investigated. It was experimentally shown that the temperature of the ignition limit over Pd at $P = 1.75$ atm, measured with a bottom-up approach by temperature, of the mixtures 30% methane + 70% hydrogen + air ($\theta = 0.9$, $T = 317$ °C) and 30% propane + 70% H_2 + air ($\theta = 1$, $T = 106$ °C) markedly drops after subsequent ignitions to $T = 270$ °C for H_2–CH_4 mix and to $T = 32$ °C for the H_2–C_3H_8 blend. The catalytic ignition limit returns to the initial value after treatment of the reactor with O_2 or the air; i.e., a hysteresis phenomenon occurs. The ignition limit of the mixtures 30% (C2, C4, C5, C6) + 70% H_2 + air ($\theta = 0.6$, 1.1, 1.2, 1.2, correspondingly) over Pd amounts to 25–35 °C at $P = 1.75$ atm; the hysteresis effect is missing. It was found that the lean 30% C_2H_6 + 70% H_2 + air mix ($\theta = 0.6$) shows the lowest temperature of the ignition limit: 24 °C at 1 atm. The estimate of the effective activation energy of the ignition of the mixes over Pd is ~ 2.4 ± 1 kcal/mol that is characteristic of a surface process. Thus, the usage of Pd catalyst allows igniting H_2–hydrocarbon mixtures at 1–2 atm at initial room temperature without external energy sources. The features of ignition of hydrogen–oxygen and hydrogen–methane–oxygen mixes at low pressure with hot Pd, Pt, Nichrome and Kanthal wires were revealed. Numerical calculations allowed elucidating the role of an additional branching step $H + HO_2 \rightarrow 2OH$. The peculiarities of ignition of premixed stoichiometric n-pentane–air mixtures were studied in a rapid mixture

N. M. Rubtsov et al., *Catalytic Ignition of Hydrogen and Hydrogen-Hydrocarbon Blends Over Noble Metals*, Heat and Mass Transfer,
https://doi.org/10.1007/978-3-031-28416-8_3

injection static reactor in the presence of metallic Pt and Pd in the region of negative temperature coefficient (NTC). It is shown that in the absence of noble metals thermoacoustic oscillations occur within NTC region. In the presence of Pt catalyst surface, which reacts with oxygen at the flame temperature and generates catalytic centers propagating into volume, thermoacoustic regimes of thermal ignition disappear; in other words, the catalytic Pt surface eliminates a certain inhibition stage of kinetic mechanism after the occurrence of the cool flame and NTC phenomenon vanishes. The stage may be e.g. the decomposition of some intermediate peroxide on Pt surface with the formation of a more reactive radical. In the presence of the catalytic surface (Pd), which does not react at the flame temperature and does not generate catalytic centers propagating into volume, NTC phenomenon occurs. It is found out that in Pd sample treated with ignitions, the defects in the form of openings, which are focused on etching patterns, arise. In the process, PdO particles originate in the process of oxidation of Pd surface; PdO particles decompose to Pd and O_2 at the temperature of flame products. This means that Pd is spent in the reaction of chemical etching with active intermediates of combustion. It should restrict the applicability of palladium in ignition devices. Low-pressure combustion of hydrogen–methane and hydrogen–isobutene mixtures over Rh and Pd surfaces at total pressures from 80 to 180 Torr and initial temperatures of 200–500 °C was studied. It was shown that, at total pressures up to 200 Torr, the catalytic ignition areas over the Rh and Pd surfaces are larger for $2H_2 + O_2$ mixtures than for $(H_2 + CH_4)_{stoich} + O_2$ and $(H_2 + C_4H_8)_{stoich} + O_2$ mixtures; mixtures containing more than 50% hydrocarbons do not ignite. It has been shown that the dark reaction in the (80% H_2 + 20% $C_4H_8)_{stoich}$ + O_2 mixture leads to the formation of carbon nanotubes with a diameter within 10–100 nm; here noble metal acts both as a heater and catalyst.

Keywords Ignition · Hydrogen · Methane · Ethane · Propane · Butane
n-pentane · Hexane · Isobutene · Oxidation · Rhodium · Palladium · Platinum ·
Catalytic limits · Carbon nanotubes · Speed filming · Hyperspectrometer

It was found that the temperature of the catalytic ignition limit over the palladium surface at 1.75 atm for mixtures of 30% methane + 70% hydrogen + air ($\theta = 0.9$, T = 317 °C) and 30% propane + 70% hydrogen + air ($\theta = 1$, 106 °C), measured by the "bottom approach" temperature method, decreases during subsequent ignitions of the same mixtures. The flammability limit returns to the initial value after the reactor is treated with oxygen or air, i.e. hysteresis takes place. The temperature of the catalytic ignition limits of mixtures of 30% (C2, C4, C5, C6) + 70% H_2 + air ($\theta = 0.6$, 1.1, 1.2, 1.2, respectively) over the palladium surface is 19 ÷ 35 °C at 1.75 atm; there is no hysteresis. It is shown that the lean ($\theta = 0.6$) mixture of 30% ethane + 70% hydrogen + air has the lowest temperature of the ignition limit: 24 °C at 1 atm. The effective activation energy for the ignition of mixtures over palladium is estimated as ~ 2.4 ± 1 kcal/mol. It was found that the detected separation of the CH and Na emission bands in time during the combustion of a mixture of 30% propane

+ 70% H_2 + air ($\theta = 1$), is due to the occurrence of hydrodynamic instability of the flame when it touches the end of the cylindrical reactor.

It was found that the ignition temperatures of hydrogen–oxygen and hydrogen–methane–oxygen mixtures above wires of palladium, platinum, nichrome and kantal (fechral) heated by external source at a total pressure of 40 Torr increase with a decrease in the hydrogen content in the mixture; only heated palladium wire exhibits a noticeable catalytic effect. A qualitative numerical calculation made it possible to assume the role of the additional branching reaction $H + HO_2 \rightarrow 2OH$, in which a weakly active radical HO_2 is replaced by OH.

It is known that methane and oxygen on a heated platinum wire can release a significant amount of heat in a dark reaction [1]. Interest in catalytic oxidation processes and their mechanisms is constantly growing due to the broad prospects of using this technology in combustion in power generation systems [2–4], to reduce the concentration of methane in the air [5]; in the use of catalytic converters in vehicles to reduce emissions of harmful gases [6]. The issue of ensuring hydrogen safety at nuclear power plants using catalytic afterburners is a topical issue [7]. There is also a great deal of interest in catalytic partial oxidation leading to the intermediates that are critical in the synthesis of target industrial compounds.

3.1 Study of the Combustion of Hydrogen–Air and Hydrogen–Methane–Air Mixtures over the Surface of Palladium Metal with the Combined Use of a Hyperspectral Sensor and High-Speed Color Filming

The mechanism of the oxidation of hydrogen and hydrocarbons on noble metals has not yet been sufficiently understood. Experiments on isotope exchange [8] have shown that chemisorption of methane on noble metals results in the formation of adsorbed methyl or methylene radicals. Their interaction with adsorbed oxygen can lead either to direct oxidation to carbon dioxide and water or to the formation of adsorbed formaldehyde [9]. Until now, the nature of the active surface is generally unknown. In the case of palladium, oxidation can occur at the same time on the metal itself, on the surface of Pd (II) oxide, or even on the surface partially covered with adsorbed oxygen. According to X-ray photoelectron spectroscopy (XPS) data [10], the smaller the size of the palladium crystallites is, the more likely they are to exist in the oxide form. It should be noted that because of a certain degree of conversion of the reagent, a significant amount of heat can be released. This leads to a significant increase in temperature, thus, the stability of the catalyst at high operating temperatures must be known [2]. As the temperature rises, the activation energy of methane oxidation on the Pd catalyst changes sharply. The temperature, at which this transition occurs is a function of the catalyst composition [11]. It should be emphasized that noble metals form oxides, which, depending on their reactivity, determine

the rate and mechanism of the catalytic process. This significantly complicates the search for optimal conditions for catalysis. For example, Pd readily transforms into PdO at temperatures lower than 1100 K, but PtO_2 already decomposes at temperatures above 825 K. Due to the greater stability of PdO compared to PtO_2, in the case of a Pd-containing catalyst, the active phase is most likely PdO, in while in the case of a Pt catalyst, the active phase is Pt. The activity of PdO is higher than that of Pt. This allows to achieve higher conversions when using PdO. Controlling the presence of PdO in the gas phase, which is necessary to establish the mechanism of catalysis, is complicated by the fact that the spectroscopic data on PdO are scattered and contradictory [12–14]. In [15], the emission spectra of PdO obtained during the pyrolysis of polymer complexes ($PtCl_2$) upon excitation at a wavelength of 355 nm are presented. Thus, the appearance and participation of a chemically active surface in gas combustion significantly complicate the understanding of the process, not only due to the emergence of new control parameters, but also to difficulties in registering catalyst molecules or particles.

It is worth reminding that the hyperspectrometers used in this chapter and discussed in the previous chapter are the devices that allow remote registration of reflected, scattered and emitted radiation, obtaining its spectra in a wide wavelength range [16, 17]. The hyperspectrometer makes it possible to study temporal characteristics of the processes occurring on a narrow strip of the investigated surface. 4D dimension is formed by the x coordinate, the spectral coordinate—by the wavelength λ, the intensity of the spectral line I and the time t. The work [18] demonstrated the possibility of studying combustion and explosion processes using remote hyperspectral sensing.

High-speed filming is also used in this book as a remote study of various processes. In [19, 20], the method of high-speed color cinematography was used to study spark-initiated ignition of hydrogen–air and pentane–air mixtures. This method makes it possible to visualize the propagation of the flame front and reveal the features of combustion processes, in particular, the transition of a smooth flame front into a cellular structure.

This chapter is devoted to identifying the regularities of the combustion of hydrogen and mixtures of hydrogen with methane over metallic palladium, among them using an optoelectronic complex based on a hyperspectral sensor and high-speed color filming.

3.1.1 Experimental

The experiments were carried out in a heated horizontal cylindrical stainless steel reactor 25 cm in length and 12 cm in diameter, equipped with a tangential gas inlet, collapsible covers, and an optical quartz window in one of the coatings (Fig. 3.1). In experiments, in which it was required to avoid gas circulation due to the presence of a tangential inlet (Fig. 3.1), an aluminum ring with an outer diameter of 11.2 cm and

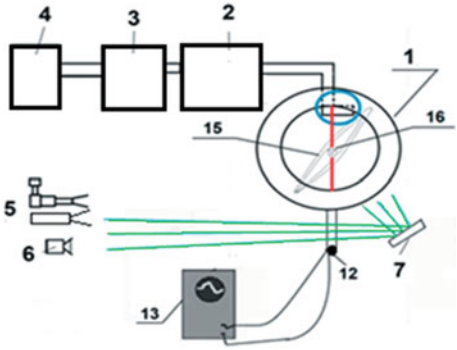

Fig. 3.1 Block diagram of the experimental setup, end view **a** and side view **b**. The strip, along which the 4D spectral survey was carried out is indicated in red. The width of this strip is about 1 mm. (1) reactor, (2) solenoid valve, (3) buffer volume, (4) gas cylinder, (5) hyperspectrometer, (6) digital video camera, (7) folding mirror, (8) internal insulation, (9) heater, (10) external insulation, (11) optical window, (12) pressure sensor, (13) ADC converter and computer for receiving and accumulating data, (14) millivoltmeter for taking thermocouple readings, (15) aluminum ring to prevent gas circulation, (16) Pd spiral, (17) Wheatstone bridge. The unit for tangential gas injection into the reactor is highlighted with a blue circle

an inner diameter of 11 cm was introduced into the reactor perpendicular to the gas flow (see also paragraph 1 of Chap. 2).

The temperature measurement accuracy was 0.3 K. The evacuated and heated to the required temperature reactor was quickly filled with a gas mixture from the high-pressure buffer volume to the required pressure. An electromagnetic valve was used to open and close gas lines. Due to a sharp pressure drop in the buffer volume and in the reactor, a gas vortex arises in the reactor, leading to a reduction in the time for establishing a uniform temperature distribution. To prevent gas circulation, an aluminum ring was introduced into the reactor perpendicular to the gas flow, as described in the first paragraph of Chap. 2. The pressure during the gas input and combustion process was recorded using a "Karat-DI" tensoresistive sensor, a signal from which was fed through an ADC to a computer. Pd wire (in a number of experiments, Pt wire) 80 mm long and 0.3 mm in diameter in the form of a spiral was placed into the reactor. This wire was used to initiate the ignition of the combustible mixture. In addition, the wire was connected as a shoulder of the Wheatstone bridge, which allowed controlling its average temperature. Before each experiment, the reactor was evacuated to 0.1 Torr. The total pressure in the reactor and the pressure in the buffer volume were monitored with a pressure gauge. We used chemically pure gases and 99.85% Pd.

The registration of the ignition and FF propagation was carried out through the optical window with VID-IK3 hyperspectrometers (see Chap. 2), BIK, as well as a color high-speed film camera Casio Exilim F1 Pro (frame rate — 1200 s^{-1} at a resolution of 336 × 96 pixels, 600 frames per second at a resolution of 432 × 192 pixels or 300 frames per second at a resolution of 512 × 384 pixels) or PHANTOM

(frame rate − 4000 s^{-1} at a resolution of 1300 × 800 pixels). The obtained data were written into the computer memory, and then they were processed. We used hyperspectrometers of both the visible and near infrared range (400–970 nm VID-IK3 [16]) and the BIK1 [17] hyperspectrometer in the wavelength range 970–1700 nm.

It is worth reminding that the optical system of the BIK hyperspectrometer is similar to the optical system of the VID-IK3 hyperspectrometer, only a diffraction grating is used as a spectral splitter.

3.1.2 Results and Discussion

The typical results of simultaneous recording of the pressure change (a) and the change in the resistance Pd of the wire (b, c) upon ignition of the mixture of 40% H_2 air at 128 °C at $P_0 = 1$ atm are shown in Fig. 3.2 a. As seen from Fig. 3.2 a, the total pressure in the reactor reaches 1 atm before ignition, i.e. ignition occurs after the completion of the gas injection. Since palladium wire does not heat up uniformly due to heat dissipation at the soldering points, the dependence of resistance on time is somewhat more inertial than the pressure curve. The vertical segment of this dependence corresponds to the change in resistance at the moment of ignition.

Temperature calibration was performed by changing the temperature of the reactor. However, the temperature measured by means of a Pd wire is the lower limit of the actual temperature of the ignition site [21]. The main result of the experiment is that the temperature of the reactor upon ignition of the mixture of 40%

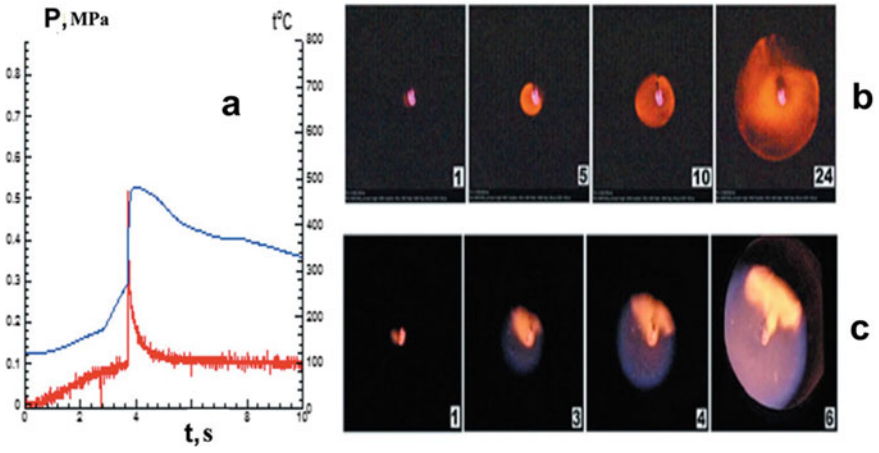

Fig. 3.2 **a** Simultaneous registration of the heating and average temperature of the Pd coil upon initiation of the ignition of the mixture of 40% H_2 with air over palladium. $T_0 = 128$ °C, $P_0 = 1.08$ atm; **b** a sequence of video frames of the initiated ignition of the mixture of 40% H_2 with air. $T_0 = 120$ °C, $P_0 = 1.25$ atm, 600 frames/s; **c** a sequence of video frames of initiated ignition of a stoichiometric mixture (80% H_2 + 20% CH_4)$_{stoich}$ + air. $T_0 = 190$ °C, $P_0 = 1.17$ atm, 600 frames/s

H_2–air over Pd (108 °C, 1 atm) is at least ~ 160 °C less than above the surface of Pt (260 °C, 1 atm, 40% H_2–air) [21]. It should be noted that the heating recorded on a Pd wire (360 °C, Fig. 3.2a) is insufficient for thermal initiation of the ignition of a 40% H_2–air mixture [21]. Thus, the contribution of surface catalytic reactions to the direct initiation of hydrogen combustion over palladium, in contrast to platinum is very noticeable. It is worth reminding that the role of catalytic processes on a Pt surface is only to heat the surface to the ignition temperature. The role of the emission of active centers from the surface is insignificant.

The spatial development of ignition and flame propagation in a 40% mixture of H_2–air and (80% H_2 + 20% $CH_4)_{stoich}$ + air was studied over a Pd wire (Fig. 3.2b, c). In the same way as in the case of Pt, Pd is heated before and after ignition due to catalytic reactions on the Pd surface. It can be seen that in the presence of a Pd wire, the cellular structure of the flame front is not observed in comparison with the results obtained on the Pt surface [22]. This is due to the greater stability of PdO in comparison with PtO_2, which decomposes even at 500 °C and is a very unstable compound [22].

The temperature dependence of the hydrogen concentration at the catalytic ignition limit was determined experimentally to reveal the contribution of surface reactions (including those responsible for heating the Pd wire). The catalytic ignition limits of stoichiometric mixtures 6–40% H_2 + air (indicated by crosses) and (20–60% H_2 + 80–40% $CH_4)_{stoich}$ + air are shown in Fig. 3.3 a. As is seen, Pd wire ignites a mixture of 40% H_2–air in the reactor, which is heated only to 70 °C. For comparison, ignition of the same mixture with Pt wire requires heating to 260 °C [21]. In addition, as can be seen from the Fig. 3.3, the minimum H_2 concentration at the limit is approximately 5%, which is very close to the concentration limit of H_2 ignition at atmospheric pressure when initiated by a spark [23, 24]. This means that CH_4 in H_2–CH_4–air mixtures reacts only in the gas phase and not on the Pd surface.

It should be emphasized also that Pt wire of the same size does not ignite any of the mixtures (20 ÷ 60% H_2 + 80 ÷ 40% $CH_4)_{stoich}$ + air at reactor temperatures up to 450 °C.

On the contrary, Pd wire ignites mixtures (H_2 30 ÷ 60% + 70 ÷ 40% $CH_4)_{stoich}$ + air (circles in Fig. 3.3a). However, the mixture (20% H_2 + 80% $CH_4)_{stoich}$ + air at temperatures up to 450 °C cannot be ignited with Pd wire, probably because the H_2 concentration in the mixture (2.2%) turned out to be lower than the concentration limit of hydrogen ignition [23, 24].

The temperature dependence of the H_2 fraction in combustible mixtures in Arrhenius coordinates is shown in Fig. 3.3b. As can be seen in Fig. 3.3b, this dependence can be approximated by a straight line (correlation coefficient 0.98). The data were processed using the Statistica 9 software package (Statsoft).

We can conclude from Fig. 3.3b, that the dependence for H_2–CH_4–air mixtures is determined only by the H_2 fraction in the mixture. We limited ourselves to 40% H_2 in the mixture, because after a further increase in H_2 content, the hydrogen oxidation reaction slows down [24]. For this reason, the value of the effective activation energy obtained below is only an estimate.

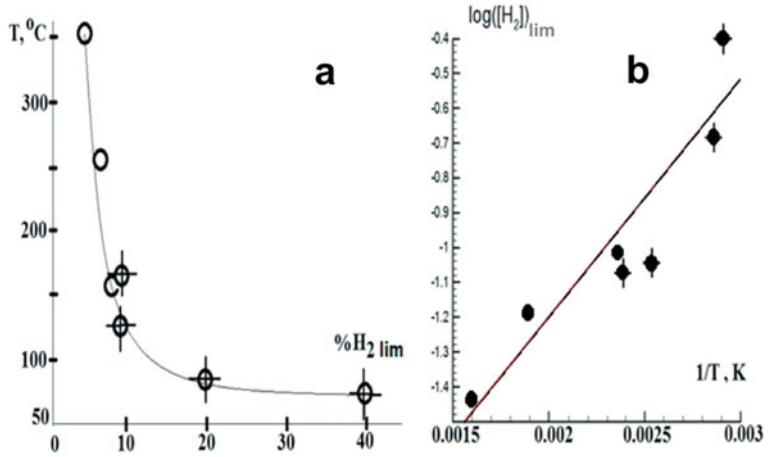

Fig. 3.3 **a** Experimental dependence of the ignition temperature at the concentration limit on the hydrogen content in the mixture, crosses refer to the hydrogen–air mixture; **b** Dependence **a** in Arrhenius coordinates

Let's consider the nature of the resulting dependence. We will point out that this approximation is rather rough; but it will allow us systematizing the experimental results for the limits of catalytic ignition over the studied noble metals quite consistently below. For the absence of nonlinear branching in a stoichiometric mixture $2H_2 + O_2$, the lower flammable limit (marked with the subscript $_{lim}$) at low pressures (see also Chap. 1): $2\,k_2\,(O_2)_{lim} = k_4$ i.e. $(O_2)_{lim} = 1/2\,(H_2)_{lim} = k_4/k_2$, where k_4—the rate constant of heterogeneous termination of active combustion centers (weakly dependent on temperature) and k_2 is the activated rate constant of branching (16.7 kcal/mol [25]).

Thus, we obtain Arrhenius dependence ln $(H_2)_{lim}$ on 1/T with a positive slope. Obviously, the heterogeneous nature of the process on Pd significantly complicates the analysis. However, it can be assumed that in the catalytic oxidation of H_2, the reaction rate depends mainly on H_2 concentration, which can be expressed for the steady state as the ratio of some two effective constants [25].

The experimental value of the effective activation energy of the process is $E = 3.5 \pm 1$ kcal/mol, which is typical for surface processes [25]. It should be noted that the value of the effective activation energy is close to the activation energy of adsorption–desorption of hydrogen on Pd [26]. However, in order to ensure ignition, the cycle of reactions must occur, in which branching is realized [24]. The activated ($E = 16.7$ kcal/mol [25]) homogeneous branching reaction $H + O_2 \rightarrow O + OH$ is the slowest elementary reaction of the cycle. Therefore, the activation energy of branching should determine the temperature dependence of the overall process, as it happens for experiments with metallic Pt ([21], see also Chap. 2). This means that in the case of Pd, the branching can be of a heterogeneous nature, because the effective

activation energy is close to ~ 3.5 kcal/mol. The obtained approximate value of E along with the results presented in Fig. 3.3a, b, can be used in practical applications to estimate the flammability of mixtures H_2–CH_4–air in the presence of metallic palladium.

It can be seen from Fig. 3.2b, c that, upon initiation with Pd wire, combustion is accompanied by orange luminescence for both hydrogen and hydrogen–methane mixtures, while for the latter mixture, this luminescence propagates nonuniformly and independently on the spherical flame front. An attempt was made to establish the nature of this luminescence using the hyperspectral method. The optical and IR spectra of radiation from a flame of hydrogen and a mixture (80% H_2 + 20% $CH_4)_{stoich}$ + air, recorded along a vertical strip along the diameter of the optical window (red strip, Fig. 3.1 a) are shown in Fig. 3.4a, b, c.

Let us preliminarily point out that a hydrogen flame at low pressures is practically invisible, since its radiation is mainly due to the radiation of hydroxyl radicals OH $A^2\Sigma - X^2\Pi$ in the ultraviolet region at 306 nm [24]. The combustion spectrum of a stoichiometric mixture of pentane with air contains intense lines of atoms of alkali metals sodium (581 nm) and potassium (755 nm), inherent in all hot flames [24] and water vapor bands of water vapor bands in the range 900–970 nm [27, 28]. In the IR spectrum, broad bands of water are observed between $\lambda = 1300$ nm and 1600 nm. A relatively narrow band of the OH* radical is recorded at about 1400 nm [29].

It should be noted that the spectra presented in [28] and in this work were recorded in the same reactor using the same hyperspectral technique. It follows from Fig. 3.4a, b that the main features of the spectra of the flame of 40% H_2 + air, initiated by palladium in the visible region, in comparison with the optical spectra of the emission of a hydrogen flame initiated by a platinum wire and a spark discharge ([28], Fig. 13a) are:

(a) the absence of a system of emission bands in the range of 570–650 nm, referred to H_2O* in [30]. This may be because we used in this paragraph an optical window made of leucosapphire rather than quartz, as in [28]. Leucosapphire, unlike quartz, does not contain active surface OH groups. Thus, the emergence of water bands in the region of 570–650 nm may be due to the adsorboluminescence of water on quartz. Such a process is impossible on leucosapphire.
(b) increased intensity of water bands in the region 900–970 nm in comparison with the intensities of lines of alkali metals.

This indicates the emergence of an additional source of excited H_2O molecules. Earlier, we showed [31] that the catalytic activity of the palladium surface in the hydrogen combustion reaction is higher than that of the platinum surface. In other words, there is a fast catalytic reaction of hydrogen oxidation on the hot Pd surface along with the initiation of gas combustion. This reaction can lead to the formation of an additional amount of excited water molecules.

We summarize the results obtained in this paragraph.

It has been shown experimentally that the ignition temperature of a 40% H_2–air mixture over metallic Pd (70 °C, 1 atm) is ~ 200 °C lower than over the Pt surface (260 °C, 1 atm). In addition, the Pd wire initiates the ignition of mixtures (H_2 for

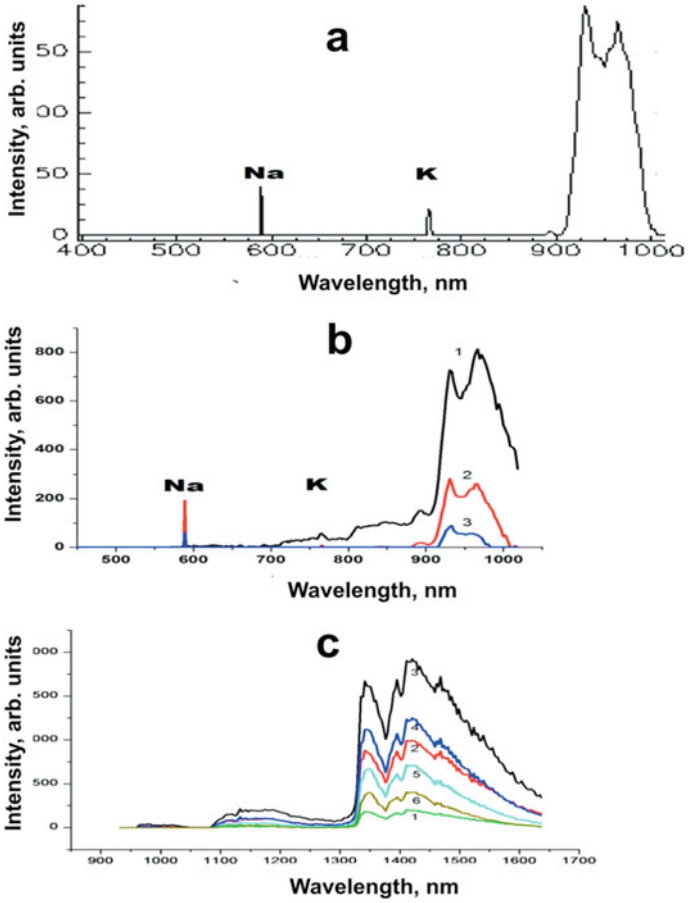

Fig. 3.4 Emission spectrum of combustion of the mix on time. **a** 40% H_2 + air, hyperspectrometer VID-IK-3, 30 fps; **b** (80% H_2 + 20% $CH_4)_{stoich}$ + air, hyperspectrometer VID-IK-3, 300 frames/s; **c** 40% H_2 + air, NIR hyperspectrometer, 300 frames/s. The emission spectra of the mixture of 40% H_2 + air in this spectral region do not differ qualitatively. As the number of the spectrum increases, time grows

30–60% + 70–40% $CH_4)_{stoich}$ + air; Pt wires of the same size cannot ignite these mixtures up to 450 °C. This means that Pd wire is more efficient than Pt wire.

It was shown that the cellular structure of the flame front during ignition on a Pd wire is not observed in comparison with the results obtained on the Pt surface. Therefore, Pd is more applicable for hydrogen recombiners in nuclear power plants, since catalytic particles do not appear in the gas phase, as is the case when using Pt.

The experimental value of the effective activation energy of the process is estimated as 3.5 ± 1 kcal/mol, which is typical for the surface process. This indicates a significant role of the dark reaction of the consumption of H_2 and O_2 on Pd,

which is observed directly at low pressures. The presence of this reaction reduces the likelihood of an accidental explosion as compared to Pt.

It was found that in the presence of leucosapphire the system of H_2O^* emission bands in the region of 570–650 nm is missing. A possible explanation of this phenomenon is given. An explanation is proposed for the appearance of an additional source of excited water molecules emitting in the range of 900–970 nm.

3.2 Features of Ignition of Hydrogen–Hydrocarbon (C1–C6)–Air Mixtures Over the Palladium Surface at 1–2 atm

In the previous paragraph, we showed experimentally that the ignition temperature of a 40% H_2–air mixture over metallic Pd (70 °C, 1 atm) is lower than over Pt metal (260 °C, 1 atm). In addition, a Pd wire initiates the ignition of the mixtures, which cannot be ignited with Pt wires of the same size, i.e. Pd wires are more efficient than Pt wires. It was shown that the cellular structure of the flame front during ignition on the Pd wire is not observed in comparison with the results obtained on the Pt surface, therefore catalytic particles do not appear in the gas phase, as is the case when using Pt. The value of the effective activation energy of the process was estimated as 3.5 ± 1 kcal/mol, which is typical for the surface process. This indicates an important role of the dark reaction of H_2 oxidation over Pd, which is observed at low pressures. The presence of this reaction reduces the possibility of an accidental explosion as compared to Pt.

It was found that in the presence of leucosapphire the system of H_2O^* emission bands in the region of 570–650 nm is missing. An explanation is given for the appearance of an additional source of excited water molecules emitting in the range of 900–970 nm.

This paragraph discusses the catalytic oxidation of hydrogen with the addition of higher paraffin hydrocarbons. Mixed hydrogen–hydrocarbon fuels have attracted increased attention as alternative fuels for energy production for two main reasons. First, there is increased efficiency available from methane–hydrogen fuel, which improves the characteristics of combustion devices, widens the range of their use, and reduces pollutant emissions when using lean mixtures in stationary [32] and mobile [33] systems. The second reason relates to developments in hydrogen energy and the prospects of using hydrogen in fuel cells and combustion devices [34]. Using the combustion of premixed lean mixtures is a promising method for fulfilling the modern need to limit NO_x emissions in energy production, including in internal combustion engines [35, 36]. The reduction in the combustion temperature that is achieved by using lean mixtures may significantly reduce NO_x emissions. However, more research is needed to address the issues that impede the widespread adoption of these technologies. For example, due to the lower combustion temperatures of premixed mixtures, problems associated with suppression of oxidation reactions, increased CO

emissions, and decreased operational stability of the combustion chamber may arise [37].

Natural gases, mainly methane, may contain up to 18% other gases, depending on their field of origin [33]. These impurities are usually ethane and propane. Changes in the natural gas composition cause changes in the chemistry of its combustion and NO_x emissions. Catalytic ignition is most effective with the use of lean combustible fuels [38]: there are no extinction effects at electrical breakdown that occurs when using electrodes of a conventional spark plug, and the ignition source can be placed in the combustion chamber. Catalytic ignition does not require electrodes and the ignition system, so there is no erosion of the electrodes while the operation time of the catalytic ignition system will be significantly longer than that for a device using a conventional spark plug. There is a need to develop catalysts that provide oxidation at low temperatures (<300 °C) for a new generation of highly efficient internal combustion engines [39]. The combustion of fuels over metallic palladium (as one of the most used catalysts) is of great interest. For example, methane combustion over metallic palladium was experimentally studied during the flame penetration through obstacles [40]. The catalyst stability issues were studied, for example, in [41]. The alumina-based palladium catalyst was found to be not stable during methane conversion while the platinum addition to such catalysts provides significantly higher stability. On the other hand, the poisoning of Pd–Pt catalysts with water vapor is known to be reversible, i.e., their activity is restored after the water is removed. In this case, a decrease in the catalytic activity of Pd/Al_2O_3 is observed not for all fuels, as a result of the combustion of which water vapor is formed. Hydrogen is very stably oxidized on Pd/Al_2O_3. The degree of ethane conversion slightly decreases over time, but not to the extent that is observed at methane conversion.

Noble metals Pt and Pd affect the flammability of methane and hydrogen-based fuel in different ways. The ignition temperature of a 40% H_2–air mixture on palladium (70 °C, 1 atm) was shown to be ~ 200 °C lower than temperature on the platinum surface (260 °C, 1 atm) [21, 31]. Besides, Pd ignites stoichiometric mixtures (30–60% H_2 + 70–40% CH_4) + air [$\theta = 1$, where θ is the fuel fraction in mixtures with air: $\theta H_2 + 0.5\,(O_2 + 3.76\,N_2)$]. Platinum metal does not ignite these mixtures up to 450 °C, i.e., metallic palladium is more effective than platinum. The cellular structure of the flame front during ignition was also not observed above the palladium surface as compared to the results obtained for the platinum surface. Thus, palladium seems to be a more suitable material for use in hydrogen recombiners at nuclear power plants because catalytic particles, as ignition centers, producing from the thermal decomposition of labile oxide (PtO_2) cannot appear in the gas phase [42]. The experimental value of the effective activation energy of the process was estimated to be (3.5 ± 1) kcal/mol. This value is characteristic of surface processes; it indicates the noticeable role of the dark hydrogen oxidation reaction observed above the palladium surface at low pressures [31]. Obviously, this reaction reduces the probability of an accidental explosion of hydrogen as compared to Pt.

This paragraph is devoted to the establishment of combustion characteristics of fuels containing hydrogen–hydrocarbon (C1–C6, as in CH_4, C_2H_6, C_3H_8, C_4H_{10}, C_5H_{12}, and C_6H_{14}) mixtures with $\theta = 0.6$–1.2 above the palladium surface at total

pressure of 1–2 atm. The study is aimed at identifying the propagation characteristics of the flame front in mixed fuels, establishing the temperature dependence of the ignition limit above the palladium surface, and investigating the spectral features during combustion of a 30% propane + 70% H_2 + air mixture using hyperspectrometers.

3.3 Experimental

The experiments were performed with 30% hydrocarbon (C1–C6) + 70% H_2 + air gas mixtures with $\theta = 0.6$–1.2 at 1–2 atm equipped with a leukosapphire window at one of the ends, a heated cylindrical stainless steel reactor with a length of 25 cm and an internal diameter of 14 cm was used (Fig. 3.5).

A more detailed description of the setup can be found in [43, 44]. The accuracy of the temperature measurement was 0.3 K. Ignition and flame propagation were recorded using a Casio Exilim F1 Pro color high-speed video recorder (the frame rate is 600 fps). The video file was stored in the computer memory, and then it was processed frame-by-frame [31].

Spectroscopic measurements were carried out using hyperspectrometers allowing simultaneous measurements of spectral and spatial coordinates [45]. A hyperspectrometer (such as push-broom one, see Chap. 2) registers a narrow strip on the probed object at the same moment. Simultaneous registration is carried out using a two-dimensional photodetector matrix, along one coordinate of which the spatial coordinate is measured while the spectral (wavelength) coordinate is measured along

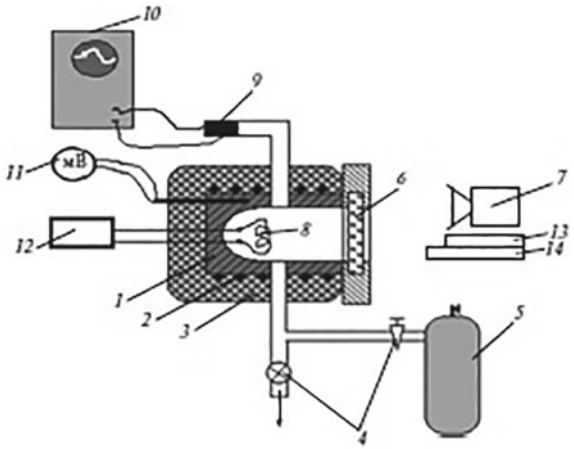

Fig. 3.5 Schematic of the experimental setup: (1) stainless steel reactor, (2) electric heater, (3) thermal insulation, (4) valves, (5) high-pressure buffer volume, (6) leucosapphire optical window, (7) digital video recorder, (8) palladium spiral, (9) pressure gauge, (10) recording system, (11) digital millivoltmeter, (12) Wheatstone bridge, (13) hyperspectrometer with a spectral range of 400–1000 nm, and (14) hyperspectrometer with a spectral range of 1000–1700 nm

the other coordinate. The image of a narrow strip on the probed object is formed by the confining slit of the diaphragm unit of the hyperspectrometer. Because the data are taken from the photodetector matrix of the hyperspectrometer with a frame frequency of up to 300 Hz, the time dependence of the emission spectra of the combustion process is also recorded. In this paragraph, both the video recording of combustion by a video recorder and the registration of the combustion process by a hyperspectrometer were performed simultaneously, and the obtained data were subsequently compared. The VID-IK3 hyperspectrometer [17] was used for measurements in the wavelength range of 400–1000 nm, and the NIR hyperspectrometer was used for measurements in the 900–1700 nm range [46].

The evacuated and heated reactor was rapidly filled with the studied gas mixture from the buffer volume to the required pressure. The ignition limit was determined as the average of two close temperatures at a given pressure: at higher temperature ignition occurred, and at lower temperature ignition was missing. For fast opening and closing of gas communications, an electromagnetic valve was used. A capacitive pressure sensor recorded the pressure during gas inlet and combustion. A palladium spiral with a wire length of 70 mm and a diameter of 0.3 mm was used both to initiate ignition of the combustible mixture and to estimate the amount of wire heating as a shoulder of the bridge circuit was placed in the reactor. Prior to each experiment, the reactor was pumped out to 0.01 Torr. After each ignition, the reactor was pumped out for 1.5 h for water vapor removal. The total pressure in the reactor was recorded with a vacuum gauge, and the pressure in the buffer volume was monitored by a reference pressure gauge. Gases and palladium of the chemical grade (99.85% purity) were used.

3.3.1 Results and Discussion

Typical sequences of video frames of spatial development of ignition initiated by the palladium wire and flame propagation of previously prepared mixtures of 30% CH_4 + 70% H_2 + air and 30% C_2H_6 + 70% H_2 + air with $\theta = 0.6$–0.9 at 1.75 atm are presented in Fig. 3.6a and b. The palladium wire is heated before and after ignition due to catalytic reactions on the metallic palladium surface in the same way as that in the case of Pt [42–44]. As can be seen in Fig. 3.6, the cellular structure of the flame front is observed in lean mixtures: the thermal diffusion instability of the flame in lean fuel leads to the appearance of cellular structures [47, 48].

Figure 3.7 shows the results of simultaneous recording of pressure changes and changes in the resistance of a palladium wire (proportional to self-heating) during ignition at $P = 1.75$ atm of mixtures: (a) 30% C_2H_6 + 70% H_2 + air, $\theta = 0.6$, 39 °C and (b) 30% C_6H_{14} + 70% H_2 + air, $\theta = 1.2$, 36 °C.

Because the Pd wire is heated nonuniformly [21] (see also Fig. 3.7a and b), the time dependence of the resistance that represents the relative temperature is somewhat delayed in comparison with video recording. The kink on this dependence corresponds to the resistance change at the time of ignition. Obviously, the temperature value measured using the palladium resistance is the lower bound of the true

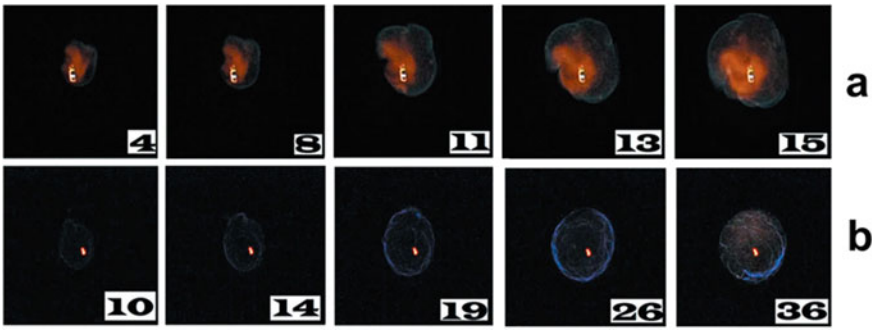

Fig. 3.6 Video recording frames: high-speed recording of the combustion initiation by the Pd spiral and flame propagation in mixtures: **a** 30% CH_4 + 70% H_2 + air, $\theta = 0.7$, $P = 1.75$ atm, 270 °C, 600 fps; **b** 30% C_2H_6 + 70% H_2 + air, $\theta = 0.6$, $P = 1.75$ atm, 390 °C, 300 fps. Frame numbering corresponds to the frame number after initiation during ignition

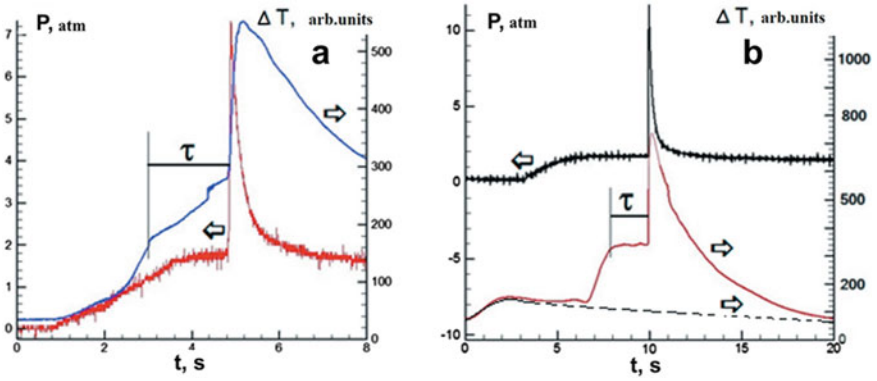

Fig. 3.7 Dependences of the simultaneous recording of changes in pressure and resistance of a Pd spiral during ignition: **a** mixture of 30% C_2H_6 + 70% H_2 + air, $\theta = 0.6$, $P = 1.75$ atm, 39 °C; **b** mixture of 30% C_6H_{14} + 70% H_2 + air, $\theta = 1.2$, $P = 1.75$ atm, 36 °C. τ is the ignition delay. The dashed line is the change in the resistance of a Pd spiral when a 30% Ar + 70% H_2 + air mixture is injected into the reactor to a pressure of $P = 1.75$ atm

temperature of the ignition center initiating the combustion of the gas, as it takes a certain amount of time to heat the whole palladium spiral uniformly.

The dashed line in Fig. 3.7b shows a change in the resistance of the palladium spiral when a 30% Ar + 70% H_2 + air mixture is introduced into the reactor. Thus, the first maximum in the time dependence of resistance during combustion does not relate to the ignition process but to the interaction of hydrogen with the palladium surface.

As can be seen in Fig. 3.7a and b, the total pressure in the reactor reaches 1.75 atm before ignition, and ignition occurs after gas inlet is complete. The ignition delay period τ for a 30% C_2H_6 + 70% H_2 + air mixture is ~ 2 s at $P = 1.75$ atm. Note that

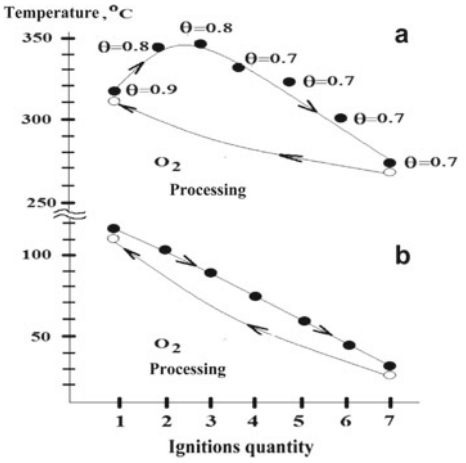

Fig. 3.8 Dependence of the mixture flammability on the number of sequential ignitions: top—30% CH_4 + 70% H_2 + air, $\theta = 0.7$–0.9; bottom—30% C_3H_8 + 70% H_2 + air, $\theta = 1$, $P =$ 1.75 atm. Filled circles: ignition, empty circles: no ignition

τ is 8 s for the same mixture at 24 °C and $P = 1$ atm. This means that the combustion of this fuel can be initiated by the palladium surface at room temperature without additional physical stimulation. The 30% C_2H_6 + 70% H_2 + air mixture with $\theta =$ 0.6 has the lowest ignition limit temperature of 23 °C at $P = 1$ atm.

The mixtures of 30% CH_4 + 70% H_2 + air and 30% C_3H_8 + 70% H_2 + air were shown to have two values of ignition limit temperature. A higher value can be achieved with a bottom-up temperature approach, while a lower value can be achieved by treating the reactor with ignitions. The foregoing is illustrated by the flammability dependences of 70% CH_4 + 30% H_2 + air (Fig. 3.8a) and 30% C_3H_8 + 70% H_2 + air mixtures (Fig. 3.8b) on the number of consecutive ignitions at $P =$ 1.75 atm.

As is shown in Fig. 3.8, the ignition temperature in the fresh reactor (bottom-up approach: no previous ignition in the reactor) is ~ 315 °C at $\theta = 0.9$. At this temperature, the mixtures with $\theta < 0.9$ at the same pressure in the fresh reactor do not ignite. However, during the treatment with ignitions, the catalytic ignition limit decreases markedly to 274 °C at $\theta = 0.7$ after seven ignitions. This process was shown to be reversible: after treating the reactor with oxygen (1 atm O_2 for 10 min) or air, the ignition limit temperature returns to its initial value of ~ 315 °C. Similar dependences were also observed in the case of ignition of 30% C_3H_8 + 70% H_2 + air mixture (Fig. 3.8b). The catalytic ignition limit temperature in a fresh reactor is ~ 108 °C at $\theta = 1$.

During subsequent ignitions of the same mixture, the ignition limit temperature decreases and is 30 °C after seven ignitions. The process is also reversible: after treating the reactor with oxygen (1 atm O_2 for 10 min) or air, the ignition limit temperature returns to its initial value of ~ 108 °C.

Thus, the observed phenomenon is a hysteresis, the cause of which may be reversible changes in the palladium surface and, consequently, the catalyst activity.

Table 3.1 Catalytic ignition limits for mixtures 70% H_2 + 30% (C2, C4-C6) at 1.75 atm

Fuel	30% C_2H_6 + 70% H_2 $\theta = 0.6$	30% C_4H_{10} + 70% H_2 $\theta = 1.1$	30% C_5H_{12} + 70% H_2 $\theta = 1.2$	30% C_6H_{14} + 70% H_2 $\theta = 1.2$
Temperature at the catalytic ignition limit, °C	20	28	24	36

Note that reversible changes in the palladium surface are observed only for H_2–methane and H_2–propane fuels, while there is no hysteresis effect for other mixtures studied. This means that the catalytic ignition limit above palladium is also determined by the features of the kinetic mechanism of hydrocarbon oxidation. The ignition limit temperatures for these mixtures at total pressure of 1.75 atm are presented in Table 3.1.

To evaluate the effective activation energy of the brutto-reaction for those mixtures that do not exhibit the features associated with reversible changes in the catalyst activity, the temperature values of the ignition delay periods were obtained. The experimental temperature dependences of ignition delay periods in Arrhenius coordinates for 30% (C_2H_6, C_4H_{10}, C_5H_{12}, and C_6H_{14}) + 70% H_2 + air mixtures are shown in Fig. 3.9. As can be seen in Fig. 3.9, these values can be approximated by a straight line (the correlation coefficient is $r = 0.983$). The data were processed using Statistica 9 (StatSoft) software package. Based on the data presented in Fig. 3.9, the experimental value of the effective activation energy of the brutto-process was found to be $E = (2.4 \pm 1)$ kcal/mol, which is specific to the surface process [25].

This value is very close to the value of $E = (3.5 \pm 1)$ kcal/mol obtained in [21] from the temperature dependence of the H_2 content in H_2–air and H_2 + CH_4 + air mixtures. Based on this result, we can conclude that the temperature dependences for 30% (C2, C4, C5, and C6) + 70% H_2 + air mixtures are determined only by

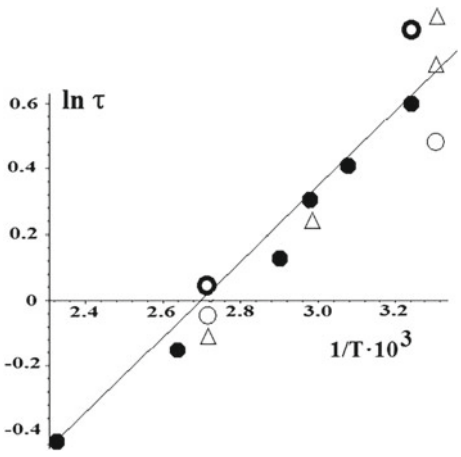

Fig. 3.9 Experimental temperature dependences of the ignition delay periods of mixtures with various compositions in Arrhenius coordinates at $P = 1.75$ atm (circles) 30% C_2H_6 + 70% H_2 + air, $\theta = 0.6$; (black circles) 30% C_4H_{10} + 70% H_2 + air, $\theta = 1.1$; (triangles) 30% C_5H_{12} + 70% H_2 + air, $\theta = 1.2$; and (bold circle) 30% C_6H_{14} + 70% H_2 + air, $\theta = 1.2$

the H_2 content in them, as is shown for H_2–air and H_2–CH_4–air mixtures in [21]. It can be assumed that the obtained estimates of the effective activation energy refer to the same process, perhaps a branching process or chain propagation one [21]. If so, then this process has a heterogeneous nature. The lowest ignition limit temperature of the hydrogen–air mixture on the palladium surface is ~ 70 °C for 40% H_2 + 60% air mixture [21]. Because the catalytic ignition limit for 70% hydrogen + 30% hydrocarbon (C2–C6) + air mixtures is ~ 40 °C lower (see Table 3.1), this indicates the importance of the role of reactions involving hydrocarbon molecules (except methane, see above) on the palladium surface.

Figure 3.10 shows the frame-by-frame processing results of video recording of the palladium-initiated ignition of a 70% H_2 + 30% C_3H_8 + air mixture ($\theta = 1$, $P =$ 1.73 atm). Figure 3.10 shows that, upon initiation by a Pd wire, spatially nonuniform combustion of the combustible mixture occurs until the flame touches the reactor walls (frames 10–19), followed by a sharp increase in the combustion intensity (frames 23–26) when the flame touches the back reactor wall (which is closer to the Pd spiral). As is seen in frames 146 and 176, after the combustion in the volume is completed, the burning of the combustible mixture continues on the palladium spiral.

We attempted to establish the nature of this chemiluminescence using the hyperspectral method. Figure 3.11a–c show the visible and IR emission spectra during combustion of a 60% H_2 + 40% C_3H_8 + air mixture ($\varphi = 1$) recorded along the vertical line over the diameter of the optical window. This approximately corresponds to the red strip in Fig. 3.5a. Intensive lines of the alkali metal atoms sodium (581 nm) and potassium (755 nm) that are inherent to all hot flames [24] and water vapor bands (900–970 nm) are observed in the spectrum in Fig. 3.11a [27, 28].

Wide absorption bands of water in the range of $\lambda = 1300$–1600 nm are observed in the IR spectrum. The problem was to establish the features of the appearance

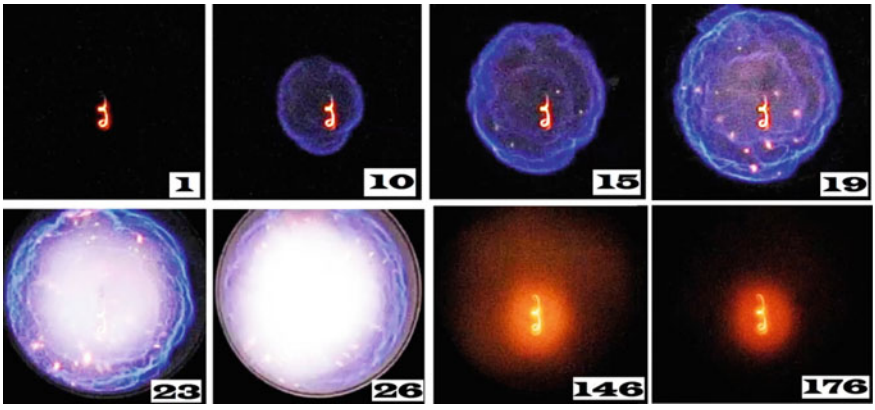

Fig. 3.10 Frames for the high-speed registration of Pd spiral-initiated ignition and flame propagation in a mixture of 70% C_3H_8 + 30% H_2 + air, $\theta = 1$, $P = 1.75$ atm, 35 °C, 600 fps. The frame numbering corresponds to the sequential frame number during ignition

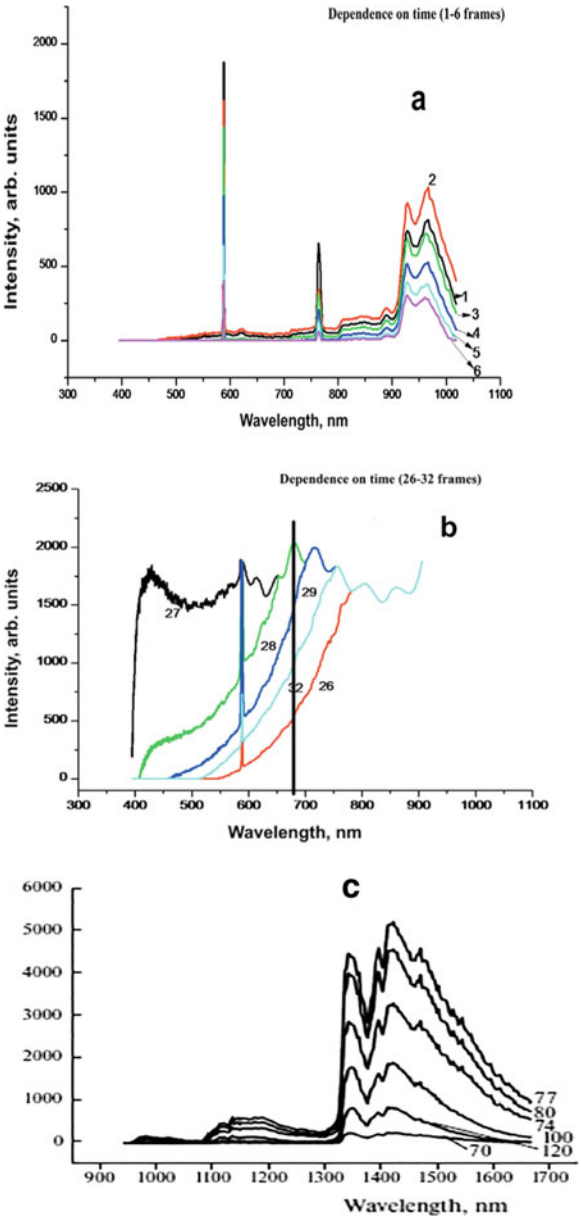

Fig. 3.11 Graphs of experimental time dependences of: **a** intensities of the combustion emission spectra of a mixture of 60% $H_2 + 40\%$ $C_3H_8 +$ air ($\theta = 1$, $P = 1.9$ atm), VID-IK3 hyperspectrometer, recording speed is 70 fps; **b** intensities of the combustion emission spectra of a mixture of 60% $H_2 + 40\%$ $C_3H_8 +$ air ($\theta = 1$, $P = 1.9$ atm), VID-IK3 hyperspectrometer, the blue region of the spectrum, recording speed is 70 fps; a black vertical line limits the spectrum distortion area to the right, which is associated with a sharp increase in the device sensitivity; **c** intensities of the emission spectra of the combustion mixture 40% $H_2 +$ air, BIK hyperspectrometer, recording speed is 300 fps. The number in the figures means the frame number. As the spectrum number increases, the time increases

in time and space of active intermediate particles [for CH ($A^1\Delta - X^2\Pi$), 431 nm [24] and 590 nm for the Na line). Thus, it was expected that the presence of active intermediate particles and self-heating would be revealed, as the emission of Na atoms is caused by their thermal excitation [24] at flame temperature not lower than 1200 °C [49]. As seen in Fig. 3.11b, blue CH emission is detected at the beginning of the process (spectrum 27) (the spectral band at 431 nm is not resolved due to collisional broadening at 1.9 atm [24]), while the maximum of the Na line is recorded much later. Note that the observed separation in time of the CH and Na emission bands is consistent with the results obtained in [50] when a methane–air flame passed through a small hole in a plane obstacle, i.e., during the gas flow turbulization. As is seen in Fig. 3.12 (taken from [50]), there is a blue emission before the obstacle in the reactor due to the emission of CH radicals, while C_2 radicals ($A^3\Pi g - X^3\Pi u$) in the detected amounts are observed only beyond the first obstacle.

When registering the radiation of a propagating flame using glass filters in the wavelengths 435, 520, and 590 nm, it can be clearly seen that both C_2 radicals in the detected amounts and the main heat release during the Na luminescence are observed beyond the first obstacle, i.e., after the gas flow turbulization. Note that we earlier experimentally and theoretically established that the combustion front is turbulized

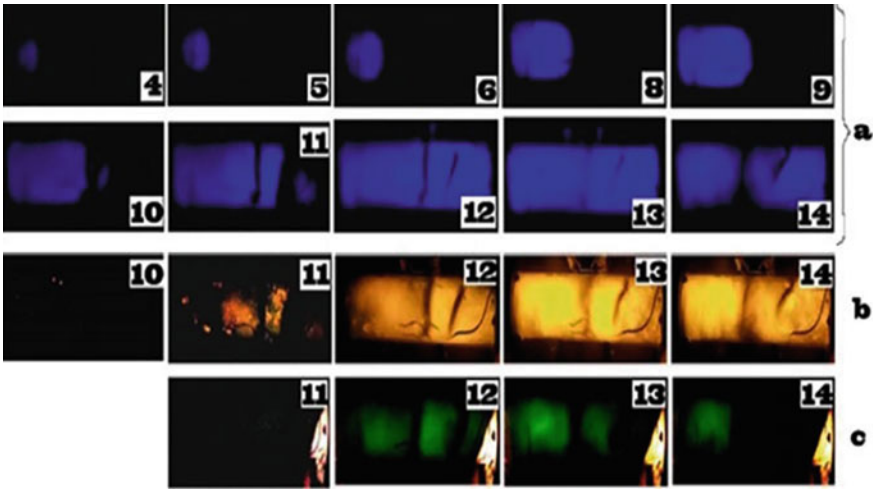

Fig. 3.12 High-speed video recording of the combustion flame front propagation of a mixture of 15.4% CH_4 + 30.8% O_2 + 46% CO_2 + 7.8% Kr at an initial pressure of 180 Torr through a combined obstacle consisting of a first flat obstacle with a diameter of 14 cm with a single hole with a diameter of 25 mm and a second flat obstacle with a single hole with a diameter of 25 mm covered with a flat grid: **a** glass filter in the region of 435 nm (CH transmittance at a maximum is 70%, ± 35 nm), **b** combined glass filter in the region of 590 nm (Na—transmission at a maximum is 70%, ± 25 nm); recording speed is 300 fps. **c** glass filter in the region of 520 nm (C_2 transmittance at a maximum is 35%, ± 60 nm). The numbering corresponds to the sequence frame number after the moment of initiation

due to the appearance of hydrodynamic instability [51] when a flame of a methane–air mixture touches the end of a cylindrical reactor (see, for example, Fig. 3 from [51]). Thus, the separation in time of the CH and Na emission bands observed in this study is due to the occurrence of hydrodynamic instability of the flame when it touches the end of the cylindrical reactor.

This result means that the used experimental technique allows separating the cold flame from the hot one in time and space in a single experiment. This result is also important for verification of numerical methane combustion models. It should be noted the enhanced intensity of the water absorption bands in the spectral region of 900–970 nm compared to the intensities of the spectral lines of the alkali metals. In this case, according to Fig. 3.11a, water absorption bands are observed at the end of the combustion process when the Na line is almost not observed in the spectrum (Fig. 3.11a, spectrum 5). As is indicated in the previous paragraph, this emission can be associated with a catalytic oxidation reaction of unreacted hydrogen atoms and, possibly, propane on the hot Pd surface.

Let us briefly summarize the obtained results.

The temperature of the ignition limit above the palladium surface at $P = 1.75$ atm measured by the bottom-up approach by temperature for 30% methane + 70% hydrogen + air ($\theta = 0.9$, $T = 317$ °C) and 30% propane + 70% H_2 + air ($\theta = 1$, $T = 106$ °C) mixtures was experimentally shown to decrease noticeably after subsequent ignitions down to $T = 270$ °C for the H_2–CH_4–air mixture and to $T = 32$ °C for the H_2–C_3H_8–air mixture.

The ignition limit returns to its initial value after treating the reactor with oxygen or air, i.e., hysteresis occurs. The ignition limit temperature of 30% (C2, C4, C5, and C6) + 70% H_2 + air ($\theta = 0.6$, 1.1, 1.2, and 1.2, respectively) mixtures above the metallic palladium surface is 25–35 °C at $P = 1.75$; there is no the hysteresis effect. A lean mixture of 30% C_2H_6 + 70% H_2 + air ($\theta = 0.6$) was found to have the lowest ignition limit temperature of 24 °C at $P = 1$ atm. The estimate of the effective activation energy of ignition of mixtures over Pd is ~ (2.4 ± 1) kcal/mol, which is specific of the surface process. It is shown that the use of Pd allows igniting combustible mixtures of the 30% hydrocarbon + 70% H_2 composition at 1–2 atm and initial room temperature without the use of external energy sources. It was established that the separation in time of the CH and Na emission bands during the combustion of a mixture of 30% propane + 70% H_2 + air ($\theta = 1$) is due to the occurrence of hydrodynamic instability of the flame when it touches the end of a cylindrical reactor.

3.4 Ignition of Hydrogen–Oxygen and Hydrogen–Methane–Oxygen Mixtures with Heated Wires

It was found in the previous paragraph that the temperature of the ignition limit above the palladium surface at $P = 1.75$ atm measured by the bottom- up approach by temperature decreases noticeably after subsequent ignitions to almost room one ($T = 32$ °C) for the H_2–C_3H_8–air mixture. The ignition limit returns to its initial value after treating the reactor with oxygen or air, i.e., hysteresis occurs. However, the ignition limit temperature of 30% (C2, C4, C5, and C6) + 70% H_2 + air mixtures above the metallic palladium surface is 25–35 °C at $P = 1.75$; there is no hysteresis effect. A lean mixture of 30% C_2H_6 + 70% H_2 + air ($\theta = 0.6$) has the lowest ignition limit temperature of 24 °C at $P = 1$ atm. The estimate of the effective activation energy of ignition of mixtures over Pd is ~ (2.4 ± 1) kcal/mol, which is specific of the surface process. It is shown that the use of Pd allows igniting combustible mixtures of the 30% hydrocarbon + 70% H_2 composition at 1–2 atm and initial room temperature without the use of external energy sources. It was established that the separation in time of the CH and Na emission bands during the combustion of a mixture of 30% propane + 70% H_2 + air ($\theta = 1$) is due to the occurrence of hydrodynamic instability of the flame when it touches the end of a cylindrical reactor.

This paragraph discusses the features of the chemical mechanism of hydrogen oxidation on heated wires from various metals in order to identify one of the possible reactions responsible for catalytic ignition.

Hydrogen is a renewable energy source for the future, combustion products of which do not pollute the environment. However, before the widespread use of hydrogen, the issues of explosion safety of production, transportation and storage of hydrogen must be resolved. Accidental ignition is one of the largest hazards, as hydrogen has much wider flammability limits than conventional fuels [52].

By analyzing the risk of accidental ignition in the event of an uncontrolled hydrogen leak, as can occur during a vehicle collision or pipeline breakdown, the most likely ignition source is a hot surface. Therefore, it is important to be able to predict and thus prevent the situation, in which ignition can occur when a flammable mixture is in contact with a hot surface.

The use of hydrogen as a fuel requires the ability to ignite it predictably. The problem with refueling spark ignition engines with hydrogen is that the hydrogen–air mixture entering the combustion chamber can be ignited immediately upon contact with a hot surface, such as an intake valve. In diesel engines with direct fuel injection, the pre-ignition problem does not arise. However, hydrogen is difficult to ignite when compressed, an additional device is required such as a spark plug and some ignition helps, usually a glow plug [53]. Therefore, the design of both spark ignition and diesel engines should be based on the analysis of hot surface ignition information.

Many experimental works [54] are devoted to the investigation of hydrogen ignition by a hot surface. Most measurements were carried out for gas mixtures at atmospheric pressure. Measurements of the surface temperature required to initiate the

ignition of hydrogen (T_{ign}) in air or oxygen at 1 atm, as a rule, were in the range from 640 °C [5] to 930 °C [55]. The value T_{ign} ~ 70 °C was observed for a mixture of 40% hydrogen—60% air over the palladium surface, i.e. with a significant catalytic effect [56, 57, see Sect. 1]. In addition, in some works, there is practically no dependence of T_{ign} on H_2 content [54, 58]. However, in other works, for example, [59], this dependence is observed.

We showed earlier that T_{ign} at 40 Torr on a heated palladium foil is ~ 100 °C lower than on a heated platinum foil [31]. For thermal ignition, it was found that at pressures up to 180 Torr at 288 °C, the catalytic activity of the palladium surface is higher than that of the Pt surface [31]. We showed in [41] that the dependence of T_{ign} on the hydrogen content for H_2–CH_4–air mixtures is determined only by the H_2 content in the mixture. Thus, the dependence of T_{ign} on [H_2] exists. The wide range of measured values also shows that the hot surface temperature required for the ignition is not only a property of the gas, but also depends on a number of factors such as mixture composition and pressure, the nature and state of the surface as determined by the surface history, etc.

This paragraph is devoted to the establishment of the regularities of the ignition of mixtures of hydrogen–oxygen and hydrogen–methane–oxygen at low pressures with heated wires of Pd, Pt, nichrome and kanthal (fechral). The paragraph is aimed at revealing the dependence of the ignition temperature on the fuel concentration as well as assessment the contribution of the catalytic properties of the materials used.

3.4.1 Experimental

Experiments were carried out with stoichiometric gas mixtures $2H_2 + O_2$, $(20\% H_2 + 80\% CH_4)_{stoich} + O_2$, $(40\% H_2 + 50\% CH_4)_{stoich} + O_2$, $(50\% H_2 + 50\% CH_4)_{stoich} + O_2$, $(60\% H_2 + 40\% CH_4)_{stoich} + O_2$ $(80\% H_2 + 20\% CH_4)_{stoich} + O_2$. In a number of experiments, CH_4 was replaced with nitrogen N_2. The reactor was a quartz cylinder 12 cm high and 8 cm in diameter, equipped with a replaceable window CsI on the generatrix of the cylinder, inlet holes for gas injection, pumping and electrodes, on which an igniting wire was located (Fig. 3.13).

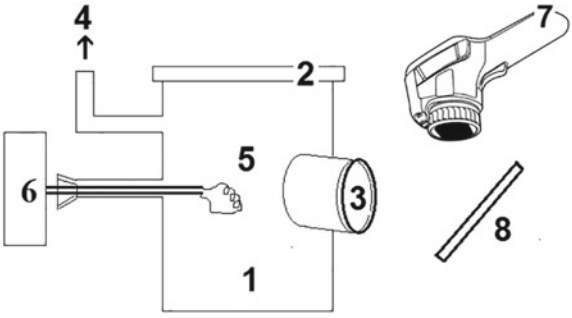

Fig. 3.13 Experimental setup for investigation of initiated ignition: (1) quartz cylinder 12 cm high and 8 cm in diameter, (2) quartz vacuum lid, (3) CsI window, (4) to the pump, (5) Pt or Pd spiral, (6) heater, (7) IR thermal imager Flir 60, (8) rotary mirror

The quartz reactor was used to study initiated ignition, which was provided by heating polished wires Pd, Pt, nichrome and kanthal (0.3 mm in diameter and 80 mm long). The optical window CsI (40 mm in diameter and 5 mm thick) withstands only 5–6 ignitions at an initial pressure of 40 Torr, after which it was changed to a new one. The Flir 60 infrared camera (60 frames/s, 320 × 240 pix, sensitivity range 8–14 mm) was used to determine the ignition temperature T_{ign} wires during ignition. Video recording was turned on at arbitrary time before initiation. The video file was stored in the computer memory and processed frame-by-frame. The evacuated reactor was filled with a gas mixture from the buffer volume to the required pressure. The wires were quickly heated to initiate ignition of the gas mixture. Before each experiment, the reactor was evacuated to 10^{-2} Torr. The total pressure in the reactor was monitored with a VIT-2 vacuum gauge, the pressure in the buffer volume was recorded with a manometer. We used chemically pure gases, 99.99% Pt and 99.85% Pd, commercial nichrome and kanthal.

The ignition temperatures of the mixtures under study with heated wires were measured. It was previously shown that replacing methane with nitrogen does not significantly affect the T_{ign} value, in agreement with [21]. Typical results of IR video recording at a total initial pressure of 40 Torr are shown in Fig. 3.14. The temperature presentation by the Flir 60 camera lags somewhat behind in time due to the inertia of the temperature sensor; therefore, the maximum temperature $T_{exp} = 306$ °C (shown in the upper left corner of each frame) in the 3rd and 4th frames of Fig. 3.14 corresponds to the temperature of the wire immediately before ignition. The temperature in the 5th frame (T_{exp} = 380 °C) corresponds to the temperature of the wire heated by the flame. This temperature is underestimated because the ignition is fast, but the temperature during the ignition delay can be measured accurately and reproducibly. The emissivity was set 0.95 in these experiments (close to a black body).

The recommended emissivity in the range of 8–14 mm for polished palladium wire is ε ~ 0.07 (http://www.zaoeuromix.ru/) and ε ~ 0.07–0.1 (http://www.thermalinfo.ru/) for Pt wire. The value ε ~ 0.1 for Pt and Pd wires, ε ~ 0.1 for kanthal and ε ~ 0.15 for nichrome wire was accepted (http://www.thermalinfo.ru/). The actual ignition temperature on the wire immediately before the explosion at 40 Torr can be estimated from the Stefan-Boltzmann law: $0.95\ T^4_{exp} \approx \varepsilon\ 0.07\ T^4_{ign}$. The results are shown in Fig. 3.15. As is seen in Fig. 3.15, the dependence of T_{ign} on $[H_2]$ takes place; Pd shows the highest catalytic activity (T_{ign} values are the lowest ones) according to [31].

The purpose of the numerical calculation was to establish the limiting ignition conditions in temperature at a wall temperature of 300 K, depending on the H_2 content in the combustible mixture. The model reflects the experimental fact that at the initial stages of the combustion process, the development of the primary heating source leads to the propagation of the flame front [42] with a velocity U.

The surface chain initiation reaction (generation of active combustion centers) was also taken into account, as well as the peculiarities of the mechanism of branched-chain hydrogen oxidation (see Chap. 1). The reduced kinetic mechanism of hydrogen oxidation in the region of the upper ignition limit can be presented as follows [42]:

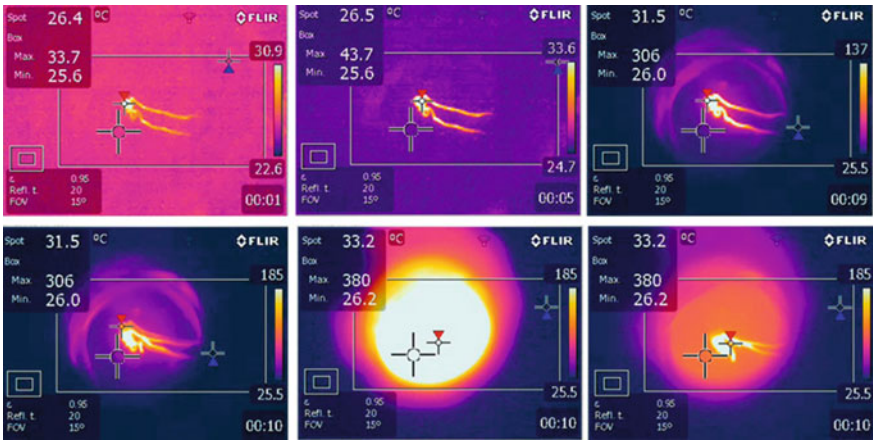

Fig. 3.14 IR—filming of initiated ignition with a heated Pd wire. 60 frames/s, $T_0 = 20$ °C. A mixture (60% H_2–40% methane)$_{stoich}$–oxygen. $P_0 = 40$ Torr. The time in seconds is given on the bottom right of each frame. The red triangle shows the maximum temperature in the rectangle. The blue triangle shows the minimum temperature in the rectangle, the cross indicates the temperature at the point. Emissivity is set to 0.95 (lower left corner of the frame)

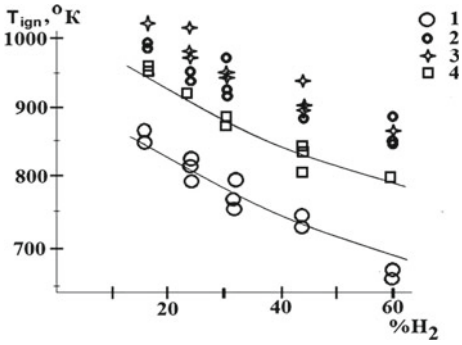

Fig. 3.15 Experimental dependences of T_{ign} on wires on the H_2 content in the mixture, (1) Pd, (2) Pt, (3) nichrome, (4) kanthal, curves-calculations with the values $k_{0cat} = 4 \times 10^{12}$ exp $(-3500/T)$ cm^3/(mol/s) for initiation by the heated Pd surface (lower curve), and $k_{0cat} = 2 \times 10^{15}$ exp $(-5000/T)$ cm^3/(mol/s) for Pt (upper curve)

$$H_2 + O_2 \rightarrow 2OH \quad (0)\ k_0 = 1.92 \times 10^{14} \exp(-21890/T) \mathrm{cm}^3/(\mathrm{mol/s})$$
$$OH + H_2 \rightarrow H_2O + H \quad (1)\ k_1 = 4.63 \times 10^{12} \exp(-2100/T) \mathrm{cm}^3/(\mathrm{mol/s})$$
$$H + O_2 \rightarrow OH + O \quad (2)\ k_2 = 1.99 \times 10^{14} \exp(-8460/T) \mathrm{cm}^3/(\mathrm{mol/s})$$
$$O + H_2 \rightarrow OH + H \quad (3)\ k_3 = 1.88 \times 10^{14} \exp(-6897/T) \mathrm{cm}^3/(\mathrm{mol/s})$$

$$H + O_2 + M \rightarrow HO_2 + M \quad (4)\ k_4 = 6.47 \times 10^{15} (T/298)^{-0.8} \mathrm{cm}^6/\left(\mathrm{mol}^2/\mathrm{s}\right)$$
$$H + HO_2 \rightarrow 2OH \quad (5)\ k_5 = 1.69 \times 10^{14} \exp(-440/T) \mathrm{cm}^3/(\mathrm{mol/s})$$
$$H_2 + HO_2 \rightarrow H_2O_2 + H \quad (6)\ k_6 = 3 \times 10^{13} \exp(-14400/T) \mathrm{cm}^3/(\mathrm{mol/s})$$
$$OH + O \rightarrow H + O_2 \quad (7)\ k_7 = 9.29 \times 10^{12} \mathrm{cm}^3/(\mathrm{mol/s})$$

$$O + HO_2 \rightarrow OH + O_2 \quad (8)\ k_8 = 3.25.10^{13} \mathrm{cm}^3/(\mathrm{mol/s})$$
$$OH + HO_2 \rightarrow H_2O + O_2 \quad (9)\ k_9 = 2.89.10^{13} \exp(250/T) \mathrm{cm}^3/(\mathrm{mol/s})$$

$2HO_2 \rightarrow H_2O_2 + O_2 \quad (10)\ k_{10} = 2.10^{12}cm^3/(mol/s)$
$H_2O_2 + M \rightarrow 2OH + M\ (11)\ k_{11} = 1.3.10^{17}exp(-22750/T)cm^6/\left(mol^2/s\right)$
$H + H + M \rightarrow H_2 + M \quad (12)\ k_{12} = 2.2.10^{15}cm^6/\left(mol^2/s\right)$

A two-dimensional problem was studied. The characteristic scales of the process were chosen as follows: $t_0 = 1/(k_1{}^0\ [H_2]_0)$, $x_0 = (D_3/\ k_1{}^0[H_2]_0)^{1/2}$, $U_0 = x_0/t_0 = (D_3\ k_1{}^0[H_2]_0)^{1/2}$ (scales of time, length and velocity, respectively, D_3 is the diffusion coefficient of H_2). We define dimensionless variables and parameters $\tau = t/t_0$, $\xi = x/x_0$, $\eta = y/y_0$, $\varpi = U/U_0$, $Y_i =$ [concentration of the i-th component]/$[H_2]_0$, $\delta_i = D_i/D_3$ (D_i is the diffusion coefficient of the ith component). The velocity and coordinates of the propagating flame front were determined through D_3: $\varpi = U/(D_3\ k_1{}^0[H_2]_0)^{1/2}$, $\xi = x/(D_3/\ k_1{}^0[H_2]_0)^{1/2}$, $\eta = y/(D_3/\ k_1{}^0[H_2]_0)^{1/2}$. Here U, x and y are the corresponding dimensional quantities, k_{10} is the preexponential factor of reaction (1). Diffusion coefficients (D_i/D_3, i = 0–6) δ_0, δ_1, δ_2, $\delta_3 = 1$, δ_4, δ_5, δ_6 in a hydrogen–oxygen mixture refer to OH, O, H, H_2, O_2, HO_2, H_2O_2, respectively. The system of equations for the above reaction mechanism takes the form (m, n = 0 ÷ 6 refer to the reacting particles OH, O, H, H_2, O_2, HO_2, H_2O_2, respectively):

$$\partial Y_i/\partial t = \delta_i(\partial^2 Y_i/\partial\xi^2 + \partial^2 Y_i/\partial\eta^2) + \sum_{m\neq i,n} k_n Y_m Y_n - \sum_{m=i,n} k_n Y_m Y_n$$
$$\partial T/\partial t = \delta_7(\partial^2 T/\partial\xi^2 + \partial^2 T/\partial\eta^2) + 1/(C_p\rho)\sum_{m,n} Q_n k_n Y_m Y_n \qquad (3.1)$$

The rate of heat release in the component of the reaction chain [42] is given by the last equation of system (3.1). Here C_p is the average specific heat at constant pressure, $\delta_7 \approx \delta_3$ is the thermal diffusivity for near-stoichiometric mixtures, and $\delta_7 \approx \delta_4$ for lean mixtures [42], T is the temperature (K), ρ is the mixture density g/cm^3, taken from [60]. Specific heats Q_i and diffusion coefficients were taken from [42]. f is the molar fraction of the initial component.

The reaction–diffusion equation for O atoms is shown below as an example:

$$\partial Y_1/\partial t = \delta_1(\partial^2 Y_1/\partial\xi^2 + \partial^2 Y_1/\partial\eta^2) + k_2 Y_2 Y_4 - k_3 Y_1 Y_3 - k_7 Y_0 Y_1 - k_8 Y_1 Y_5$$

The solutions of system (3.1) satisfy the following boundary conditions for flame propagation from right to left (L is the dimensionless distance between the reactor axis and the reactor wall, symmetry conditions are set on the axis):

$Y_i(\xi,\eta) \rightarrow 0\ (i \neq 3,4),\ (\xi,\eta) \rightarrow 300\,K, \quad \xi \rightarrow \pm\infty Y_3(\xi,\eta) \rightarrow f_{H2},$
$Y_4(x,h) \rightarrow f_{O2}, \quad \xi \rightarrow -\infty; \quad \partial Y_3(\xi,\eta)/\partial\eta \rightarrow 0,$
$\partial Y_4(\xi,\eta)/\partial\eta \rightarrow 0, \quad \xi \rightarrow +\infty$
$(\partial Y_i(\xi,\eta)/\partial\eta)_L = 0; \quad (\xi, L) = 300^\circ K$

When solving system (3.1), the initial fronts of the initial components Y_3 [H_2] and Y_4 [O_2] at zero time were determined according to the composition of the mixture. For the numerical solution, a finite-difference approximation of system (3.1) on a uniform grid of Cartesian coordinates was used. The two-step implicit scheme provided the second order of approximation of system (3.1) in spatial and temporal variables [61]. The distribution of the initial components in sections parallel to the central plane of the channel was approximated as follows: $Y_3 = 1/2 - 1/\pi(\text{arctg}(\xi + \eta))$, $Y_4 = 1/2 - 1/\pi(\text{arctg}(\xi + \eta))$, the initial temperature front was defined as $T = T_{ign} \exp((\xi + \eta)^2/50)$ [42], where T_{ign} is an a priori (trial) estimate. These initial fronts correspond essentially to the initiation of flame propagation by an external source. In the calculations, we used 500 partition points along the ξ and $70 \div 350$ points of division along η coordinate. The Laplace operator was approximated according to the "cross" scheme. The boundary conditions on the wall and the plane of symmetry were also approximated with a second order accuracy, while the partial derivatives with respect to time were approximated by one-sided differences, providing first-order accuracy. The calculations used such values of steps in spatial and temporal coordinates, which did not change the solution of the original problem with a further decrease in the step. Integration was performed according to an explicit scheme using the "predictor–corrector" procedure. The change in the concentration and temperature distribution was displayed on the screen, which made it possible to control the calculated parameters during the computation and determine the time of its completion in the dialogue mode. In the course of integration, either the regime of propagation of all the fronts of the Y_i concentrations at the same velocity was achieved, or the process of chemical transformation faded. It was assumed that the traveling reaction wave mode was achieved when the average value of the velocity did not change at a distance of 100 characteristic dimensions of the flame front, which was defined as the distance on the central plane of the channel where the dimensionless concentration of hydrogen atoms decreased by a factor of e ($e = 2.71828 \ldots$). If it was necessary to carry out long-term calculations (near the limits of flame propagation), the following procedure was used. Because the propagating wave with the values of the governing parameters used in the calculations occupied no more than 50 grid nodes, then when the wave approached the left boundary of the computational domain, and all changes in concentration and temperature occurred at 100 left grid nodes (there were only zero values on the right), the Y_i values from the left half of the grid were transferred to the right half and the calculation was continued. The reliability of this calculation method was quantitatively verified in [62].

Obviously, to ensure ignition, a cycle of reactions must occur, in which branching takes place (an increase in the number of active centers, see Chap. 1) [63]. To lower T_{ign}, namely, the flammability limit, the branching rate must increase [63], for example, due to the implementation of an additional branching reaction. Under the conditions of our experiment, this step can be reaction (5), in which a relatively inactive HO_2 radical is converted into active OH, i.e. branching occurs additionally to the reaction (2). As is shown in [63], taking into account reaction (5) makes it possible to explain the expansion of the ignition region in the presence of H atoms generated by an external source. In our case, the source of atoms is the chain initiation

reaction (0), because k_0 (a, E) increases in the presence of a hot catalyst. This rate is defined below as k_{0cat} (a is the preexponent, E is the activation energy). The higher the catalytic activity of the metal is, the greater the value of k_{0cat} is. The numerical experiment consisted in the fact that the value of $k_{0cat} \gg k_0$ for all experimental points of each curve in Fig. 3.15 was sought by means of paired linear regression analysis [64] with parameters a and E, so that the calculated curve was the closest to the experimental one. The experimental points on each curve were the average of the experimental temperatures, above which combustion occurred and below which there was no combustion. The calculated profiles of the concentration of the components, temperature and flame velocity U for one of the experimental points are shown in Fig. 3.16.

In Fig. 3.16, the shade of green determines the spatial distribution of Y_i concentrations. While the boundaries between the shades are isoconcentration ones (for the temperature distribution by isotherms), a darker color corresponds to a higher concentration (temperature) value within the range of variation between isoconcentration lines (isotherms). The interval between adjacent isoconcentration (isothermal) lines corresponds to a change in concentration (temperature) by 30%. In each of the given two-dimensional distributions, the top of the "frame" is the channel wall, and the bottom of the "frame" is the central plane. The calculation results are shown in Fig. 3.15 (curves).

As can be seen from Fig. 3.15, taking into account the elementary reaction H + HO_2 → 2OH (5) allows one to explain the experimentally discovered dependence of T_{ign} on the H_2 concentration. It also allows one to obtain satisfactory

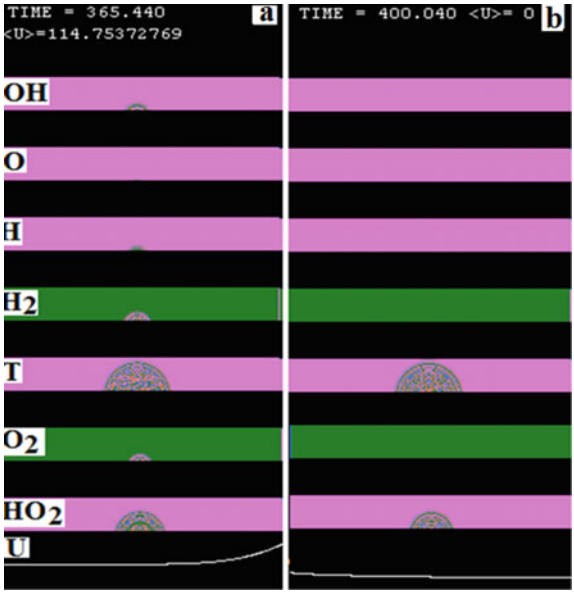

Fig. 3.16 Calculated profiles of chemical components and temperature at a given point in time (when it is clear, whether the reaction has started or not) above **a** and below **b** T_{ign}. The top of each frame is the reactor wall; bottom—the axis of the reactor. The front of the flame moves from the center to both sides. P = 40 Torr, wall temperature—300 K. **a** initial T = 680 K, ignition occurs; **b** initial T = 670 K, no ignition. U—flame velocity, arbitrary units

agreement with experimental data at $k_{0\,cat}$ (a, E) values for catalytic materials: $k_{0cat} = 4 \times 10^{12}$ exp (−3500/T) cm^3/(mol/s) for palladium and $k_{0\,cat} = 2 \times 10^{15}$ exp (−5000/T) cm^3/(mol/s) for platinum.

It should be noted that the activation energy of the gross process for a hot palladium surface (~7 kcal/mol) is higher than for a cold palladium surface (2.4 kcal/mol), while for a hot platinum surface (~10 kcal/mol). It is lower than for the cold platinum surface (19 ± 4 kcal/mol), which may be due to both the use of the reduced hydrogen combustion mechanism and errors in temperature measurements. Establishing the nature of this discrepancy requires further investigation.

3.5 The Influence of Noble Metals on Thermoacoustic Oscillations and the Boundaries of the Region of Negative Temperature Coefficient in Combustion of N-Pentane–Air Mixtures

The previous paragraph was devoted to the catalytic ignition of hydrogen, the oxidation of which is considered as a model process. The mechanism of ignition of hydrocarbons involves a significantly larger number of elementary steps, the rate constants of many of which have not been experimentally measured. The great complexity of the mechanism of oxidation of hydrocarbons causes a number of specific phenomena that are observed during their combustion.

Studying the ignition of hydrocarbons is of evident importance, but there has been no complete clarity about the puzzling phenomena intrinsic to that process. These are stepwise ignition and negative temperature coefficient (NTC), observed at considerably low temperatures. NTC is the increase of the delay time of auto (thermal) ignition with reactor temperature growth in a certain interval of temperatures. It causes undesirable phenomena in internal combustion engines [65, 66]. There is no consensus on the detailed hydrocarbon oxidation mechanisms over that temperature range as well as on an understanding of NTC phenomenon. As is known, a platinum layer on the reactor surface exhibits a promoting action on the hydrogen and hydrocarbon oxidation reactions [67], which is caused by heterogeneous development of reaction chains [68]. The occurrence of these heterogeneous reactions enhances the possibility of spontaneous ignition of gas mixture at a surface and influences markedly on delay times of ignition; the state of the reactor surface is another factor, which determines the spatial pattern of the ignition.

We emphasize once again that the design and operation of advanced reactors such as gas turbines or stationary and mobile fuel reformers require reliable micro-kinetic models to control the dynamics of combustion processes. The negative temperature coefficient phenomenon causes a reduction in mixture temperature for increasing inlet temperatures [69–71]. This behavior is known for higher hydrocarbons [70, 71]; limited data exist for methane oxidation. Under practical engine conditions, the ignition characteristics of hydrocarbon fuels can be divided into two classes: those with

single-stage auto ignition such as short-alkyl chain aromatics and alcohols, and those with two-stage auto ignition such as *n*-paraffins, unsaturated and cyclic hydrocarbons, with NTC phenomenon usually observed at temperatures below 850 K. When two-stage ignition occurs, the first-stage ignition assumes an essential role because the second-stage ignition depends on the heat release and intermediate species generated in the first stage. Furthermore, the negative temperature coefficient regime of the total ignition delay covers exactly the temperature range, which is relevant to engine knock and related combustion phenomena [72, 73]. Since hydrocarbons with two-stage auto ignition typically represent more than a half of practical fuels [74], engine processes controlled by combustion kinetics, such as homogeneous charge compression ignition, would occur in two stages as well; a low-temperature heat release stage is followed by a high-temperature heat release stage. It is then important to note that fuels with two-stage ignition have been found to offer significant advantages in controlling combustion phasing and extending the homogeneous charge compression ignition operation range [75, 76]. Consequently, it is essential to better understand the NTC phenomenon to develop novel control strategies for optimal fuel economy and lower pollutant emissions. Yu et al. [77] numerically investigated the transitions from ignition to the flames as well as the combustion dynamics in stratified n-heptane/air mixture, which showed that the rich mixtures with fuel stratification can demonstrate knocking and acoustic phenomena. One-dimensional simulations were performed to study the auto ignition and flame propagation of n-heptane/air mixture in a broad temperature range including NTC regime under elevated pressure conditions. According to one-dimensional simulations, steady premixed flame propagation affected by NTC chemistry shows a two-stage behavior, including both hot and cool flames [78]. It turns out that, despite all the variety of reacting systems and the conditions of development of chemical reactions in them, it is extremely difficult to determine the mechanism of ignition of the system.

Indeed, all kinetic studies based on measuring the ignition delay time show that a homogeneous ignition of a mixture at considerably low temperatures is an exception rather than a rule (see, e.g., [19, 79–81]). An initial center of ignition originates on the reactor surface; in each subsequent experiment under the same conditions, the site of origin of the initial center varies. This means that the initiation of the thermal ignition process is always determined by the presence of reactive centers on the surface, the properties of which are determined by both surface defects having an excess of free energy and their catalytic properties; the ignition process includes stages of warming-up, local ignition, and flame propagation. The basic feature of ignition process lies in the fact that ignition occurs at separate sites of surface at uniform temperature of the reactor surface. Therefore, combustion originates on the surface of the reactor even under conditions of almost homogeneous warming up of a gas mixture.

It should be noted in this connection that the ignition of the combustible mix in the heated reactor in swirling flow is on the contrary homogeneous [81]. In addition, in the presence of the surface in the form of aerosol, the ignition takes place on aerosol particles [19].

We earlier performed the following experiments to determine whether the reactor surface produces a catalytic effect on the ignition of hydrocarbons [69]. To do this, we introduced into the heated reactor a platinum wire 0.3 mm in diameter and 0.5 m in length. It was shown that multiple ignition kernels occur along the wire at higher temperatures (see Chap. 1). Without the wire, only one kernel occurs on the reactor surface over the temperatures in the NTC interval.

The pressure oscillograms for ignition under the same conditions in the absence and the presence of the catalytic surface showed the following. In the absence of the catalyst, cool flame ignition accompanied with considerably small warming up (if any occurred at all) quickly transforms into a hot one. Ignition kernels develop very rapidly, signifying in fact the beginning of hot ignition, while stepwise ignition and cool flames precede the stage of hot ignition. Although the pressure time history of the process is indicative of a cool flame ignition of the mixture, which manifests itself as a small step that precedes the main rise in pressure and appears much earlier than the ignition kernel recorded by the camera; filming frames show no detectable cool flames.

A specific effect on the ignition produced by the introduction a catalytic surface into the reactor in the form of a platinum wire is not limited to speed filming and pressure recording. In addition, in different temperature regions, this catalytic surface influences the ignition differently, namely at low temperature, the catalytic surface has no appreciable effect on the ignition delay time, but over the temperature region, in which NTC is usually observed, the presence of that surface completely eliminates this phenomenon [69]. In this case, a center of catalyzed ignition is located along the surface of the wire, i.e., it serves as an ignition source; at higher temperatures, several ignition centers are observed. Since the ignition delay in this case behaves as if there is no difference between cool flame and hot ignition in the temperature region corresponding to NTC, we can conclude that the catalytic surface eliminates a certain stage of the kinetic mechanism (an inhibition step) after the emergence of the cool flame. This fact seems to be very significant for elucidating the nature of the intermediate products of the reaction probably causing the existence of NTC phenomenon. However, it remains unclear how platinum wire localized in a small volume of the reactor has such a noticeable effect on the volume process.

This paragraph is aimed at the establishment of the features of the impact of noble metals (Pt, Pd) on specific combustion modes in the region of NTC.

3.5.1 Experimental

The ignition of n-pentane–air mixtures was studied in a rapid mixture injection static reactor (Fig. 3.17). A premixed fuel–air mixture passed from a storage vessel through a solenoid valve into a reactor, preliminary evacuated and heated to the desired temperature.

A stainless steel reactor, 12 cm in inner diameter and 25 cm in length, consisted of two hemispherical parts and narrow cylindrical one between them. The design of

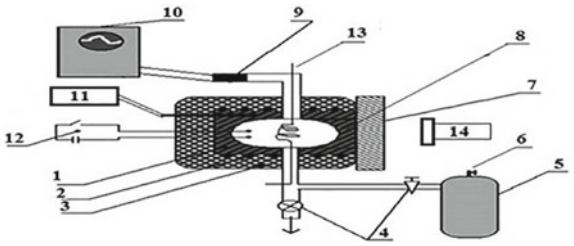

Fig. 3.17 Schematic diagram of the experimental setup: (1) reactor, (2) electric heater, (3) thermal insulation, (4) valves, (5) mixer, (6) pressure-reducer safety valve, (7) removable cover, (8) semi-spherical inset, (9) pressure transducer, (10) ADC–computer based data acquisition system, (11) digital measuring device for thermocouple, (12) spark ignition circuit, (13) noble metal wire, (14) digital video camera

the heater provided a uniform temperature distribution in the reactor volume [82], which was controlled with a movable thermocouple placed at the reactor surface. In a number of experiments Pt or Pd wires (0.3 mm in diameter and 40 cm long) were placed perpendicular the axis of the reactor in its central part.

Experiments were carried out with stoichiometric n-pentane–air mixtures over the pressure range of 2–3 atm. The pressure time history was recorded with a Karat-CI piezoelectric transducer (4 kHz), the signal from which was fed through an ADC to the computer. In a number of experiments, the reactor was equipped with an optical sapphire window at one of the ends (Fig. 3.17). Then ignition delays were additionally determined by a Casio Exilim F1 Pro color high-speed video camera (the frame rate is 600 fps). The video file was stored in the computer memory, and then it was processed frame-by-frame. Before each experiment, the reactor was evacuated with a 2NVR 5D vacuum pump to 10^{-2} Torr. The pressure in the reactor was measured by a vacuum meter and a standard vacuum gauge. An electromagnetic valve was used to open and close gas lines. N-pentane "Merck" of chemical pure grade, 99.9% Pt and 99.85% Pd were used.

The sets of experiments were always performed starting from low temperatures. When getting desired temperature, the gas mix was supplied into the reactor in 3 min. The reactor surface was scraped if there was a necessity to eliminate the noble metal from the walls of the reactor. The ignition delays were measured from the moment, at which gas supply ends, to the time of maximum pressure value. Then ignition delays were additionally determined by a Casio Exilim F1 Pro color high-speed video camera from the end of gas supply estimated from the corresponding pressure curve to the moment of appearance of the primary ignition center on the catalytic wire [19] at the frame rate 600 fps. It was shown that delay times of ignition measured both using maximum pressure with pressure transducer and occurrence of chemiluminescence with digital camera are very close to each other, because ignition delay time is much more than the time of pressure rise, therefore it is correct to identify the ignition moment as a peak pressure.

3.5.2 Results and Discussion

First, by means of the direct measurements of temperature in the center of the reactor (10 cm in diameter and 10 cm in length) with thin 25 μm thermocouples at atmospheric pressure and 800–980 K, it was shown that the time of warming up of gas mixture does not exceed 0.2 s. It is in agreement with results of Ref. [82] obtained in the same installation; that is much less than the time obtained by the equation considering the only conductive heat exchange.

Before the experiment 3 (Fig. 3.18a), 0.5 mm thick inner surface layer of the reactor was scraped off mechanically. In Fig. 3.18a, the sets of experimental data on ignition delay times for a stoichiometric n-pentane–air mixture in the reactor in the absence and presence of the catalytic Pt surface are compared. As is seen in Fig. 3.18a, in the region of a positive temperature coefficient at lower temperatures, the catalytic Pt surface has almost no effect on the ignition delay time, i.e. on the process of ignition. However, in the region of the negative temperature coefficient, the role of the catalytic Pt surface becomes very significant in agreement with [69]. However, not all Pt is eliminated from the surface layer after scraping. The initial "fresh" surface layer manifests longer ignition delay times, i.e. NTC over an untreated surface is observed at longer delay times than over scraped one.

Figure 3.19 displays typical pressure oscillograms at ignition under the same conditions in the absence and the presence of Pt and Pd. These oscillograms are shortened to increase the time resolution of oscillations: gas injection and most of ignition delay are not shown. It should be noted that the full pressure oscillograms show the stages in the process of ignition in the absence of a catalytic Pt surface in the reactor, whereas in the presence of the Pt catalyst, cool flame ignition immediately

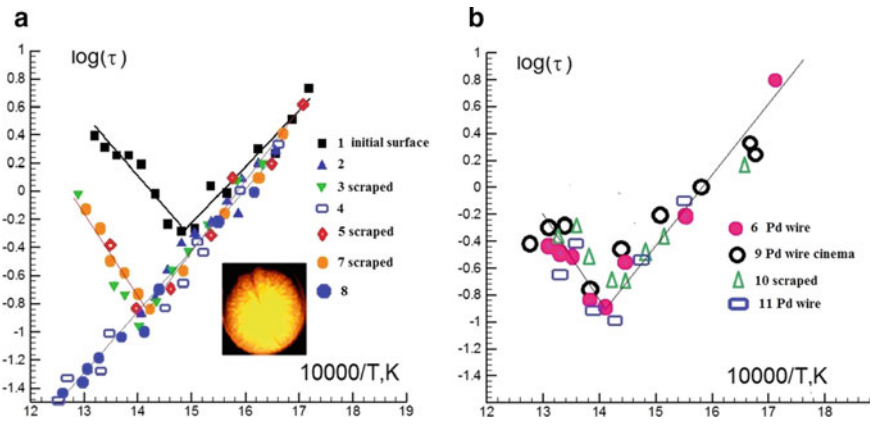

Fig. 3.18 Temperature dependence of the ignition delay time τ for n-pentane–air stoichiometric mixture at initial pressure of 3 atm. The figures at the symbols specify the sequence of the experimental sets; **a** Pt catalytic surface, **b** Pd catalytic surface. In the box: The frame of cellular combustion of 40% H_2 + 60% air mixture at the reactor walls temperature of 316 °C; Pt wire is placed in the stainless steel reactor [83]

transforms into hot one. The cool flame delay times (when a cool flame was observed) are rather close under our conditions to overall delays (the difference does not exceed 0.15 s at lower temperatures), see also [69]. Pt catalyzed ignition is located along the surface of the wire, i.e. it serves as an ignition source.

It should be noted that Pt and Pd experiments differ only in the material of the noble metal wire. The procedure and geometry of the apparatus are the same in the experiments; initial temperatures are very close to each other. Thus, the reproducibly

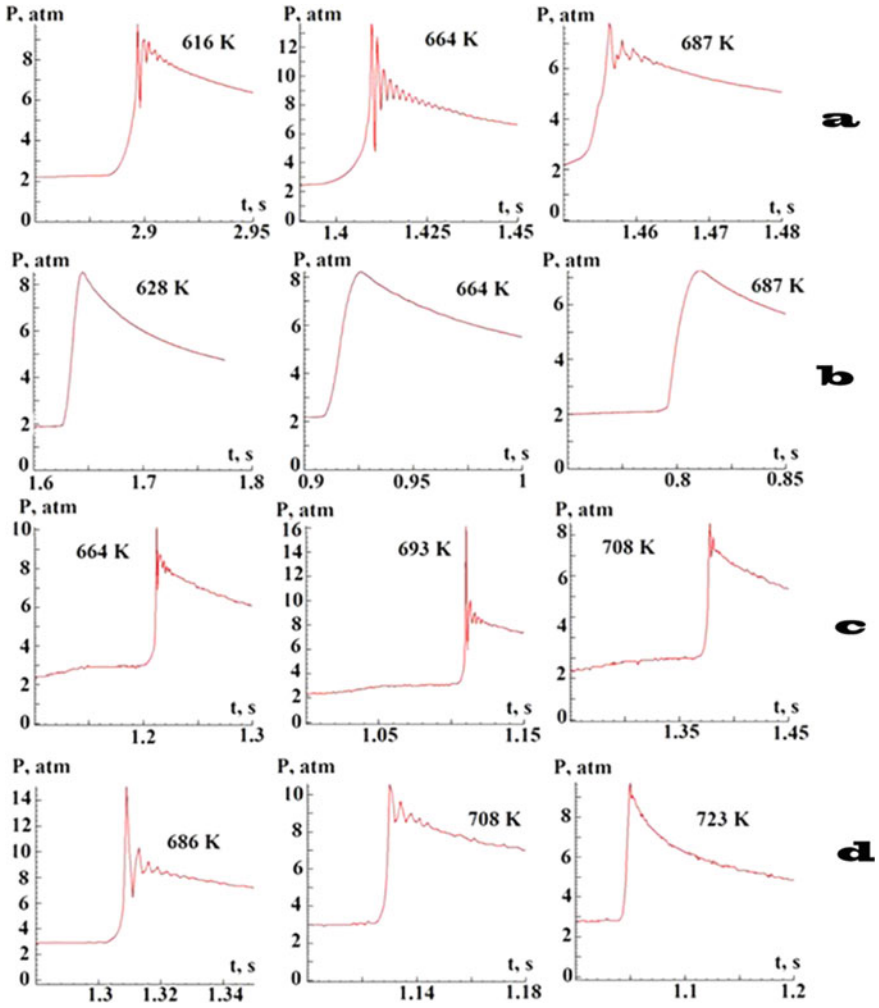

Fig. 3.19 Oscillograms of change in pressure for the ignition of n-pentane–air stoichiometric mixtures within the NTC region **a** in the absence of the catalytic surface, **b** in the presence of Pt wire, **c** in the absence of the catalytic surface (inner surface layer is previously scraped off), **d** in the presence of Pd wire

observed occurrence or absence of chemical oscillations is due to the chemical nature of the catalyst.

Notice that the process of ignition of the hydrocarbon–air mixtures at atmospheric pressure begins with the occurrence of the initial centers at the most chemically active sites of the surface, which initiate propagation of hemispherical flame fronts. The localization of the center is determined by the state of reactor surface and the temperature. These factors determine the geometry of the interaction of the flame fronts with acoustic waves. It in turn influences the number and intensity of the pressure oscillations because these occur from the very moment of the flame initiation as a feedback loop caused by the interaction between a flame front as a heat source and acoustic waves repeatedly passing through the front (see, e.g. Ref. [84]). In addition, Fig. 3.19a presents the results over scraped surface, but as is shown in Fig. 3.18a, not all Pt is eliminated from the surface layer after scraping, therefore the surface states for Fig. 3.19a and c are somewhat different from each other.

Because the delay time of ignition in this case behaves like if there is no difference between a cool flame and hot ignition within the temperature region corresponding to NTC [69, 85], we can infer that the catalytic Pt surface eliminates a certain step of ignition mechanism, probably an inhibition reaction [83], after the occurrence of the cool flame.

As is seen in Fig. 3.19a, hot ignition in the absence of catalytic Pt surface within NTC region is accompanied by thermoacoustic oscillations; their maximum amplitude is attained around the middle of the NTC region by temperature. As we noted above, thermoacoustic oscillations occur from the very moment of the flame initiation. At a small length of a spherical flame front at the beginning of combustion, the amplitude of thermoacoustic oscillations will also be quite small. Under our conditions, the process of amplification of the oscillations can be resolved by enhancing frequency and sensitivity of a pressure transducer. In Fig. 3.20a, typical oscillogram with increased sensitivity and frequency available for the pressure transducer used in the work is shown. In Fig. 3.20b, the oscillogram recorded with desensitized parameters is presented for comparison. As is seen in Fig. 3.20a, the amplification of oscillations on the section of pressure rise is clearly seen. However, this was not part of the task of this paragraph. It is aimed at establishment, under which conditions the oscillations are observed, or not observed. The frequency of the oscillations is about 500 Hz; this value roughly corresponds to the first mode of oscillations of the hollow vessel with dimensions close to the reactor used in this paragraph [86]. However, in the presence of catalytic Pt surface the oscillations are no longer observed (Fig. 3.19b). According to Lord Rayleigh principle [87] for heat driven pressure oscillations, thermoacoustic instability is encouraged when the heat release fluctuates in phase with the pressure perturbation. It means that in the presence of Pt, heat release and pressure perturbations during the combustion occur out of phase. It agrees with the statement cited above that the catalytic Pt surface eliminates a certain stage of combustion (an inhibition step) after the occurrence of the cool flame. The stage may be e.g. the decomposition of some slow reacting intermediate peroxide on the Pt surface with the formation of a more reactive surface radical, for instance O and/or OH, which then can be desorbed. Such a mechanism was proposed in [88] for

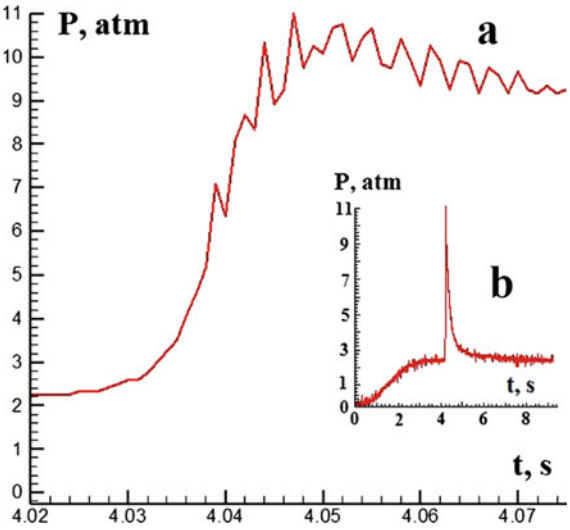

Fig. 3.20 Oscillogram of change in pressure for the ignition of n-pentane–air stoichiometric mixture at 615 K in the presence of Pd wire

hydrogen peroxide decomposition on platinum. It results in changing the rate of heat release during the hot ignition. The detailed mechanism of that stage in hydrocarbon oxidation obviously requires further consideration because experimental data on the reactions of gaseous alkyl peroxides on the surface of platinum are very scarce to date.

Seemingly, thin Pt wire occupies a low volume and cannot influence the combustion process in a gas. However, it is known [89] that at the temperature over 500 °C the molecules or clusters of both platinum oxide and platinum metal occur in gaseous phase. It was experimentally shown by the example of H_2 oxidation at 1 atm in [22] that the catalytic effect of Pt particles expanding into the reactor volume (see box in Fig. 3.18a) leads to the sharp reduction of the time of the steady flame front formation. The normal velocity of the flame front in the presence of a catalytic particles in the volume is much higher, than without the catalyst.

The catalytic effect of Pt in this work is almost similar to one described above.

Thus, the chemistry of the process is that the thin film of feebly stable, solid platinum oxide is formed on platinum surfaces in air or oxygen at room temperature and thickens as the temperature is raised to about 500 °C; then it decomposes. It means that molecules or clusters of both platinum oxide and platinum metal exist in gaseous phase at temperatures over 500 °C. Therefore, Pt containing particles, which expand into the volume during combustion, are the catalytic centers, where catalytic reaction can take place in the course of flame front propagation and strongly influence the combustion mechanism.

In the following series of experiments, the Pt wire was extracted out of the reactor and the dependence of the logarithm of an ignition delay time on reciprocal temperature for the stoichiometric n-pentane–air mixture within NTC region was measured again. It turned out that NTC phenomenon was still missing. It is evidently due to the

catalytic action of Pt-containing particles deposited on the reactor walls [89] after previous ignitions.

To restore initial material of the surface (stainless steel), 0.5 mm thick inner surface layer of the reactor was again scraped off mechanically. In Fig. 3.18b, the experimental data on ignition delay times for a stoichiometric n-pentane–air mixture in the reactor in the absence and presence of the catalytic Pd surface are compared. As is seen in Fig. 3.18b, both in the region of positive temperature coefficient and in the region of negative temperature coefficient the catalytic Pd surface has almost no effect on the ignition delay time, i.e. on the process of ignition. The obtained result is in agreement with the data [90]. It was shown in the work that in the presence of Pd foil, the cellular structure of the flame front of the H_2–CH_4–air mixtures is not observed, as compared with the results obtained on the Pt surface. This is due to the greater stability of PdO in comparison with PtO_2, which is very unstable and decomposes over 500 °C (see above). Figure 3.19c, d display pressure oscillograms for ignition under the same conditions in the absence (c) and the presence (d) of the catalytic Pd surface. As is seen in the Fig. 3.19c, the reactor inner surface was recovered from the mechanical treatment; hot ignition both in the absence and in the presence of catalytic Pd surface within NTC region is accompanied by thermoacoustic oscillations; their maximum amplitude is achieved in the middle of NTC region. It is an additional indication that in the presence of the catalytic surface, which does not noticeably react with oxygen at flame temperature and does not generate catalytic centers propagating into a volume, NTC phenomenon occurs.

Let us summarize the main experimental results.

(a) In the region of a positive temperature coefficient at lower temperatures, catalytic Pt surface has almost no effect on the ignition delay time, i.e. on the process of ignition. However, in the region of the negative temperature coefficient NTC, the role of the catalytic Pt surface becomes very significant: the NTC phenomenon vanishes;

(b) We can infer that the catalytic Pt surface eliminates a certain step of ignition mechanism, probably an inhibition reaction, after the occurrence of the cool flame;

(c) In the presence of Pt, heat release and pressure perturbation during the combustion occur out of phase. It agrees with the statement cited above that the catalytic Pt surface eliminates a certain stage of combustion (an inhibition step) after the occurrence of the cool flame. The stage may be e.g. the decomposition of some slow reacting intermediate peroxide on Pt surface with the formation of a more reactive surface radical, for instance O and/or OH, which then can be desorbed;

(d) Seemingly, thin Pt wire occupies a low volume and cannot influence the combustion process in a gas. However, at the temperature over 500 °C the molecules or clusters of both platinum oxide and platinum metal occur in gaseous phase. We showed earlier that these particles enter the reactor volume by diffusion and convection and act as catalytic centers, on which ignition takes place in the course of flame front propagation. These are the centers, which reactions strongly influence the combustion mechanism;

(e) The absence of Pd effect on NTC is due to the greater stability of PdO in comparison with PtO_2; it is additional evidence that in the presence of the catalytic surface, which does not noticeably react with oxygen at flame temperature and does not generate catalytic centers propagating into a volume, NTC phenomenon occurs.

In the further kinetic analysis, we wanted to build on the reliable kinetic data. However, the analysis of the detailed kinetic mechanism of n-pentane oxidation is premature due to lack of information (see below). In addition, in Ref. [91], the detailed mechanism of adsorption–desorption and surface oxidation of hydrogen on platinum is considered, elementary constants of 23 elementary reactions are given. It is obvious that these are estimates rather than experimental data; therefore, the reliability of the mechanism of catalysis is doubtful. Also, in the calculations of the ignition temperature of H_2–O_2 mixes over Pd foil decreases for leaner mixtures; it is contrary to experiment [92]. Therefore, there is no reliable kinetic data on the $H_2 + O_2$ kinetics over Pt particularly with the participation of n-pentane.

Notice that numerical investigations including kinetic mechanisms are considerably speculative; their value is often exaggerated. Really, any comparison of e.g. experimentally detected flame front propagation with a result of numerical modeling is credible only in a qualitative aspect, namely on velocity change of movement of the boundary between initial and actively reacting gas, as well as on the shape of this border and on the degree of its "smoothness" or perturbations of its structure. The consideration of detailed kinetics in calculations provides additional uncertainty since most of kinetic parameters (e.g. preexponent and activation energy for every reaction step) are not accurate enough to draw sufficient conclusions. The completeness of the kinetic mechanism is reasonably always under question because a certain important reaction can be overlooked. This is particularly true for n-pentane oxidation as well as for the reactions of the alkylperoxide responsible for NTC phenomenon. Moreover, there are no unicity theorems on reactive Navier–Stokes equations; thus, any agreement between calculated and experimental quantities does not argue for agreement between calculation and experiment, as there can be other sets of governing parameters describing the same experimental data [42].

The above can be illustrated by the example of the mechanism of methane oxidation. For the mathematical analysis, the mechanism, which includes all possible reactions is first reduced; namely the reactions in this system are excluded by means of various algorithms e.g. the program environment "Chemical Workbench". However, in literature the question of uniqueness of the optimum reduction process using a certain algorithm is not strictly proved. Therefore, there are several similar algorithms leading to different mechanisms. Thus, simplification of a probably incomplete mechanism is a non-strict process, which can lead to an unacceptable error. For instance, one of the most popular is the methane oxidation mechanism known as the GRI-Mech; one of its versions consists of 325 elementary steps and 53 components. However, this mechanism does not describe some aspects of methane combustion, such as soot formation. Though there are such components as methanol and acetylene, the mechanism cannot be applied to the description of the processes of their

oxidation. Thus, the mechanism fails to describe accurately the important features of methane oxidation. It means that the mechanism has no predictive force, because it incorrectly describes known regularities of that process. One can conclude that the contemporary results based on calculations can serve at best only for qualitative illustration of experimental data [93]. This applies even more so to the mechanism of n-pentane oxidation in the presence of a catalyst.

Due to aforesaid, we used the qualitative approach, namely the simplest kinetic mechanism only to illustrate the experiment; because the analysis of detailed chemical kinetics will have no scientific value since it will be reduced to fitting a few hundred kinetic parameters.

Thus, we took an attempt to illustrate qualitatively the influence of the chemical mechanism and heat release by a simple example of a sequence of two chain chemical reactions by means of numerical modeling. The system of compressible dimensionless reactive Navier–Stokes equations in low Mach number approximation presented in [42, 92, 93], which describes the flame propagation in a two-dimensional area was used.

The following reaction set was analyzed. The combustion process for certainty was presented by an elementary chain mechanism: $C \rightarrow 2n$ (w0) and $n + C \rightarrow 2n + n1 +$ products (β_0, $Q = \beta_1$) and $n1 + C \rightarrow n +$ products (β, $Q = \beta_2$), Q—heat release in a step. The second reaction can be considered as some kind of gross process involving molecular clusters containing a catalyst. We will specify that by consideration of the process of stationary flame propagation, a reaction of chain origination w_0 can be neglected [94]. The set of dimensionless reactive Navier–Stokes equations is presented in Chap. 2, Sect. 2.5, Appendix. We will recall it in order not to refer the reader to Chap. 2. When considering the problem, the designations given in Chap. 2 are kept below.

$$
\begin{aligned}
&\rho T = P && \text{(a)}\\
&\rho_t + (\rho v)_y + (pu)_x = 0 && \text{(b)}\\
&\rho(u_t + vv_y + uv_x) + P_y/\gamma M^2 = 1/Fr + Sc(\nabla^2 v + 1/3K_y) && \text{(c)}\\
&\rho(v_t + vu_y + uu_x) + P_x/\gamma M^2 = 1/Fr + Sc(\nabla^2 u + 1/3K_x) && \text{(d)}\\
&\rho[T_t + vT_y + uT_x] - (\gamma - 1)/\gamma P_t - (\gamma - 1)\gamma M^2[P_t + uP_x + vP_y] = \nabla^2 T + \beta_1 W + \beta_2 W_1 && \text{(e)}\\
&\rho[C_t + v\,C_y + uC_x] = \Delta^2 C + w0 - \beta_0 n\,W - \beta n1\,W_1 && \text{(f)}\\
&\rho[n_t + v\,n_y + u\,n_x] = \Delta^2 n + w0 + 2\beta_0 n\,W + \beta n1\,W_1 && \text{(g)}\\
&\rho[n1_t + v\,n1_y + u\,n1_x] = \Delta^2 n + \beta_0 n\,W - \beta n1\,W_1 && \text{(h)}\\
&W = C\exp(\zeta - \zeta/T) && \text{(i)}\\
&W_1 = C\exp(\zeta_1 - \zeta_1/T) && \text{(j)}\\
&P_{tt} - -1/M^2\nabla^2 P = q(C_P - 1)[\beta_1 W_t + \beta_2 (W_1)_t] && \text{(k)}
\end{aligned}
\qquad (3.2)
$$

where $\nabla^2 = (\ldots)_{yy} + (\ldots)_{xx}$ is the two-dimensional Laplace operator, $K^v = v_y + u_x$ is the viscous dissipation, M - Mach number, $P(x,y,t) = P_0(t) + \gamma M^2 p_2(x,y,t) + O(M^3)$, $P_0(t)$—static pressure (computed as in [95]), $p_2(x,y,t)$—dynamic pressure. $P_{tt} = d^2P/dt^2$, $d(\ldots)/dt$ is a material derivative, u and v are the velocity components in the directions x, y, respectively, ρ is the density and T is the temperature. C—reagent concentration, $1 - C$—extent of transformation, ζ—dimensionless coefficient proportional to E/R. Dimensionless parameters—Schmidt's criterion Sc

$= \nu/D$, D—diffusivity (0.3 cm^2/s at 1 atm [60]), ν—gas kinematic viscosity (10^{-5} cm^2/s [60]), γ—the relation of constant pressure and constant volume thermal capacities; β_1 characterizes heat release allocation for concentration, β is a kinetic coefficient proportional to Damköhler number. The initial values are the following: $\rho_0 = 0.001$ g/cm^3 [60], $T_0 = 1$, $P_0 = \rho_0 T_0$, $\zeta = 10.5$, $\gamma = 1.4$, $\beta = 0.2$, $\beta_1 = 0.3$, $C_P = 0.3$ kal/g grad [60] and $C_0 = 0$, respectively. These values were used for calculations in Fig. 3.21. Lewis's number is equal $Le = 1$ that assumes equality of $Sc = Pr$ where $Pr = \rho_0 Cp\ \nu/\lambda$, λ—heat conductivity and Cp—thermal capacity at constant pressure. Scales of length and speed are determined as $l_d^2 = Dt_d$, and $U_d = l_d/t_d$, respectively. Then Reynolds's number is $l_d\ U_d/\nu = 1/Sc$. Mach number is $M = U_d/c_0$; it is accepted equal 0.025, where c_0—the speed of sound. If the standard representation of pressure is used, then usual replacement of variables $P = P_0 p$ leads to occurrence of a factor $1/M^2$ in the term *grad p* in impulse equation [96, 97]. It is accepted that pressure values satisfy wave equation [the last equation (k) of the set (a)–(k)], which can be obtained from the continuity and impulse equations taking into account internal power sources and neglecting terms of order 1/M [96, 97]. The equation (k) of the set (a)–(k), describing waves in the moving non-uniform media with a heat source, follows from continuity and impulse equations ($q = l_d^2/(U_d^4 \rho_0) \approx 1$—the parameter arising at the reduction to a dimensionless form), therefore the set (a)–(k) is overdetermined. In order that the quantity of the equations must correspond to the number of unknowns, Eq. (a) is excluded from the set (a)–(k) in the further analysis.

The parameters were assumed to be $\zeta = 4$, $\zeta_{1=}7.5$ $\beta_0 = 0.1$, $\beta = 0.15$, $\beta_1 = 0.22$, $\beta_2 = 0.3$. Diffusivities $D_n = D_{n1} = 0.3$, $T_t = T - T_0$.

The solution of the problem was carried out by finite element analysis with the package (FlexPDE 6.08, 1996-2008 PDE Solutions Inc. [98]). The results of calculation of thermoacoustic oscillations in the reaction set (b)–(k) are shown in Fig. 3.21. On the top, the calculation of temperature field is shown. At the bottom, kinetic pressure curves calculated at the point of the top of the reactor (indicated by a square), corresponding to the conversion degree specified on the top of Fig. 3.21 are shown. Each column corresponds to the initial dimensionless wall temperature specified at the bottom of Fig. 3.21. It is seen that at $T = 6$ the oscillations during combustion are most intense, and at $T = 3$ and $T = 9$ the oscillations are less intense; it qualitatively illustrates the experiment.

As is also seen in Fig. 3.21, the interchange of activation energies of two radical reactions leads to marked changes in the modes of thermoacoustic oscillations. This is most likely because the heat release and pressure perturbation at $\zeta = 4$, $\zeta_1 = 7.5$ during the combustion occur to a greater extent out of phase than at $\zeta = 7.5$, $\zeta_1 = 4$ at the expense of change in time dependencies of heat release during combustion.

It should be noted that the analysis of a single chemical reaction when the second one is excluded ($\beta = 0$), which is equivalent to its complete inhibition, does not lead to an effect when, with an increase in the initial temperature, the intensity of thermoacoustic oscillations first increases and then decreases. It means that this simple model allows a qualitative representation of NTC phenomenon.

Therefore, it is clear that the reliable micro-kinetic model must take into account the occurrence of thermoacoustic oscillations; the exclusion of a certain stage of the

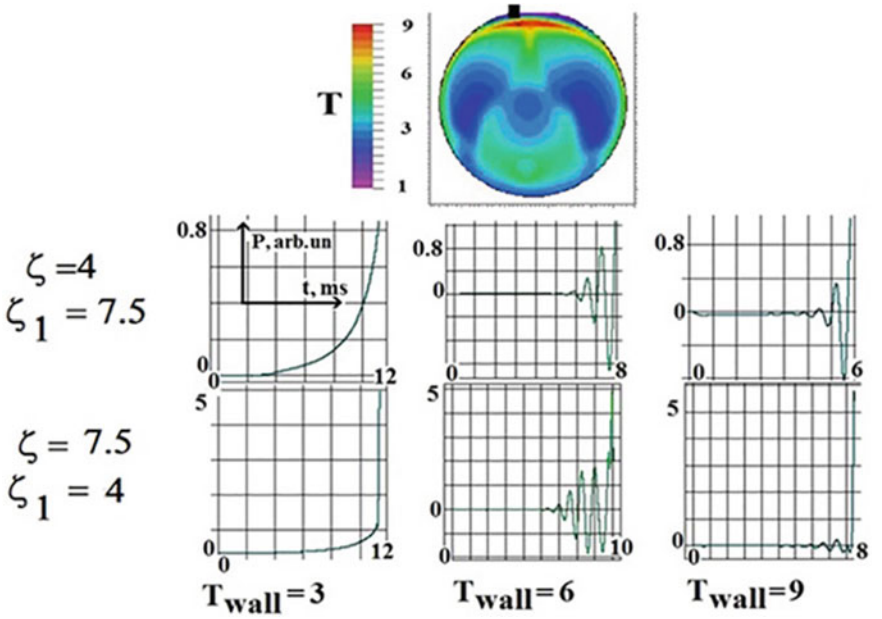

Fig. 3.21 The results of numerical calculation of the set of compressible dimensionless reactive Navier–Stokes equations in low Mach number approximation. A detailed explanation of this figure is given in the text

kinetic mechanism (probably of superficial character) should cause the NTC reaction mode to disappear. It is obvious that the establishment of the detailed combustion mechanism satisfying the conditions obtained in the present work requires not only additional experimental information but also an increase in the amount of calculations using a significantly large computer capacity for going through all possible variants of the reaction steps.

We summarize shortly the results obtained.

The peculiarities of ignition of premixed stoichiometric n-pentane–air mixtures were studied in a rapid mixture injection static reactor in the presence of metallic Pt and Pd in the region of negative temperature coefficient (NTC). It is shown that in the absence of noble metals thermoacoustic oscillations occur within NTC region. However, in the presence of Pt catalyst surface, which reacts with oxygen at the flame temperature and generates catalytic centers propagating into volume, thermoacoustic regimes of thermal ignition disappear. In other words, the catalytic Pt surface eliminates a certain inhibition stage of kinetic mechanism after the occurrence of the cool flame and NTC phenomenon vanishes; the stage may be e.g. the decomposition of some intermediate slow reacting peroxide on Pt surface with the formation of a more reactive radical. In the presence of the catalytic surface (Pd), which does not react at the flame temperature and does not generate catalytic centers propagating into volume, NTC phenomenon occurs.

Thus, the detected regularities must be taken into account in numerical simulations of NTC phenomenon. In other words, the oscillations and NTC phenomenon must both disappear in calculations after excluding a certain reaction or a series of reaction steps from the mechanism. The step must include the superficial reaction of an active intermediate of combustion on Pt surface, in which more active intermediates are formed from a low-active one.

3.6 A Negative Temperature Coefficient Phenomenon in the Combustion of Hydrogen–Propane–Air Mixtures Over Pd Foil

The existence of a negative temperature coefficient region in hydrocarbon oxidation reactions suggests the existence of a similar region in the catalytic oxidation of hydrogen–hydrocarbon mixtures, but caused by a change in surface state from ignition to ignition, which we described in Chap. 2. Experimental observation of such a region will be described below.

The investigation of ignition of fuels, mainly hydrocarbons or hydrogen–hydrocarbon mixed fuels, is of obvious practical importance, but even to this day, there is no complete clarity about the mysterious phenomena accompanying this process. One of the most poorly understood are stepwise ignition and negative temperature coefficients (NTC), observed at considerably low temperatures [42]. NTC is the increase of the delay time of ignition with temperature growth in a certain interval of temperatures. As it was discussed in the previous paragraph, it causes undesirable phenomena in internal combustion engines [66, 99]. There is no consensus on the detailed mechanisms of hydrocarbon oxidation in this temperature range as well as on the nature of NTC phenomenon. We have shown in Sect. 3.4 of this chapter, using rapid mixture injection static reactor that at temperatures < 660 K, the catalytic Pt surface has no appreciable effect on the ignition delay time of thermal ignition of stoichiometric n-pentane–air mixture. However, in the temperature region in which negative temperature coefficient is usually observed, the presence of Pt surface eliminates NTC occurrence [69]. The revealed feature seems to be the key one for understanding NTC phenomenon.

Noble metals impact on the flammability of hydrogen–hydrocarbon blends differently. We showed above that the ignition temperature of the mixture 40% H_2–air over Pd metal (70 °C, 1 atm) is ~ 200° less than over the Pt surface (260 °C, 1 atm) [31, 90]. In addition, Pd ignites stoichiometric mixes (30 ÷ 60% H_2 + 70 ÷ 40% CH_4) + air ($\theta = 1$, equivalence ratio θ is a fraction of fuel in the mix with air: $\theta\ H_2 + 0.5\ (O_2 + 3.76N_2)$); metallic Pt cannot ignite these up to 450 °C, i.e. Pd is more effective than Pt. We also showed that the cellular structure of a flame front at ignition with Pd is not observed as compared with the results obtained over Pt surface. Thus, Pd to a greater extent meets the requirements for hydrogen recombinators in NPP, because no catalytic particles as ignition centers formed by decomposition of volatile

oxide can appear in gas phase as compared to Pt [42]. The experimental value of the effective activation energy of the process is estimated as 3.5 ± 1 kcal/mol that is characteristic of surface processes. It indicates the noticeable role of the dark reaction of consumption of H_2 and O_2 observed directly at low pressures [31].

We found that the temperature of the "upper" ignition limit over palladium surface at 1.75 atm, measured with a bottom-up approach by temperature, of the mixtures 30% methane + 70% hydrogen + air ($\theta = 0.9$, T = 317 °C) and 30% propane + 70% hydrogen + air ($\theta = 1$, 106 °C) decreases after subsequent ignitions to the "lower" ignition limit and amounts to 270 °C, for the hydrogen–methane mix and to 32 °C for the hydrogen-propane mix. The limit returns to the initial "upper" value after processing of the reactor with oxygen or air, i.e. a hysteresis effect occurs. Thus, the "lower" ignition limit corresponds to the reactor or Pd surface treated with ignitions; the "upper" one corresponds to the "fresh" reactor or Pd surface.

As is seen from above, noble metals influence on the NTC phenomenon and give rise to hysteresis phenomena in H_2–hydrocarbon blends combustion as well. These factors give good grounds for expecting NTC phenomena in low temperature area as well as the hysteresis phenomenon in the combustion of H_2–hydrocarbon blends over catalytic surface.

The present paragraph concentrates on both the detection and the establishment the nature of the low temperature NTC phenomenon in the hysteresis area of combustion of (70 ÷ 40%) hydrogen– (30 ÷ 60%) propane–air mixtures with $\theta = 1$ over Pd at total pressures 1 ÷ 2 atm. The paragraph is also aimed at the establishment of both dependencies of the ignition delay period on time and the relationship of a flammability limit over Pd surface on temperature.

3.6.1 Experimental

The experiments were performed with gas mixtures of (70 ÷ 40%) hydrogen– (30 ÷ 60%) propane–air mixtures with $\theta = 1$ over Pd at total pressures 1 ÷ 2 atm. A heated cylindrical stainless steel reactor 25 cm in length and 14 cm in diameter, equipped with demountable covers and an optical sapphire window in one of the covers was used in experiments [90]. The accuracy of temperature measurements was 0.3 K. Recording of ignition and flame propagation was performed by means of a color high-speed camera Casio Exilim F1 Pro (frame frequency—600 s^{-1}). A video file was stored in computer memory and its time-lapse processing was performed [42]. The pumped and heated reactor was quickly filled with the gas mixture from a high-pressure buffer volume with the necessary pressure. We recall that the ignition limit was determined as the mean of two temperatures at the given pressure; e.g. for a bottom-up approach by temperature: at lower temperature the ignition was missing, at a higher one the ignition occurred. An electromagnetic valve was used to open and close gas communications. A pressure transducer recorded pressure in the course of gas intake and combustion. A Pd foil 80 mm long, 1 mm wide and 0.066 mm thick was placed in the reactor. The Pd wire was used both to ignite the flammable mix and

to estimate the warming-up of the wire as a bridge arm. Before each experiment, the reactor was pumped down to 0.01 Torr; after each ignition, the pumping continued during 1.5 h to pump out most of the water vapor. Total pressure in the reactor was monitored with a vacuum gauge, and the pressure in the buffer volume was controlled with a manometer. Chemically pure gases and 99.85% Pd were used. X-ray photoelectron spectroscopy (XPS) measurements were performed by means of Kratos AXIS Ultra DLD device. The microstructure of Pd foil and wire was examined using field emission ultra-high resolution scanning electron microscope Zeiss Ultra Plus (Germany) equipped with an X-ray microanalysis console INCA 350 Oxford Instruments.

3.6.2 Results and Discussion

Time dependencies of the Pd wire resistance during the ignition of $C_3H_8 + H_2 +$ air mixtures are shown in Fig. 3.22a, b. The dependencies correspond to the successive temperature values below the "upper" catalytic ignition limit measured with a bottom-up approach. As is seen in Fig. 3.22a, b, the ignition delay periods τ first decrease with a decrease in temperature; but then τ values increase until the "lower" catalytic ignition limit is achieved. Thus, we observe the NTC phenomenon somewhat similar to one known in literature [42]. In our case, the NTC phenomenon we found has an obvious explanation. It is caused by the changes in the state of Pd surface.

The dependence of H_2 fraction at the "upper" ignition catalytic ignition limits (a bottom-up approach) in the mixtures under investigation in Arrhenius coordinates similarly to [90] is presented in Fig. 3.22c. As is seen in Fig. 3.21c, the dependence can be approximated by a straight line (the correlation coefficient is 0.978, the data were processed with the use of the program package Statistica 9 (Statsoft)). The experimental value of effective activation energy of the process is $E = 2.2 \pm 1$ kcal/mol that is characteristic of surface processes [25]. It should be noted that the value of effective activation energy is close to one obtained from the dependence of the H_2 fraction in the flammable mixtures on temperature in Arrhenius coordinates for H_2–air and H_2–CH_4–air mixes [90]. It is also evidence that the detected NTC phenomenon is strongly associated with the state of Pd surface.

In this regard, studies have been conducted in order to examine the state of Pd surface. An initial sample of Pd foil was compared with one treated with 70 ignitions by means of X-ray photoelectron spectroscopy and scanning electron microscopy.

As is revealed in [100], in examining the partial oxidation of methane over Pd/Al_2O_3 catalyst, the peaks at lower binding energies (335 eV) are characteristic of metallic Pd with PdO_x species appearing slightly higher at 336–337 eV. Due to the catalyst preparation method and storage (i.e. exposure to air), Pd shows some degree of oxidation for all samples at 500 °C, but metallic Pd peaks at 335 eV are dominant at these lower temperatures. As the temperature is increased to 600 °C and again to 650 °C, XPS signal characteristic of a PdOx species at 336.0–336.2 eV becomes dominant for most particle sizes. In addition, metallic Pd (335 eV) also has a strong

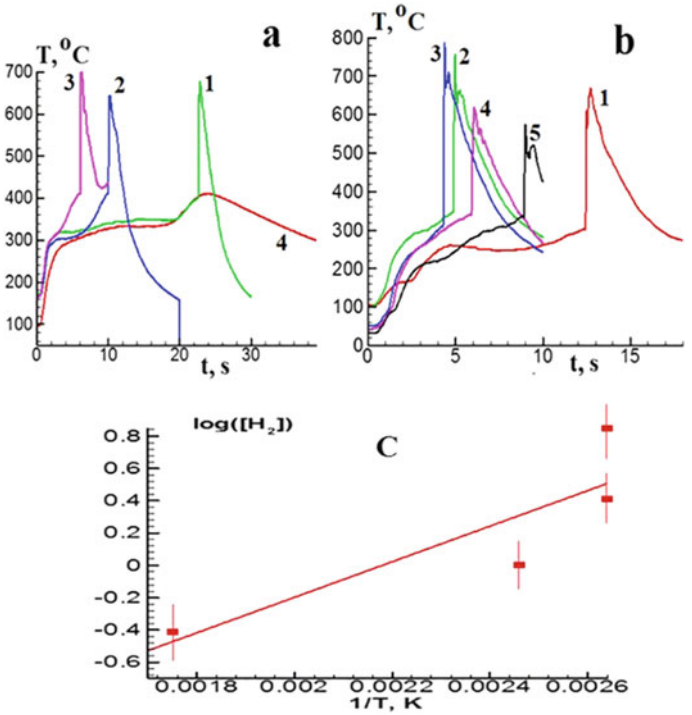

Fig. 3.22 Monitoring of the change in the Pd wire resistance during the ignition of **a** 60% C_3H_8 + 40% H_2 + air mixture; initial temperature. (1) 174 °C, (2) 168 °C, (3) 165 °C, (4) 98 °C, P = 1.75 atm. **b** 40% C_3H_8 + 60% H_2 + air mixture; initial temperature. (1) 104 °C, (2) 102 °C, (3) 58 °C, (4) 45 °C, (5) 38 °C, P = 1.75 atm. The ignition delay τ is indicated in the figure. **c** The dependence of the H_2 fraction at the "upper" ignition limits in the mixtures under investigation in Arrhenius coordinates (a bottom-up approach by temperature) at P = 1.75 atm

contribution in the XPS spectra, and the data show that a mixture of both Pd metal and Pd oxide is needed to continue the reaction, after the oxide has initially been formed. At temperatures above 700 °C, the oxide species is reduced to metallic Pd. According to above, as is seen in Fig. 3.23, the treated Pd sample contains greater amount of PdO than initial sample. PdO species arise due to gaseous oxidation and then decompose again to Pd and O_2 at 900 °C [101]. It means that both Pt oxide and Pt metal in the form of molecules or clusters of exist in gaseous phase at temperatures over 900 °C. Notice that the maximum temperature of hydrogen- propane–air flame attains 1600 °C under our conditions.

The results of electron spectroscopy investigation are presented in Fig. 3.24. As is seen, the initial sample represents the surface with rolling marks (Fig. 3.24a). In the sample treated with ignitions, the defects in the form of openings develop (Fig. 3.24b). It was found that their depth reaches 1 μm. These defects are focused on the patterns having the form of etching figures (Fig. 3.24c); the etching substances are evidently active intermediates of H_2 and CH_4 oxidation.

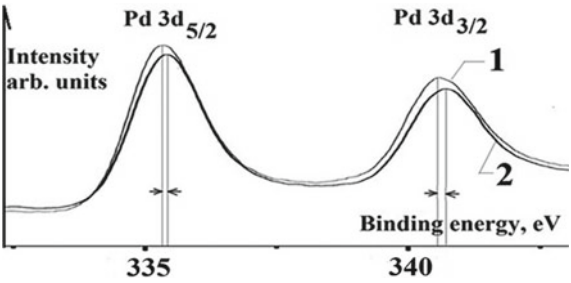

Fig. 3.23 Pd $3d_{5/2}$ and Pd $3d_{3/2}$ photoemission spectra obtained from (1) initial Pd foil and (2) Pd foil treated with 70 ignitions of mixes (30 ÷ 60% H_2 + 70 ÷ 40% CH_4) + air. Photon energy is 460 eV

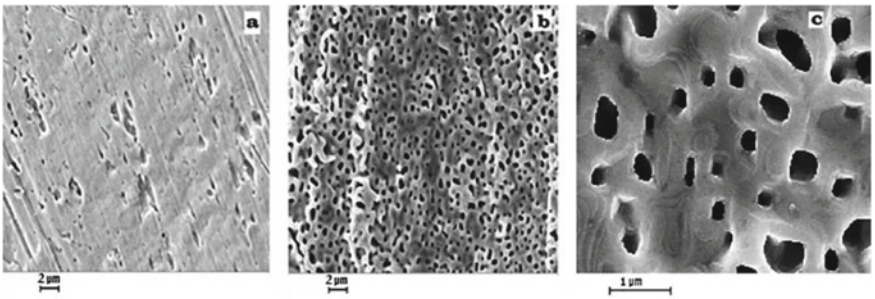

Fig. 3.24 Micrographs of the Pd foil surface **a** of initial Pd foil, **b**, **c** of treated Pd foil

The etching process can be easily vizualised by means of speed color cinematography (Fig. 3.25). As is seen in Fig. 3.24, an orange flow of particles moves up simultaneously with propagating flame front. The fact that the particles rise up indicates that the particles are hot. It is clearly seen from the sequence of frames that these particles occur in the immediate vicinity of the surface of palladium metal. We may conclude, therefore, that we observe PdO particles, which originate in the process of oxidation of Pd surface; these partially decompose to Pd and O_2 at the temperature of flame products. This means that the catalyst Pd is consumed in the reaction of chemical etching with (most likely) active intermediates of the flame. It should restrict the applicability of palladium in stationary ignition devices.

As is seen from the above, the catalytic ignition in the vicinity of the ignition limit over palladium surface, measured with a bottom-up approach by temperature, provides etching and a corresponding increase in Pd surface area (see Fig. 3.24b, c). It leads to acceleration of the surface reaction of H_2 oxidation and hence to the acceleration of the overall process. Each subsequent ignition causes a further increase in the catalysic surface area, therefore the values of ignition delay decrease by temperature; then τ values increase until the "lower" catalytic ignition limit is achieved.

It is shown that at combustion of (70 ÷ 40%) hydrogen– (30 ÷ 60%) propane–air mixtures ($\theta = 1$) over palladium at total pressures 1 ÷ 2 atm the ignition delay periods τ first decrease with a decrease in temperature; but then τ values increase until

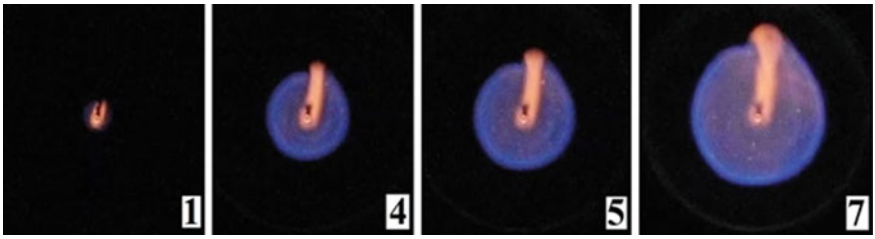

Fig. 3.25 High speed color registration of the initiation with a palladium wire and flame propagation in mixes 60% CH_4 + 40% H_2 + air mix, $\theta = 1$, P = 1.75 atm, 174 °C, 600 s^{-1}. Numbers in each frame correspond to a consecutive number of the video image during the catalytic ignition

the ignition limit is achieved i.e. NTC phenomenon occurs. The effective activation energy of the process is $E = 2.2 \pm 1$ kcal/mol that is characteristic of a surface process. Thus, NTC phenomenon is strongly associated with the state of Pd surface. It is found out that in the sample treated with ignitions, the defects in the form of openings, which are focused on etching patterns, arize. In the process, PdO particles form, which originate in the process of oxidation of Pd surface; they decompose to Pd and O_2 at the temperature of flame products. Thus, the negative temperature coefficient at combustion of hydrogen–propane–air mixtures over palladium at total pressures $1 \div 2$ atm is caused by an increase in Pd surface area due to the reaction of chemical etching with active intermediates of combustion. This means that Pd is spent in the reaction of chemical etching with active intermediates of combustion. It should limit the applicability of palladium in ignition devices.

3.7 Ignition of Hydrogen–Methane and Hydrogen–Isobutene Mixes with Oxygen Over Rh and Pd at Low Pressures

In the previous paragraphs, we considered the features of catalytic ignition of hydrocarbons and their mixtures with hydrogen. However, the factors determining the boundaries of the catalytic ignition regions of hydrogen–hydrocarbon mixtures, the knowledge of which is important, for example, to address the issues of explosion safety, remained unaffected in above consideration. In addition, in this paragraph, the regularities of the process in the conditions of the dark reaction and, accordingly, incomplete combustion of fuel are established.

As is well known, methane reaction with oxygen occurs in a dark on hot platinum wire as a catalyst [1]. This has stimulated a great interest in the study of catalytic oxidation processes in view of a potential for the industrial applications. For instance, this is promising for use in electric power generation systems [4], for reducing methane emissions in mines [5], and in automobile emission control systems [6]. Hydrogen–hydrocarbon blends attract attention as alternative fuels for

power generation for the following two reasons. The first refers to the opportunity of adding hydrogen to methane in order to improve performance and to reduce pollutant emissions of lean combustion [6]. The second reason is due to concerns about global warming possibly reduced by using hydrogen in both fuel cells and combustion devices [34]. Note, however, that this reason makes sense only in the case of the fairness of the theory of global warming. As indicated in the introduction, this hypothesis is more connected with the desire of a number of bureaucratic structures to earn more money.

Noble metals can also catalyze reactions during chemical vapor deposition (CVD) in the synthesis of carbon nanostructures. These were synthesized on Al_2O_3 supported Pd nanoparticles [102]. The addition of hydrogen or oxygen to acetylene highly influences the growth products on Pd [103]. Different carbon nanostructures could be synthesized by catalytic CVD on palladium (Pd) nanoparticles. Multi-walled carbon nanotubes (MWCNTs) and carbon nanofibers (CNFs) were grown selectively, dependent on temperature, using acetylene as carbon precursor [104].

There are many modes of noble metals impact on the flammability of hydrogen–methane blends. It was shown that the ignition temperature of the mixture 40% H_2–air over Pd metal (70 °C, 1 atm) is ~ 200° less than over the Pt surface (260 °C, 1 atm) [31, 69]. In addition, Pd ignites stoichiometric mixes (30 ÷ 60% H_2 + 70 ÷ 40% CH_4) + air ($\theta = 1$, equivalence ratio θ is a fraction of fuel in the mix with air: θ H_2 + 0.5 (O_2 + 3.76 N_2)); metallic Pt cannot ignite these up to 450 °C, i.e. Pd is more effective than Pt. The experimental value of the effective activation energy of the process is estimated as 3.5 ± 1 kcal/mol that is characteristic of surface processes. It indicates the noticeable role of the dark reaction of consumption of H_2 and O_2 observed at low pressures [31].

It was experimentally shown that the temperature of the catalytic ignition limit over Pd at P = 1.75 atm, measured with a bottom-up approach by temperature (when increasing temperature from a state of no ignition), of the mixtures 30% methane + 70% hydrogen + air ($\theta = 0.9$, T = 317 °C) and 30% propane + 70% H_2 + air ($\theta = 1$, T = 106 °C) markedly drops after subsequent ignitions to T = 270 °C for H_2–CH_4 mix and to T = 32 °C for the H_2–C_3H_8 blend. The catalytic ignition limit returns to the initial value after treatment of the reactor with O_2 or air, i.e. a hysteresis phenomenon occurs. The ignition limit of the mixtures 30% (C_2, C_4, C_5, C_6) + 70% H_2 + air ($\theta = 0.6$, 1.1, 1.2, 1.2, correspondingly) over Pd amounts to 25 ÷ 35 °C at P = 1.75 atm; the hysteresis effect is missing. It was found that the lean 30% C_2H_6 + 70% H_2 + air mix ($\theta = 0.6$) shows the lowest temperature of the ignition limit: 24 °C at 1 atm. The estimate of the effective activation energy of the ignition of the mixes over Pd is ~ 2.4 ± 1 kcal/mol that is inherent to surface processes [90].

This paragraph focuses on experimental studies of low-pressure combustion of hydrogen–methane and hydrogen-isobutene mixtures over Rh and Pd surfaces at total pressures from 80 to 180 Torr and initial temperatures of 200–500 °C. It is aimed at establishment the relationships of flammability limits over noble metals on temperature and determination the possibility of carbon nanotube synthesis from these gas precursors.

3.7.1 Experimental

The experiments were performed with previously prepared stoichiometric gas mixtures $2H_2 + O_2$, $((20 \div 80\%)\ H_2 + (80 \div 20\%)$ hydrocarbon$)_{stoich} + O_2$. The reactor was quartz one 4 cm in diameter and 30 cm long heated up with an electric furnace (Fig. 3.26); the temperature was controlled by a thermocouple. The reactor was supplied with an optical quartz window at its butt-end. The reactor was used for studying thermal/catalytic ignition provided by Pd wire (0.3 mm thick 80 mm long) and Pd foil (0.06 mm thick, 1 mm wide and 80 mm long) as well as Rh samples, which was made by electrochemical deposition of Rh layer 15 mm thick on Pd wire (0.3 mm thick 80 mm long). Pd was chosen because its coefficient of thermal expansion is the closest to that of Rh [105], since Rh wire is rather expensive.

The overall intensity of chemiluminescence was recorded with a FD–24 photodiode (Russia) sensitive in the range 450–900 nm. The recording of the experiment was performed with a Nikon 1J2 digital camera (Fig. 3.26). A video recording was turned on at an arbitrary moment before initiation. A video file was stored in computer memory and its time-lapse processing was performed. The pumped and heated reactor was filled with the gas mixture from a high-pressure buffer volume to necessary pressure; the resistivity of the wires during ignition was measured. The pressure ignition limit was considered as a mean pressure P Torr, at P + 0.03P the ignition occurs, at P-0.03P it does not occur, all other things being equal. The pump-down time between experiments was 30 min. The ignition limit was measured at increasing pressure with a step 2 Torr until the ignition occurred (a bottom-up approach, when increasing temperature from a state of no ignition).

The mean temperature of the wire during ignition was recorded by an ADC based acquisition system, taking into account the temperature dependence of metal electrical resistivity during computer analysis of the signal. The microstructures of carbon residues on noble metal surfaces were examined using field emission, ultra-high resolution scanning electron microscope Zeiss Ultra Plus (Germany) equipped with an X-ray Microanalysis console INCA 350, Oxford Instruments. Before each experiment, the reactor was pumped down to 10^{-2} Torr. Total pressure in the reactor was monitored with a vacuum gauge (Fig.S1a, 10), and the pressure in the buffer volume was monitored with a manometer. Chemically pure gases and 99.85% Pd were used.

3.7.2 Results and Discussion

Temperatures of thermal/catalytic ignition of $2H_2 + O_2$ and $((20 \div 80\%)\ H_2 + (80 \div 20\%)$ hydrocarbon$)_{stoich} + O_2$ mixtures over Pd and Rh/Pd were determined. Typical experiments are shown in Fig. 3.27 a, b, in which the experiments above the ignition limit over Pd wire, and below the limit correspondingly are shown. As is seen in Fig. 3.27 b, the wire becomes red-hot even without ignition near the ignition limit, i.e. the flameless "dark" reaction of hydrocarbon consumption occurs.

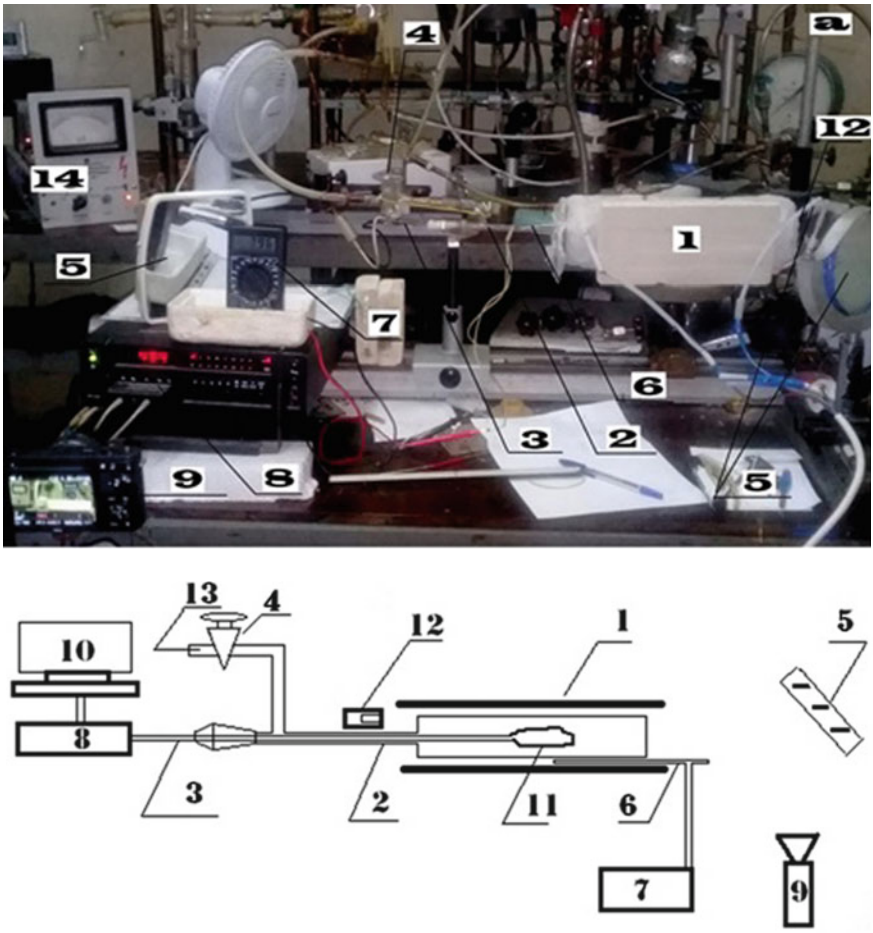

Fig. 3.26 Schematic of the experimental installation for the study of thermal/catalytic ignition over the wire **a**, **b**. (1) electric furnace, (2) quartz reactor of 4 cm in diameter and 30 cm long, (3) vacuum feed-through, (4) vacuum valve, (5) rotating mirror, (6) thermocouple, (7) millivoltmeter for thermocouple, (8) ADC computer based system, (9) Nikon 1J2 digital camera, (10) computer, (11) noble metal wire, (12) FD-24a photodiode, (13) to pressure gauge, gas inlet, to the pump, (14) pressure gauge

Warming-up kinetics was monitored by means of ADC computer based acquisition system using the temperature dependence of resistivity of Pd wire in combustion of $(80\%\ H_2 + 20\%\ CH_4)_{stoich} + O_2$ (Fig. 3.27c). According to Fig. 3.27c, the activity of catalytic wire expresses itself in both the occurrence ignition transition from the surface into the reactor volume, and the flameless "dark" catalytic reaction of the consumption of the flammable mixture. The preheating catalytic process provides the warming-up, which is enough to ignite the mixture at given pressure [curve (2)]. At lower pressure, even the greater warming up is insufficient to cause ignition [curve (3)],

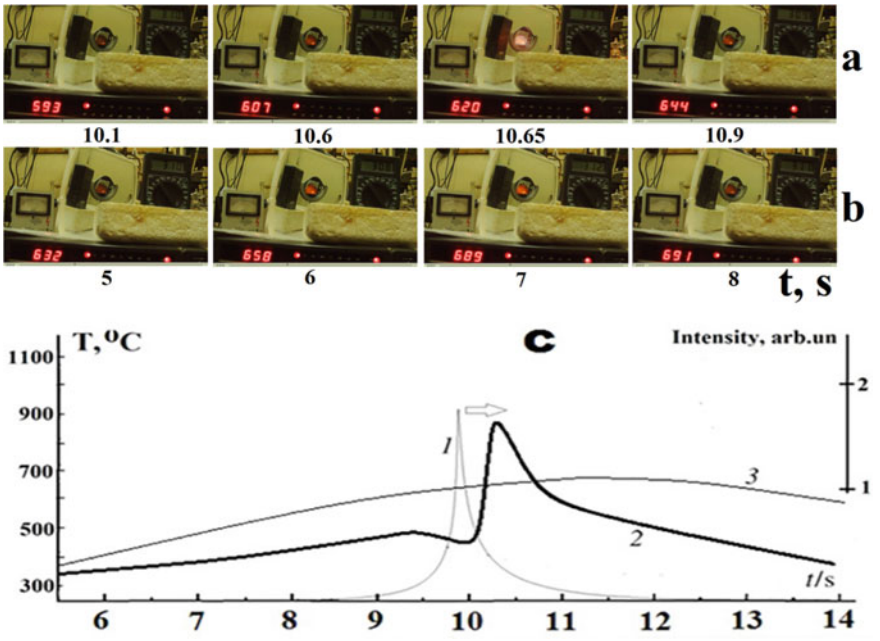

Fig. 3.27 **a** Experiment (80% H_2 + 20% $CH_4)_{stoich}$ + O_2 above the catalytic ignition limit, Pd wire, 30 frames/s, 310 °C, 139 Torr (the pressure gauge is off, because the maximum of the gauge range is 100 Torr); **b** experiment (80% H_2 + 20% $CH_4)_{stoich}$ + O_2 below the catalytic ignition limit, Pd wire, 30 frames/s, 310 °C, 70 Torr; **c** measurement of chemiluminescence by photodiode and warming-up by the dependence of resistivity on temperature in (80% H_2 + 20% $CH_4)_{stoich}$ + O_2 using ADC computer based acquisition system, over Pd wire, (1) ignition recorded with FD-24a photodiode, T_0 = 233 °C, P_0 = 139 Torr; (2) mean temperature of the wire, T_0 = 233 °C, P_0 = 139 Torr, ignition occurred; (3) mean temperature of the wire, T_0 = 310 °C, P_0 = 70 Torr, no ignition

since the mixture is far beyond the ignition region. Obviously, the value of the warming-up is underestimated because the wire is nonuniformly heated during ignition [69] (see also Chap. 2).

Catalytic ignition areas of $2H_2 + O_2$ mixes over noble metal wires are presented in Fig. 3.28 in P–T coordinates. As is seen in the Fig. 3.28, Rh is the most active surface, Pd surface is less active. Notice that the hysteresis phenomenon for $2H_2 + O_2$ ignition is observed only over Pd wire. The ignition limit value measured over the wire, which is not treated with ignitions (a bottom-up approach, when increasing temperature from a state of no ignition) is higher than the value measured with a top-down approach; the same applies to the delay periods of ignition. The catalytic ignition limit is reversible: after reactor treatment with air or O_2, the ignition limit returns to the value corresponding to the bottom-up approach (when decreasing temperature from a state of catalytic ignition).

In the case of $(H_2 + CH_4)_{stoich} + O_2$ mixes, the catalytic ignition limit pressure value measured over the Pd wire with a bottom-up approach is the lowest one. Then,

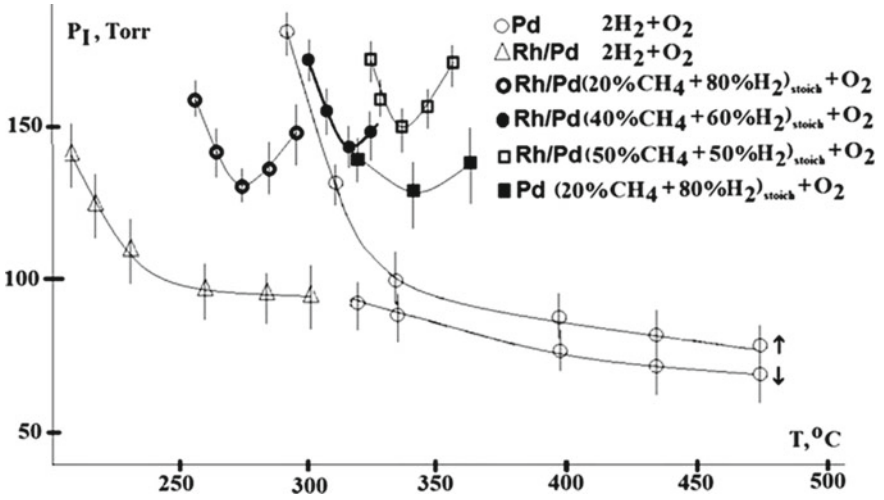

Fig. 3.28 Catalytic ignition areas of $(H_2 + CH_4)_{stoich} + O_2$ mixes over noble metal wires in pressure–temperature coordinates. The arrow oriented upwards corresponds to a bottom-up approach and the arrow oriented downwards corresponds to a top-down approach in measuring an ignition limit. To the right of each curve the ignition occurs, to the left—the ignition does not occur

with an increase in temperature the ignition limit increases until the auto-ignition area takes the characteristic V-shape. The V-shape is probably determined by the following. With an increase in temperature, the value of the ignition limit initially decreases due to the increasing rate of the activated volume branching step or the cycle of elementary steps [24]. As temperature increases further, the rate of the dark surface reaction increases resulting in an increase in the degree of fuel conversion; thus, the fuel content of the mixture decreases and therefore the value of the ignition limit increases for the leaner mixture. In addition, only mixtures (80% H_2 + 20% $CH_4)_{stoich} + O_2$, (60% H_2 + 40% $CH_4)_{stoich} + O_2$, (50% H_2 + 50% $CH_4)_{stoich} + O_2$ ignite over Rh/Pd wire, and only the mix (80% H_2 + 20% $CH_4)_{stoich} + O_2$ ignites over Pd wire (or foil). Under conditions of our work, other mixtures are consumed only in the "dark" reaction (see Fig. 3.27b).

Notice that hysteresis phenomenon for ignition of $(H_2 + CH_4)_{stoich} + O_2$ is missing. To return to the ignition limit to the initial value corresponding to the bottom-up approach, one must dissolve or mechanically remove the film deposited on the noble metal wire.

The further part of the paragraph was aimed at the establishing morphology of the residue deposited on the noble metal surface using the mix (80% H_2 + 20% $C_4H_8)_{stoich} + O_2$ as the main precursor.

The preliminary analysis of the formed residue did not show any noticeable structures in the product deposited on the noble metal surface, both in ignition (140 Torr) and "dark" reaction (70 Torr) regimes in combustion of $(H_2 + CH_4)_{stoich} + O_2$ mix. Therefore, we chose the "dark" reaction regime at 140 Torr in the (80% H_2 + 20%

$C_4H_8)_{stoich} + O_2$ mix, which does not ignite under conditions of this work. The results of SEM investigation of the black residue formed in the reaction on the noble metal surface are shown in Fig. 3.29. As is seen, carbon nanotubes form in the "dark" reaction regime. In the case of the synthesis of carbon nanotubes by this method, the noble metal plays both, the role of a catalyst for the growth of nanostructures and a heating element; for this, the presence of hydrogen and oxygen in the gas mixture is necessary.

In Fig. 3.29a, SEM micrographs of nanotubes formed on Pd wire first treated with 2 ignitions $(80\%\ H_2 + 20\%\ CH_4)_{stoich} + O_2$ at and further processing with $(80\%\ H_2 + 20\%\ C_4H_8)_{stoich} + O_2$ in the dark reaction regime for three times are presented. Three times mean three actions of filling the reactor with a $(80\%\ H_2 + 20\%\ C_4H_8)_{stoich} + O_2$ gas mixture to 140 Torr for 15 s and pumping. This sequence of procedures leads to the formation of carbon nanotubes ~ 30 nm of mean diameter with comparably small variance. In Fig. 3.29b, SEM micrographs of nanotubes formed on Rh/Pd wire treated with $(80\%\ H_2 + 20\%\ C_4H_8)_{stoich} + O_2$ for three times are presented. The processing with ignitions of $(80\%\ H_2 + 20\%\ CH_4)_{stoich} + O_2$ was not performed. As is seen in Fig. 3.29, the nanotubes have more than one mean size. One can see

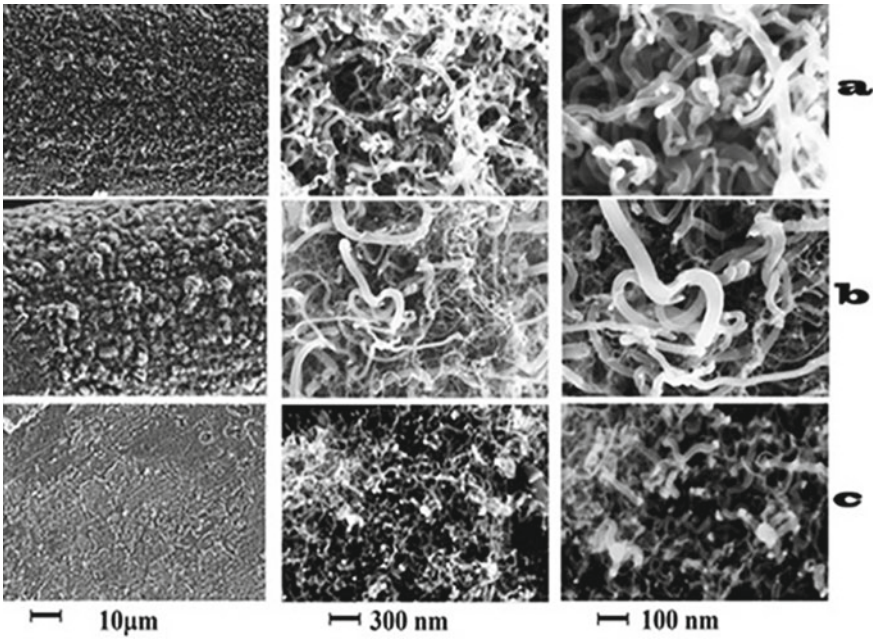

Fig. 3.29 SEM micrographs of nanotubes **a** Pd wire first treated with 2 ignitions $(80\%\ H_2 + 20\%\ CH_4)_{stoich} + O_2$ at and processing with $(80\%\ H_2 + 20\%\ C_4H_8)_{stoich} + O_2$ for three times, P = 140 Torr, T = 310 °C; **b** Rh/Pd wire treated with $(80\%\ H_2 + 20\%\ C_4H_8)_{stoich} + O_2$ for three times, P = 140 Torr, T = 230 °C; **c** Pd foil treated with $(80\%\ H_2 + 20\%\ C_4H_8)_{stoich} + O_2$ for three times P = 140 Torr, T = 310 °C. Three times mean three procedures of filling the rector with a gas mixture to 140 Torr for 15 s and pumping

nanotubes up to 100 nm in diameter as well as nanotubes about 10 nm in diameter. In Fig. 3.29c, SEM micrographs of nanotubes deposited on Pd foil treated with (80% H_2 + 20% $C_4H_8)_{stoich}$ + O_2 for three times are shown. These nanotubes have in general the mean diameter less than in cases (a) and (b), however the variance in diameters seems rather high. Thus, the optimization of the process needs further investigation.

We summarize the results as follows.

It was shown that at total pressures up to 200 Torr catalytic ignition areas of $2H_2$ + O_2 mixes over Rh and Pd surfaces are broader than these of $(H_2 + CH_4)_{stoich}$ + O_2 mixtures; the mixtures containing more than 50% CH_4 as well as (80% H_2 + 20% $CH_4)_{stoich}$ + O_2 mixtures do not ignite. This is directly related to the formation of carbon-containing film on the noble metal surface. The fuel in the mixtures is consumed in dark reaction. It was shown that the dark reaction in (80% H_2 + 20% $CH_4)_{stoich}$ + O_2 mixture leads to the formation of carbon nanotubes over the range 10 ÷ 100 nm of mean diameter. In the case of the synthesis of carbon nanotubes by this method, the noble metal plays both, the role of a catalyst for the growth of nanostructures and a heating element; for this, the presence of hydrogen and oxygen in the gas mixture is necessary.

3.8 Conclusions

It was shown experimentally that the catalytic ignition temperature of the 40% H_2 + air mixture over metallic Pd (70 °C, 1 atm) was ~ 200 °C lower than over the Pt surface (260 °C, 1 atm). In addition, Pd wire initiates the ignition of the (30–60% H_2 + 70–40% $CH_4)_{stoich}$ + air mixtures; Pt wire of the same size cannot ignite these mixtures at reactor temperatures below 450 °C. This means that Pd wire is more effective in initiation of ignition than Pt wire. The cellular structure of the flame front during ignition in the presence of Pd wire was not observed in contrast to the results obtained on the Pt surface. Therefore, Pd is more suitable than Pt for hydrogen recombiners in nuclear power plants because the catalytic particles do not appear in the gas phase. The experimental value of the effective activation energy of the process was estimated at (3.5 ± 1) kcal/mol, which is characteristic of surface processes. This indicates the significant role of the dark reaction of H_2 and O_2 consumption on the Pd surface observed directly at low pressures. The presence of this reaction reduces the probability of accidental explosion compared to the Pt surface. It was found that in the presence of leucosapphire, there was no system of emission bands of H_2O^* in the range 570–650 nm, and a possible explanation of this effect was given. The appearance of an additional source of excited water molecules emitting in the range 900–970 nm was explained.

It was experimentally shown that the temperature of the catalytic ignition limit over Pd at $P = 1.75$ atm, measured with a bottom-up approach by temperature for the mixtures 30% methane + 70% hydrogen + air ($\theta = 0.9$, $T = 317$ °C), and 30% propane + 70% H_2 + air ($\theta = 1$, $T = 106$ °C) markedly drops after subsequent ignitions to $T = 270$ °C for H_2–CH_4 mix and to $T = 32$ °C for the H_2–C_3H_8 blend.

Equivalence ratio θ is a fraction of fuel in the mix with air: θ H_2 + 0.5 (O_2 + 3.76 N_2)). The ignition limit returns to the initial value after treatment of the reactor with O_2 or the air; i.e., a hysteresis phenomenon occurs. The ignition limit of the mixtures 30% (C2, C4, C5, C6) + 70% H_2 + air (θ = 0.6, 1.1, 1.2, 1.2, correspondingly) over Pd amounts to 25–35 °C at $P = 1.75$ atm; the hysteresis effect is missing. It was found that the lean 30% C_2H_6 + 70% H_2 + air mix (θ = 0.6) shows the lowest temperature of the ignition limit: 24 °C at 1 atm. The estimate of the effective activation energy of the ignition of the mixes over Pd is ~ 2.4 ± 1 kcal/mol that is characteristic of a surface process. Thus, the usage of Pd catalyst allows igniting H_2–hydrocarbon mixtures at 1–2 atm at initial room temperature without external energy sources.

It was found that the ignition temperatures of hydrogen–oxygen and hydrogen–methane–oxygen mixes at low pressure over heated Pd, Pt, Nichrome and Kanthal wires at 40 Torr increase with a decrease in H_2 concentration; only a heated Pd wire shows the pronounced catalytic action. Numerical calculations allowed revealing the role of an additional branching step H + HO_2 → 2OH, in which the slightly active radical HO_2 is replaced by a more active OH.

The peculiarities of ignition of premixed stoichiometric n-pentane–air mixtures were studied in a rapid mixture injection static reactor in the presence of metallic Pt and Pd in the region of negative temperature coefficient (NTC). It is shown that in the absence of noble metals thermoacoustic oscillations occur within NTC region. However, in the presence of Pt catalyst surface, which reacts with oxygen at the flame temperature and generates catalytic centers propagating into volume, thermoacoustic regimes of thermal ignition disappear. In other words, the catalytic Pt surface eliminates a certain inhibition stage of kinetic mechanism after the occurrence of the cool flame and NTC phenomenon vanishes; the stage may be e.g. the decomposition of some intermediate slow reacting peroxide on Pt surface with the formation of a more reactive radical. In the presence of the catalytic surface (Pd), which does not react at the flame temperature and does not generate catalytic centers propagating into volume, NTC phenomenon occurs.

Thus, the detected regularities must be taken into account in numerical simulations of NTC phenomenon. In other words, the oscillations and NTC phenomenon must both disappear in calculations after excluding a certain reaction or a series of reaction steps from the mechanism. The step must include the superficial reaction of an active intermediate of combustion on Pt surface, in which more active intermediates are formed from a low-active one.

It was found that the ignition delay (induction) period during the combustion of (70–40% hydrogen + 30–60% propane) + air mixtures over palladium at a total pressure of 1–2 atm first decreases with a decrease in temperature and then increases until the ignition limit is reached, i.e., the NTC phenomenon occurs. The effective activation energy E of the process is 2.2 ± 1 kcal mol^{-1} that is characteristic of a surface process. Therefore, the detected NTC phenomenon is closely related to the surface state of Pd. In the sample treated with ignitions, defects in the form of holes were found, which are focused on the etching patterns. In this process, PdO particles are formed during the oxidation of the Pd surface and decompose to Pd and O_2 at the temperature of flame products. Thus, Pd is consumed in the chemical etching

reaction with active combustion intermediates. It should limit the applicability of palladium in ignition devices.

It was shown that, at total pressures up to 200 Torr, the catalytic ignition areas over the Rh and Pd surfaces are larger for $2H_2 + O_2$ mixtures than for $(H_2 + CH_4)_{stoich} + O_2$ and $(H_2 + C_4H_8)_{stoich} + O_2$ mixtures; mixtures containing more than 50% hydrocarbons do not ignite. This behavior is directly related to the formation of a carbon-containing film on the noble metal surface. The fuel in the mixtures is consumed in a dark reaction. In the case of the synthesis of carbon nanotubes by this method, the noble metal plays both, the role of a catalyst for the growth of nanostructures and a heating element; for this, the presence of hydrogen and oxygen in the gas mixture is necessary. It has been shown that the dark reaction in the $(80\% H_2 + 20\% C_4H_8)_{stoich} + O_2$ mixture leads to the formation of carbon nanotubes with a mean diameter in the range of 10–100 nm.

References

1. H. Davy, Some new experiments and observations on the combustion of gaseous mixtures with an account of a method of preserving a continuous light in mixtures of inflammable gases and air without flame. Phil. Trans. R. Soc. London A **107**, 77 (1817)
2. J. Lee, D.L. Trimm, Catalytic combustion of methane. Fuel Process. Technol. **42**, 339 (1995)
3. O. Deutschmann, L.I. Maier, U. Riedel et al., Hydrogen assisted catalytic combustion of methane on platinum. Catalysis Today **59**, 141 (2000)
4. M. Lyubovsky, H. Karim, P. Menacherry et al., Complete and partial catalytic oxidation of methane over substrates with enhanced transport properties. Catalysis Today **83**, 183 (2003)
5. S. Salomons, R.E. Hayes, M. Poirier et al., Flow reversal reactor for the catalytic combustion of lean methane mixtures. Catalysis Today **83**, 59 (2003)
6. J.K. Lampert, M.S. Kazia, R.J. Farrauto, Palladium catalyst performance for methane emissions abatement from lean burn natural gas vehicles. Appl. Catal. B **14**, 211 (1997)
7. IAEA Safety Standards Series. Design of Reactor Containment Systems for Nuclear Power Plants Safety Guide. No. NS-G-1.10 (2004)
8. A. Frennet, Chemisorption and exchange with deuterium of methane on metals. Catal. Rev. Sci. Eng. **10**, 37 (1974)
9. C.F. Cullis, B.M. Willatt, Oxidation of methane over supported precious metal catalysts. J. of Catalysis **83**, 267 (1983)
10. R.F. Hicks, H. Qi, M.L. Young, R.G. Lee, Structure sensitivity of methane oxidation over platinum and palladium. J. of Catalysis **122**, 280 (1990)
11. R.E. Hayes, S. Kolaczkowskii, P. Lib, S. Awdryb, The palladium catalyzed oxidation of methane: reaction kinetics and the effect of diffusion barriers. Chem. Eng, Science **56**, 4815 (2001)
12. S. Choudhury, R. Sasikala, V. Saxena, D. Kumar-Aswalb, D. Bhattacharyac, A new route for the fabrication of an ultrathin film of a PdO–TiO_2 composite photocatalyst. Dalton Trans. **41**, 12090 (2012)
13. P.O. Nilsson, M.S. Shivaraman, Optical properties of PdO in the range of 0.5–5.4 eV. J. Phys. C: Solid State Phys. **12**, 1423 (1979)
14. F. Ling, O.C. Anthony, Q. Xiong, M. Luo, X. Pan, L. Jia, J. Huang, D. Sun, Q. Li, PdO/$LaCoO_3$ heterojunction photocatalysts for highly hydrogen production from formaldehyde aqueous solution under visible light. Int. J. hydrogen energy **41**, 6115 (2016). https://doi.org/10.1016/j.ijhydene.2015.10.036

15. C. Diaz, M.L. Valenzuela, C. Rios, M. Segovia, Oxidation facility by a temperature dependence on the noble metals nanostructured $M°/M_xO_y$ phase products using a solid state method: the case of Pd. J. Chilean Chem. Soc. **61**, 4 (2016). https://doi.org/10.4067/S0717-97072016000400024
16. I.D. Rodionov, A.I. Rodionov, L.A. Vedeshin, V.V. Egorov, A.P. Kalinin, Airborne hyperspectral systems for solving remote sensing problems. Izv. Atmos. Ocean. Phys. **50**(9), 989 (2014). https://doi.org/10.1134/S0001433814090175
17. A.N. Vinogradov, V.V. Egorov, A.P. Kalinin, A.I. Rodionov, I.D. Rodionov, A line of aviation hyperspectrometers in the UV, visible, and near-IR ranges. J. Opt. Technology **83**(4), 237 (2016). https://doi.org/10.1364/JOT.83.000237
18. A.P. Kalinin, A.G. Orlov, A.I. Rodionov, K.Y. Troshin, Demonstration of the possibilities to study combustion and explosion processes on the base of hyperspectral remote sensing. Physical-Chemical Kinetics in Gas Dynamics **8** (2009). http://chemphys.edu.ru/issues/2009-8/articles/202/
19. N.M. Rubtsov, B.S. Seplyarskii, K.Y. Troshin, V.I. Chernysh, G.I. Tsvetkov, Investigation into spontaneous ignition of hydrogen–air mixtures in a heated reactor at atmospheric pressure by high-speed cinematography. Mendeleev Commun. **22**(4), 222 (2012). https://doi.org/10.1016/j.mencom.2012.07.001
20. N.M. Rubtsov, B.S. Seplyarskii, K.Y. Troshin, V.I. Chernysh, G.I. Tsvetkov, High-speed color cinematography of the spontaneous ignition of propane–air and n-pentane–air mixtures, Mendeleev Commun. **21**(3), 31 (2011). https://doi.org/10.1016/j.mencom.2011.01.013
21. N.M. Rubtsov, V.I. Chernysh, G.I. Tsvetkov, K.Y. Troshin., I.O. Shamshin, Ignition of hydrogen–air mixtures over Pt at atmospheric pressure. Mendeleev Commun. **27**(3), 307 (2017). https://doi.org/10.1016/j.mencom.2017.05.031
22. N.M. Rubtsov, A.N. Vinogradov, A.P. Kalinin., A.I. Rodionov, V.I. Chernysh, Cellular combustion and delay periods of ignition of a nearly stoichiometric H_2–air mixture over a platinum surface. Mendeleev Commun. **26**(2), 160 (2016). https://doi.org/10.1016/j.mencom.2016.03.027
23. K.L. Cashdollar, I.A. Zlochower, G.M. Green, R.A. Thomas, M. Hertzberg, Flammability of methane propane and hydrogen gases. J. Loss Prevention in the Process Industries **13**(3), 327 (2000). https://doi.org/10.1016/S0950-4230(99)00037-6
24. B. Lewis, G. Von Elbe, *Combustion, Explosions and Flame in Gases* (London. Acad. Press, New York, 1987)
25. S.M. Repinski, Vvedenie v himicheskuy fiziku poverchnosti tverdych tel (Introduction into chemical physics of the surface of solids) (Novosibirsk: Nauka, Sibir publishing company, 1993)
26. L. Kristinsdóttir, E. Skúlason, A systematic DFT study of hydrogen diffusion on transition metal surfaces. Surf. Sci. **606**(17–18), 1400 (2012). https://doi.org/10.1016/j.susc.2012.04.028
27. L.S. Rothman, I.E. Gordon, Y. Babikov, A. Barbe, D. Chris Benner et al., The HITRAN 2012 molecular spectroscopic database. J. Quantitative Spectroscopy & Radiative Transfer **130**, 4 (2013)
28. N.M. Rubtsov, A.N. Vinogradov, A.P. Kalinin, A.I. Rodionov, I.D. Rodionov, K.Y. Troshin, G.I. Tsvetkov, V.I. Chernysh, High speed multidimensional optical complex in research of ignition and combustion features of 40% H_2–air mix in the presence of platinum. Physical-Chemical Kinetics in Gas Dynamics **17**(1) (2016). http://chemphys.edu.ru/issues/2016-17-1/articles/615/
29. R.G. Stützer, S. Kraus, M. Oschwald, Characterization of Light Deflection on Hot Exhaust Gas for a LIDAR Feasibility Study, 4th Conference on Space Propulsion (2014). https://www.researchgate.net/publication/263586493
30. T. Icitaga, Emission spectrum of the oxy-hydrogen flame and its reaction mechanism. (1) Formation of the activated water molecule in higher vibrational states. The Review of Physical Chemistry of Japan **13f**(2), 96 (1939)

31. N.M. Rubtsov, V.I. Chernysh, G.I. Tsvetkov, K.Y. Troshin, I.O. Shamshin, A.P. Kalinin, The features of hydrogen ignition over Pt and Pd foils at low pressure. Mendeleev Commun. **28**, 216 (2018). https://doi.org/10.1016/j.mencom.2017.05.031
32. C. Tang, Y. Zhang, Z. Huang, Progress in combustion investigations of hydrogen enriched hydrocarbons. Renew. Sustain. Energy Rev. **30**, 195 (2016)
33. D.A. Knyazkov, V.M. Shvartsberg, A.M. Dmitriev, K.N Osipova, A.G. Shmakov, O.P. Korobeinichev, Combustion chemistry of ternary blends of hydrogen and C1–C4 hydrocarbons at atmospheric pressure. Combustion, Explosion, and Shock Waves **53**(5), 491 (2017). https://doi.org/10.1134/S001050821705001X
34. S. Biswas, S. Tanvir, H. Wang, L. Qiao, On ignition mechanisms of premixed CH_4/air and H_2/air using a hot turbulent jet generated by pre-chamber combustion. Appl. Therm. Eng. **106**, 925 (2016). https://doi.org/10.1016/j.applthermaleng.2016.06.070
35. E.-S. Cho, S.H. Chung improvement of flame stability and NO_x reduction in hydrogen-added ultralean premixed combustion. J. Mech. Sci. Technol. **23**(3), 650 (2009). https://doi.org/10.1007/s12206-008-1223-x
36. H. Razali, K. Sopia, S. Mat, Green fuel: 34% reduction of hydrocarbons via hydrogen (Al+HCl) blended with gasoline at maximum torque for motorcycle operation. ARPN Journal of Engineering and Applied Sciences **10**(17), 7780 (2015)
37. R.M. Flores, V.G. McDonell, G.S. Samuelsen, Impact of ethane and propane variation in natural gas on performance of a model gas turbine combustor. J. Eng. Gas Turbines Power **125**(3), 701 (2003). https://doi.org/10.1115/1.1584480
38. H. Hassan, B. Khandelwa, Reforming technologies to improve the performance of combustion systems. Aerospace **1**, 67 (2014). https://doi.org/10.3390/aerospace1020067
39. H. Xiong, M.H. Wiebenga, C. Carrillo, J.R. Gaudet, H.N. Pham, D. Kunwar et al., Design considerations for low-temperature hydrocarbon oxidation reactions on Pd based catalysts. Appl. Catal. B **236**(15), 436 (2018). https://doi.org/10.1016/j.apcatb.2018.05.049
40. N.M. Rubtsov, A.P. Kalinin, G.I. Tsvetkov, K.Y. Troshin, A.I. Rodionov, Experimental study of methane combustion over metallic palladium upon flame penetration through obstacles. Russ. J. Phys. Chem. B **12**, 1017 (2018)
41. K. Persson, L.D. Pfefferle, W. Schwartz, A. Ersson, S.G. Jaras, Stability of palladium-based catalysts during catalytic combustion of methane: the influence of water. Appl. Catal. B **74**, 242 (2007). https://doi.org/10.1016/j.apcatb.2007.02.015
42. N.M. Rubtsov, *The Modes of Gaseous Combustion* (Springer International Publishing, Cham, 2016). https://doi.org/10.1007/978-3-319-25933-8
43. A.A. Borisov, N.M. Rubtsov, G.I. Skachkov, K.Y. Troshin, Gas-phase spontaneous ignition of hydrocarbons. Russ. J. Phys. Chem. B **6**, 517 (2012)
44. K.Y. Troshin, I.O. Shamshin, V.A. Smetanyuk, A.A. Borisov, Self-ignition and combustion of gas mixtures in a medium with vortex flow. Russ. J. Phys. Chem. B **11**, 952 (2017). https://doi.org/10.7868/S0207401X17110115
45. Vision system overview, C&PS Flight Technical Services (2013) https://www.mygdc.com/assets/public_files/gdc_services/pilot_services/presentations/Vision_Systems_Overview.pdf
46. A.N. Vinogradov, V.V. Egorov, A.P. Kalinin, A.I. Rodionov, I.D. Rodionov, Hyperspectrometer for the 900–1700 nm near-infrared region. J. Opt. Technol. **84**, 683 (2017)
47. G.H. Markstein, Cell structure of propane flames burning in tubes. J. Chem. Phys. **17**, 428 (1949). https://doi.org/10.1063/1.1747278
48. Y.B. Zeldovich, Teoria gorenia i detonacii gazov (Theory of Combustion and Detonation of Gases) (Moscow, Acad. Sci. USSR. 1944)
49. A. P. Kreshkov, Osnovy analiticheskoi himii (Fundamentals of analytical chemistry, vol. 3) (M: "Khimiya", 1970)
50. N.M. Rubtsov, A.N. Vinogradov, A.P. Kalinin et al., Gas dynamics and kinetics of the penetration of methane–oxygen flames through complex obstacles, as studied by 3D spectroscopy and high-speed cinematography. Mendeleev Commun. **27**, 192 (2017)
51. I.M. Naboko, N.M. Rubtsov, B.S. Seplyarskii, K.Y. Troshin, G.I. Tsvetkov, V.I. Chernysh, Cellular combustion at the transition of a spherical flame front to a flat front at the initiated

ignition of methane–air, methane–oxygen and n-pentane–air mixtures. Mendeleev Commun. **23**(6), 35 (2013). https://doi.org/10.1016/j.mencom.2013.11.020
52. M. Fisher, Safety aspects of hydrogen combustion in hydrogen energy systems. Int. J. Hydrogen Energy **11**, 593 (1986)
53. A.B. Welch, J.S. Wallace, Performance characteristics of a hydrogen-fueled diesel engine with ignition assist, SAE Paper 902070 (1990). https://doi.org/10.4271/902070
54. R.K. Kumar, Ignition of hydrogen oxygen diluent mixtures adjacent to a hot, non-reactive surface. Comb. Flame **75**, 1975 (1989)
55. R.S. Silver, The ignition of gaseous mixtures by hot particles. The Philosophical Magazine and Journal of Science **23**(156), 633 (1937)
56. K.B. Brady. Master Thesis. Case Western Reserve University (2010)
57. M. Rinnemo, O. Deutschmann, F. Behrendt, B. Kasemo, Experimental and numerical investigation of the catalytic ignition of mixtures of hydrogen and oxygen on platinum. Comb. Flame **111**, 312 (1997). https://doi.org/10.1016/S0010-2180(97)00002-3
58. S.K. Menon, P.A. Boettcher, B. Ventura, G. Blanquart, J.E. Shepherd, Investigation of hot surface ignition of a flammable mixture, Western States Sect. Comb. Inst. (WSSCI). Arizona University, Tempe, Paper # 12S-39 (2012)
59. K. Dong-Joon, Ignition temperature of hydrogen/air mixture by hot wire in pipeline. Fire Science and Engineering **28**(4), 8 (2014). https://doi.org/10.7731/KIFSE.2014.28.4.008
60. Tablitsy fizicheskikh velichin. Spravochnik (Tables of Physical Values. Handbook), ed. by I.K. Kikoin (Atomizdat Moscow, 1976)
61. G.I. Marchuk, Metody vychislitel'noy matematiki (Methods of computational mathematics) (Nauka, Moscow, 1989)
62. N.M. Rubtsov, V.D. Kotelkin, V.P. Karpov, The transition of flame propagation from isothermal mode to the mode of chain processes with non-linear chain branching. Kinet. Catal. **45**(1), 3 (2004)
63. N.N. Semenov, *O nekotorykh problemakh khimicheskoi kinetiki I reaktsionnoi sposobnosti (On Some Problems of Chemical Kinetics and Reactivity)*, 2nd edn. (AN SSSR, Moscow, 1958)
64. D.C. Montgomery, E.A. Peck, G. Vining, Introduction to linear regression analysis, 5th edn. (Wiley, New Jersey, 2012)
65. A.G. Merzhanov, B.I. Khaykin, Teoria Voln Gorenia v Gomogennych Sredach (Theory of Combustion Waves in Homogeneous Media), (ISMAN RAS, Chernogolovka, 1992)
66. J. Warnatz, U. Maas, C. Dibble. *Combustion. Physical and Chemical Aspects, Modeling, Experiments, Formation of Pollutants* (Springer, Berlin, 2001)
67. V.V. Azatyan, Y.I. Pyatnitskii, N.A. Boldyreva, Detection of chemoluminescence during oxidation of hydrogen-containing compounds on the surface of platinum metals. Russ. J. Phys. Chem. A **72**, 235 (1998)
68. V.V. Azatyan, Heterophase development of chains in processes of combustion and pyrolysis. Russ. J. Phys. Chem. A **72**, 199 (1998)
69. N.M. Rubtsov, A.A. Borisov, G.I. Skachkov, K.Y. Troshin, On the features of the negative temperature coefficient phenomenon in combustion of n-pentane-air mixtures. Int. J. Chem. Proc. Eng. Res. **1**, 51 (2014). https://doi.org/10.18488/journal.65/2014.1.6/65.6.51.58
70. A. Naidja, C.R. Krishna, T. Butcher, D. Mahajan, Cool flame partial oxidation and its role in combustion and reforming of fuels for fuel cell systems. Prog. Energy Comb. Science **29**, 155 (2003). https://doi.org/10.1016/S0360-1285(03)00018-2
71. L. Hartmann, K. Lucka, H. Köhne, Mixture preparation by cool flames for diesel-reforming technologies. J. Pow. Sources **118**, 286 (2003). https://doi.org/10.1016/S0378-7753(03)00100-9
72. J.F. Griffiths, J.P. MacNamara, C.G.W. Sheppard, D.A. Turton, B.J. Whitaker, The relationship of knock during controlled autoignition to temperature inhomogeneities and fuel reactivity. Fuel **81**, 2219 (2002). https://doi.org/10.1016/S0016-2361(02)00134-5
73. Y. Qi, Z. Wang, J. Wang, X. He, Effects of thermodynamic conditions on the end gas combustion mode associated with engine knock. Comb. Flame **162**, 4119 (2015). https://doi.org/10.1016/j.combustflame.2015.08.016

74. J.T. Farrell, N.P. Cernansky, F.L. Dryer, C.K. Law, D.G. Friend, C.A. Hergart, R.M. McDavid, A.K. Patel, C.J. Mueller, H. Pitsch, Development of an experimental database and kinetic models for surrogate diesel fuels. SAE Technical Paper 2007-01-0201 (2007)
75. K. Kuwahara, T. Tada, M. Furutani, Y. Sakai, H. Ando, Chemical kinetics study on two-stage main heat release in ignition process of highly diluted mixtures. SAE Int. J. Engines **6**, 520 (2013). https://doi.org/10.4271/2013-01-1657
76. G. Shibata, K. Oyama, T. Urushihara, T. Nakano, The effect of fuel properties on low and high temperature heat release and resulting performance of an HCCI engine. SAE World Congress 2004-01-0553 (2004). https://doi.org/10.4271/2004-01-0553
77. Y. Ju, W. Sun, M.P. Burke, X. Gou, Z. Chen, Multi-timescale modeling of ignition and flame regimes of n-heptane-air mixtures near spark assisted homogeneous charge compression ignition conditions. Proc. Combust. Inst. **33**, 1245 (2011). https://doi.org/10.1016/j.proci.2010.06.110
78. J. Pan, H. Wei, G. Shu, Z. Chen, P. Zhao, The role of low temperature chemistry in combustion mode development under elevated pressures. Comb. Flame **174**, 179 (2016). https://doi.org/10.1016/j.combustflame.2016.09.012
79. S.G. Saytzev, R.I. Soloukhin, Study of combustion of adiabatically heated gas mixture, in *Proceedings of 8th Symposium (International) on Combustion* (The Combust. Inst., Pittsburgh, 1962), p. 2771
80. J.C. Livengood, W.A. Leary, Autoignition by rapid compression. Ind. and Engin. Chem. **43**, 2797 (1951)
81. K.Y. Troshin, I.O. Shamshin, V.A. Smetanuik, A.A. Borisov, Self-ignition and combustion of gas mixtures in the volume with vortex flow. Russ. J. Phys. Chem. B **11**, 952 (2017). https://doi.org/10.1134/S1990793117060112
82. A.A. Borisov, V.G. Knorre, E.L. Kudryashova, G.I. Skachkov, K.Y. Troshin, On temperature measurement in an induction period of the ignition of homogeneous gas mixtures in rapid mixture injection static setup. Rus J Phys Chem B **17**, 80 (1998)
83. N.M. Rubtsov, V.I. Chernysh, G.I.T Svetkov, K.Y. Troshin, I.O. Shamshin, Ignition of hydrogen–air mixtures over Pt at atmospheric pressure, Mendeleev. Commun. **27**, 307 (2017). https://doi.org/10.1016/j.mencom.2019.07.039
84. J.F. van Kampen, Acoustic pressure oscillations induced by confined turbulent premixed natural gas flames. Dissertation, University of Twente: Enschede The Netherlands (2006)
85. Y.B. Zel'dovich, G.I. Barenblatt, V.B. Librovich, G.M. Machviladze, The mathematical theory of combustion and explosions (2011). https://doi.org/10.1007/978-1-4613-2349-5, Corpus ID 91204935
86. C.B. Goates, Analytical Expressions for Acoustic Radiation Modes of Simple Curved Structures, Dissertation, Brigham Young University 2019; 7494. https://scholarsarchive.byu.edu/etd/7494
87. J.W. Strutt, *The Theory of Sound*, V.2. 2nd edn. (London Macmillan and Co: New York, 1894)
88. R. Serra-Maia, M. Bellier, S. Chastka, K. Tranhuu, A. Subowo, J.D. Rimstidt, P.M. Usov, A.J. Morris, F.M. Michel, Mechanism and kinetics of hydrogen peroxide decomposition on platinum nanocatalysts. ACS Appl Mater Interfaces **10**, 21224 (2018). https://doi.org/10.1021/acsami.8b02345
89. J.C. Chaston, Reaction of oxygen with the platinum metals. The oxidation of platinum. Platinum Metals Rev. **8**, 50 (1964)
90. N.M. Rubtsov, V.I. Chernysh, G.I. Tsvetkov, K.Y. Troshin, I.O. Shamshin, Ignition of hydrogen–methane–air mixtures over Pd foil at atmospheric pressure. Mendeleev Commun. **29**, 69 (2019). https://doi.org/10.1016/j.mencom.2017.05.031
91. O. Deutschmann, R. Schmidt, F. Behrendt, J. Warnatz, Numerical modeling of catalytic ignition. Proc. Combust. Inst. **26**, 1747 (1996)
92. N.M. Rubtsov, G.I. Tsvetkov, V.I. Chernysh, K.Y. Troshin, Features of hydrogen and deuterium ignition over noble metals at low pressures. Comb. Flame **218**, 179 (2020). https://doi.org/10.1016/j.combustflame.2020.05.006

93. N.M. Rubtsov, Key factors of combustion. from kinetics to gas dynamics (Springer International Publishing, 2017)
94. V.S. Posvyanskii, Skorost I predely rasprostranenia izotermicheskich plamen (Velocity and Propagation Limits of Isothermal Flames), Dissertation, Moscow: Inst. of Chemical Physics USSR (1976)
95. F. Nicoud, Conservative high-order finite-difference schemes for low-mach number flows. J. Comput. Phys. **158**, 71 (2000). https://doi.org/10.1006/jcph.1999.6408
96. D.I. Abugov, V.M. Bobuylev, *Teoria i raschet tverdotoplivnych raketnych dvigatelei (Theory and calculations of solid fuel rocket jets)* (Mashinostroenie, Moscow, 1987)
97. M.J. Lighthill, On sound generated aerodynamically. II. Turbulence as a source of sound, Proc. R. Soc. Lond. A **222**, 1 (1954)
98. G. Backstrom, *Simple Fields of Physics by Finite Element Analysis* (GB Publishing, 2005)
99. A.S. Sokolik, Self-ignition, flame, and detonation in gases (Israel Program for Scientific Translations; [available from the Office of Technical Services, U.S. Department of Commerce, Washington] (1963)
100. R. Price, T. EralpErden, E. Crumlin, S. Rani, S. Garcia, R. Smith, L. Deacon, C. Euaruksakul, G. Held, The partial oxidation of methane over Pd/Al_2O_3 catalyst nanoparticles studied in-situ by near ambient-pressure x-ray photoelectron spectroscopy. Top. Catal. **59**, 516 (2016)
101. N.N. Greenwood, A. Earnshaw, *Chemistry of the Elements* (Pergamon Press, Oxford, 1984)
102. C. Lai, Q. Guo, X.-F. Wu, D.H. Reneker, H. Hou, Growth of carbon nanostructures on carbonized electrospun nanofibers with palladium nanoparticles. Nanotechnology **19**, 195303 (2008)
103. M.A. Atwater, J. Phillips, Z.C. Leseman, The effect of powder sintering on the palladium-catalyzed formation of carbon nanofibers from ethylene-oxygen mixtures. Carbon **48**, 1932 (2010)
104. F. Nitze, Synthesis and characterization of palladium based carbon nanostructure-composites and their clean energy application, Dissertation, Umeå University, Sweden (2013)
105. https://tehtab.ru/Guide/GuidePhysics/GuidePhysicsHeatAndTemperature/HeatexpansionCoefficient/linearExtensionManyMaterials/

Chapter 4
Features of Combustion of Hydrogen–Methane–Air Fuels Over Surfaces of Noble Metals

Abstract This chapter is aimed at the establishment of the regularities of catalytic ignition mainly of H_2–methane mixtures; in a series of experiments methane blends were replaced with ethane, ethylene and n-pentane. It was shown that in the reactor, treated with ignitions, the ignition temperature of the mixture 70% H_2 + 30% methane with air over rhodium surface is 62 °C. The result indicates the potential of using rhodium catalyst to lower markedly the catalytic ignition temperature of the fuels based on hydrogen–methane mixtures. The critical condition for volume reaction is revealed: the volume process occurs at 45% H_2, but it is missing at $\leq$ 40% H_2. If $H_2 \leq 40\%$, only a slow surface reaction occurs; this phenomenon is qualitatively described by our calculations. It is revealed that the effective activation energies both of "upper" and "lower" limits of H_2 + methane oxidation over the range of linearity are roughly equal (2.5 ± 0.6) kcal/mol; it means that the key reactions, responsible for the occurrence of "upper" and "lower" ignition limits are almost certainly the same. It was shown that the obtained values of effective activation energy are in mutual agreement and are characteristic of the surface nature of Rh action; Rh is more catalytically active than Pd. It was shown that under conditions of our experiments not the chemical nature of the catalyst but that of C_2 hydrocarbon in the mix with H_2 is the determining factor of catalytic ignition. The catalytic ignition limits of synthesis gas over Rh/Pd are qualitatively different from the dependencies for combustible hydrogen-hydrocarbon. Long delay periods of catalytic ignition of hydrogen—n-pentane mixes (tens of seconds) and the absence of the dependence of the periods on the initial temperature allow us to conclude that the catalytic ignition of hydrogen—n-pentane mixes is determined by the transfer of the molecules of the hydrocarbon blend to the surface of the catalytic wire. It was shown that the ignition limits of $2H_2 + O_2$ and $(80\%\ H_2 + 20\%\ CH_4)_{stoich} + O_2$ mixes over Pt wire do not depend on the applied voltage without discharge up to 1200 V. We showed that for $(80\%\ H_2 + 20\%\ CH_4)_{stoich} + O_2$ mixes the application of an electric field (1200 V) leads to the disappearance of Pt containing particles from the reaction volume formed by decomposition of volatile platinum oxide in gas phase, which indicates that these particles are charged. This may be due to the chemiionization phenomenon observed in the combustion of hydrocarbons and then adsorption of the charged particles onto the Pt containing particles.

N. M. Rubtsov et al., *Catalytic Ignition of Hydrogen and Hydrogen-Hydrocarbon Blends Over Noble Metals*, Heat and Mass Transfer,
https://doi.org/10.1007/978-3-031-28416-8_4

Keywords Catalytic · Ignition · Limit · Rhodium · Palladium · Platinum · Hydrogen · Methane · Air oxygen · Kinetics · Chemiionization

Note that below we will constantly focus the reader's attention on the description of the procedures for processing wires and foils made of noble metals, which were carried out to ensure the reproducibility of the measurements described in this book.

We recall the important remark made at the beginning of the Chap. 2. Because the quantitative features of the ignition processes of the catalytic surface are investigated below, it becomes important to control the state of the surface. However, it is not possible to provide a micro-level control for a macro sample. In the present study, the same samples of wires and foils were made from the same Pt (and Pd) ingot, and Rh and Ru coatings were applied from the same samples of liquid reagents from the same jeweler. Since the heat losses at the ends of the sample where the contacts are attached plays a prominent role, the samples were used of sufficient (and the same) length and thickness so that the heat losses did not affect the results of the experiments. Thus, the length and diameter of the wires used below are those that increasing their length and decreasing the diameter did not affect the values of the measured limits of catalytic ignition.

Experimental determination of ignition temperatures and effective activation energies of ignition of mixes (40 ÷ 70% H_2 + 60 ÷ 30% $CH_4)_{stoich}$ + air over Rh was performed at 1 ÷ 2 atm over temperature range 20 ÷ 300 °C under static conditions. This was aimed at both establishment catalytic effectiveness of Rh as a promising igniter, and clarification the factors, which determine the values of effective activation energies and to find out whether NTC phenomenon exists in the ignition.

It was shown that in the reactor, treated with ignitions, the ignition temperature of the mixture 70% H_2 + 30% methane with air over rhodium surface is 62 °C. The result indicates the potential of using rhodium catalyst to lower markedly the catalytic ignition temperature of the fuels based on hydrogen–methane mixtures. The critical condition for volume reaction is revealed: the volume process occurs at 45% H_2, but it is missing at ≤ 40% H_2. If $H_2 \leq 40\%$, only a slow surface reaction occurs, this phenomenon is qualitatively described by our earlier calculations. It is revealed that the effective activation energies both of "upper" and "lower" limits of H_2 + methane oxidation over the range of linearity are roughly equal (2.5 ± 0.6) kcal/mol; it means that the key reactions, responsible for the occurrence of "upper" and "lower" ignition limits are almost certainly the same.

It was shown that for Rh/Pd catalyst the chain development process has most likely heterogeneous nature because the effective activation energy is < 3 kcal/mol. Experimental determination of ignition temperatures and effective activation energies of ignition of mixtures 5% ÷ 40% H_2–air over Rh and (30 ÷ 70% H_2 + 70 ÷ 30% C_2H_6 (and C_2H_4))$_{stoich}$ + air over Rh and Pd at 1 atm was performed over temperature range 20–300 °C under static conditions in order to compare catalytic effectiveness of Rh and Pd and to establish factors that determine the values of effective activation energies. It was shown that the obtained values of effective activation energy are in mutual agreement and are characteristic of the surface nature of Rh

action; Rh is more catalytically active than Pd. The key features of catalytic ignition on metallic rhodium and palladium in a series of mixed fuels: namely hydrogen + synthesis gas and hydrogen + hydrocarbon (ethane, ethylene, propane, pentane) + air were identified to establish the boundaries of catalytic ignition regions, dependencies of effective ignition activation energies on the nature of a hydrocarbon, and the role of dark oxidation processes. It was found out that under conditions of our experiments not the chemical nature of the catalyst but that of C_2 hydrocarbon in the mix with H_2 is the determining factor of catalytic ignition. The catalytic ignition limits of synthesis gas over Rh/Pd are qualitatively different from the dependencies for combustible hydrogen-hydrocarbon: the "lower" catalytic limit dependence has a distinct maximum, which indicates a complex mechanism of the catalytic process; the Arrhenius dependence of $\ln [H_2]_{lim}$ on $1/T$ can not obviously be applied. Therefore, the interpretation of the "upper" and "lower" limits of catalytic ignition given in the literature should be cleared up. Long delay periods of catalytic ignition of hydrogen—n-pentane mixes (tens of seconds) and the absence of the dependence of the periods on the initial temperature allow us to conclude that the catalytic ignition of hydrogen–n-pentane mixes is determined by the transfer of the molecules of the hydrocarbon blend to the surface of the catalytic wire.

Experimental studies of low-pressure combustion of hydrogen–methane mixtures were carried out over Pt surface at total pressures from 20 to 180 Torr and initial temperatures of 400–600 °C in order to establish the relationships of catalytic ignition limits over Pt on temperature and to reveal the features of ignition of hydrogen-methane mixes over Pt in a constant electric field in the absence of discharge. It was shown that the ignition limits of $2H_2 + O_2$ and $(80\%\ H_2 + 20\%\ CH_4)_{stoich} + O_2$ mixes over Pt wire do not depend on the applied voltage without discharge up to 1200 V. We showed that for $(80\%\ H_2 + 20\%\ CH_4)_{stoich} + O_2$ mixes the application of an electric field (1200 V) leads to the disappearance of Pt containing particles formed by decomposition of volatile platinum oxide in gas phase from the reaction volume, which indicates that these particles are charged. This may be due to the chemiionization phenomenon observed in the combustion of hydrocarbons. Is was shown that in combustion of $(80\%\ H_2 + 20\%\ CH_4)_{stoich} + O_2$ mix carbon nanotubes practically do not form as distinct from $(H_2 + C_4H_8)_{stoich} + O_2$ mix.

The peculiarities of penetration of a flame front of the diluted methane-oxygen mixture in the volumes of complex geometry in the laboratory scale installation were established. It was shown that a flame propagation process in a conditional room containing an indoor space with two openings and a flammable material inside shows a wide variety of combustion modes depending on the geometry of this complex volume. The preliminary numerical calculation of the expected flame propagation patterns may not always be successful. Thus, a real experiment under laboratory conditions, assuming the possibility of scaling the process, seems to be the most informative one.

The investigation into Pt behavior in the flame of methane combustion under conditions of turbulent flow was performed. We revealed that under certain conditions Pt catalyst can suppress combustion and thereby show the opposite effect due to the high efficiency of Pt surface coated with a Pt oxide layer in the reaction of

chain termination. Therefore, kinetic factors could be the determining even under conditions of high turbulence. Specific features of oxidation of hydrogen and methane over platinum and palladium at low pressures (70–200 Torr) were established. The value of effective activation energy of the dark reaction over Pd is evaluated as $E = 4.1 \pm 1$ kcal/mol that is characteristic of a surface process. Under our conditions, no dark reaction on Pt wire was observed. It was shown that the rate of chain termination determines the value of the critical diameter for flame penetration through Pt or Pd cylinders; the efficiency of Pd surface in chain termination reaction is much greater than that of Pt.

4.1 Ignition Limits of Hydrogen–Methane Air Mixtures Over Metallic Rh at Pressure 1–2 atm

Hydrogen-hydrocarbon mixed fuels attract attention as alternative fuels for energy production for two main reasons. The first reason is related to improved efficiency of mixed fuel methane-hydrogen, which leads to improved performance of combustion devices, increased range of their use and reduced emissions of pollutants when using lean mixtures in stationary and mobile systems. The second reason is related to the development of hydrogen energy and the prospect of using H_2 in fuel cells and devices using combustion [1, 2]. With the commercialization of new hydrogen technologies, the problem of hydrogen safety becomes increasingly important. However, explosive concentrations of H_2 in the mixture with air range from 4 to 75% by volume, thus, transportation and storage of H_2 is dangerous in a high range of its concentration. Meanwhile, it is known that as the methane content of the hydrogen–methane mix increases, the upper combustion concentration limit of such a mix markedly decreases [3]; this makes the mix much safer [4]. Natural gas and hydrogen can be mixed in the engine directly during engine operation [5]. The methane-hydrogen mixture "Haitan" was invented in the USA [6]. The figure in the haitan marking means the energy share of hydrogen in the mixture: HY-5 = 5% (for gasoline cars) and HY-7 = 7% (for diesel cars). The volume fraction of H_2 in the mix can reach up to 20% and even up to 32%, as was the case of a Cummins-Westport gas engine. It has been theoretically and experimentally confirmed that the addition of hydrogen significantly increases the environmental safety and economy of the engine [7].

The challenges in the safety of producing, transporting and storing hydrogen-hydrocarbon fuels need to be fixed before widespread use. One of the main problems is accidental ignition [8]. One of the usual possible sources of ignition is a hot surface. Thus, it is urgent to be able to prevent conditions, under which the ignition can occur when a flammable mixture flows above a hot surface. The catalytic combustion of pure hydrogen is of interest because the boilers using this principle operate at relatively low temperatures and can generate heat for household applications without CO_2 and NO_x emissions [9]. The combustion catalysts should possess the oxygen storage capacity and thermal stability; these should be able to ensure that

fuel oxidation occurs without explosion. That can be achieved using noble metals [10]. Noble metals influence the flammability of hydrogen–methane blends in various ways. We experimentally found that Pd foil ignites mixtures (30–60% H_2 + 70–40% $CH_4)_{stoich}$ + air, whereas Pt foil cannot ignite these up to 450 °C. The estimated effective activation energy of the process is 3.5 ± 1 kcal mol^{-1}, which is indicative of surface processes [11]. It indicates the noticeable role of the dark reaction of H_2 and O_2 consumption observed directly at low pressures [12]. It was also found that the temperature of the ignition limit over palladium surface at 1.75 atm, measured with a bottom-up approach by temperature, of the mixtures 30% CH_4 + 70% H_2 + air ($\theta = 0.9$, T = 317 °C) decreases after subsequent ignitions and amounts to 270 °C, for the hydrogen–methane mix. The ignition limit returns to the initial value after processing of the reactor with oxygen or air; i.e. a hysteresis effect occurs [13]. It was shown [14] that in combustion of hydrogen- propane—air mixtures ($\theta = 1$) over palladium at total pressures 1 ÷ 2 atm the ignition delay periods τ first decrease with a decrease in temperature; but then τ values increase until the ignition limit is achieved i.e. negative temperature coefficient (NTC) phenomenon exists. It was shown that NTC phenomenon is strongly associated with the state of Pd surface.

The paragraph is aimed at experimental determination of ignition temperatures and effective activation energies of ignition of mixes (40 ÷ 70% H_2 + 60 ÷ 30% $CH_4)_{stoich}$ + air over Rh at 1 ÷ 2 atm over temperature range 20 ÷ 300 °C under static conditions. The objective was both, to establish catalytic effectiveness of Rh as a promising igniter, to reveal factors, which determine the values of effective activation energies and to find out whether NTC phenomenon exists in ignition.

4.1.1 Experimental

The experiments were performed with gas stoichiometric mixtures of (40 ÷ 70% H_2 + 60 ÷ 30% $CH_4)_{stoich}$ + air over Rh (stoichiometry composition was calculated for the sum of fuels) at 20° ÷ 300 °C. A heated cylindrical stainless steel reactor 25 cm in length and 12 cm in diameter, equipped with demountable covers and an optical sapphire window in one of the covers was used in experiments [12]. The accuracy of temperature measurements was 0.3 °C. The pumped and heated reactor was quickly filled with the gas mixture from a high-pressure buffer volume to necessary pressure. An electromagnetic valve was used to open and close gas communications. Registration of ignition and flame propagation was performed by means of a color high-speed camera Casio Exilim F1 Pro (frame frequency—1200 s^{-1}). A video file was stored in computer memory and its time-lapse processing was performed [13]. A pressure transducer recorded pressure in the course of gas intake and combustion. The reactor was used to study thermal/catalytic ignition provided by Rh sample, which was made by electrochemical deposition of Rh layer 15 μm thick on Pd wire (0.3 mm thick 80 mm long). Pd was chosen because its coefficient of thermal expansion is the closest to that of Rh [14], since wire made of pure Rh is relatively expensive. The Rh/Pd wire was used both to ignite the flammable mix and to measure

the temperature of the foil as Wheatstone bridge arm. Before each experiment, the reactor was pumped down to 0.1 Torr. The upper ignition limit was determined as the temperature of the first ignition at the given pressure for a bottom-up approach by increase in temperature in the "fresh" reactor, which was not treated with ignitions: at lower temperatures the ignition was missing, at higher one the ignition occurred. For a top-down approach by decrease in temperature in the treated reactor the lower ignition limit was determined as a mean of two temperatures: at higher one the ignition occurred at lower one the ignition was missing. Total pressure in the reactor was monitored with a vacuum gauge, and the pressure in the buffer volume was controlled with a manometer. Chemically pure gases, and 99.85% Pd were used.

4.1.2 Results and Discussion

All experiments on high-speed registration of catalytic ignition of the H_2–methane–air mixtures over Rh/Pd wire (1200 s^{-1}) have shown that an initial center of ignition originates on the wire surface [13] (Fig. 4.1). In subsequent experiments under the same conditions, the site of origin of the initial center varies similarly to catalytic ignition over Pd surface [15]. Thus, the thermal/catalytic ignition over noble metal is determined by the reactions of adsorbed active centers on the surface, their behavior is determined by both surface defects with an excess of free energy and the nature of the catalysts; the ignition consists of the stages of warming-up, local ignition, and flame propagation. The chemical activity of various sites of surface changes from one ignition to another.

The dependencies of the pressure on time at catalytically initiated ignition of 45% H_2 + 55% CH_4 + air mixture at $P_0 = 1.75$ atm over Rh/Pd wire at three temperatures (201 °C, 189.8 °C, 181.4 °C) are shown in Fig. 4.2.

Let us recall that the "upper" catalytic ignition limit is measured with a bottom-up approach by temperature (at lower temperatures the ignition in the "fresh" reactor is missing, at higher one the ignition occurs) [15]. When the "upper" ignition limit is

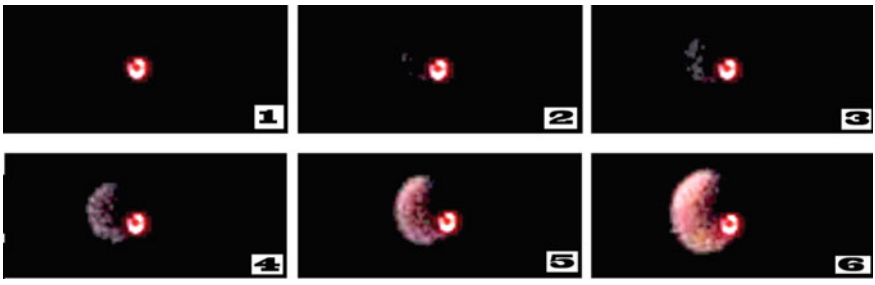

Fig. 4.1 High speed color detection of the initiation and flame propagation in 70% H_2 + 30% CH_4 + air mixture with Rh/Pd wire, 1200 s^{-1}, P_0 = 1. 7 atm, T_0 = 71.1 °C. Numbers in each frame correspond to the consecutive numbers of video images during the ignition

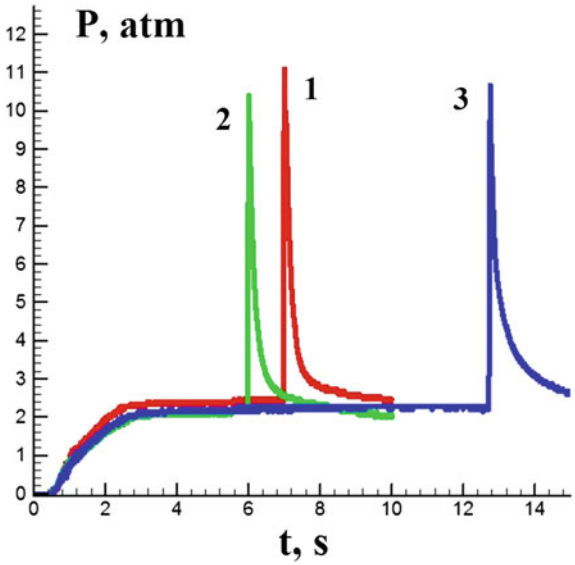

Fig. 4.2 The change in pressure at catalytic ignition of 45% H_2 + 55% CH_4 + air mixture over Rh/Pd wire as a function of time. P_0 = 1.75 atm (1) T_0 = 201 °C, (2) T_0 = 189.8 °C, (3) T_0 = 181.4 °C

attained, the further ignitions in the reactor already treated with combustion take place at decreasing temperatures lower than the "upper" limit until the "lower" ignition limit is attained (a top-down approach). Thus the "lower" ignition limit corresponds to the catalyst (in this paragraph, Rh) surface treated with ignitions; the "upper" one corresponds to the "fresh" reactor, in which no ignitions occurred before.

The typical dependencies corresponding to the successive temperature values below the "upper" ignition limit are shown in Fig. 4.2. As is seen in Fig. 4.2, the ignition delay periods τ first decrease with a decrease in temperature; but then τ values increase until the "lower" temperature ignition limit (at higher temperatures the ignition occurs, at lower one the ignition is missing) is achieved. Thus, we observe the NTC phenomenon similar to one described in [13, 14], see also Chap. 3, Sect. 3.4. NTC phenomenon is caused by the changes in the state of Rh surface. As is shown in [15], in the samples treated with ignitions, the defects in the form of openings develop (Fig. 5 from [15]), i.e. the surface area and the surface state change from ignition to ignition.

To establish the boundaries of catalytic ignition of H_2–CH_4 mixtures over Rh, temperature dependences of hydrogen concentration at both the "upper" and the "lower" ignition limit were experimentally determined. Experimental dependences of H_2 content in the mixture at 1.7 atm on the temperature at "upper" (filled circles) and "lower" (circles) ignition limits of gas stoichiometric H_2–methane–air mixtures, over Rh/Pd wire are presented in Fig. 4.3.

Figure 4.3a shows that in the reactor, treated with ignitions, the ignition temperature of the mixture 70% H_2 + 30% methane with air over rhodium surface is 62 °C. By comparison, the "lower" ignition limit of the same mix is 270 °C over palladium surface at 1.75 atm [16]. The result indicates the potential of using rhodium catalyst

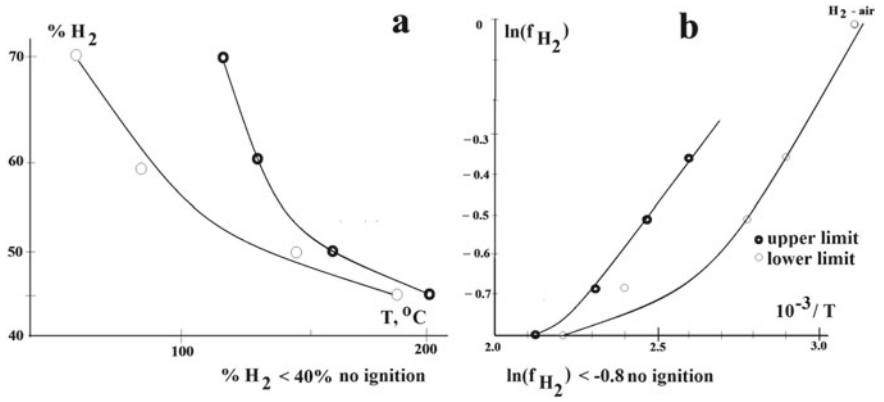

Fig. 4.3 **a** Experimental dependences of the H_2 content in the mixture at the ignition limit over Rh/Pd wire on temperature; filled circles: "upper" limit of H_2–methane–air mix over Rh/Pd,; circles: "lower" limit of H_2–methane–air mix over Rh/Pd, $P_0 = 1.7$ atm. **b** Arrhenius plots: filled circles—dependences of logarithm of the H_2 fraction at "upper" limit of H_2–methane–air mix of catalytic ignition on reciprocal of the temperature over Rh/Pd; circles—dependences of logarithm of the H_2 fraction at "lower" limit of H_2–methane–air mix of catalytic ignition on reciprocal of the temperature over Rh/Pd

to markedly lower the ignition temperature of the fuels based on hydrogen–methane mixtures.

In addition, Rh catalyst is most stable in $H_2 + O_2$ flame than Pd, Ru and Pt, see Chap. 2, Sect. 2.5. As is seen in Fig. 4.3a, the critical condition for volume reaction exists: the volume process occurs at 45% H_2, but it is missing at $\leq$ 40% H_2. If H_2 $\leq$ 40%, only a slow surface reaction takes place: the Rh/Pd wire remains bright red within several minutes. The chemical mechanism of that process needs further investigation.

The dependences of H_2 fraction in the flammable mixtures on temperature in Arrhenius coordinates as justified in [11], (see also Chap. 3) are presented in Fig. 4.3b. As is seen in Fig. 4.3, the dependences at $H_2 > 50\%$ can be approximated by straight lines (the correlation coefficients are > 0.98). The data was processed with the use of the program package Statistica 9 (Statsoft). Figure 4.3b shows that the effective activation energies both of upper and lower limits of H_2 + methane oxidation over the range of linearity are roughly equal (2.5 $\pm$ 0.6) kcal/mol; it means that the key reactions, responsible for the occurrence of upper and lower ignition limits are almost certainly the same. Notice that to provide the ignition, the set of reactions, in which the development of chains (an increase or conservation [15] in the number of free valences) occurs, must be realized [11]. Therefore, activation energy of the chain development should determine the temperature dependence of the overall process, as observed for similar experiments with Pt catalyst [17]. Thus, in case of Rh/Pd catalyst, the chain development process has most likely heterogeneous nature because the effective activation energy is < 3 kcal/mol.

The presence of upper and lower limits of catalytic ignition can be interpreted using the results of Sect. 2.5, Chap. 2. When the temperature rises and the Rh/Pd wire is treated with a hydrogen-containing gas mixture, an effective rhodium hydride catalyst is formed on the surface of the wire. When the temperature corresponding to the upper limit is reached, the mixture ignites above the rhodium hydride layer. Then, with a decrease in temperature, the lower limit of catalytic ignition over the same rhodium hydride is reached. Then the fact that the activation energies of the upper and lower limits are very close is due to the fact that ignition at both limits occurs over the same surface—rhodium hydride.

The feasible illustration of the occurrence of catalytic ignition limits was given in [18] by means of numerical modeling using compressible dimensionless reactive Navier–Stokes equations in low Mach number approximation [15, 18–20], see also Sect. 2.5, Chap. 2.

We will recall the course of this illustrative calculation. The reaction velocity in the volume was presented by an elementary chain mechanism [15, 18]. Chemical exothermic reaction of chain development occurred on the boundaries of the wire (a rectangular region in the middle of the reactor). The Newmann's boundary condition on the "wire" for temperature took into account the heat release in the reaction of chain development; these for initial reagent and a single active center accounted for surface chain development and adsorption of the initial reagent [15]. On the reactor walls the Derichlet's boundary condition hold true for active center and velocity components; The Newmann's boundary conditions hold true for density, initial reagent and temperature. Initial temperature of the gas was given by the initial conditions: $T_0 = 1$ for dark reaction, $T_0 = 2$ to provide ignition [15], see also Sect. 2.5, Chap. 2.

The model showed that in the dark reaction ($T_0 = 1$), the rate of consumption of initial reagent is slower than during the ignition ($T_0 = 2$); thus, it allowed obtaining both, the mode of the emergence of primary ignition centers on the wire followed by a local ignition, and the mode of a dark catalytic reaction of the consumption of the initial reagent (Fig. 8 [15], Fig. 3 [18], Fig. 2.39, Chap. 2).

We summarize briefly the main results.

It was shown that in the reactor, treated with ignitions, the ignition temperature of the mixture 70% H_2 + 30% methane with air over rhodium surface is 62 °C. The result indicates the potential of using rhodium catalyst to markedly lower the ignition temperature of the fuels based on hydrogen–methane mixtures.

The critical condition for volume reaction is revealed: the volume process occurs at 45% H_2, but it is missing at $\leq$ 40% H_2. If $H_2 \leq 40\%$, only a slow surface reaction occurs; this phenomenon is qualitatively described by our earlier calculations.

It is revealed that the effective activation energies both of "upper" and "lower" limits of H_2 + methane oxidation over the range of linearity are roughly equal (2.5 $\pm$ 0.6) kcal/mol^{-1}; it means that the key reactions, responsible for the occurrence of "upper" and "lower" ignition limits are almost certainly the same.

It was shown that for Rh/Pd catalyst, the chain development process has most likely heterogeneous nature because the effective activation energy is < 3 kcal/mol.

4.2 Ignition Limits of Hydrogen–Air Mixtures Over Metallic Rh and Hydrogen-Ethane/Ethylene–Air Mixtures Over Pd and Rh at Atmospheric Pressure

In the previous paragraph, the areas of hydrogen ignition in the presence of the simplest carbon-hydrogen additive—methane are considered and it was established that in the reactor, treated with ignitions, the ignition temperature of the mixture 70% H_2 + 30% CH_4 with air over rhodium surface is 62 °C. The result points to the possibility of using rhodium catalyst to lower markedly the ignition temperature of the fuels based on hydrogen–methane mixtures. It is found that the critical condition for volume ignition exists: the volume process occurs at 45% H_2, but it is missing at $\leq$ 40% H_2. If $H_2 \leq 40\%$, only a slow surface reaction occurs. It is shown that the effective activation energies both of "upper" and "lower" limits of H_2 + methane oxidation over the range of linearity are roughly equal (2.5 $\pm$ 0.6) kcal/mol; thus, the key reactions, responsible for the occurrence of "upper" and "lower" ignition limits are almost certainly the same. In this paragraph, the regularities obtained for methane are compared with those for ethane/ethylene blends.

As we stated above, the challenges in the safety of producing, transporting and storing hydrogen need to be fixed before widespread use of hydrogen as fuel. One of the main problems is accidental ignition, since hydrogen has much wider flammability limits than most conventional fuels [8]. One of the most frequent sources of ignition is a hot surface. Thus, it is essential to be able to prevent conditions, under which the ignition can occur when a flammable hydrogen-oxidizer mixture is exposed to a hot surface, especially if the surface has catalytic nature.

The catalytic combustion of hydrogen is of interest because the devices using this principle operate at comparably low temperatures and therefore, can generate heat for various applications without CO_2 and NO_x emissions [9]. We drew attention that for H_2 combustion reaction, the catalysts should possess the oxygen storage capacity and thermal stability; these should be able to ensure that H_2 oxidation occurs without explosion. That can be attained using noble metals, which, in addition, have the high adsorption capability of H_2 and O_2 at low temperatures [10].

Along with hydrogen, mixed hydrogen–hydrocarbon fuels have attracted increased attention as alternative ones for instance due to the fact that using the combustion of premixed mixtures is a promising method to lower the combustion temperature, and consequently, to fulfill the modern need to limit NO_x emissions in energy production, including internal combustion engines [11, 21, 22].

We showed that at the ignition temperature of the mixture 40% H_2–air over Pd metal (70 °C, 1 atm) is ~ 200° less than over the Pt surface (260 °C, 1 atm) [11] i.e. Pd is more effective than Pt. Thus, Pd seems to be more usable for hydrogen recombiners in NPP, in part, because no catalytic particles as ignition centers formed by decomposition of volatile oxide can appear in gas phase as compared to Pt [23]. The experimental value of the effective activation energy of catalytic ignition over Pd is ~ 3.5 kcal/mol that is characteristic of surface processes [11]. It indicates the noticeable role of the dark reaction of consumption of H_2 and O_2 what is known as

"flameless combustion", which is observed at low pressures [12]. The occurrence of that reaction reduces the probability of an accidental explosion at the expense of fuel consumption and accordingly leads to shifting the boundaries of catalytic explosion area.

Hydrogen combustion over Rh, Ru, Pd and Pt wires at total pressures up to 200 Torr and initial temperatures up to 500 °C is investigated in [15] in order both to establish the dependencies of autoignition limits over noble metal surfaces on temperature and to indicate the governing factors of the problem of gas ignition by a catalytic surface. At the total pressures, it was shown that Rh is the most effective catalyst of $2H_2 + O_2$ ignition, the lowest ignition temperature over Rh coated Pd wire (Rh/Pd) is 210 °C, for Ru/Pd and Pd—300 °C, for Pt wire—410 °C.

It is shown [13, 16] that at the combustion of (70 ÷ 40%) hydrogen- (30 ÷ 60%) propane–air mixtures ($\theta = 1$) over palladium at total pressures 1 ÷ 2 atm the ignition delay periods τ first decrease with a decrease in temperature; but then τ values increase until the ignition limit is achieved i.e. NTC phenomenon occurs. The effective activation energy of the process is $E = 2.2 \pm 1$ kcal/mol that is characteristic of a surface process. Thus, NTC phenomenon is strongly associated with the state of Pd surface.

The paragraph is focused on experimental establishment of ignition temperatures and effective activation energies of ignition of mixtures 5% ÷ 40% H_2–air and 10% ÷ 20% D_2–air over Rh and (30 ÷ 70% H_2 + 70 ÷ 30% C_2H_6 (or C_2H_4))$_{stoich}$ + air over Rh and Pd at 1 atm over temperature range 20–300°C under static conditions in order to compare catalytic effectiveness of Rh and Pd, and to establish factors that determine the values of effective activation energies and to find out whether NTC exists in ignition of hydrogen over Rh.

4.2.1 Experimental

The experiments were performed with gas stoichiometric mixtures of 5% ÷ 40% H_2–air and 10% ÷ 20% D_2–air over Rh and (30 ÷ 70% H_2 + 70 ÷ 30% C_2H_6 (and C_2H_4))$_{stoich}$ + air over Rh and Pd (stoichiometry composition was calculated for the sum of fuels) and 5 ÷ 40% H_2 + air at 20^0 ÷ 300 °C. A heated cylindrical stainless steel reactor 25 cm in length and 12 cm in diameter, equipped with demountable covers and an optical sapphire window in one of the covers was used in experiments [12]. The accuracy of temperature measurements was 0.3 K. Registration of ignition and flame propagation was performed by means of a color high-speed camera Casio Exilim F1 Pro (frame frequency–600 s^{-1}). A video file was stored in computer memory and its time-lapse processing was performed [13, 16]. The pumped and heated reactor was quickly filled with the gas mixture from a high-pressure buffer volume to necessary pressure. An electromagnetic valve was used to open and close gas communications. A pressure transducer recorded pressure in the course of gas intake and combustion. The reactor was used for studying thermal/catalytic ignition provided by Pd wire (0.3 mm thick 80 mm long) as well as Rh sample, which was

made by electrochemical deposition of Rh layer 15 μm thick on Pd wire (0.3 mm thick 80 mm long). Pd was chosen because its coefficient of thermal expansion is the closest to that of Rh and Ru [24]. The Pd or Rh/Pd wires were used both to ignite the flammable mix and to measure the temperature of the wire as a bridge arm. Before each experiment, the reactor was pumped down to 0.1 Torr. The ignition limit was determined as the mean of two temperatures at the given pressure; e.g. for a bottom-up approach by temperature: at lower temperatures the ignition was missing, at higher one the ignition occurred. Total pressure in the reactor was monitored with a vacuum gauge, and the pressure in the buffer volume was controlled with a manometer. Chemically pure gases and 99.85% Pd were used.

4.2.2 Results and Discussion

All experiments on high-speed registration of catalytic ignition of the mixture 40% H_2 + air over Rh/Pd wire (600 s^{-1}) have shown that an initial center of ignition originates on the wire surface [23] (Fig. 4.4).

In subsequent experiments under the same conditions, the site of origin of the initial center varies similarly to catalytic ignition over Pd surface [15]. Thus, the thermal ignition over noble metal is determined by the reactions of adsorbed active centers on the surface, their behavior is determined by both surface defects with an excess of free energy and the nature of the catalyst; the ignition consists of the stages of warming-up, local ignition, and flame propagation. The chemical activity of various sites of surface changes from one ignition to another.

The dependencies of the resistance of the Rh/Pd wire on time at catalytically initiated ignition of 40% H_2–air mixture at P_0 = 1.75 atm at three temperatures (98 °C, 80 °C, 68 °C) are shown in Fig. 4.5.

The dependencies correspond to the successive temperature values below the "upper" ignition limit measured with a bottom-up approach (at lower temperatures the ignition occurs, at higher one the ignition is missing) [13]. As is seen in Fig. 4.5, the ignition delay periods τ first decrease with a decrease in temperature; but then τ values increase until the "lower" temperature ignition limit (at higher temperatures the ignition occurs, at lower one the ignition is missing) is achieved. The "lower" ignition limit corresponds to the Pd surface treated with ignitions; the "upper" one

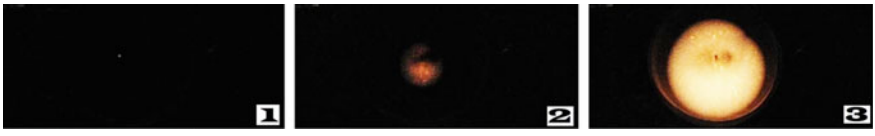

Fig. 4.4 High-speed filming of the catalytic ignition of the mixture 40% H_2 + air over Rh wire, 600 s^{-1}, T_0 = 80 °C, P_0 = 1.7 atm. The first number of the frame corresponds to the moment of the occurrence of a primary ignition center on the wire

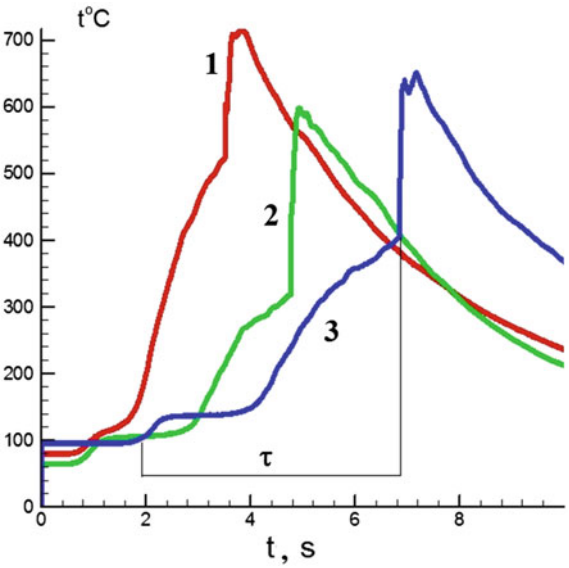

Fig. 4.5 Monitoring of the change in the Rh/Pd wire resistance during the ignition of 40% H_2 + air mixture; initial temperature 1–80 °C, 2–68 °C, 3–98 °C, P = 1.75 atm. The ignition delay τ is indicated

corresponds to the "fresh" reactor, in which no ignitions occurred before. Thus, we observe the NTC phenomenon similar to one described in [13]. The phenomenon is caused by the changes in the state of Rh surface. As is shown in [15], in the samples treated with ignitions, the defects in the form of openings develop (Fig. 5 from [15], see also Sect. 2.5, Chap. 2). Their depth reaches < 1 μm in the case of Pd wire. These defects seemingly focus on chemical etching patterns; the etching substances are evidently active intermediates of H_2 oxidation.

To bring out the influence of chemical nature of both a catalyst and a hydrocarbon on the surface processes, the catalysts Pd and Rh/Pd as well as ethylene and ethane were used in the mixtures with hydrogen and temperature dependences of hydrogen concentration at the "lower" ignition limit were experimentally determined.

Experimental dependences of the temperature at "upper" and "lower" ignition limits of gas stoichiometric mixtures H_2–ethane–air mix (filled circles), and H_2–ethylene–air mix (circles) over Pd wire on H_2 content in the mixture at 1.7 atm are presented in Fig. 4.6a.

The dependences of "lower" ignition limits over Pd and Rh/Pd wires on H_2 and D_2 content in the mixtures H_2–air over Rh/Pd (filled circles), D_2–air over Rh/Pd (circles), H_2–air mixes over Pd (squares), H_2–ethylene–air mixtures over Rh/Pd (bold circles) at $P_0 = 1.7$ atm are shown in Fig. 4.7a. To get reproducible results, before ignitions of D_2–air mix over Rh/Pd the wire was kept in the reactor filled with 500 Torr D_2 for 2 h (see Chap. 2).

Figure 4.6a shows that H_2–ethane–air mix ignites at higher temperatures, than H_2–ethylene–air mix, i.e. ethylene reacts more readily with active centers on the catalytic surface of palladium. As is seen in Fig. 4.7a, Rh/Pd wire ignites H_2–air mixture at temperatures lower than Pd wire does. The result is in an agreement with

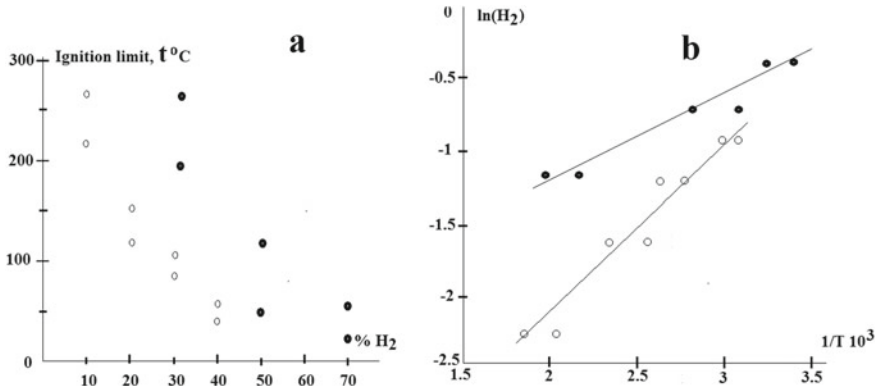

Fig. 4.6 **a** Experimental dependences of the temperature at the ignition limit over Pd wire on H_2 content in the mixture; filled circles: H_2–ethane–air mix, circles: H_2–ethylene–air mix. **b** Arrhenius plots of the dependences. Effective activation energies E_{eff}: fuel H_2–ethane—1.25 ± 0.50 kcal/mol; fuel H_2–ethylene—2.8 ± 1.0 kcal/mol

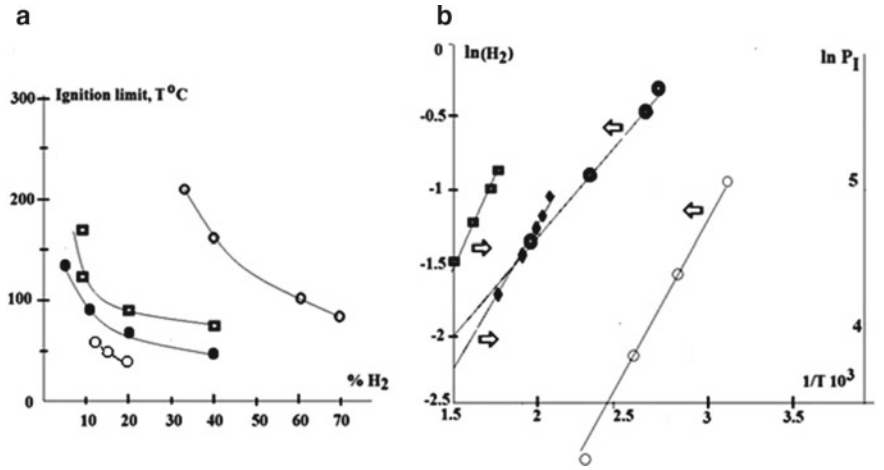

Fig. 4.7 **a** Experimental dependences of the temperature at the "lower" ignition limit over Pd and Rh/Pd wires on H_2 content in the mixture; filled circles: H_2–air mix over Rh/Pd, squares: H_2–air mix over Pd, bold circles: H_2–ethylene- air mix over Rh/Pd, $P_0 = 1.7$ atm, D_2—air mix over Rh/Pd, circles. **b** Arrhenius plots: dependences of lower pressure limit of catalytic ignition of $2H_2 + O_2$ mixes (Figs. 6, 7 [15]) on temperature over Pd—squares; over Rh/Pd—diamonds; dependences of H_2 content in the mixture on temperature over Rh/Pd: filled circles—H_2–ethylene–air; circles—40% H_2–air

Fig. 4 from [15], where it is shown that Rh is the most active surface in the reaction $H_2 + O_2$, Ru and Pd surfaces are less active at total pressures < 200 Torr. As is also seen in Fig. 4.7a the lower catalytic ignition limit of $2D_2 + O_2$ over rhodium deuteride is noticeably lower than that of $H_2 + O_2$ over Rh hydride; thus, D_2 is more flammable than H_2 over Rh. It is in agreement with the results of Sect. 2.5, Chap. 2.

It should be noted that at pressures > 1 atm at successive catalytic ignitions over Rh/Pd of the H_2–hydrocarbon mixtures near the lower limit under the same conditions, the ignition delay period increases, that is, the lower ignition limit increases. This can be prevented by igniting a mixture of 40% H_2–air before each ignition of the mixtures of H_2–hydrocarbon-air.

As is stated above, the reaction ability of noble metal is caused by the changes in the state of its surface. Thus, the rhodium surface is more efficiently poisoned by a hydrocarbon than the palladium surface; this hydrocarbon is removed from the surface during its treatment by ignition of H_2–air mix.

The dependences of H_2 fraction in the flammable mixtures on temperature in Arrhenius coordinates as justified in [11], are presented in Figs. 4.6b and 4.7b. As is seen in the Figures, the dependence can be approximated by straight lines (the correlation coefficients are > 0.98). The data was processed with the use of the program package Statistica 9 (Statsoft).

Figure 4.6 b shows that the effective activation energy of H_2 + ethane oxidation is 1.25 ± 0.6 kcal/mol; it is noticeably less than the effective activation energy of H_2 + ethylene oxidation (2.8 ± 0.7 kcal/mol), hence, the chemical nature of hydrocarbon in the mix with H_2 is one of the determining factors of catalytic ignition. Though the value of effective activation energy is close to activation energies of adsorption—desorption of hydrogen on Pd [25], to provide the ignition, the set of reactions, in which the branching (an increase in the number of free valences) occurs, must be realized [6]. The activated (E = 16.7 kcal/mol [8, 26]) homogeneous branching reaction $H + O_2 \rightarrow O + OH$ is the slowest step in the set. Therefore, activation energy of the branching should determine the temperature dependence of the overall process, as observed for similar experiments with Pt metal [17]. Thus, in case of Pd and Rh/Pd, the branching reaction has most likely heterogeneous nature because the effective activation energy is < 3 kcal/mol.

Figure 4.7 b shows Arrhenius dependences of H_2 content in the mixture at the "lower" limit on temperature over Rh/Pd for H_2–ethylene–air mix; the value of effective activation energy is 2.4 ± 0 0.7 kcal/mol, the value is lower than that over Pd and indicates a greater reactivity of rhodium as compared to palladium.

The value of effective activation energy from Arrhenius dependence of H_2 content in the mixture at the "lower" limit on temperature over Rh/Pd for H_2–air mix is 3.5 $\pm$ 0.8 kcal/mol.

The value is close to that taken from Arrhenius dependence of the low-pressure limit of catalytic ignition of $2H_2 + O_2$ mix over Rh/Pd: 3.6 ± 0.8 kcal/mol (Fig. 6 [15]). The value of effective activation energy determined for low pressure limit of catalytic ignition of 2 $H_2 + O_2$ mix over Pd (3.9 ± 0.8 kcal/mol, Fig. 6 [15]) also satisfactorily agrees with that obtained from Arrhenius dependence of H_2 content in the mixture at the "lower" limit on temperature over Pd for H_2–air mix ~ 3.5 kcal/mol.

The obtained values of effective activation energy are in mutual agreement and are characteristic of the surface nature of Rh action; Rh is more catalytically active than Pd.

4.3 Features of Ignition of Mixtures of Hydrogen with Hydrocarbons (C_2, C_3, C_5) Over Rhodium and Palladium at Pressures of 1–2 atm

In the previous paragraph, it was shown that the obtained values of effective activation energy of ignition of hydrogen–ethane/ethylene blends are in mutual agreement and are characteristic of the surface nature of Rh action; Rh is more catalytically active than Pd. It is also found that the reaction ability of noble metal is caused by the changes in the state of its surface. Thus, the rhodium surface is more efficiently poisoned by hydrocarbon than the palladium surface; this hydrocarbon is removed from the surface during its treatment by ignition of H_2–air mix.

In this paragraph, the regularities obtained in Sects. 4.4.1 and 4.4.2 are compared with those for propane and n-pentane blends.

Along with hydrogen, mixed hydrogen–hydrocarbon fuels as well as synthesis gas have attracted increased attention as alternative fuels. It is because the usage of their combustion is a promising method for fulfilling the modern need to limit NO_x emissions in energy production, including internal combustion engines [22] as well as for obtaining target intermediate reagents for commercial organic synthesis. The advancement in catalytically stabilized (CS) combustion technology requires the development of catalysts with improved activity (desired light-off temperature less than 450 °C), understanding of the catalytic surface processes, knowledge of low temperature homogeneous kinetics and their respective coupling with heterogeneous kinetics. Of particular interest in natural gas-fueled turbines is the concept of hydrogen-assisted CS combustion [27]. As is known, the extensive quantities of H_2 and steam generated in the boiling water reactor (BWR) system create high pressure and temperatures. This may lead to the reactor failure. Thus, the removal of excess amount of H_2 is necessary, and extensive research is required to overcome the highly undesirable phenomenon in nuclear industries. The use of noble metal catalysts for hydrogen afterburning at nuclear power plants (NPPs) is also of great interest [28]. Methane oxidation on noble metals has been insufficiently studied [29]; the nature of the surface processes is generally unknown.

The features of catalytic ignition of mixtures of hydrogen with hydrocarbons and synthesis gas with air above the surface of metallic Rh are not practically considered in contemporary literature. Ignition temperatures and effective activation energies of ignition limits of mixes $(40 \div 70\%\ H_2 + 60 \div 30\%\ CH_4)_{stoich}$ + air over Rh were experimentally determined at 1 atm over 20–300 °C. Over the surface treated with ignitions, the ignition temperature of the mix 70% H_2 + 30% methane + air over Rh is 62 °C indicating the potential of using Rh to lower markedly the ignition temperature

of the fuels based on hydrogen–methane mixes (see Sect. 4.1 of this chapter). Ignition temperatures and effective activation energies of ignition of mixtures 5% ÷ 40% H_2–air over Rh and (30 ÷ 70% H_2 + 70 ÷ 30% C_2H_6 (and C_2H_4))$_{stoich}$ + air over Rh and Pd were experimentally determined at 1 atm over temperature range 20 ÷ 300°, see previous paragraph. It was shown that metallic Rh is more effective than Pd; effective activation energies of ignition depend both on the nature of the catalyst and on the chemical nature of the hydrocarbon (see Sect. 4.2 this chapter). Ignition limits of stoichiometric mixtures (20 ÷ 80% H_2 + 80 ÷ 20% CH_4) + O_2 over Rh and Pd were determined at 0 ÷ 200 Torr and 200 ÷ 500 °C [30].

Similar data for Pd metal as a catalyst are also rather disparate. We showed previously that the effective activation energy of the process the combustion of (70 ÷ 40%) hydrogen—(30 ÷ 60%) propane–air mixtures over Pd at total pressures 1–2 atm is $E = (2.2 \pm 1)$ kcal/mol [18] that is characteristic of a surface process [25]. It was found out that in the sample treated with ignitions, the defects in the form of openings, which are focused on etching patterns, arise [15]. This means that Pd is spent in the reaction of chemical etching with active intermediates of combustion. It was shown that before ignition, catalytic wire is not heated up uniformly; initial centers of the ignition occur. In addition, in sequential ignitions, primary ignition centers change their location on the wire from the first ignition to the next one [18].

We indicate that the effective activation energies of catalytic ignition of mixed fuels were determined taking into account the fact that it is hydrogen that provides catalytic ignition over a noble metal, which is confirmed by the fact that under our conditions catalytic ignition of pure hydrocarbons does not take place. In this case, the following dependence of the hydrogen content in the mixture on the temperature of the catalytic ignition limit was assumed [11]. We recall (see Chap. 2 and 3) that for the stoichiometric $2H_2 + O_2$ mixture, the ignition limit at low pressures is $2k_2$ $[O_2]_{lim} = k_4$; i.e., $[O_2]_{lim} = (1/2)$ $[H_2]_{lim} = k_4/k_2$, where k_4 is the rate constant of the heterogeneous break (weakly dependent on temperature) and k_2 is the branching rate constant. Thus, we obtain Arrhenius dependence of ln $[H_2]_{lim}$ on $1/T$ with a positive slope. The heterogeneous nature of the process in the presence of noble metal considerably complicates the analysis. This reflects the fact that in the catalytic oxidation of H_2, the reaction rate depends mainly on the H_2 concentration, which can be expressed as the ratio of some two effective constants for the steady state [25]. We will point out that this approximation is rather rough; but it allows us systematizing the experimental results for the limits of catalytic ignition over the studied noble metals.

Obviously, in order to understand the mechanism of the catalytic process, it is necessary to establish the features of the influence of hydrocarbon on the catalytic oxidation of the mixed fuel.

The work is aimed at identifying the key features of catalytic ignition on metallic rhodium and palladium in a series of mixed fuels, namely hydrogen + synthesis gas and hydrogen + hydrocarbon (ethane, ethylene, propane, pentane) + air to establish the boundaries of catalytic ignition regions, dependencies of effective ignition activation energies on the nature of hydrocarbon, and the role of dark oxidation process.

4.3.1 Experimental

The experiments were performed with gas stoichiometric mixtures of 5% ÷ 40% H_2–air over Rh and (30 ÷ 70% H_2 + 70 ÷ 30% C_2H_6 (C_2H_4, C_3H_8, n-C_5H_{12}))$_{stoich}$ + air over Rh and Pd (stoichiometry composition was calculated for the sum of fuels) and 5 ÷ 40% H_2 + air at 20 ÷ 300 °C. A heated cylindrical stainless steel reactor 25 cm in length and 12 cm in diameter, equipped with demountable covers and an optical sapphire window in one of the covers was used in experiments [11]. The accuracy of temperature measurements was 0.3 K. Registration of ignition and flame propagation was performed by means of a color high-speed camera Casio Exilim F1 Pro (frame frequency—600 s^{-1}). A video file was stored in computer memory and its time-lapse processing was performed [11]. The pumped and heated reactor was quickly filled with a gas mixture from a high-pressure buffer volume to necessary pressure. An electromagnetic valve was used to open and close gas communications. A pressure transducer recorded pressure in the course of gas intake and combustion. The reactor was used for studying thermal/catalytic ignition provided by Pd wire (0.3 mm thick 80 mm long) as well as Rh sample, which was made by electrochemical deposition of Rh layer 15 μm thick on Pd wire (0.3 mm thick 80 mm long). Pd was chosen because its coefficient of thermal expansion is the closest to that of Rh [24], since Rh wire is relatively expensive. The Pd or Rh/Pd wires were used both to ignite the flammable mix and to measure the temperature of the wire as a bridge arm. Before each experiment, the reactor was pumped down to 0.1 Torr. Catalytic ignition limits were considered as the mean of two temperatures at the given pressure:

(a) for a bottom-up approach by temperature at lower temperature, the ignition was missing, at higher one the ignition occurred, all other things being equal; the temperature was increased in steps of 10°, there were no ignitions above the noble metal wire before
(b) for a top-down approach at higher temperature the ignition occurred, at lower one the ignition was missing; the temperature was reduced in steps of 10°. It is evident that the ignition limit value measured over the wire, which is not treated with ignitions (a bottom-up approach), is higher than the value measured with a top-down approach. Each value of the catalytic ignition limit given in the graphs below is the arithmetic mean of 6 experimental values.

Total pressure in the reactor was monitored with a vacuum gauge, and the pressure in the buffer volume was controlled with a manometer. Chemically pure gases and 99.85% Pd were used.

4.3.2 Results and Discussion

We recall that the “upper” ignition limit is measured with a bottom-up approach by temperature (at lower temperatures the catalytic ignition over the “fresh” noble metal

wire reactor is missing, at higher one the ignition occurs) [15]. When the "upper" ignition limit is attained, the further ignitions over the wire already treated with combustion take place at decreasing temperatures lower than "upper" limit until the "lower" ignition limit is attained (a top-down approach). Thus, the "lower" ignition limit corresponds to the catalyst (Pd or Rh) surface treated with ignitions; the "upper" one corresponds to the "fresh" catalyst, over which no ignitions occurred before.

In Fig. 4.8 a, experimental dependences of the temperature at "upper" and "lower" ignition limits of gas mixtures H_2–ethane- air mix (filled circles), H_2–ethylene- air mix (circles) over Pd wire and synthesis gas H_2–CO mix (squares) over Rh/Pd wire on H_2 content in the mixture at $P_0 = 1.7$ atm are shown. Crosses on the symbols indicate "lower" catalytic ignition limits.

To bring out the influence of chemical nature of both catalyst and hydrocarbon on the surface processes, the catalysts Pd and Rh/Pd as well as ethylene and ethane were used in the mixes with hydrogen. Temperature dependences of hydrogen concentration at the catalytic ignition limits were experimentally determined. Figure 4.8 a shows that H_2–ethylene–air mix ignites at lower temperatures, than H_2–ethane–air mix, i.e. ethylene reacts more readily with active centers on the catalytic surface of palladium.

The dependences of H_2 fraction in the flammable mixtures on temperature in Arrhenius coordinates as justified above (see also [11]) are presented in Fig. 4.8b. As is seen in Fig. 4.8, the dependences can be approximated by straight lines (the correlation coefficients are > 0.98). The data was processed with the use of the program package Statistica 9 (Statsoft). Figure 4.8b shows that the effective activation energy of H_2 + ethane oxidation is 1.25 ± 0.4 kcal/mol both over Pd and Rh/Pd wires;

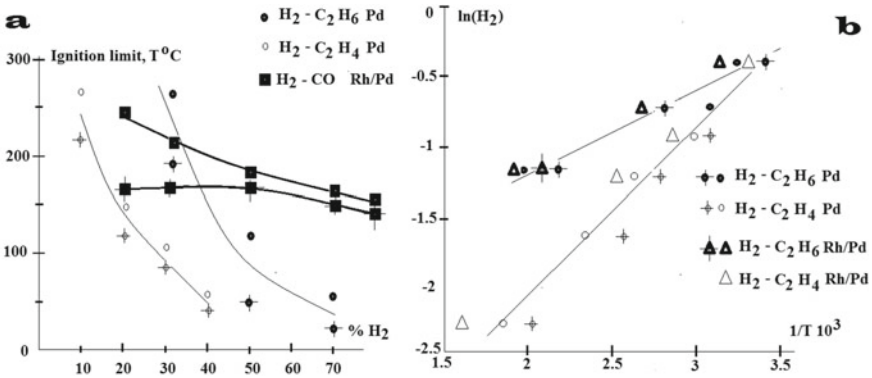

Fig. 4.8 **a** Experimental dependences of the temperature at "upper" and "lower" ignition limits of gas mixtures H_2–ethane–air mix (filled circles), H_2–ethylene–air mix (circles) over Pd wire H_2–CO mix (squares) over Rh/Pd wire on H_2 content in the mixture. $P_0 = 1.7$ atm. Crosses on the symbols indicate "lower" catalytic ignition limits. **b** Arrhenius plots: dependences of "upper" and "lower" catalytic ignition limits of H_2–ethylene–air mixes (circles, over Pd; triangles, over Rh/Pd); H_2–ethane–air mixes (filled circles, over Pd; bold triangles, over Rh/Pd)

it is noticeably less than the effective activation energy of H_2 + ethylene oxidation (2.8 ± 0.5 kcal/mol) both over Pd and Rh/Pd wires.

Therefore, under conditions of our experiments, not the chemical nature of the catalyst but that of C_2 hydrocarbon in the mix with H_2 is the determining factor of catalytic ignition. However, to provide the ignition, the set of reactions, in which the branching (an increase in the number of free valences) occurs, must be realized [8]. The activated (E = 16.7 kcal/mol [8]) homogeneous branching reaction $H + O_2 \rightarrow O + OH$ is the slowest step in the set. Therefore, activation energy of the branching should determine the temperature dependence of the overall process, as we observed in similar experiments with Pt metal [23]. Thus, in case of Pd and Rh/Pd, the branching reaction (or chain propagation one, see Sect. 2.5 of Chap. 2) has most likely heterogeneous nature because the effective activation energy is < 3 kcal/mol.

It can be seen in Fig. 4.8a that both the upper and lower limits of catalytic ignition over Rh/Pd are observed during combustion of the synthesis gas, however, hydrogen rich mixtures ignite less actively than H_2–ethane/ethylene–air mixes. In addition, Fig. 4.8a shows that the dependencies of the catalytic ignition limits of synthesis gas over Rh/Pd are qualitatively different from the dependencies for combustible hydrogen-hydrocarbon: the "lower" catalytic limit dependence has a distinct maximum, which indicates a more complex mechanism of the catalytic process. Therefore, the straight-line Arrhenius relation of $\ln [H_2]_{lim}$ on $1/T$ is not in principle fulfilled.

It means that the interpretation of the "upper" and "lower" limits of catalytic ignition given in the work [15] should be clarified. Notice that according to [15], as the temperature rises and the Rh/Pd wire is treated with a hydrogen-containing gas mixture, an effective rhodium hydride catalyst is formed on the surface of the wire. When the temperature corresponding to the "upper" limit is attained, the mixture ignites over the rhodium hydride layer. Then, as the temperature decreases, the lower limit of catalytic ignition over the same rhodium hydride layer is reached. Then the fact that the activation energies of the upper and lower limits are very close to each other is due to the fact that ignition at both limits occurs over the same surface. *However, both for the synthesis gas and hydrocarbons with longer chains, due to the different adsorption capacity of fresh and ignition-treated rhodium hydride with respect to CO molecules, initial reagents and combustion products must be taken into account to describe the behavior of catalytic ignition limits.*

In Fig. 4.9 a, experimental dependences of the temperature at "upper" and "lower" ignition limits of gas mixtures H_2–propane- air mix (filled circles, over Rh/Pd wire), H_2–propane–air mix (circles, over Pd wire) and H_2–n-pentane–air mix (triangles, over Rh/Pd wire) on H_2 content in the mixture at P_0 = 1.7 atm are shown. Crosses on the symbols indicate "lower" catalytic ignition limits.

As is seen in Fig. 4.9, the value of effective activation energy from Arrhenius dependence of logarithm of H_2 content at both "upper" and "lower" limits over both Pd and Rh/Pd for all mixes on inverse temperature is 1.2 ± 0.3 kcal/mol. Thus, the effective activation energy does not depend on the chemical nature both of the hydrocarbon in the mix and of the catalyst.

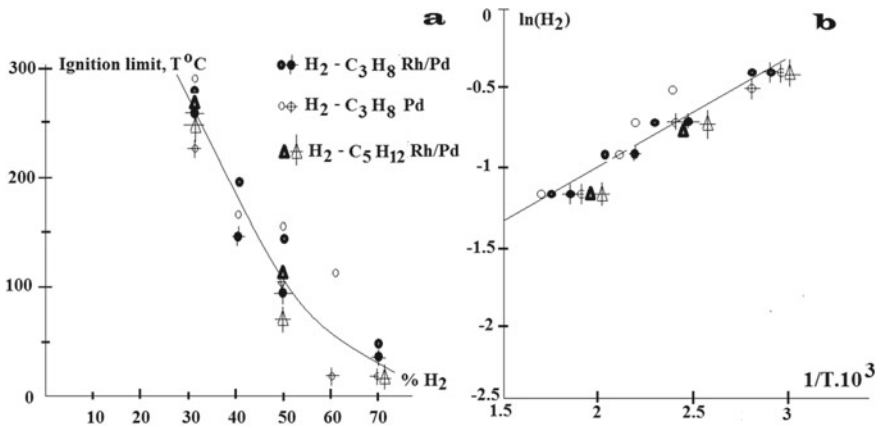

Fig. 4.9 **a** Experimental dependences of the temperature at "upper" and "lower" ignition limits of gas mixtures H_2–propane–air mix (filled circles, over Rh/Pd wire), H_2–propane–air mix (circles, over Pd wire) and H_2—n-pentane—air mix (triangles, over Rh/Pd wire) on H_2 content in the mixture. $P_0 = 1.7$ atm. Crosses on the symbols indicate "lower" catalytic ignition limits. **b** Arrhenius plots: dependences of "upper" and "lower" catalytic ignition limits of H_2–propane–air mix (filled circles, over Rh/Pd wire) on temperature; H_2–propane–air mix (circles, over Pd wire) on temperature; H_2–n-pentane–air mix (triangles, over Rh/Pd wire)

It was found that the values of delay periods of catalytic ignition of hydrogen–propane mixes weakly depend on initial temperature (Fig. 4.10).

This means that the delay period in this combustible mixture is determined by at least two processes, which can be qualitatively represented by the sum of two terms, one of which depends on the temperature and is determined by the proximity of the mixture to the catalytic ignition limit (a true delay period). The second one weakly depends on temperature, while this term is much larger than the first one. The second process, which weakly depends on temperature can be the diffusion of one of the reagents to (or within) the surface of the catalyst. The foregoing is evidence in favor of the following. These relatively long delay periods of catalytic ignition and the absence of their dependence on the initial temperature allow us concluding that the catalytic ignition of hydrogen—propane (n-pentane) mixes is determined by the process of transfer of hydrocarbon molecules to the surface of the catalytic wire either from the volume, or within the surface to some active center.

We briefly summarize the obtained results. It was shown that under conditions of our experiments not the chemical nature of the catalyst but that of C_2 hydrocarbon in the mix with H_2 is the determining factor of catalytic ignition. The catalytic ignition limits of synthesis gas over Rh/Pd are qualitatively different from the dependencies for combustible hydrogen-hydrocarbon: the "lower" catalytic limit dependence has a distinct maximum, which indicates a more complex mechanism of the catalytic process; the straight-line Arrhenius relation of ln $[H_2]_{lim}$ on $1/T$ is not fulfilled. Therefore, it is necessary to clarify the interpretation of the "upper" and "lower" limits of catalytic ignition given in the literature and take into account the adsorption of CO

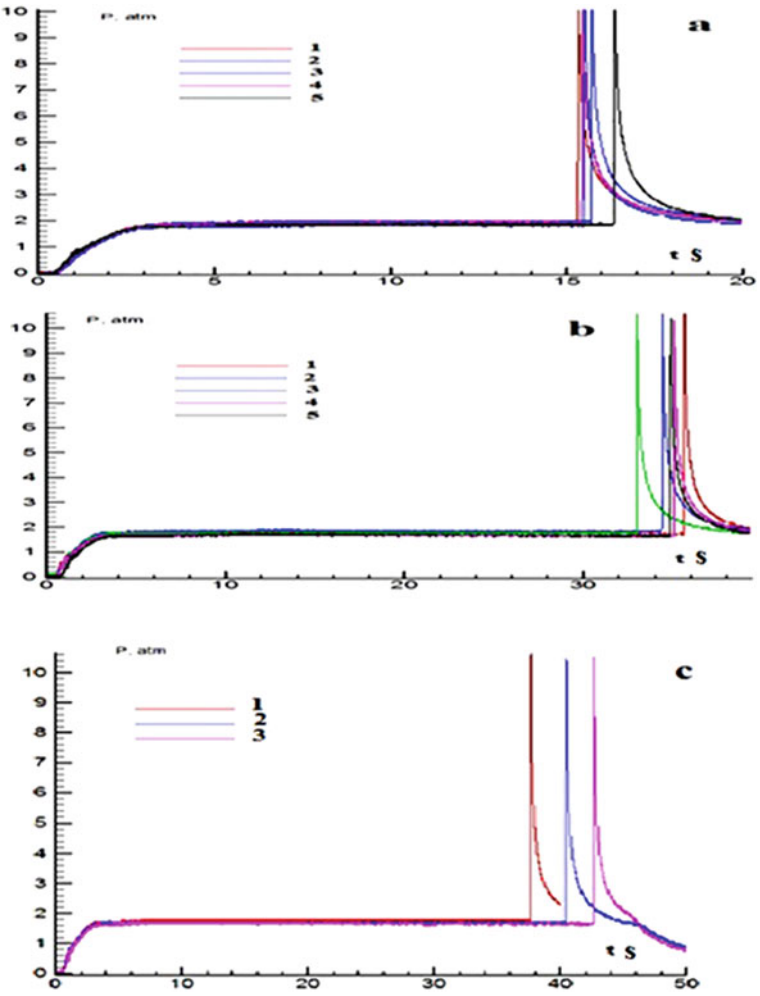

Fig. 4.10 Delay periods of catalytic ignition of hydrogen–propane and hydrogen–pentane mixes. **a** (50% H_2 + 50% $C_3H_8)_{stoich}$ + air over Rh, (1) T = 129.5 °C, (2) T = 125 °C, (3) T = 117.1 °C, (4) T = 111 °C, (5) T = 101 °C. **b** (60% H_2 + 40% $C_3H_8)_{stoich}$ + air over Rh, (1) T = 193.3 °C, (2) T = 185 °C, (3) T = 173.4 °C, (4) T = 165 °C, (5) T = 155 °C. **c** (50% H_2 + 50% $C_5H_{12})_{stoich}$ + air over Rh, 1 − T = 94.5 °C, (2) T = 79.7 °C, (3) T = 70.1 °C

molecules, initial hydrocarbons and combustion products on the catalytic surface. The relatively long delay periods of catalytic ignition of hydrogen—n-pentane mixes (tens of seconds) and the absence of the dependence of the periods on the initial temperature allow concluding that the catalytic ignition of hydrogen—propane/n-pentane mixes is determined by the transfer of the hydrocarbon molecules to (or within) the surface of the catalytic wire.

Thus, during the oxidation of hydrogen-hydrocarbon mixtures for methane, the main factor determining catalytic ignition is the reaction of hydrogen oxidation on the catalytic surface. With an increase in the number of carbon atoms in the hydrocarbon, the factors related to the chemical structure, that is, the reactivity of the hydrocarbon during catalytic oxidation, begin to play a significant role; and then the oxidation rate is already determined by the transfer of hydrocarbon molecules to the surface (or along the surface) of the catalyst.

4.4 The Features of Ignition of Hydrogen–Methane Mixes Over Pt at Low Pressures in a Constant Electric Field in the Absence of Discharge

The boundaries of ignition area may also be determined by the occurrence of a new solid phase during combustion, on which the reaction of chain termination can occur; in this case, for example, the boundaries of ignition area are narrowing. Thus, the possible role of charged particles at phase formation can be caused by the heterogeneous nature of processes with the participation of these particles.

As is well known, methane oxidation occurs in a dark on hot platinum wire as a catalyst [31]. This is of a great interest in the study of catalytic oxidation processes in view of the industrial applications in the near future. For instance, this is promising for use in electric power generation systems [32], for reducing methane emissions in mines [33], and for automobile emission control [34].

Noble metals can also catalyze reactions during chemical vapor deposition (CVD) in the synthesis of carbon nanostructures [35]. Cellular combustion regime of 40% H_2–air mixture in the presence of Pt wire over the interval 270–350 °C was observed for the first time in [17]. The regime is caused by the catalytic action of Pt containing particles (probably Pt oxides) formed by decomposition of volatile platinum oxide in gas phase. The ultra-disperse Pt-containing particles are emitted under heating according to [36]. The particles extending into the reactor volume by diffusion and convection act as catalytic centers.

Noble metals strongly impact on the flammability of hydrogen–methane blends. It was experimentally shown that the temperature of the ignition limit over Pd at P = 1.75 atm, measured with a bottom-up approach by temperature (when increasing temperature from a state of no ignition), of the mixtures 30% methane + 70% hydrogen + air ($\theta = 0.9$, T = 317 °C) markedly drops after subsequent ignitions to T = 270 °C for H_2–CH_4–air mix. The ignition limit returns to the initial value after treatment of the reactor with O_2 or air, i.e. a hysteresis phenomenon occurs [16]. It was shown that in the reactor, treated with ignitions, the ignition temperature of the mixture 70% H_2 + 30% methane with air over rhodium surface is 62 °C. The result indicates the potential of using rhodium catalyst to markedly lower the ignition temperature of the fuels based on hydrogen–methane mixtures (see Sect. 4.1 this chapter).

The critical condition for volume reaction is revealed: the ignition in the volume occurs at 45% H_2 + 55% CH_4, but it is missing at ≤ 40% H_2 + 60% CH_4. If H_2 ≤ 40%, only a slow dark reaction on the catalyst surface occurs. It is revealed that the effective activation energies of the catalytic ignition limits of H_2 + methane oxidation are (2.5 ± 0.6) kcal/mol; it means that the key reactions, responsible for the occurrence of ignition limits are almost certainly the same for both limits. It was shown that for Rh/Pd catalyst, the chain development process has most likely heterogeneous nature because the effective activation energy is < 3 kcal/mol (see Sect. 4.1 this chapter).

This paragraph focuses on experimental studies of low-pressure combustion of hydrogen–methane mixtures over Pt surface at total pressures from 20 to 180 Torr and initial temperatures of 400–600 °C in order to establish the dependencies of catalytic ignition limits over Pt surface on temperature and to reveal the features of hydrogen- methane mixes ignition over Pt in a constant electric field in the absence of discharge.

4.4.1 Experimental

The experiments were performed with previously prepared stoichiometric gas mixtures $2H_2 + O_2$, $(80\%\ H_2 + 20\%\ CH_4)_{stoich} + O_2$ (the stoichiometry was calculated for the sum of fuels. A quartz reactor 4 cm in diameter and 30 cm long was heated up with an electric furnace (Fig. 4.11); the temperature was controlled by a thermocouple. The accuracy of temperature measurements was ± 0.3 K. The reactor was supplied with an optical quartz window at its butt-end. The molybdenum electrode 1 mm in diameter and 40 cm long was placed along an axis of the reactor. The external cylindrical electrode 300 mm long made of copper foil was tight around the external surface of the reactor. A narrow loop of platinum wire 50 cm long and 0.3 mm in diameter was soldered to the end of the molybdenum electrode (Fig. 4.11).

Constant stabilized voltage 0 ÷ 1200 V from B5-24A power supply was applied to the internal electrode. Electrodes were connected via a capacitor (3 mF) and a resistor (50 kΩ), from which the signal was transmitted if necessary to A/D converter and

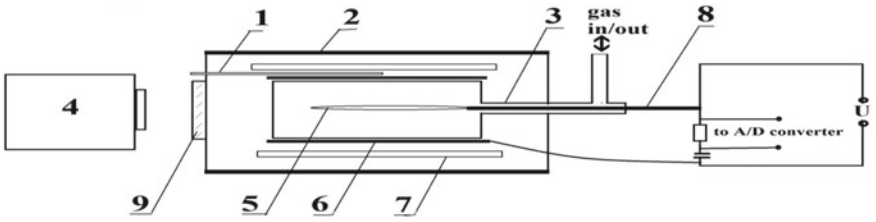

Fig. 4.11 Experimental installation: (1) thermocouple, (2) furnace, (3) reactor, (4) color speed video camera, (5) internal Pt electrode in the shape of a narrow loop, (6) external copper electrode, (7) isolating quartz cylinder, (8) internal Mo electrode, (9) optical window

was stored in computer memory exercising control of breakdown between electrodes. The reactor was used for studying thermal/catalytic ignition provided by Pt wire. A video recording was turned on at an arbitrary moment before gas inlet. A color high-speed camera Casio Exilim F1 Pro (frame frequency ÷ 1200 frames per second) was used. A video file was stored in computer memory and its time-lapse processing was performed. The pumped and heated reactor was filled with the gas mixture from a high-pressure buffer volume to necessary pressure. The ignition limit was measured at increasing pressure with a step 2 Torr until the ignition occurred (a bottom-up approach, when increasing pressure from a state of no ignition). Before each experiment, the reactor was pumped down to 10^{-2} Torr. Total pressure in the reactor was monitored with a vacuum gauge and the pressure in the buffer volume was monitored with a manometer. Chemically pure gases and 99.9% Pt were used.

The microstructures of carbon residues on Pt were examined using field emission, ultra-high resolution scanning electron microscope Zeiss Ultra Plus (Germany) equipped with an X-ray Microanalysis console INCA 350, Oxford Instruments.

4.4.2 Results and Discussion

Catalytic ignition areas (indicated with +) of 2 H_2 + O_2 and (80% H_2 + 20% $CH_4)_{stoich}$ + O_2 mixes over Pt wire are presented in Fig. 4.12 in pressure–temperature coordinates. As is seen in Fig. 4.12, the ignition limit pressures for both gas fuels do not depend on the applied voltage up to 1200 V.

In the case of (80% H_2 + 20% $CH_4)_{stoich}$ + O_2 mix, the catalytic ignition limit value first decreases with increasing temperature and then the ignition limit increases until the auto-ignition area takes the characteristic V-shape (Fig. 4.12). The V-shape is probably determined by the following. With an increase in temperature, the value of the ignition limit initially decreases due to the increasing rate of the activated volume branching step or the certain activated cycle of elementary steps [8]. As temperature increases further, the rate of the dark surface reaction increases resulting

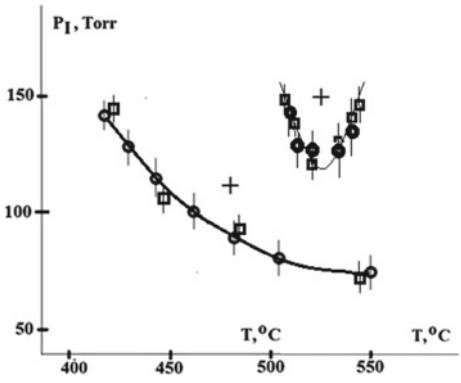

Fig. 4.12 Areas of catalytic ignition (indicated with + ; filled circles, 0 V; squares, 1200 V) over Pt wire: lower curve—2H_2 + O_2; upper curve (80% H_2 + 20% $CH_4)_{stoich}$ + O_2. The areas below the curves correspond to the dark reaction

in an increase in the degree of fuel conversion; thus, the fuel content of the mixture decreases and therefore the value of the ignition limit increases because the mixture becomes leaner.

However, the certain features of developed ignition depend on the applied voltage. In Fig. 4.13, typical frames of high-speed filming of the catalytic ignition of mixtures $2H_2 + O_2$ (a) and $(80\%\ H_2 + 20\%\ CH_4)_{stoich} + O_2$ (b, c) over Pt wire are presented at different values of applied voltage.

Note that the sequences of the frames of hydrogen catalytic ignition in the absence of a field and in the applied field do not differ. This means that the solid particles occurring during combustion, which are formed by decomposition of volatile platinum oxide in gas phase [17] to metallic Pt conduct electricity. It agrees with literature data [37], according to which α-PtO_2 is the n-type semiconductor with high electrical conductivity (as well as Pt itself).

From Fig. 4.13, one can estimate the relative visible propagation velocities of the flames in experiments a–c, by the time it takes the intensity of chemiluminescence to reach its maximum [8]. As is seen in Fig. 4.13, hydrogen flame (Fig. 4.13a) propagates at the highest velocity, since the maximum intensity of chemiluminescence is reached already at approximately the third frame. As is seen in Fig. 4.13 (b), the hydrogen–methane flame in the absence of an applied electrical field has a visible velocity less than the hydrogen flame (the maximum intensity of chemiluminescence is reached at approximately the fifth frame) in accordance with literature data [8] indicating that the methane-oxygen flames propagate at lower velocities than the hydrogen–oxygen flame.

From Fig. 4.13c, it can be seen that the application of an electric field (1200 V) leads to the disappearance of solid particles from the reaction volume, which indicates

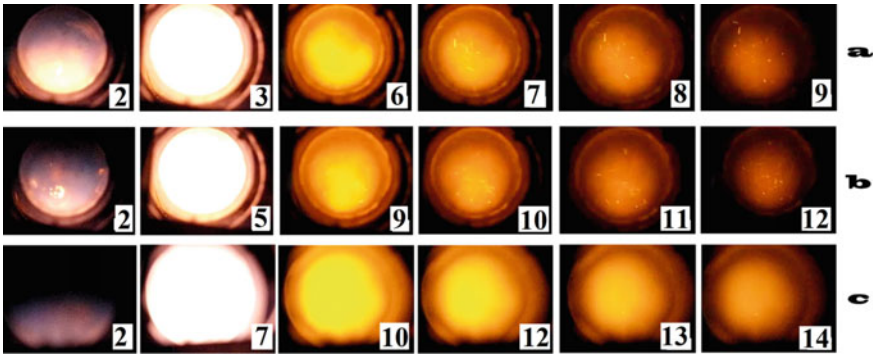

Fig. 4.13 **a** High-speed filming of the catalytic ignition of a 40% H_2 + air mixture over Pt wire. 1200 frames per second, $T_0 = 525$ °C, $P_0 = 135$ Torr. 1200 V applied. **b** High-speed filming of the catalytic ignition of a mixture $(80\%\ H_2 + 20\%\ CH_4)_{stoich} + O_2$ over Pt wire. 1200 frames per second, $T_0 = 525$ °C, $P_0 = 135$ Torr. 0 V applied. **c** High-speed filming of the catalytic ignition of a mixture $(80\%\ H_2 + 20\%\ CH_4)_{stoich} + O_2$ over Pt wire. 1200 frames per second, $T_0 = 525$ °C, $P_0 = 135$ Torr. 1200 V applied. The first frame corresponds to the moment of the occurrence of the flame

that these particles are charged. This may be due to the chemiionization phenomenon observed in the combustion of hydrocarbons [38]. For instance, positive ions and electrons formed in the flame front can be trapped by Pt-containing particles and the latter acquire a charge [39, 40].

As is also seen in Fig. 4.13c, the hydrogen–methane flame in the presence of an electrical field has a visible velocity even less than that in the absence of it (the maximum intensity of chemiluminescence is reached at approximately the seventh frame). At this point, we showed in [17] that Pt-containing particles extending into the reactor volume by mass transfer processes act as catalytic centers, on which the ignition occurs in the course of flame front propagation. Thus, if the electric field is applied, catalytic centers acquire a charge and are removed from the volume, which should lead to a decrease in the flame velocity.

Thus, the interpretation of the patterns given in Fig. 4.13 is in agreement with literature data.

The furher part of the work was aimed at the establishing morphology of the residue on the noble metal surface using the mix (80% H_2 + 20% $CH_4)_{stoich}$ + O_2 as the precursor. SEM analysis of the wire surface did not show any noticeable structures on the noble metal surface, both in ignition (140 Torr) and "dark" reaction (70 Torr) regimes of combustion of $(H_2 + CH_4)_{stoich} + O_2$ mix. The results of SEM investigation of the noble metal surface treated under conditions of both combustion regimes are shown in Fig. 4.14. The elemental analysis is given in Table 4.1.

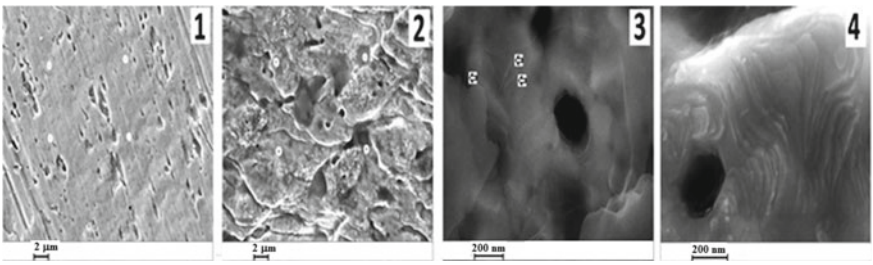

Fig. 4.14 (1) SEM micrograph of untreated Pt wire; (2) SEM micrograph of Pt wire treated with 20 ignitions of (80% H_2 + 20% $C_4H_8)_{stoich}$ + O_2 mix (P = 140 Torr) and 20 treatments with the dark reaction (P = 100 Torr), T = 530 °C; 3, 4—Micrograph 2 in higher magnification. White circles in micrographs 1, 2 indicate the points of analysis. Mean values are given in Table 4.1

Table 4.1 Surface elemental analysis of samples 1 and 2

Mean	1	4.05	6.25	10.29	79.41
Mean	2	41.55	13.12	6.80	38.53
Spectrum		C	Al	Cu	Pt

All results are given in atomic %
Processing option: All elements analysed (Normalized)

As is seen in Table 4.1, the surface of treated wire contains more carbon than untreated one. However, Fig. 4.13 (3, 4) shows that carbon nanotubes practically do not form, only perhaps very rarely (shown by the arrows in Fig. 4.13 (3)] as distinct from $(H_2 + C_4H_8)_{stoich} + O_2$ mix, in which the synthesis of carbon nanotubes proceeds in an efficient way in a "dark" regime (see Sect. 3.6, Chap. 3).

Notice that the untreated sample represents the surface with rolling marks [Fig. 4.13 (1)]. In the sample treated with ignitions, the defects in the form of openings develop [Fig. 4.13 (2–4)]. These defects focus on etching patterns; the etching substances are obviously active intermediates of H_2 oxidation, the similar etching was earlier observed for Rh, Ru and Pd surfaces [15] under their treatment with H_2 combustion.

We briefly summarize the results.

It was shown that the ignition limits of $2H_2 + O_2$ and $(80\%\ H_2 + 20\%\ CH_4)_{stoich} + O_2$ mixes over Pt wire do not depend on the applied voltage without discharge up to 1200 V.

It was shown that for $(80\%\ H_2 + 20\%\ CH_4)_{stoich} + O_2$ mixes the application of an electric field (1200 V) leads to the disappearance of Pt containing particles formed by decomposition of volatile platinum oxide in gas phase from the reaction volume, which indicates that these particles are charged. This may be due to the chemiionization phenomenon observed in the combustion of hydrocarbons.

It was shown that in combustion of $(80\%\ H_2 + 20\%\ CH_4)_{stoich} + O_2$ mix carbon nanotubes practically do not form as distinct from combustion of $(H_2 + C_4H_8)_{stoich} + O_2$ mix.

4.5 Conclusions

Experimental determination of ignition temperatures and effective activation energies of ignition of mixes $(40 \div 70\%\ H_2 + 60 \div 30\%\ CH_4)_{stoich}$ + air over Rh was performed at $1 \div 2$ atm over temperature range $20 \div 300$ °C under static conditions in order both, to establish catalytic effectiveness of Rh as a promising igniter, and to reveal the factors, which determine the values of effective activation energies and to find out whether NTC phenomenon exists in the ignition.

It was shown that in the reactor, treated with ignitions, the ignition temperature of the mixture 70% H_2 + 30% methane with air over rhodium surface is 62 °C. The result indicates the potential of using rhodium catalyst to lower markedly the catalytic ignition temperature of the fuels based on hydrogen–methane mixtures. The critical condition for volume ignition is revealed: the ignition in the volume occurs at 45% H_2, but it is missing at $\leq 40\%$ H_2. If $H_2 \leq 40\%$, only a slow surface reaction occurs; this phenomenon is qualitatively described by our earlier calculations. It is revealed that the effective activation energies both of "upper" and "lower" limits of H_2 + methane oxidation over the range of linearity are roughly equal (2.5 ± 0.6) kcal/mol; it means that the key reactions, responsible for the occurrence of "upper" and "lower" ignition limits are almost certainly the same. It was shown that for

Rh/Pd catalyst, the chain development process has most likely heterogeneous nature because the effective activation energy is < 3 kcal/mol. Experimental determination of ignition temperatures and effective activation energies of ignition of mixtures 5% ÷ 40% H_2–air over Rh and (30 ÷ 70% H_2 + 70 ÷ 30% C_2H_6 (and C_2H_4))$_{stoich}$ + air over Rh and Pd at 1 atm was performed over temperature range 20–300° under static conditions in order to compare catalytic effectiveness of Rh and Pd and to establish the factors that determine the values of effective activation energies. It was shown that the obtained values of effective activation energy are in mutual agreement and are characteristic of the surface nature of Rh action; Rh is more catalytically active than Pd. The key features of catalytic ignition on metallic rhodium and palladium in a series of mixed fuels: namely hydrogen + synthesis gas and hydrogen + hydrocarbon (ethane, ethylene, propane, pentane) + air were identified to establish the boundaries of catalytic ignition regions, dependencies of effective ignition activation energies on the nature of hydrocarbon, and the role of dark oxidation processes. It was shown that under conditions of our experiments not the chemical nature of the catalyst but that of C_2 hydrocarbon in the mix with H_2 is the determining factor of catalytic ignition. The catalytic ignition limits of synthesis gas over Rh/Pd are qualitatively different from the dependencies for combustible hydrogen-hydrocarbon: the "lower" catalytic limit dependence has a distinct maximum, which indicates a complex mechanism of the catalytic process; Arrhenius dependence of ln $[H_2]_{lim}$ on $1/T$ could not be applied. Therefore, the interpretation of the "upper" and "lower" limits of catalytic ignition given in the literature should be cleared up. In our opinion, both for the synthesis gas and hydrocarbons with longer chains, due to the different adsorption capacity of fresh and ignition-treated rhodium hydride with respect to CO molecules, initial hydrocarbons and combustion products must be taken into account to describe the behavior of catalytic ignition limits. Long delay periods of catalytic ignition of hydrogen–n-pentane mixes (tens of seconds) and the absence of the dependence of the periods on the initial temperature allow us concluding that the catalytic ignition of hydrogen–n-pentane mixes is determined by the transfer of the molecules of the hydrocarbon blend to the surface of the catalytic wire. Thus, in the oxidation of hydrogen-hydrocarbon blends for methane, the main factor determining catalytic ignition is the oxidation reaction of hydrogen on the catalytic surface. With an increase in the number of carbon atoms in the hydrocarbon, the factors associated with the chemical structure, that is, the reactivity of the hydrocarbon in catalytic oxidation, begin to play a significant role; and then the oxidation rate is already determined by the processes of transfer of the hydrocarbon molecules to (or within) the catalyst surface.

Experimental studies of low-pressure combustion of hydrogen–methane mixtures were carried out over Pt surface at total pressures from 20 to 180 Torr and initial temperatures of 400–600 °C in order to establish the relationships of catalytic ignition limits over Pt on temperature and to reveal the features of ignition of hydrogen-methane mixes over Pt in a constant electric field in the absence of discharge. It was shown that the ignition limits of $2H_2 + O_2$ and (80% H_2 + 20% CH_4)$_{stoich}$ + O_2 mixes over Pt wire do not depend on the applied voltage without discharge up to 1200 V. We showed that for (80% H_2 + 20% CH_4)$_{stoich}$ + O_2 mixes the application

of an electric field (1200 V) leads to the disappearance of Pt containing particles formed by decomposition of volatile platinum oxide in gas phase from the reaction volume, which indicates that these particles are charged. This may be due to the chemiionization phenomenon observed in the combustion of hydrocarbons. Is was shown that in combustion of $(80\%\ H_2 + 20\%\ CH_4)_{stoich} + O_2$ mix carbon nanotubes practically do not form as distinct from $(H_2 + C_4H_8)_{stoich} + O_2$ mix.

References

1. B. Nagalim, F. Duebel, K. Schmillen, Performance study using natural gas, hydrogen-supplemented natural gas and hydrogen in AVL research engine. Int. J. of Hydrogen Energy **8**, 715 (1983)
2. A.A. Korzhavin, P.K. Senachin, Osnovi teorii gorenia, (Fundamentals of combustion theory) (Polzunov Altai State Technical University, Voevodsky Institute of Chemical Kinetics and Combustion, 2014). http://elib.altstu.ru/eum/download/dvs/Korjavin-otg.pdf
3. V.A. Bunev, V.S. Babkin, A.V. Baklanov, V.V. Zamashikov, I.G. Namyatov, Selective oxidation of hydrogen in rich hydrogen–methane–air flames. Combustion, Explosion and Shock Waves **43**, 493 (2007)
4. S.O. Akansu, Z. Dulger, N. Kahranman, N.T. Veziroglu, Internal combustion engines fueled by natural gas—hydrogen mixtures. Int. J. Hydrogen Energy **29**, 1527 (2004)
5. F. Ma, S. Ding, Y. Wang, Y. Wang, J. Wang, S. Zhao, Study on combustion behaviors and cycle-by-cycle variations in a turbocharged lean burn natural gas SI engine with hydrogen enrichment. Int. J. Hydrogen Energy **33**, 7245 (2008)
6. F.E. Lynch, R.W. Marmaro, U.S. Patent 5139002A, 18 Aug 1992
7. F. Ma, H. Liu, Y. Wang, J. Wang, S. Ding, S. Zhao, Effects of combustion phasing, combustion duration, and their cyclic variations on Spark-Ignition (SI) engine efficiency, SAE Paper 2008-01-1633 (2008)
8. B. Lewis, G. Von Elbe, *Combustion, Explosions and Flame in Gases* (Acad. Press, New York, London, 1987)
9. K. Persson, L.D. Pfefferle, W. Schwartz, A. Ersson, S.G. Jaras, Stability of palladium-based catalysts during catalytic combustion of methane: the influence of water. Appl. Catal. B: Environmental **74**, 242 (2007)
10. A. Fernández, G.M. Arzac, U.F. Vogt, F. Hosoglu, A. Borgschulte, M.C.J. Jiménez de Haro, O. Montes, A. Züttel, Investigation of a Pt containing washcoat on SiC foam for hydrogen combustion applications. Appl. Catal. **180**, 336 (2016)
11. N.M. Rubtsov, V.I. Chernysh, G.I. Tsvetkov, K.Y. Troshin, O.I. Shamshin, Ignition of hydrogen-methane-air mixtures over Pd foil at atmospheric pressure. Mendeleev Commun. **29**, 469 (2019)
12. N.M. Rubtsov, V.I. Chernysh, G.I. Tsvetkov, K.Y. Troshin, O.I. Shamshin, The features of hydrogen ignition over Pt and Pd foils at low pressures. Mendeleev Commun. **28**, 216 (2018)
13. N.M. Rubtsov, V.I. Chernysh, G.I. Tsvetkov, K.Y. Troshin, I.O. Shamshin, The phenomenon of negative temperature coefficient in palladium-initiated combustion of hydrogen–propane–air mixtures. Mendeleev Commun. **31**, 274 (2021)
14. N.M. Rubtsov, B.S. Seplyarski, M.I. Alymov, *Initiation and Flame Propagation in Combustion of Gases and Pyrophoric Metal Nanostructures* (Springer Nature Switzerland AG, 2021)
15. N.M. Rubtsov, G.I. Tsvetkov, V.I. Chernysh, K.Y. Troshin, Features of hydrogen and deuterium ignition over noble metals at low pressures. Comb. Flame **218**, 179 (2020)
16. A.P. Kalinin, N.M. Rubtsov, A.N. Vinogradov, V.V. Egorov, N.A. Matveeva, A.I. Rodionov, A.Y. Sazonov, K.Y. Troshin, G.I. Tsvetkov, V.I. Chernysh, Ignition of hydrogen-hydrocarbon (C1–C6)–air mixtures over the palladium surface at 1–2 atm. Russ. J. Phys. Chem. B **14**, 413 (2020)

17. N.M. Rubtsov, A.N. Vinogradov, A.P. Kalinin, A.I. Rodionov, K.Y. Troshin, G.I. Tsvetkov, V.I. Chernysh, Cellular combustion and delay periods of ignition of a nearly stoichiometric H_2–air mixture over a platinum surface. Mendeleev Commun. **26**, 160 (2016)
18. N.M. Rubtsov, V.I. Chernysh, G.I. Tsvetkov, K.Y. Troshin, I.O. Shamshin, Surface modes of catalytic ignition of flammable gases over noble metals. Mendeleev Commun. **32**, 564 (2022)
19. T. Alasard, Low Mach number limit of the full Navier-Stokes equations. Arch. Ration. Mech. Anal. **180**, 1 (2006)
20. V. Akkerman, V. Bychkov, A. Petchenko, L.-E. Eriksson, Accelerating flames in cylindrical tubes with nonslip at the walls. Comb. Flame **145**, 206 (2006)
21. E.-S. Cho, S.H. Chung, Improvement of flame stability and NO_x reduction in hydrogen-added ultralean premixed combustion. J. Mech. Science and Technology **23**(3), 650 (2009). https://doi.org/10.1007/s12206-008-1223-x
22. H. Razali, K. Sopia, S. Mat, Green fuel: 34% reduction of hydrocarbons via hydrogen (Al+HCl) blended with gasoline at maximum torque for motorcycle operation. ARPN Journal of Engineering and Applied Sciences **10**(17), 7780 (2015)
23. N.M. Rubtsov, *The Modes of Gaseous Combustion* (Springer International Publishing, 2015)
24. Engineering ToolBox, Coefficients of Linear Thermal Expansion (2003) https://www.engineeringtoolbox.com/linear-expansion-coefficients-d_95.html
25. S.M. Repinski, Vvedenie v himicheskuyu fiziky poverhnosti tvyordych tel (Introduction into chemical physics of the surface of solids) (Novosibirsk:; "Nauka", Sibir publishing company, 1993)
26. N.N. Semenov, *O nekotorych problemah himicheskoi kinetiki i reaktsionnoi sposobnosti, (On some problems of chemical kinetics and reaction ability)* (Academy of Sciences of the USSR, Moscow, 1958)
27. C. Appel, J. Mantsaras, R. Schaeren, R. Bombach, A. Inauen, Catalytic combustion of hydrogen–air mixtures over platinum: validation of hetero-homogeneous reaction schemes. Clean Air **5**, 21 (2004)
28. IAEA safety standards series. Design of reactor containment systems for nuclear power plants safety guide no. NS-G-1.10 (2004)
29. R. Horn, K. Williams, N. Degenstein, A. Bitschlarsen, D. Dallenogare, S. Tupy et al., Methane catalytic partial oxidation on autothermal Rh and Pt foam catalysts: oxidation and reforming zones, transport effects, and approach to thermodynamic equilibrium. J Catal. **249**, 380 (2007)
30. N.M. Rubtsov, V.I. Chernysh, G.I. Tsvetkov, K.Y. Troshin, I.O. Shamshin, The features of ignition of hydrogen–methane and hydrogen–isobutene mixtures with oxygen over Rh and Pd at low pressures. Mendeleev Commun. **32**, 405 (2022)
31. H. Davy, Some new experiments and observations on the combustion of gaseous mixtures with an account of a method of preserving a continuous light in mixtures of inflammable gases and air without flame. Phil. Trans. R. Soc. London A **107**, 77 (1817)
32. J.M. Herreros, S.S. Gill, I. Lefort, A. Tsolakis, P. Millington, E. Moss, Enhancing the low temperature oxidation performance over a Pt and a Pt-Pd diesel oxidation catalyst. Appl. Catal. B Environ **147**, 835 (2014)
33. V. Dupont, S.-H. Zhang, A. Williams, Catalytic and inhibitory effects of Pt surfaces on the oxidation of $CH_4/O_2/N_2$ mixtures. Chem. Eng. Science **56**, 1291 (2001)
34. D.J. Worth, M.E.J. Stettler, P. Dickinson, K. Hegarty, A.M. Boies, Characterization and evaluation of methane oxidation catalysts for dual-fuel diesel and natural gas engines. Emiss. Control Sci. Technol. **2**, 204 (2016)
35. Z.A.C. Ramli, S.K. Kamarudin, Platinum-based catalysts on various carbon supports and conducting polymers for direct methanol fuel cell applications: a review. Nanoscale Res. Lett. **13**, 410 (2018)
36. J.C. Chaston, Reaction of oxygen with the platinum metals. The oxidation of platinum. Platinum Met. Rev. **8**, 50 (1964)
37. N.P. Ivanova, I.A. Velikanova, P.B. Kubrack , Ehlektroximicheskii-sintez (Elecrtrochemical Synthesus) (Minsk, BGTU, 2011) elib.belstu.by ehlektroximicheskii-sintez-n.p.-ivanova-i.a.-velikanova-p.b.-kubrak.pdf

38. H.F. Calcote, R.J. Gill, Development of the chemical kinetics for an ionic mechanisms of soot formation in flames, in *Proceedings of Zel'dovich Memorial International Conference on Combustion*, Moscow, 2, 16 (1994)
39. J. Lahaye, G. Prado, Formation of carbon particles from a gas phase: nucleation phenomenon. Water Air Soil Pollut. **3**, 473 (1974)
40. N.M. Rubtsov, B.S. Seplyarskii, V.I. Chernysh, G.I. Tsvetkov, Yu.A. Gordopolov, V.E. Fortov, Formation of liquid and solid dusty crystals in gas-phase combustion reactions. EPL **97**, 15003 (2012)

Chapter 5
Features of Interaction of the Surfaces of Noble Metals with Propagating Flame Front

Abstract This chapter is focused on the features of interaction of the surfaces of noble metals with a propagating flame front. It was shown that a flame propagation process in a conditional room containing an indoor space with two openings and a flammable material inside shows a wide variety of combustion modes depending on the geometry of this complex volume. Preliminary numerical calculation of the expected flame propagation patterns may not always be successful, a real experiment under laboratory conditions, assuming the possibility of scaling the process, seems to be the most informative one. The investigation into Pt behavior in the flame of methane combustion under conditions of turbulent flow was performed. We revealed that under certain conditions Pt catalyst can suppress combustion and thereby show the opposite effect due to the high efficiency of Pt surface coated with a Pt oxide layer in the reaction of chain termination. Therefore, kinetic factors could be the determining even under conditions of high turbulence. It was shown that the rate of chain termination determines the value of the critical diameter for flame penetration through Pt or Pd cylinders; the efficiency of Pd surface in chain termination reaction is much greater than that of Pt.

Keywords Flame propagation · Rhodium · Palladium · Platinum · Combustion · Methane · Oxygen · Air · Obstacle · Complex geometry · Turbulence

The influence of the obstacles located in different volumes, filled with combustible mixture, on the propagation of flame front (FF) is investigated for a long time. These researches were performed to find out both the dependence of combustion regime on the type of obstacles and possibility to influence on combustion regimes by varying obstacle shape. In our investigations, the obstacle material is also varied. It is known that if the composition of a gas mixture is far from concentration limits of ignition then the velocity of flame propagation in the presence of obstacles can quickly increase to supersonic values. On studying the quickly accelerated flames, it is possible to observe DDT (deflagration to detonation transition), however, the velocity of supersonic combustion wave in the presence of obstacles is often below Chapman–Jouquet velocity. Therefore, from the practical point of view the most prominent aspect in the investigation of accelerated flames is caused by problems of engines operation or

N. M. Rubtsov et al., *Catalytic Ignition of Hydrogen and Hydrogen-Hydrocarbon Blends Over Noble Metals*, Heat and Mass Transfer,
https://doi.org/10.1007/978-3-031-28416-8_5

explosion safety and connected mainly with transition of fast combustion to nonstationary quasi-detonation regimes, which destructive influence is more effective than in Chapman–Jouquet regime. It is necessary to notice that influence of obstacles, can manifest themselves doubly: in the maintenance of detonation wave as a result of reflections of shock waves and in quenching of detonation wave as a result of heat losses. It is possible to transfer the previously mentioned to an initial stage of flame acceleration, namely to the moment when the laminar flame meets an obstacle; that is the subject of the present Chapter. This interaction causes the development of flame instability, promoting its acceleration. On the other hand, the contact of FF with a reactor surface leads to an increase in the contribution of heterogeneous reactions, in particular, chain termination. This should promote flame suppression. This ambiguous mechanism of the action of obstacles underlies that physical means of detonation suppression (nets, nozzles, etc.) is not always effective.

The contributions of both of these processes are also determined by the geometry of the confinement, in which the flame propagates and the material of the obstacle, with which the flame interacts.

The purpose of this Chapter was to establish the gas-dynamic and kinetic features of the penetration of methane-oxygen flames through obstacles of various geometries and materials (including noble metals) using high-speed filming.

5.1 Propagation of Laminar Flames of Natural Gas-Oxygen Mixtures in the Volumes of Complex Geometry

Combustion processes in large volumes have attracted great interest in recent decades. Tests in large volumes are performed to characterize the explosion and detonation characteristics of hydrogen-air and hydrogen–oxygen mixtures. Most of the existing experiments use shock tubes for these types of explosions. A small part of these works is devoted to experiments in spherical geometry [1, 2]. However, the large scale transfer of small fire tests emerges as the major problem encountered by researchers. Therefore, it is difficult to predict and anticipate the development of a full-scale fire. To solve this problem, the development of an approach combining experiments and modeling is necessary. Moreover, multi-scale analysis is a required strategy [3].

At the same time, one can conclude from existing publications that modeling, and, accordingly, understanding ignition and combustion in large volumes in the presence of mesh and other obstacles, is still at an early stage. In particular, this is due to the lack of experimental data because of the cost and danger of creating large-scale experimental stands.

As is shown in [4], propagation velocities of the spherical combustion front within the framework of the acoustic approximation of the reactive Navier–Stokes equations for a compressible medium taking into account the chain reaction mechanism, are practically the same both for a small scale and for large one. This means that for subsonic flames one should not probably expect the manifestation of scale effects.

However, the exception can be thermoacoustic instabilities of the spherical flame front in lean hydrogen–air mixtures while in the process of flame propagation, long-wave disturbances arise, which are excited noticeably later than the moment when the flame front touches the side walls of the small laboratory reactor. The data obtained in [5] are an argument in favor of the existence of a large-scale effect when this type of instability occurs.

As is seen from above, one can expect the lack of the large-scale effect in subsonic combustion of stoichiometric hydrocarbon-oxidizer mixtures. Therefore, taking into account the fact that the multi-scale analysis is the required strategy, the experiments on the propagation of combustion waves in methane-oxygen mixtures in the volumes of the laboratory scale of complex geometry were performed. The experimental data are qualitatively illustrated on the basis of the reactive Navier–Stokes equations for a compressible medium taking into account the chain reaction mechanism. The results must be important for the modeling of explosion safety problems for volumes of complex geometry.

The paragraph is aimed at establishing the regimes of penetration of a flame front of the diluted methane-oxygen mixture through obstacles in the volumes of complex geometry in the laboratory scale installation.

5.1.1 Experimental

The experiments were performed with stoichiometric methane-oxygen mixes diluted with CO_2 and Kr at initial pressures of 100–200 Torr and 298 K in the horizontally located cylindrical quartz reactor of 70 cm in length and of 14 cm in diameter. A spark ignition electrode was located near the left butt-end of the reactor (Fig. 5.1).

The reactor was fixed in two stainless steel gateways at butt-ends, supplied with inlets for gas pumping and blousing and a safety shutter, which swung outward when the total pressure in the reactor exceeded 1 atm [6]. The obstacles shown in the Fig. 5.1 were placed inside the reactor. These included a plastic cone with the cone hole $d = 40$ mm directed towards the propagating flame front, and 110 mm long (Fig. 5.1a), and a plastic cone with the cone hole $d = 40$, 110 mm long and a hole on the cone generator; the Rh/Pd spiral was placed at the cone point (Fig. 5.1b). In the paragraph, plastic cylinders 110 mm long and diameters $d = 25$, 40, 50, 60, 110 mm (Fig. 5.1c) and a plastic cylinder $d = 40$ mm with a hole on the generatrix of the cylinder were used; the Rh/Pd spiral was placed at the butt-end of the cylinder (Fig. 5.1d). Rh sample was made by electrochemical deposition of Rh layer 15 μm thick on Pd wire (0.3 mm thick 80 mm long).

A combustible mixture (15.4% CH_4 + 30.8% O_2 + 46% CO_2 + 7.8% Ar) was prepared prior to experiment; CO_2 was added to decrease a flame front velocity and to enhance the quality of filming; Ar was added to diminish the discharge threshold. The reactor was filled with the mixture up to necessary pressure. Then, spark initiation was performed (the discharge energy was 1.5 J). Speed filming of ignition dynamics and flame front propagation was carried out from the side of the reactor with a Casio

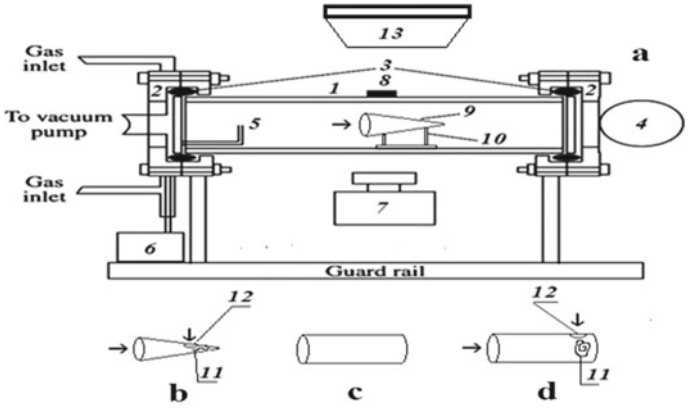

Fig. 5.1 **a** experimental installation. (1) quartz reactor, (2) stainless steel gateway, (3) silicone laying, (4) stainless steel shutter, (5) spark electrodes, (6) discharge power supply, (7) high-speed color movie camera, (8) microphone, (9) hollow cone, (10) fastening element, (11) Rh/Pd wire coil, (12) hole, (13) rotary mirror; **b** a hollow cone with a hole and Rh/Pd wire coil inside; **c** a hollow cylinder; d- a hollow cone with a hole and Rh/Pd wire coil inside

Exilim F1 Pro color high-speed digital camera (frames frequency of 600 s^{-1}) [7]. The video file was stored in computer memory and its time-lapse processing was performed [7]. The pressure change in the course of combustion was recorded by a piezoelectric gage synchronized with the discharge. The reagents of chemically pure grade and 99.85% Pd were used.

5.1.2 Results and Discussion

Figure 5.2 shows the results of high-speed filming of flame propagation in the hollow cylinder (Fig. 5.2a) and cone (Fig. 5.2b) located in the larger reactor. As is seen in (Fig. 5.2a, b) the flame propagation in both the hollow cylinder and the cone occurs similar to the flame propagation in the larger cylinder, namely the flame reaches the end of the cylinder (or the tip of the cone) and the end of the larger cylinder almost simultaneously. In addition, in the hollow cylinder and in the larger cylinder, the gas dynamic instability ("tulip flame" [8]) also arises simultaneously.

In the hollow cone, this instability is missing. As is seen in (Fig. 5.2c), the visible flame velocity V_v (determined from the dependence of a flame front position on a frame number) does not depend on the diameter of the hollow cylinder. It means that the rates of both, heat losses and heterogeneous chain termination are relatively small. Notice that the V_v value in the hollow cone (85 cm/s) is less than that for the hollow cylinder (112 cm/s) indicating greater contribution of the losses of both types during flame propagation in the cone. Notice that the value of the flame velocity in the

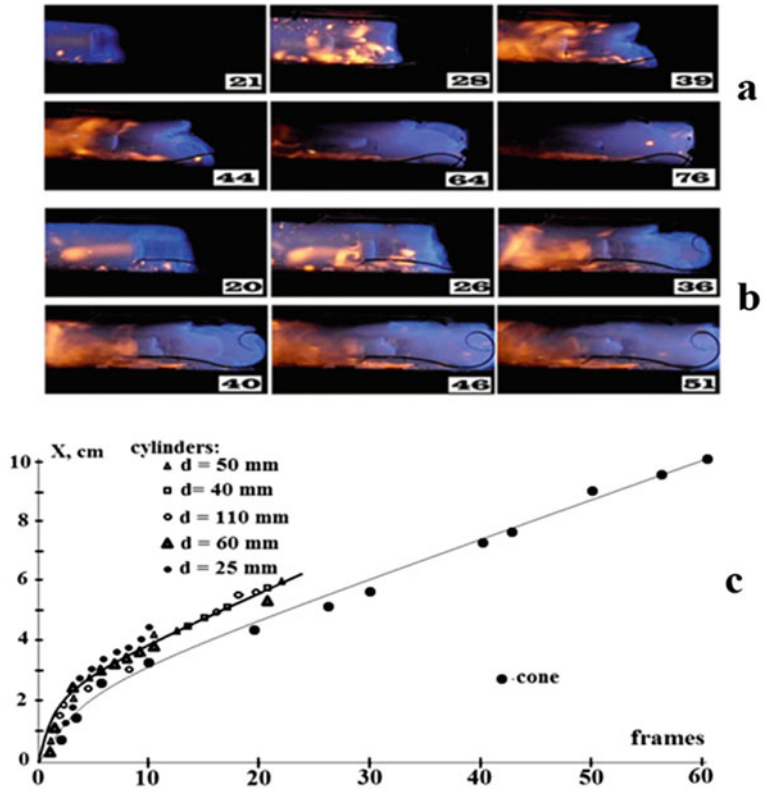

Fig. 5.2 High-speed filming of a flame front propagation in **a** hollow cone, **b** hollow cylinder. **c** dependence of a flame front position on a frame number. $T_0 = 298$ K. $P_0 = 170$ Torr. The figure on each frame corresponds to the frame number after discharge

hollow cylinder is close to the experimental value for the $CH_4 + O_2$ stoichiometric mixture + 40% CO_2 [9].

In (Fig. 5.3a), the frames of high-speed filming of flame propagation in a hollow cone with a hole and Rh/Pd wire coil inside (Fig. 5.1b) are presented. Such geometry allows observing the propagation of counter flames in the hollow cone. In the experiment, one of the flames (on the left) is initiated by the initial flame front, the second one (on the right) arises at the top of the hollow cone when initiated by an external flame through a hole in the presence of a Rh/Pd catalyst: in the absence of the latter, the counter flame does not occur.

In (Fig. 5.4a), the frames of high-speed filming of flame propagation in a hollow cylinder with a hole and Rh/Pd wire coil inside (Fig. 5.1d) are shown. Such geometry provides a generation of the vortex ring from reaction products (the vortex ring propagation is highlighted by white curcles) under same conditions (instead of counter flames, occurring in the hollow cone), which arises at the butt-end of the hollow cylinder (on the left) being initiated by an external flame through a hole in

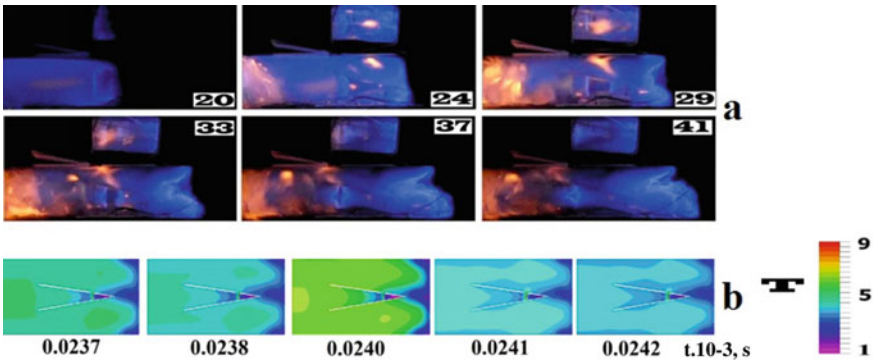

Fig. 5.3 **a** High-speed filming of a flame front propagation in a hollow cone with a hole and Rh/Pd wire coil inside (b, Fig. S1). $T_0 = 298$ K. $P_0 = 170$ Torr. The figure on each frame corresponds to the frame number after discharge. **b** Results of calculation of the change in dimensionless temperature for flame in a hollow cone with a hole and Rh/Pd wire coil inside

the presence of a Rh/Pd catalyst: in the absence of the latter, the vortex ring does not occur.

In Fig. 5.5, the frames of high-speed filming of flame propagation in a hollow cylinder (d = 25 mm) with a hole and Rh/Pd wire coil inside (Fig. 5.1d) are presented. As is seen in the Figure, a blue flame front propagates from the left to the right, then the catalyst initiates a yellow flame, which propagates in the opposite direction. As is known, the flame front in a hydrocarbon-air mixture in a heated cylindrical reactor is always of yellow color (so-called "hot" flame, [4, 10]), although the flame at the

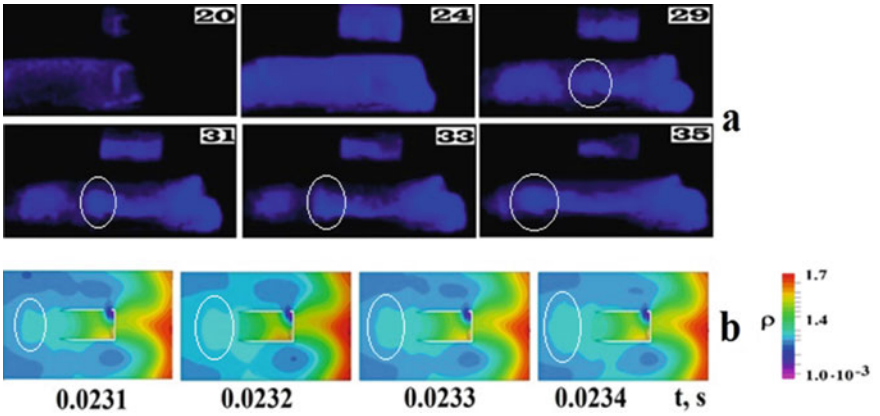

Fig. 5.4 **a** High-speed filming of a flame front propagation in a hollow cylinder with a hole and Rh/Pd wire coil inside (Fig. 5.1d). $T_0 = 298$ K. $P_0 = 170$ Torr. The figure on each frame corresponds to the frame number after discharge. The vortex ring propagation is highlighted by white circles. **b** Results of calculation of the change in dimensionless density for flame in a hollow cylinder with a hole and Rh/Pd wire coil inside. The vortex ring propagation is highlighted by white circles

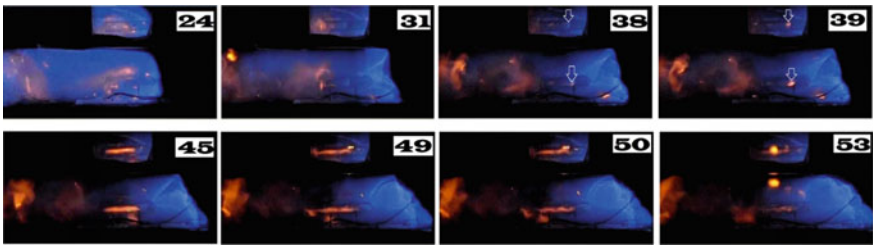

Fig. 5.5 High-speed filming of a flame front propagation in a hollow cylinder d = 20 mm with a hole and Rh/Pd wire coil inside (Fig. 5.1d). $T_0 = 298$ K. $P_0 = 170$ Torr. The figure on each frame corresponds to the frame number after discharge. The arrows indicate the occurrence of the ignition center on the surface of Rh/Pd wire

initial room temperature in the same mixture and in the same reactor is of blue color ("cold" flame, [4, 10]). The color of the flame is due to the emission of CH (431 nm) and, possibly, CH_2O (470 nm) radicals. The yellow color of the hot flame is caused by the emission of excited Na atoms or a lack of an oxidizing agent, i.e. the formation of soot [10]. A block of reactions of hydrocarbon oxidation to CO is considered [10] to be realized in a "blue", "cold" flame, and in a "yellow", "hot" flame, the next block of reactions of CO oxidation to CO_2 is realized. The result obtained means that the technique used allows one to separate in time and space the "cold" and "hot" flames in a single experiment. The result obtained is also important for the verification of numerical models of methane combustion.

Notice that the given example of combustion of a methane-air mixture in a complex volume does not even make it possible to qualitatively predict the behavior of the flame front and reaction products; it is obvious that there can be no question of achieving any quantitative agreement between calculation and experiment.

We attempted to qualitatively take into account the main factors in consideration of the ignition with catalytically heated wire [11] using compressible dimensionless reactive Navier–Stokes equations in low Mach number approximation [4, 12–14] see also Sect. 2.5 Chap. 2. The reaction velocity in the volume was presented by an elementary chain mechanism: $C \rightarrow 2n$ (w_0) and $n + C \rightarrow 3n +$ products. In this case, the simple Arrhenius equation, as in [4] and Sect. 2.5 Chap. 2, Appendix, set (2) was replaced with the following ones:

$$\rho\left[C_t + v\,C_y + u\,C_x\right] = \Delta^2 C - \beta_0 n\,W$$
$$\rho\left[n_t + v n_y + u n_x\right] = \Delta^2 n + 2\beta_0 n\,W$$

$$W = C \exp\left(\zeta - \zeta/T\right) \quad \text{volume reaction}$$
$$W_1 = C \exp\left(\varsigma_1 - \varsigma_1/T\right) \quad \text{surface reaction}$$

β_0 is a kinetic coefficient proportional to Damköhler number.

The catalytic wire was simulated by a rectangular region below the side opening in the hollow cone (Fig. 5.3c) or cylinder (Fig. 5.4c). Chemical exothermic chain propagation (without branching, but with the preservation of free valences) reaction occurred on the boundaries of the region, boundary conditions on the "wire" took the form similar to Sect. 2.5 Chap. 2, Appendix.

$T_t = \alpha\delta\beta_1 W_1$ (heat release; β_1 characterizes specific heat release, $\alpha = 1$ for homogeneous surface), $n_t = \alpha\delta\beta_0 W_1$ (surface propagation), $C_t = 0.2C$ (adsorption of the initial reagent); δ scale coefficient, which determined only the duration of the calculations. On the reactor walls $n = 0$ (heterogeneous chain termination), $u = 0$, $v = 0$, $\rho_x = 0$, $C_x = 0$, $T_x = T_0$ where x is the dimensionless coordinate (a subscript means partial derivative with respect to time t or abscissa x). The parameters were assumed to be $\zeta = 7.5$ (close to effective activation energy of the branching reaction of volume oxidation), $\zeta_1 = 1.5$ (the estimate of the value of activation energy of a surface process [15]), $\beta = 0.15$, $\beta_1 = 0.22$. Initiation condition was taken as $T = 10$ on the left boundary of the rectangular channel, in which a hollow cone or cylinder were located.

The solution of the problem was carried out by finite element analysis using a software package FlexPDE 6.08, 1996–2008, PDE Solutions Inc. [16]. The results of the calculation are shown in (Figs. 5.2c and 5.3c). As is seen in the Figures, the qualitative model allows to describe the main features of a flame front propagation in a hollow cone and cylinder with a hole and Rh/Pd wire coil inside, for instance, a generation of a vortex ring in case of the hollow cylinder.

However, a more detailed methane combustion mechanism is required to describe the occurrence of the hot flame shown in Fig. 5.5.

Thus, it can be concluded that an exemplary flame propagation process in a conditional confinement containing an indoor space with two openings and a flammable material inside shows a wide variety of combustion modes depending on the geometry of this complex volume. As is seen from above, the preliminary numerical calculation of the expected flame propagation patterns may not always be successful. Thus, a real experiment under laboratory conditions, assuming the possibility of scaling the process, seems to be the most informative one.

5.2 Experimental Investigation into the Interaction of Chemical Processes on Pt Wire and Reactive Flows at Flame Penetration Through Obstacles in the Presence of Iron Nanopowder

In the previous paragraph, we showed that a model of a flame propagation process in a conditional confinement containing a room with two openings and a flame initiating material inside provides a wide variety of combustion regimes depending on the geometry of this complex volume, i.e. gas dynamic factors play a decisive role. It means that ab initio numerical calculation of the flame propagation patterns

is successful with a low probability. Thus, it is necessary to rely on the results of experiments at least under conditions of a laboratory model installation and then interpret the obtained results taking into account the possibility of further scaling. The problems of flame interaction with catalytic surfaces, in which gas-dynamic factors play a very important role, are discussed below.

In 1818 Sir Humphrey Davy discovered that methane and oxygen on hot platinum wires can produce a considerable amount of heat in a dark reaction [17]. The interest in the catalytic oxidation process and its corresponding reaction systems has been increasing because of the wide potential applications of this technology in the usage of the catalytic combustion both in the power generation systems [18–20], and in reduction fugitive methane levels [21]; in the use of catalytic converters in the vehicles to reduce the emission levels of harmful gases as well [22, 23]. There has been considerable interest in the catalytic partial oxidation, resulting in production of intermediate raw materials, which are crucial to synthesize high value products.

The detailed mechanism of methane oxidation on noble metals is not well understood yet. Methane chemisorption and methane-deuterium exchange experiments [24] showed that the chemisorption of methane on noble metals involves dissociation to adsorbed methyl or methylene. The subsequent interaction of the methyl or methylene radicals with the adsorbed oxygen has been proposed to lead to either direct oxidation to carbon dioxide and water or the formation of chemisorbed formaldehyde [25]. Up to now the nature and oxidation states of the reactive surface are largely uncertain, and probably quite different in each of the studies. By the example of palladium, the oxidation might be occurring on the Pd metal, on a palladium (II) oxide surface, or even on a surface partially covered with oxygen. Indeed, all three types of catalytic reactions could be occurring simultaneously. As is known from X-ray photoelectron spectroscopy (XPS) measurements [26], the smaller the size of the palladium crystallites is, the greater the tendency is for them to exist in an oxide form. There are other uncertainties with regard to the catalytic oxidation of methane, that is, the role of the catalyst support, the effect of particle size and the choice of precursor salt used to prepare the catalyst.

It is worth mentioning that the kinetics of catalytic combustion is only relevant to the regions where the intrinsic surface reaction is the controlling step. In addition, the reaction will anyway reach a point where a large amount of thermal energy will be released as a result of complete consumption of the reactant. The energy can result in a significant temperature increase, so the stability of the catalyst at high operating temperatures is affecting the performance of the catalytic system [18]. It should be noted that noble metals form oxides and other chemical compounds, which, depending on the reactivity of the compound, determine both the speed and the mechanism of catalytic process; it noticeably complicates the search of optimum conditions of catalysis. For instance, Pd easily transforms to PdO at temperatures lower than 1100 K, however PtO_2 can hardly be generated below 825 K and it is a very unstable compound. Because of the greater stability of PdO in comparison with PtO_2, in the case of Pd based catalyst the active phase is the PdO while in the case of Pt based catalyst the active phase is metallic Pt. The activity of PdO is greater than that of Pt, which results in higher conversions for PdO.

The reaction temperature has a significant effect on the level of the activity of the catalyst in two ways. First, there is an apparent shift in the activation energy of methane catalytic combustion on Pd catalyst as the temperature increases. The temperature, where this transition happens, has been reported to be a function of catalyst composition [27]. Although it is crucial to differentiate changes in apparent activation energy occurring as a result of the onset of mass and heat transfer effects, there is sufficient evidence in the literature indicating that there is indeed a genuine activation energy shift in the reaction of methane catalytic combustion on Pd catalyst. Petrov et al. [25] studied methane combustion over noble metal catalysts in the temperature range of 500–800 K and they observed a sharp change in the values of reaction activation energy.

Summarizing, we conclude that the emergence and participation of chemically active surface during gas combustion (by the example of H_2 combustion over Pt surface) significantly complicates the understanding of the process due to the occurrence of a number of new governing parameters. These include the dependence of chemical activity of the catalyst on its chemical composition, temperature and conditions of mass transfer.

The paragraph is aimed at the investigation into Pt behavior in the flame of methane oxidation under conditions of turbulent flow. As is considered in [28], surface reactions on Pt surface are mainly highly activated ($\geq$ 20 kcal/mol). Therefore, one can expect not only inert behavior of Pt catalyst at comparably low temperatures, at which the catalyst does not have time to be heated, but also suppression of the process due to the complex mechanism of heterogeneous termination of atoms and radicals on a Pt surface.

5.2.1 Experimental

Flame propagation in stoichiometric mixtures of methane with oxygen diluted with CO_2 or Kr at initial pressures in the range of 100–200 Torr and 298 K (Fig. 5.6) in the pumped horizontally located cylindrical quartz reactor of 70 cm in length and of 14 cm in diameter was investigated. The reactor was fixed in two stainless steel gateways at the butt-ends, supplied with inlets for gas pumping, gas admission and a safety shutter, which swung outward when the total pressure in the reactor exceeded 1 atm. A pair of spark ignition electrodes was located near the left butt-end of the reactor [29, 30].

Four types of obstacles were used:

(1) a single flat obstacle with an opening of 25 mm in diameter closed with a flat iron net (wire $d = 0.1$ mm, cell size of 0.15 mm^2);
(2) a single flat obstacle with an opening of 25 mm in diameter closed with a flat iron net (wire $d = 0.1$ mm, cell size of 0.15 mm^2), a turn of Pt wire 0.3 mm in diameter was attached to the net;

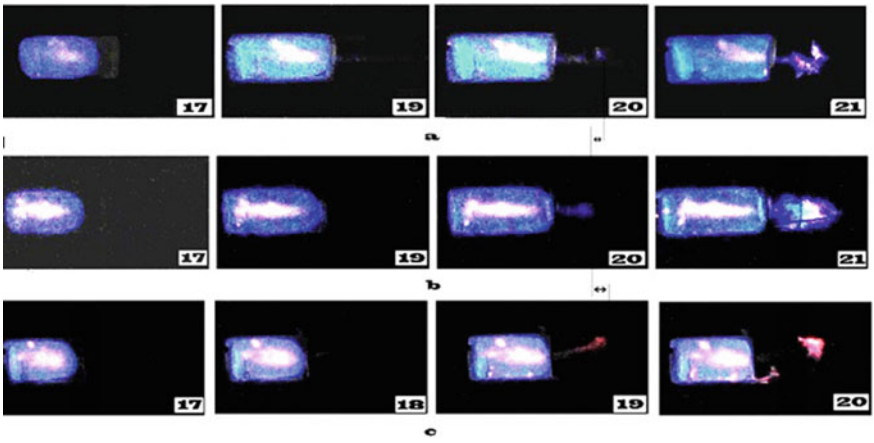

Fig. 5.6 **a** High-speed filming of FF propagation through the round opening of 2.5 cm in diameter in a planar obstacle of 14 cm in diameter, **b** high-speed filming of FF propagation through the round opening of 4 cm in diameter in a planar obstacle of 14 cm in diameter, **c** high-speed filming of FF propagation through the meshed sphere of 4 cm in diameter (wire diameter of 0.1 mm, cell size of 0.1 mm^2) inserted into a planar obstacle 14 cm in diameter, 15.4% CH_4 + 30.8% O_2 + 46% CO_2 + 7.8% Kr at initial pressure 170 Torr. The figure on a frame corresponds to frame number after discharge. Arrows specify distances of flame front occurrence after the obstacle

(3) a single flat obstacle with an opening of 25 mm in diameter with the obstacle (a) (Fig. 5.7Ia);
(4) a single flat obstacle with an opening of 25 mm in diameter with the obstacle (b) (Fig. 5.7Ib). Evidently, obstacles (3) and (4) are more effective turbulence stimulators than the obstacles (1) and (2), because they contain two consecutive obstacles, not one.

In the experiments, the obstacles with empty openings were placed first, i.e. the flame reaches the empty opening in the first instance. The second obstacle was placed at the distance of the "flame jump" [6] from the first one.

We remind that the ignition after obstacle with the central opening does not occur in the immediate vicinity of the obstacle, the first spot of ignition is observed considerably far from the obstacle surface. The less the diameter of an opening is, the farther FF from an obstacle appears (it is specified by arrows in the figure). A "flame jump" (we mean by "flame jump" the distance of flame emergence behind an obstacle) is much longer in the presence of the meshed sphere, than in the presence of a hole. For certainty, let us give an example from [5, Fig. 6.15]. The figure shows shots of a high-speed filming for the propagation of a methane flame through a narrow hole [(a) frame 20], through a wider hole [(b) frame 20] and through an obstacle in the form of a close-meshed sphere inserted into a flat obstacle [(b) frame 19].

This distance made up 12 cm under our conditions. In a number of experiments, the flat obstacle 14 cm in diameter with a single opening of 25 mm in diameter was provided with a reservoir where iron nanopowder was placed [Ref. [16] Fig. 1, (14)].

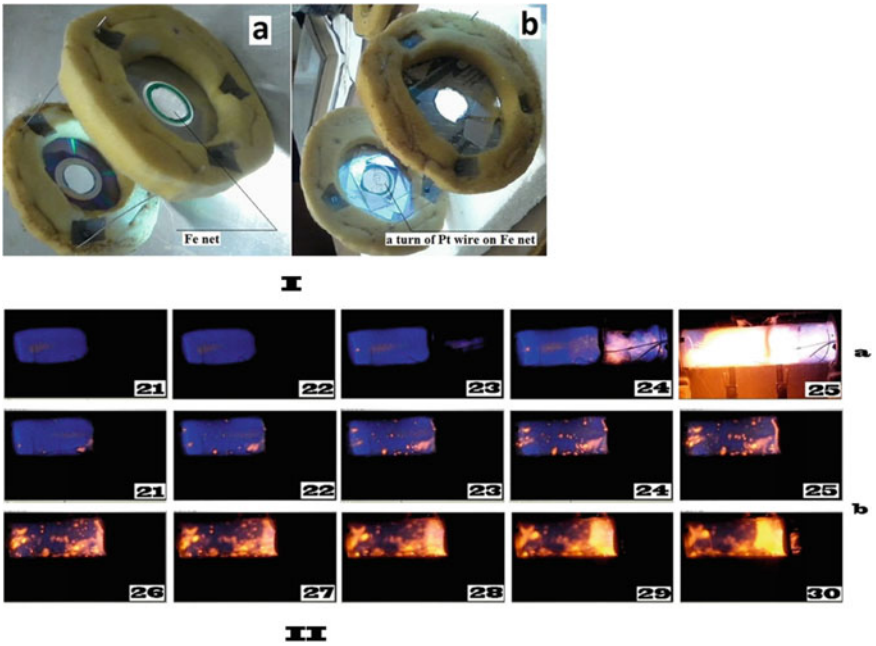

Fig. 5.7 (I) Complex obstacles. **a** flat obstacle 14 cm in diameter with a single opening of 25 mm in diameter (down) and a single opening of 25 mm in diameter (up) closed by a flat iron net (wire $d = 0.1$ mm, cell size of 0.15 mm^2), **b** flat obstacle 14 cm in diameter with a single opening of 25 mm in diameter (up) and a single opening of 25 mm in diameter (down) closed with a flat iron net (wire $d = 0.1$ mm, cell size of 0.15 mm^2) with a turn of Pt wire 0.3 mm in diameter. (II) High-speed filming of FF propagation through **a** obstacle 14 cm in diameter with a single opening 25 mm in diameter closed with a flat iron net [obstacle (1)]; **b** obstacle 14 cm in diameter with a single opening 25 mm in diameter closed with a flat iron net with a turn of Pt wire 0.3 mm in diameter [obstacle (2)]. 15.4% CH_4 + 30.8% O_2 + 46% CO_2 + 7.8% Kr. 600 frames/s. Initial pressure 170 Torr. The figure on a frame corresponds to a frame number after discharge

Iron nanoparticles, which were blown out of the reservoir through an opening with a gas flow at flame propagation from the left to the right, were ignited in a methane flame. Thus, burning iron nanoparticles visualized the gas flow during combustion. The combustible mixture (15.4% CH_4 + 30.8% O_2 + 46% CO_2 + 7.8% Kr) was prepared prior to experiment; CO_2 was added to enhance the quality of filming by decreasing FF velocity; Kr was added to diminish the discharge threshold. The reactor was filled with the mixture to necessary pressure. Then, spark initiation was performed (the discharge energy was 1.5 J). Speed filming of ignition dynamics and FF propagation was carried out from the side of the reactor [29–31] with a Casio Exilim F1 Pro color high-speed digital camera (frame frequency of 600 s^{-1}). Simultaneous detection of radicals CH ($A^1\Delta - X^2\Pi$) at 431 nm [10] was carried out with the use of two high-speed movie cameras Casio Exilim F1 Pro, one of which was equipped with a 430 nm interference filter. The video file was stored in

computer memory and its time-lapse processing was performed. The reagents were of chemically pure grade.

Iron nanopowders were obtained by the method of chemical metallurgy. The main stages of synthesis of metallic nanopowders in this method are a synthesis of the hydroxides of metals by means of alkali treatment of metal salts, sedimentation and drying of the hydroxides, their reduction and passivation [32]. Synthesis of iron hydroxide was performed by the heterophaseous interaction of solid iron salt with the solutions containing hydroxyl groups at suppression of dissolution of solid salt by the reaction of $FeCl_3$ and NH_4OH. After sedimentation of iron hydroxide it was washed out in a Buchner funnel to pH = 7 and dried in air until dusting. The reactor (described elsewhere [33]) with a sample of iron hydroxide powder 1 mm thick was maintained in the furnace during 1 h at 400 °C in hydrogen flow; then it was cooled to 20 °C in argon flow. For passivation of the iron nanopowder, which was performed in the same reactor, 0.6% of O_2 was added to argon stream at 20 °C.

5.2.2 *Results and Discussion*

The typical sequences of frames of high-speed filming of the flame front propagation through the obstacle (1) and the obstacle (2) are shown in Fig. 5.7IIa and Fig. 5.7IIb correspondingly. As is seen in Fig. 5.7II, the flame of the combustible mixture penetrates through the obstacle without Pt wire twice as fast as through the obstacle equipped with a Pt wire. It means that Pt under our experimental conditions has a noticeable suppressing influence on flame propagation even in the turbulent flow. The sequences of frames of speed filming of the flame propagation through complex obstacles (3) and (4) (obstacles a) and (b) in Fig. 5.7 I) are presented in Fig. 5.8a and Fig. 5.8b correspondingly. As is seen, the flame penetrates faster through the complex obstacle without Pt wire than through the obstacle equipped with a Pt wire. However, the suppressing influence of Pt under conditions of higher turbulence is less pronounced as compared with Fig. 5.7II.

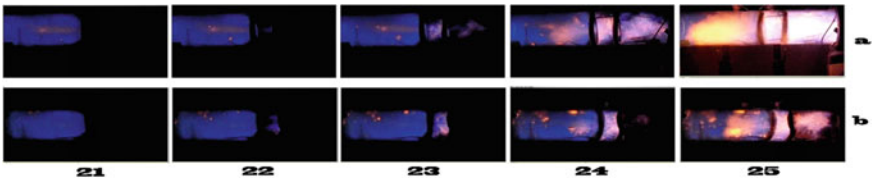

Fig. 5.8 High-speed filming of FF propagation through the complex obstacles consisting of **a** a flat obstacle 14 cm in diameter with a single opening 25 mm in diameter and the second flat obstacle with a single opening 25 mm in diameter closed with a flat iron net [obstacle (3)]; **b** a flat obstacle 14 cm in diameter with a single opening 25 mm in diameter and the second flat obstacle with the single opening 25 mm in diameter closed with a flat iron net with a turn of Pt wire 0.2 mm in diameter [obstacle (4)] 0.15.4% CH_4 + 30.8% O_2 + 46% CO_2 + 7.8% Kr. 600 frames/s. Initial pressure 170 Torr. The figure on a frame corresponds to frame number after discharge

To estimate the contribution of chemical factors, the emission of CH radicals ($A^1\Delta$–$X^2\Pi$) at 431 nm and the emission over the whole spectral interval in the presence of Fe nanopowder were recorded simultaneously. The sequences of frames obtained at flame penetration through the complex obstacle (3) in the presence of the Pt wire (I) and in the absence of the Pt wire (II) are shown in Fig. 5.9.

As is seen, Fe nanopowder ignites in the flame front, so the gas flow is visualized only when the flame front reaches the obstacle; while the usage of illumination with a laser sheet allows detecting a flow from the very beginning of the process [31]. It is seen also that the mesh on the second obstacle does not obstruct the flow of iron nanoparticles. We call attention to the fact that the intensity of emission of CH radicals after the obstacle monotonically increases after the flame reaches the obstacle.

In Fig. 5.10, the sequences of frames recorded at flame penetration through the complex obstacle (4) in the presence of a Pt wire (I) and in the presence of the Pt wire (II) are presented. The main difference in the process of flame penetration shown in Fig. 5.10 from that shown in Fig. 5.9 is that the emission of CH radicals practically passes off (frame 25); the combustible mixture ignites again at the butt-end of the reactor just as in case of absence of iron nanoparticles (Fig. 5.7b).

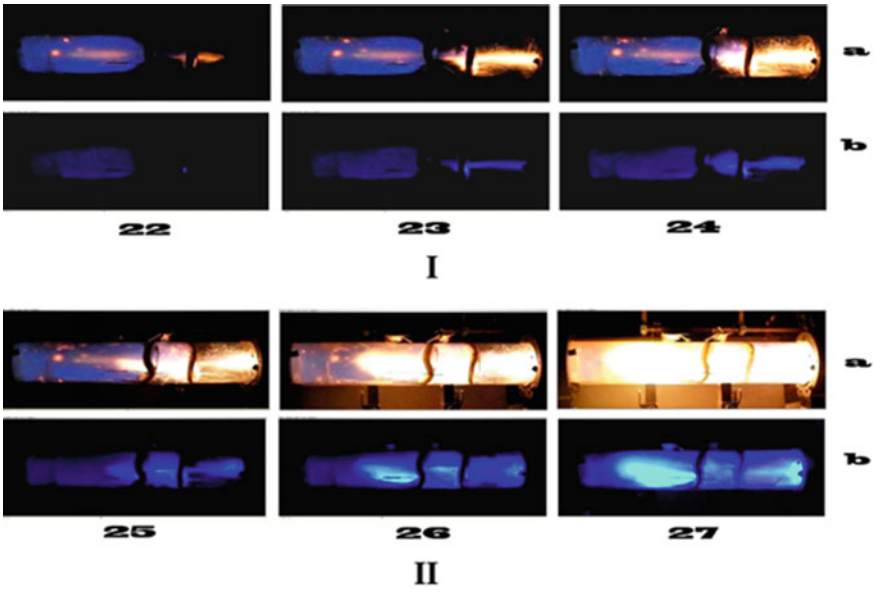

Fig. 5.9 High-speed filming of FF propagation through the complex obstacles. (I) in the presence of Pt wire turn, (II) in the absence of Pt wire turn. **a** a flat obstacle 14 cm in diameter with a single opening 25 mm in diameter and a reservoir with Fe nanopowder and the second flat obstacle with a single opening 25 mm in diameter closed with a flat iron net [obstacle (3)]; **b** the same complex obstacle, interference filter 430 nm is placed before the camera. 15.4% CH_4 + 30.8% O_2 + 46% CO_2 + 7.8% Kr. 600 frames/s. Initial pressure 170 Torr. The figure on a frame corresponds to frame number after discharge

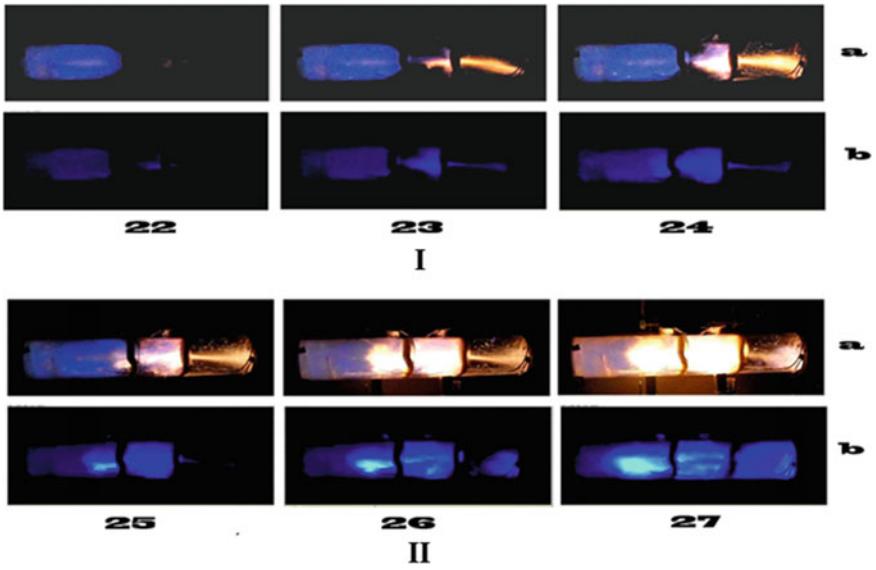

Fig. 5.10 High-speed filming of FF propagation through the complex obstacles. (I) in the presence of Pt wire turn, (II) in the absence of Pt wire turn. **a** a flat obstacle 14 cm in diameter with a single opening 25 mm in diameter and a reservoir with Fe nanopowder and the second flat obstacle with a single opening 25 mm in diameter closed with a flat iron net with a turn of Pt wire 0.3 mm in diameter [obstacle (4)]; **b** the same complex obstacle, interference filter 430 nm is placed before the camera. 15.4% CH_4 + 30.8% O_2 + 46% CO_2 + 7.8% Kr. 600 frames/s. Initial pressure 170 Torr. The figure on a frame corresponds to frame number after discharge

It means that the presence of burning Fe nanoparticles does not noticeably influence on the process of methane flame penetration; however, Pt wire in the obstacle affects the process both in the presence and in the absence of nanoparticles. As is evident from Fig. 5.10b, Pt provides a strong decrease in the intensity of emission of CH radicals, i.e. one can assume the high rate of chain termination on the Pt surface in agreement with [34]. In addition, as it was shown in [35], Pt wire is coated with a thick surface layer of Pt oxide, which exhibits some other properties than Pt. The flame penetrates through the Pt containing obstacle, apparently if Pt is heated enough (see Fig. 5.7IIb), though the heat balance on the Pt surface in a reactive turbulent flow is rather difficult to calculate. We approximately illustrated the contribution of chemical factors (chain termination on the obstacle surface) by means of numerical modeling using compressible dimensionless reactive Navier–Stokes equations in a low Mach number approximation [30, 36], which describe flame propagation in a two-dimensional channel. The equations showed a qualitative agreement with experiments [5–7, 30, 31]. The solution of the problem was carried out by finite element analysis with the package (FlexPDE 6.08, 1996–2008 PDE Solutions Inc. [16]). The simple chain mechanism [30] (see also Sect. 2.5 Chap. 2 Appendix) was used. Initiation condition was taken as $T = 10$ on the right boundary of the channel; there was a complex orifice in the channel. Boundary conditions (including the orifice)

were $C_\xi = 0$, $u = 0$, $v = 0$, $\rho_\xi = 0$, $n_\xi = 0$ (Fig. 5.11a) or $n = 0$ only on the plain mesh surface (Fig. 5.10b, the second obstacle from the right), as well as a convective heat exchange $T_t = T - T_0$ where ξ is the dimensionless coordinate. The results of calculations of flame propagation through the orifice are shown in Fig. 5.11. As is seen, the results of calculations for $n_\xi = 0$ (Fig. 5.11a) and $n = 0$ (Fig. 5.11b) show that the intensive termination of active intermediate on the mesh surface ($n = 0$) markedly influences on the flame penetration; namely, it causes the marked delay in flame penetration through the mesh in comparison with Fig. 5.11a. Therefore, regardless of the qualitative consideration, as well as a rather conventional modeling of the plain mesh, we managed to take into account the efficient action of the active surface on the features of the flame penetration.

Thus, we can conclude that under certain conditions Pt catalyst can suppress combustion and thereby show the opposite effect due to the high efficiency of Pt surface coated with a Pt oxide layer in the reaction of chain termination. Therefore, kinetic factors could be the determining even under conditions of high turbulence.

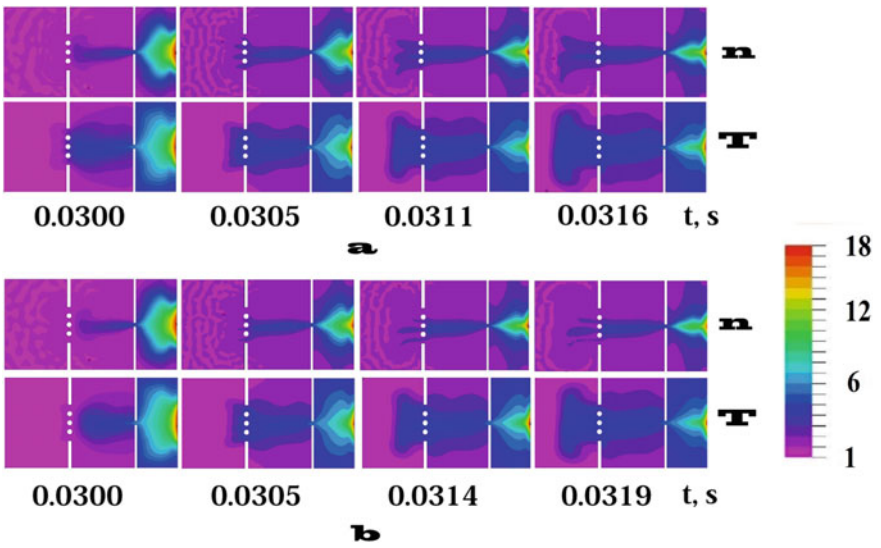

Fig. 5.11 Results of calculation of the process of flame propagation through the complex orifice. **a** change in dimensionless concentration of active intermediate n and temperature T for flame propagation through a complex opening for $n_\xi = 0$ on the mesh (II type of boundary conditions); **b** change in dimensionless concentration of active intermediate n and temperature T for flame propagation through a complex opening for n = 0 on the mesh (type I of boundary conditions); The scale of dimensionless temperature is presented on the right

5.3 Catalytic Activity of Platinum and Palladium in Gaseous Reactions of Oxidation of Hydrogen and Methane at Low Pressures

In nuclear power plant history, the major failures registered were Three Mile Island (1979), Chernobyl (1986) and Fukushima (2011). The prime reason for these disasters is because of the core meltdown in boiling water reactor (BWR) [37, 38]. At elevated temperatures (>1200 °C), reactor fuel cladding material Zircaloy (alloy of > 97% Zirconium) generates hydrogen gas upon oxidation reaction with steam [39]. The extensive quantities of H_2 and steam generated in the BWR system create high pressure and temperatures. This may lead to a reactor failure. Thus, the removal of excess amount of H_2 is necessary and extensive research is conducted to overcome the current challenge in nuclear industries. Improvement of passive catalytic hydrogen recombiners for the removal of hydrogen could avoid such disasters [40].

Further, large-scale fuel cell plants are being established for power generation for stationary, transportation and portable applications [41]. Often, fuel cells require excess amount of hydrogen to achieve stable voltage. The removal of excess hydrogen from the exhaust stream is required for safe operation [42]. In addition, residential central heating can be accomplished by hydrogen or natural gas combustion boilers (HCB or NGCB). However, direct hydrogen combustion in NGCB results in NO_x emissions because of high operating temperatures. Catalytic hydrogen combustion boilers operate at relatively low temperatures and are able to generate heat without CO_2 and NO_x emissions [43]. For hydrogen combustion reaction, the catalysts should possess properties such as oxygen storage capacity and thermal stability and should be able to provide hydrogen oxidation without explosion (that can be attained using noble metals). Noble metals have high adsorption capability of hydrogen and oxygen at low temperatures [44]. Moreover, understanding H_2 and O_2 behavior on the catalyst surface is crucial to focus on the mechanisms of various commercialized processes such as preferential oxidation and H_2 combustion.

Combustion engines running on methane-rich fuels are plagued by unburned methane slipping into the outlet. That is present in catalytic combustors used in gas turbines to burn the fuel at more moderate temperatures, and to reduce NO_x emissions. However, platinum based catalysts are not very effective with methane and only eliminate a small fraction of methane contained in the exhaust gases under normal lean burn operating conditions. Since these Pt based oxidation catalysts are not very efficient, Pd catalyst can provide high methane conversion [26]. Nevertheless, the peculiarities of catalytic action of noble metals have been under discussion.

In [45], for thermal/catalytic ignition of $2H_2 + O_2$ mixes, it was found that at pressures up to 180 Torr at 288 °C over Pd foil the catalytic activity of Pd surface is higher than over Pt foil. The activity of Pd foil expresses itself both in the occurrence of local ignition centers on the foil, from which combustion wave propagates, and in the dark catalytic reaction of consumption of the flammable mixture. In [46], the experimental value of effective activation energy of the ignition process is estimated as 3.5 ± 1 kcal/mol that is indicative of surface nature of the process. In this work,

we made an estimate of the activation energy of the dark reaction. We have shown in [47] that under certain conditions Pd catalysts can suppress the developing flame propagation in diluted methane–oxygen mix due to high efficiency of Pd surfaces in reactions of termination of active centers of the process. Therefore, even under conditions of high turbulence, kinetic factors can be determining ones.

The paragraph is aimed at establishment of specific features of oxidation of hydrogen and methane flame propagation over platinum and palladium at low pressures (70 ÷ 200 Torr).

5.3.1 Experimental

The experiments were performed with stoichiometric 2 H_2 + O_2 gas mixtures. A quartz reactor of 4 cm in diameter and 30 cm long heated up with an electric furnace, which temperature was controlled by means of a thermocouple was used. The reactor was supplied with a removable quartz window on its butt-end. Pd or Pt wires 0.3 mm in diameter, 150 mm long were placed in the reactor (Fig. 5.12 a). The pumped and heated reactor was filled with the gas mixture to necessary pressure. Before each experiment, the reactor was pumped down to 10^{-2} Torr. Total pressure in the reactor was monitored with a vacuum gauge with an indicator; its readings were recorded with a color digital camera Nikon 1J2.

Flame propagation in stoichiometric mixtures of methane with oxygen diluted with CO_2 or Kr at initial pressures in the range of 100–200 Torr and 298 K was investigated in the pumped out horizontally located cylindrical quartz reactor of 70 cm in length and of 14 cm in diameter. The reactor was fixed in two stainless steel frames, supplied with inlets for gas injection and a safety shutter, which swung outward when the total pressure in the reactor exceeded 1 atm.

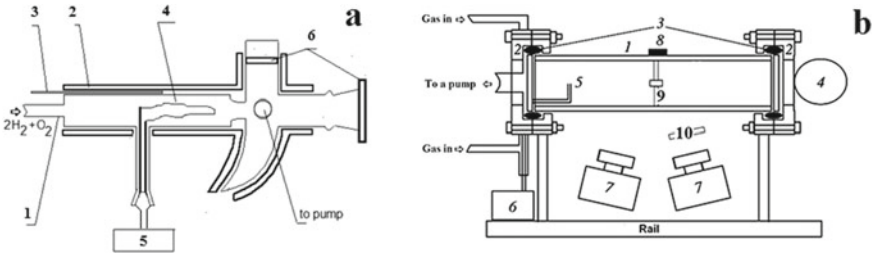

Fig. 5.12 **a** Experimental installation for the study of the dark reaction under static conditions. (1) quartz reactor of 4 cm in diameter and 30 cm long heated up in the electric furnace, (2) heater, (3) thermocouple, (4) Pd wire, (5) vacuum gauge VDG-1, (6) optical window; **b** Experimental installation for the study of initiated combustion. (1) quartz cylindrical reactor, (2) stainless steel gateway, (3) silicone laying, (4) stainless steel shutter, (5) spark electrodes, (6) power supply, (7) movie cameras Casio Exilim F1 Pro, 8- sensitive microphone "Ritmix", (9) Pt/Pd cylinder of 4 cm in length inserted into a planar obstacle 14 cm in diameter, (10) interference filter 430 nm

The obstacle was a Pt/Pd cylinder made of foil 0.3 mm thick and 40 mm in length inserted into a planar discus 14 cm in diameter (Fig. 5.12b). A pair of spark ignition electrodes was located near the left blunt end of the reactor [31]. The reactor was filled with the mixture up to necessary pressure. Then, spark initiation was performed (the discharge energy was 1.5 J). The speed filming of high speed video of ignition dynamics and flame front (FF) propagation was performed from the side of the reactor [31] by color high-speed digital cameras (frame frequency of 600 s^{-1}). Simultaneous detection of radicals CH ($A^1\Delta - X^2\Pi$) at 431 nm [31] was carried out by two high-speed movie cameras Casio Exilim F1 Pro, one of which was equipped with a 430 nm interference filter. The video file was stored in computer memory and its time-lapse processing was performed. The reagents were of chemically pure grade. The combustible mixture (15.4% CH_4 + 30.8% O_2 + 46% CO_2 + 7.8% Kr) was prepared prior to experiment; CO_2 was added to enhance the quality of filming by decreasing the flame propagation rate; Kr was added to diminish the discharge threshold. Chemically pure gases, 99.99% Pt and 99.85% Pd were used.

To evaluate the temperature dependence of the dark reaction (the branched chain reaction of H_2 oxidation below the ignition limit) the dependencies of total pressure of the 2 H_2 + O_2 mix on time were experimentally determined in the order given above (Fig. 5.13 a).

Notice that under the conditions no dark reaction in the presence of Pt wire instead of Pd was observed. As is seen in Fig. 5.13a, the experimental dependencies are practically straight lines. The dependence of tangent of the slope on temperature in Arrhenius coordinates is presented in Fig. 5.13 b. As is seen in Fig. 5.13, the dependence can be approximated by a straight line (the correlation coefficient is 0.988). The data was processed with the use of the program package Statistica 9 (Statsoft).

From Fig. 5.13b, we can estimate the value of effective activation energy of the process E = 4.1 ± 1 kcal/mol that is characteristic of surface processes [48]. It should be noted that the value of activation energy is close to one determined in [46] for the dependence of H_2 fraction at the ignition limit over Pd surface in mixtures with O_2 on temperature in Arrhenius coordinates: 3.5 ± 1 kcal/mol. The activated

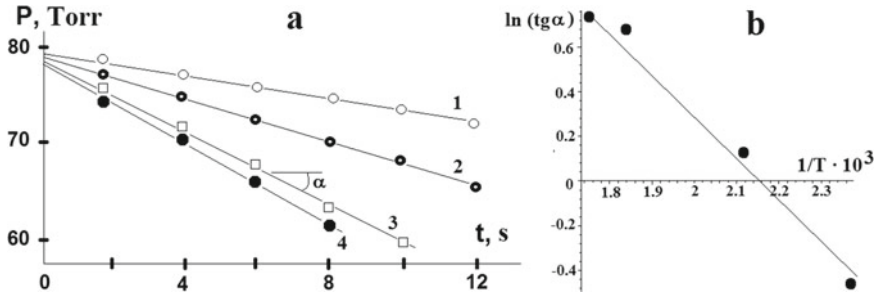

Fig. 5.13 **a** Dependencies of total pressure of the $2H_2$ + O_2 mix on time in the installation Fig. 5.12a), (1) 150 °C, (2) 200 °C, (3) 270 °C, (4) 300 °C; **b** Arrhenius plot of the dependencies **a**

(E = 16.7 kcal/mol [10]) homogeneous branching step $H + O_2 \rightarrow O + OH$ is the slowest elementary reaction of the branching (an increase in the number of active centers) cycle of reactions. However, the value of effective activation energy in the presence of Pd is markedly reduced, thus, the branching cycle must change, e.g. at the expense of the additional branching step. The step can be $H + HO_2 \rightarrow 2\ OH$, in which a relatively inactive HO_2 turns into active OH, i.e. extra branching occurs (see Sect. 3.3 Chap. 3). As is shown in [10] after ignition, laminar combustion takes place. The ignition after obstacle does not occur in the immediate vicinity of the obstacle, the first spot of ignition is observed at a certain distance from the obstacle surface (Fig. 5.14Ia, frame 24, Fig. 5.14Ib–d, frame 22), in good agreement with [31]. When the flame passes the obstacle, one can observe both flame penetration through the obstacle in case of Pt and Pd cylinders of 25 mm in diameter as well as Pt cylinder of 20 mm in diameter and a quenching effect at the smaller diameter (20 mm) of Pd cylinder, resulting in the extinction of a flame behind the orifice. It means that the critical diameter of the Pd cylinder exists, being between 20 and 25 mm.

The influence of obstacles can be expressed in the double way. On one hand, the flame interaction with obstacle can cause the development of flame instability, promoting its acceleration. On the other hand, the contact of a flame with the obstacle surface can lead to an increase in the contribution of heterogeneous reactions, in particular chain termination [49] as well as to an increase in heat losses. In our experiments, the obstacles differ by material. The rate of dark reaction even of fast H_2 oxidation on Pd surface (see Fig. 5.13) is too small to achieve noticeable degree of conversion for the time interval (1/600 s, see Fig. 5.14a–d) of flame penetration through the cylinder. It means that the rate of chain termination determines the occurrence of the critical diameter. Thus, the efficiency of Pd surface in chain termination reaction is much greater than that of Pt in agreement with [47].

It should be noted that under conditions of counter flames (the initiated ignition is carried out simultaneously from both sides of the obstacle, in our experiment at a different distance from the obstacle, Fig. 5.15) the critical diameter becomes markedly smaller: the flame penetrates through a Pd cylinder 20 mm in diameter. As is seen in the Figure, the boundaries of counter flame fronts interpenetrate each other. This means that gas dynamic factors are also important and these should be taken into consideration.

We approximately estimated the contribution of chemical factors (chain termination on noble metal surface) by numerical modeling on the basis of compressible dimensionless reactive Navier– Stokes equations in low Mach number approximation [36], which describes flame propagation in a two-dimensional channel. The equations showed a qualitative agreement with the experiments [31]. The problem was solved by a finite element analysis (FlexPDE 6.08 package [16]). The simple chain mechanism [31] was used. Initiation condition was taken as $T = 10$ on the right boundary of the channel; there was a complex orifice in the channel. Boundary conditions (including the orifice) were $C_\xi = 0$, $u = 0$, $v = 0$, $\rho_\xi = 0$, $n_\xi = 0$ and $n = 0$ only on the inner obstacle surface (this modeled the inner surface of noble metal cylinder), as well as a convective heat exchange $T_t = T - T_0$, where ξ is the dimensionless coordinate. The results of calculations showed that the intensive termination of active

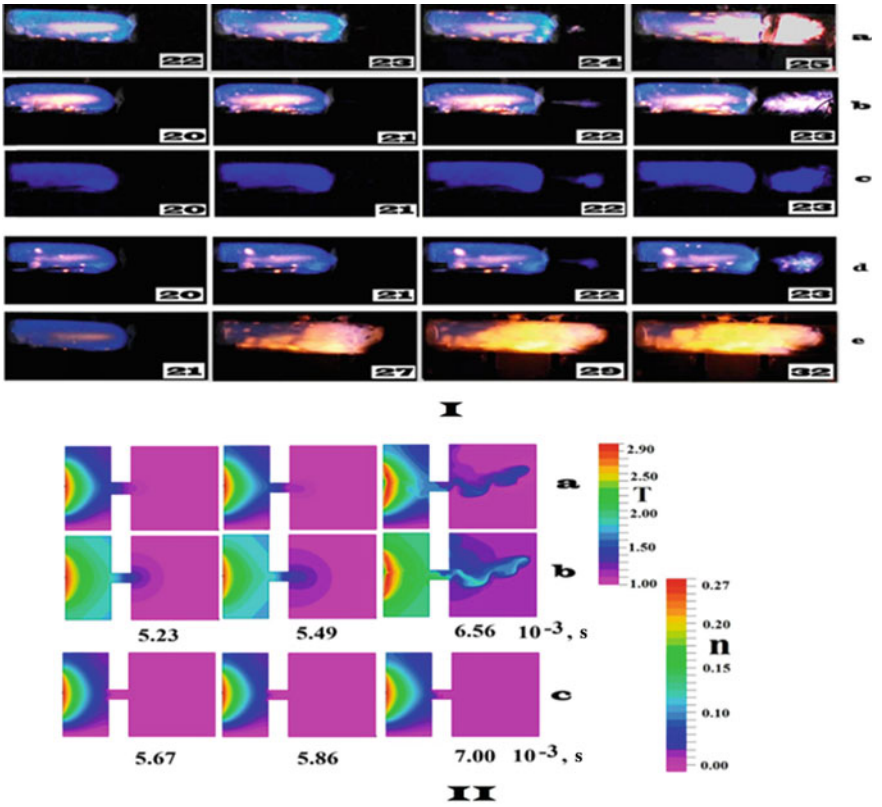

Fig. 5.14 (I) High-speed filming of FF propagation through (a) Pt cylinder 25 mm in diameter, (b) Pt cylinder 20 mm in diameter, (c) Pt cylinder 20 mm in diameter, filming through the interference filter 430 nm, (d) Pd cylinder 25 mm in diameter and (e) Pd cylinder 20 mm in diameter. Initial pressure, 170 Torr. The figure on a frame corresponds to a frame number after discharge; (II) Results of the calculation of flame propagation through a single opening. Change in (a) dimensionless temperature, (b) active intermediate n for $n_\xi = 0$ (boundary conditions of type I) in the opening, and (c) active intermediate n for $n = 0$ (boundary conditions of type II). The scales of temperature T and dimensionless active intermediate n are presented on the right

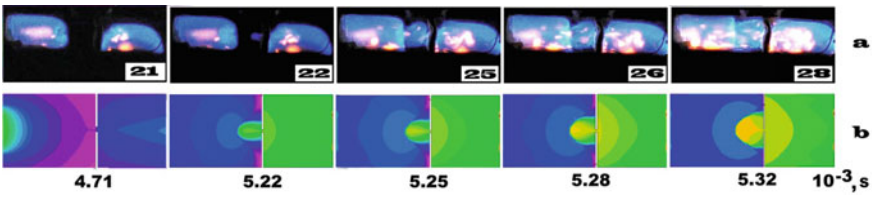

Fig. 5.15 **a** High-speed filming of counter flame propagation through the Pd cylinder 20 mm in diameter and **b** results of the numerical modeling of the change in dimensionless temperature for $n = 0$ (boundary conditions of type II). Initial pressure, 180 Torr. The figure on each frame corresponds to a frame number after discharge

intermediate on the inner obstacle surface ($n = 0$, Fig. 5.14c) markedly influences the flame penetration, namely, prevents flame penetration through the opening in comparison with the case of $n_\xi = 0$ (Fig. 5.14a, b). Hence, regardless of the qualitative consideration, we managed to illustrate the efficient action of the active surface on the features of the flame penetration.

Thus, Pd catalyst may suppress combustion as compared with Pt under certain conditions and thereby shows the effect opposite to catalytic one due to the high efficiency of Pd surface in the reaction of chain termination. Therefore, kinetic factors can be determining ones even under conditions of turbulence.

We shortly summarize the results.

The value of effective activation energy of the dark reaction over Pd is estimated as E = 4.1 ± 1 kcal/mol that is characteristic of surface processes. The values are close to one determined for the dependence of H_2 fraction at the ignition limit over Pd surface in mixtures with O_2 on temperature: 3.5 ± 1 kcal/mol. Under the conditions, no dark reaction in the presence of Pt wire instead of Pd was observed.

It was shown that the rate of chain termination determines the value of the critical diameter in flame penetration through Pt/Pd cylinders; the efficiency of Pd surface in chain termination reaction is much greater than that of Pt.

5.4 Conclusions

The peculiarities of propagation of a flame front of the diluted methane-oxygen mixture in the volumes of complex geometry in the laboratory scale installation were established. It was shown that a flame propagation process in a conditional room containing an indoor space with two openings and a flammable material inside shows a wide variety of combustion modes depending on the geometry of this complex volume, therefore, the preliminary numerical calculation of the expected flame propagation patterns may not always be successful. Thus, a real experiment under laboratory conditions, assuming the possibility of scaling the process, seems to be the most informative one.

The investigation into Pt behavior in the flame of methane combustion under conditions of turbulent flow was performed. We revealed that under certain conditions Pt catalyst can suppress combustion and thereby show the opposite effect due to the high efficiency of Pt surface coated with a Pt oxide layer in the reaction of chain termination. Therefore, kinetic factors could be determining ones even under conditions of turbulence.

Specific features of oxidation of hydrogen and methane over platinum and palladium at low pressures (70–200 Torr) were established. The value of effective activation energy of the dark reaction over Pd is evaluated as $E = 4.1 \pm 1$ kcal/mol that is characteristic of a surface process. Under our conditions, no dark reaction on Pt wire was observed. It was shown that the rate of chain termination determines the value of the critical diameter for flame penetration through Pt or Pd cylinders; the efficiency of Pd surface in chain termination reaction is much greater than that of Pt.

References

1. E. Richardson, T. Skinner, J. Blackwood, M. Hays, M. Bangham, A. Jackson, An experimental study of unconfined hydrogen–oxygen and hydrogen-air explosions, Joint Army-Navy-NASA-Air Force (JANNAF) Comb. Conf. Report Number M15-4263 (2015) 20150002596.pdf
2. J.E. Shepherd, Detonation in gases. Proc. Comb. Inst. **32**, 83 (2009)
3. C. Vincent, F. Sabatini, L. Aprin, F. Heymes, C. Longuet et al., Multi-scale experiments of household materials burning. Chem. Engineering Transactions, AIDIC **43**, 2419 (2015)
4. N.M. Rubtsov, M.I. Alymov, A.P. Kalinin, A.N. Vinogradov, A.I. Rodionov, K.Y. Troshin, *Remote Studies of Combustion and Explosion Processes Based on Optoelectronic Methods* (AUS Publishers, Melbourne, 2022)
5. N.M. Rubtsov, *The Modes of Gaseous Combustion* (Springer International Publishing, Switzerland, 2015)
6. N.M. Rubtsov, I.M. Naboko, B.S. Seplyarskii, V.I. Chernysh, G.I. Tsvetkov, K.Y. Troshin, Interaction of the laminar flames of natural gas–oxygen mixtures with planar obstacles, diffusers and confusers. Mendeleev Commun. **26**, 61 (2016)
7. N.M. Rubtsov, *Key Factors of Combustion. From Kinetics to Gas Dynamics* (Springer International Publishing, Switzerland, 2017)
8. C. Clanet, G. Searby, On the "tulip flame" phenomenon. Comb. Flame **105**, 225 (1996)
9. A. Mazas, D. Lacoste, T. Schuller, Experimental and numerical investigation on the laminar flame speed of CH_4/O_2 mixtures diluted with CO_2 and H_2O, ASME Turbo Expo, p. GT2010-22512 (Glasgow, United Kingdom, 2010) hal-00497963
10. B. Lewis, G. Von Elbe, *Combustion, Flames and Explosions of Gases* (Academic Press, London, 1987)
11. N.M. Rubtsov, G.I. Tsvetkov, V.I. Chernysh, K.Y. Troshin, Features of hydrogen and deuterium ignition over noble metals at low pressures. Comb. Flame **218**, 179 (2020)
12. T. Alasard, Low Mach number limit of the full Navier-Stokes equations. Arch. Ration. Mech. Anal. **180**, 1 (2006)
13. V. Akkerman, V. Bychkov, A. Petchenko, L.-E. Eriksson, Accelerating flames in cylindrical tubes with nonslip at the walls. Comb. Flame **145**, 206 (2006)
14. T.L. Jackson, M.G. Macaroeg, M.Y. Hussaini, Role of acoustics in flame/vortex. Interactions, NASA Contractor Report 191429 APR22, ICASE Report No. 93-4 (1993)
15. D. Chalet, A. Mahe, J. Migaud, J.-F. Hetet, A frequency modelling of the pressure waves in the inlet manifold of internal combustion engine. Appl. Energy **88**, 2988 (2011)
16. G. Backstrom, *Simple Fields of Physics by Finite Element Analysis* (GB Publishing, 2005)
17. H. Davy, Some new experiments and observations on the combustion of gaseous mixtures with an account of a method of preserving a continuous light in mixtures of inflammable gases and air without flame. Phil. Trans. R. Soc. London A **107**, 77 (1817)
18. J.H. Lee, D.L. Trimm, Catalytic combustion of methane. Fuel Process. Technol. **42**, 339 (1995)
19. O. Deutschmann, L.I. Maier, U. Riedel, A.H. Stroemman, R.W. Dibble, Hydrogen assisted catalytic combustion of methane on platinum. Catal. Today **59**, 141 (2000)
20. M. Lyubovsky, H. Karim, P. Menacherry, S. Boorse, R. LaPierre, W.C. Pfefferle, S. Roychoudhury, Complete and partial catalytic oxidation of methane over substrates with enhanced transport properties. Catal. Today **83**, 183 (2003)
21. S. Salomons, R.E. Hayes, M. Poirier, H. Sapoundjiev, Flow reversal reactor for the catalytic combustion of lean methane mixtures. Catal. Today **83**, 59 (2003)
22. J.K. Lampert, M.S. Kazia, R.J. Farrauto, Palladium catalyst performance for methane emissions abatement from lean burn natural gas vehicles. Appl. Catal. B **14**, 211 (1997)
23. P. Gelin, M. Primet, Complete oxidation of methane at low temperature over noble metal based catalysts: a review. Appl. Catal. B **9**, 1 (2002). https://doi.org/10.1016/S0926-3373(02)00076-0
24. A. Frennet, Chemisorption and exchange with deuterium of methane on metals. Catal. Rev. Sci. Eng. **10**, 37 (1974)

25. A. Petrov, D. Ferri, F. Krumeich, O. Krocher et.al, Stable complete methane oxidation over palladium based zeolite catalysts. Nature Commun. **9**, 2545 (2018). https://doi.org/10.1038/s41467-018-04748-x
26. A.W. Petrov, D. Ferri, M. Tarik, O. Kröcher, J.A. van Bokhoven, Deactivation aspects of methane oxidation catalysts based on palladium and ZSM-5. Top. Catal. **60**, 123 (2016)
27. H. Yoshida, T. Nakajima, Y. Yazawa, T. Hattori, Support effect on methane combustion over palladium catalysts. Appl. Catal. B: Environ. **71**, 70 (2007)
28. X. Zheng, J. Mantzaras, R. Bombach, Hetero-/homogeneous combustion of ethane/air mixtures over platinum at pressures up to 14 bar. Proc. Comb. Inst. **34**, 2279 (2013)
29. N.M. Rubtsov, I.M. Naboko, B.S. Seplyarskii, V.I. Chernysh, G.I. Tsvetkov, Non-steady propagation of single and counter hydrogen and methane flames in initially motionless gas. Mendeleev Commun. **24**, 308 (2014)
30. I.M. Naboko, N.M. Rubtsov, B.S. Seplyarskii, K.Y. Troshin, V.I. Chernysh, G.I. Tsvetkov, Cellular combustion at the transition of a spherical flame front to a flat front at the initiated ignition of methane–air, methane–oxygen and n-pentane–air mixtures. Mendeleev Commun. **23**, 358 (2013)
31. N.M. Rubtsov, V.I. Chernysh, G.I. Tsvetkov, K.Y. Troshin, Relative contribution of gas dynamic and chemical factors to flame penetration through small openings in a closed cylindrical reactor. Mendeleev Commun. **27**, 101 (2017)
32. N.M. Rubtsov, B.S. Seplyarskii, M.I. Alymov, *Ignition and Wave Processes in Combustion of Solids* (Springer International Publishing AG, 2017)
33. M.I. Alymov, N.M. Rubtsov, B.S. Seplyarski, A.B. Ankudinov, V.A. Zelensky, Temporal characteristics of ignition and combustion of iron nanopowders in the air. Mendeleev Commun. **26**, 452 (2016)
34. G.I. Golodets, V.M. Vorotyntsev, Temperature hysteresis in oxidation reactions on platinum. React. Kinet. Catal. Lett. **25**, 75 (1984)
35. N.M. Rubtsov, A.N. Vinogradov, A.P. Kalinin, A.I. Rodionov, K.Y. Troshin, G.I. Tsvetkov, V.I. Chernysh, Cellular combustion and delay periods of ignition of a nearly stoichiometric H_2–air mixture over a platinum surface. Mendeleev Commun. **26**, 160 (2016)
36. A. Majda, *Equations for Low Mach Number Combustion, Center of Pure and Applied Mathematics, PAM-112* (University of California, Berkeley, 1982)
37. P.C. Burns, R.C. Ewing, A. Navrotsky, Nuclear fuel in a reactor accident. Science **335**, 1184 (2012)
38. J.E. Ten Hoeve, M.Z. Jacobson, Worldwide health effects of the Fukushima Daiichi nuclear accident. Energy Environ. Sci. **5**, 8743 (2012)
39. T.K. Sawarn, S. Banerjee, S. Kumar, Study of the response of Zircaloy-4 cladding to thermal shock during water quenching after double sided steam oxidation at elevated temperatures. J. Nucl. Mater. **473**, 237 (2016)
40. S. Kelm, L. Schoppe, J. Dornseiffer, D. Hofmann, E.-A. Reinecke, F. Leistner, S. Jühe, Ensuring the long-term functionality of passive auto-catalytic recombiners under operational containment atmosphere conditions, an interdisciplinary investigation. Nucl. Eng. Des. **239**, 274 (2009)
41. T. Wilberforce, A. Alaswad, A. Palumbo, M. Dassisti, A.G. Olabi, Advances in stationary and portable fuel cell applications. Int. J. Hydrogen Energy **41**, 16509 (2016)
42. C.H. Woo, J.B. Benziger, PEM fuel cell current regulation by fuel feed control. Chem. Eng. Sci. **62**, 957 (2007)
43. P.E. Dodds, I. Staffell, A.D. Hawkes, F. Li, P. Grünewald, W. McDowall, P. Ekins, Hydrogen and fuel cell technologies for heating: a review. Int. J. Hydrogen Energy **40**, 2065 (2015)
44. A. Fernández, G.M. Arzac, U.F. Vogt, F. Hosoglu, A. Borgschulte, M.C.J. Jiménez de Haro, O. Montes, A. Züttel, Investigation of a Pt containing washcoat on SiC foam for hydrogen combustion applications. Appl. Catal. B **180**, 336 (2016)
45. N.M. Rubtsov, V.I. Chernysh, G.I. Tsvetkov, K.Y. Troshin, I.O. Shamshin, A.P. Kalinin, The features of hydrogen ignition over Pt and Pd foils at low pressures. Mendeleev Commun. **28**, 216 (2018)

46. N.M. Rubtsov, V.I. Chernysh, G.I. Tsvetkov, K.Y. Troshin, I.O. Shamshin, Ignition of hydrogen-methane-air mixtures over Pd foil at atmospheric pressure. Mendeleev Commun. **29**(4), 469 (2019). https://doi.org/10.1016/j.mencom.2019.07.039
47. N.M. Rubtsov, A.P. Kalinin, G.I. Tsvetkov K.Y. Troshin, I.D. Rodionov, Experimental study of interaction of a flame of methane oxidation and chemical processes on palladium metal at penetration of a flame through obstacles. Russ. J. Phys. Chem. B **12**, 1017 (2018)
48. S.M. Repinski, Vvedenie v himicheskuyu fiziky poverhnosti tvyordych tel (Introduction into chemical physics of the surface of solids) (Novosibirsk:; "Nauka", Sibir publishing company, 1993)

Conclusions

A cellular combustion regime of 40% H_2–air mixture in the presence of a Pt wire over the interval 270–350 °C was observed for the first time. It is shown that the regime is caused by the catalytic action of Pt containing particles formed by decomposition of volatile platinum oxide in the gas phase.

It was shown that the temperature of the initiated ignition at 40 Torr over heated Pd foil is ~ 100 °C lower than over Pt foil. Even the minimum temperature value (623 °C) is sufficient to ignite a $2H_2 + O_2$ mixture; i.e., the influence of a catalytic $H_2 + O_2$ reaction over the noble metals is negligible in case of initiated ignition. The presence of water vapor prevents ignition. For thermal ignition at 180 Torr and 288 °C over Pd foil the catalytic activity of the surface is higher than that over Pt foil. The activity of Pd foil reveals itself in both the occurrence of local ignition centers on the foil, from which combustion wave propagates; and the dark catalytic reaction of consumption of the flammable mixture.

It was shown that in the reaction of hydrogen combustion metallic Pt acts as a heat source similar to e.g. a tungsten wire heated by an external source. However, in the case under investigation, Pt is heated with an internal source, namely a surface catalytic reaction. It must be also taken into account that the composition of the surface layer changes during ignitions from Pt oxide (PtO_2) to another composition, exhibiting properties different from PtO_2.

Hydrogen and deuterium combustion over Rh, Ru, Pd and Pt wires at total pressures up to 200 Torr and initial temperatures up to 500 °C was investigated in order both to establish the dependencies of catalytic ignition limits over noble metal surfaces on temperature and to indicate the governing factors of the problem of gas ignition by a catalytic surface. It was revealed that Rh, Ru and Pd surfaces treated with $2H_2 + O_2$ ignitions show the defects in the form of openings, which are located on etching patterns; the etching substances are active intermediates of H_2 oxidation. It was found that before ignition catalytic wire is not heated up uniformly; initial centers of the ignition occur. It was shown that Rh is the most effective catalyst of $2H_2 + O_2$ ignition, the lowest ignition temperature over Rh coated Pd wire (Rh/Pd)

N. M. Rubtsov et al., *Catalytic Ignition of Hydrogen and Hydrogen-Hydrocarbon Blends Over Noble Metals*, Heat and Mass Transfer,
https://doi.org/10.1007/978-3-031-28416-8

was 210 °C, for Ru/Pd and Pd—300 °C, for Pt wire—410 °C at total pressures less than 200 Torr. The hysteresis phenomenon is observed over Ru/Pd, Pt and Pd wires; namely the ignition limit value measured over the wire, which is not treated with ignitions (a procedure of increasing temperature from a state of no ignition), is higher than the value measured with a procedure of decreasing temperature from a state of catalytic ignition. It was shown that Rh is the most effective catalyst of $2D_2 + O_2$ ignition, in this case the lowest ignition temperature over Rh coated Pd wire (Rh/Pd) was 100 °C. It is more accurate to speak about ignition over noble metals hydrides/deuterides; thus, the lowest ignition limit of $2D_2 + O_2$ over rhodium deuteride was 100 °C; thus, D_2 is more flammable than H_2 over Rh and Pd. The obtained results indicate the existence of a "kinetic inverse isotope effect", which affects the reactivity of MeH and MeD, where Me = Rh, Pd.

It was shown that the initiation of the thermal ignition process is always determined by the presence of reactive centers on the surface, the properties of which are determined by both surface defects having an excess of free energy and their catalytic properties; the ignition process includes stages of warming-up, local ignition, and flame propagation. The chemical activity of various sites of surface changes from one ignition to another. The basic feature of ignition process lies in the fact that ignition occurs at separate sites of surface at a uniform temperature of the reactor surface. Therefore, combustion originates on the surface of the reactor even under conditions of almost homogeneous warming up of a flammable gas mixture. It was found that the qualitative model based on the reactive compressible Navier–Stokes equations allows obtaining both the mode of the emergence of primary ignition centers on the wire followed by a local ignition, and the mode of a dark catalytic reaction of the consumption of the initial reagent.

It was shown experimentally that the ignition temperature of the 40% H_2 + air mixture over metallic Pd (70 °C, 1 atm) is ~ 200 °C lower than over the Pt surface (260 °C, 1 atm). In addition, Pd wire initiates the ignition of the (30–60% H_2 + 70–40% $CH_4)_{stoich}$ + air mixtures; Pt wire of the same size cannot ignite these mixtures at reactor temperatures below 450 °C. This means that Pd wire is more effective in initiation of ignition than Pt wire. The cellular structure of the flame front during ignition in the presence of Pd wire was not observed in contrast to the results obtained on the Pt surface. Therefore, Pd is more suitable than Pt for hydrogen recombiners in nuclear power plants because the catalytic particles do not appear in the gas phase. The experimental value of the effective activation energy of the process was estimated at (3.5 ± 1) kcal/mol, which is characteristic of surface processes. This indicates the significant role of the dark reaction of H_2 and O_2 consumption on the Pd surface observed directly at low pressures. The presence of this reaction reduces the probability of accidental explosion compared to the Pt surface. It was found that in the presence of leucosapphire, there was no system of emission bands of H_2O^* in the range 570–650 nm, and a possible explanation of this effect was given. The appearance of an additional source of excited water molecules emitting in the range 900–970 nm was explained.

It was experimentally shown that the temperature of the catalytic ignition limit over Pd at $P = 1.75$ atm, measured with a bottom-up approach by temperature, of

the mixtures 30% methane + 70% hydrogen + air ($\theta = 0.9$, $T = 317$ °C), and 30% propane + 70% H_2 + air ($\theta = 1$, $T = 106$ °C) markedly drops after subsequent ignitions to $T = 270$ °C for H_2–CH_4 mix and to $T = 32$ °C for the H_2–C_3H_8 blend. Equivalence ratio θ is a fraction of fuel in the mix with air: $\theta H_2 + 0.5\ (O_2 + 3.76\ N_2)$). The ignition limit returns to the initial value after treatment of the reactor with O_2 or the air; i.e., a hysteresis phenomenon occurs. The ignition limit of the mixtures 30% (C2, C4, C5, C6) + 70% H_2 + air ($\theta = 0.6$, 1.1, 1.2, 1.2, correspondingly) over Pd amounts to 25–35 °C at $P = 1.75$ atm; the hysteresis effect is missing. It was found that the lean 30% C_2H_6 + 70% H_2 + air mix ($\theta = 0.6$) shows the lowest temperature of the ignition limit: 24 °C at 1 atm. The estimate of the effective activation energy of the ignition of the mixes over Pd is ~ 2.4 ± 1 kcal/mol that is characteristic of a surface process. Thus, the usage of Pd catalyst allows igniting H_2–hydrocarbon mixtures at 1–2 atm at initial room temperature without external energy sources. It was shown experimentally that the ignition temperature of the 40% H_2 + air mixture over metallic Pd (70 °C, 1 atm) was ~ 200 °C lower than over the Pt surface (260 °C, 1 atm). In Addition, Pd wire initiates the ignition of the (30–60% H_2 + 70–40% $CH_4)_{stoich}$ + air mixtures; Pt wire of the same size cannot ignite these mixtures at reactor temperatures below 450 °C. This means that Pd wire is more effective in initiation of ignition than Pt wire.

It was found that the ignition temperatures of hydrogen–oxygen and hydrogen–methane–oxygen mixes at low pressure over heated Pd, Pt, Nichrome and Kanthal wires at 40 Torr increase with a decrease in H_2 concentration; only a heated Pd wire shows the pronounced catalytic action. Numerical calculations allowed revealing the role of an additional branching step $H + HO_2 \rightarrow 2OH$.

The peculiarities of ignition of premixed stoichiometric n-pentane-air mixtures were studied in a rapid mixture injection static reactor in the presence of metallic Pt and Pd in the region of negative temperature coefficient (NTC). It is shown that in the absence of noble metals thermoacoustic oscillations occur within NTC region. However, in the presence of Pt catalyst surface, which reacts with oxygen at the flame temperature and generates catalytic centers propagating into volume, thermoacoustic regimes of thermal ignition disappear. In other words, the catalytic Pt surface eliminates a certain inhibition stage of kinetic mechanism after the occurrence of the cool flame and NTC phenomenon vanishes; the stage may be e.g. the decomposition of some intermediate slow reacting peroxide on Pt surface with the formation of a more reactive radical. In the presence of the catalytic surface (Pd), which does not react at the flame temperature and does not generate catalytic centers propagating into volume, NTC phenomenon occurs.

Thus, the detected regularities must be taken into account in numerical simulations of NTC phenomenon. In other words, the oscillations and NTC phenomenon must both disappear in calculations after excluding a certain reaction or a series of reaction steps from the mechanism. The step must include the superficial reaction of an active intermediate of combustion on Pt surface, in which more active intermediates are formed from a low-active one.

It was found that the ignition delay (induction) period during the combustion of (70–40% hydrogen + 30–60% propane) + air mixtures over palladium at a total

pressure of 1–2 atm first decreases with a decrease in temperature and then increases until the ignition limit is reached, i.e., the NTC phenomenon occurs. The effective activation energy E of the process is 2.2 ± 1 kcal mol^{-1} that is characteristic of a surface process. Therefore, the NTC phenomenon detected in this work is closely related to the surface state of Pd. In the sample treated with ignitions, defects in the form of holes were found, which are focused on the etching patterns. In this process, PdO particles are formed during the oxidation of the Pd surface and decompose to Pd and O_2 at the temperature of flame products. Thus, Pd is consumed in the chemical etching reaction with active combustion intermediates. It should limit the applicability of palladium in ignition devices.

It was shown that, at total pressures up to 200 Torr, the catalytic ignition areas over the Rh and Pd surfaces are larger for $2H_2 + O_2$ mixtures than for $(H_2 + CH_4)_{stoich} + O_2$ and $(H_2 + C_4H_8)_{stoich} + O_2$ mixtures; the mixtures containing more than 50% hydrocarbons do not ignite. This behavior is directly related to the formation of a carbon-containing film on the noble metal surface. The fuel in the mixtures is consumed in a dark reaction. In the case of the synthesis of carbon nanotubes by this method, the noble metal plays both, the role of a catalyst for the growth of nanostructures and a heating element; for this, the presence of hydrogen and oxygen in the gas mixture is necessary. It has been shown that the dark reaction in the (80% H_2 + 20% $C_4H_8)_{stoich} + O_2$ mixture leads to the formation of carbon nanotubes with a mean diameter in the range of 10–100 nm.

It was shown that in the reactor treated with ignitions, the ignition temperature of the mixture 70% H_2 + 30% methane with air over rhodium surface is 62 °C. The result indicates the potential of using rhodium catalyst to markedly lower the ignition temperature of the fuels based on hydrogen-methane mixtures.

The critical condition for volume reaction is revealed: the volume process occurs at 45% H_2, but it is missing at ≤ 40% H_2. If $H_2 \leq 40\%$, only a slow surface reaction occurs; this phenomenon is qualitatively described by our earlier calculations. It was revealed that the effective activation energies both of "upper" and "lower" limits of H_2 + methane oxidation over the range of linearity are roughly equal (2.5 ± 0.6) kcal/mol^{-1}; it means that the key reactions, responsible for the occurrence of "upper" and "lower" ignition limits are almost certainly the same. It was shown that for Rh/Pd catalyst, the chain development process has most likely heterogeneous nature because the effective activation energy is < 3 kcal/mol.

Rh has been found to be a more effective catalyst than Pd for the studied combustion processes. The effective activation energies of catalytic ignition depend not only on the nature of the catalyst but also on the chemical nature of the hydrocarbon in the mixture. Thus, catalytic ignition is initiated by exothermic surface ignition of hydrogen oxidation reaction in the presence of a catalyst, hydrocarbon on the surface is consumed in reactions involving hydrogen oxidation intermediates that do not lead to branching of chains, then the combustion propagates into volume. It was found that in the reactor not treated with ignition, the ignition temperature of the mixture of 70% H_2 + 30% methane-air above the Pd surface at a pressure of 1.75 atm is 310 °C, and above the Rh surface—105 °C. In the ignition-treated reactor, the ignition temperature of this mixture above the Pd surface at a pressure of 1.75 atm is

270 °C and above the Rh surface is 62 °C. The obtained result indicates the prospect of using a rhodium catalyst for lowering the ignition temperature of methane and hydrogen based fuels.

It was shown that under conditions of our experiments not the chemical nature of the catalyst but that of C_2 hydrocarbon in the mix with H_2 is the determining factor of catalytic ignition. The catalytic ignition limits of synthesis gas over Rh/Pd are qualitatively different from the dependencies for combustible hydrogen-hydrocarbon: the "lower" catalytic limit dependence has a distinct maximum, which indicates a more complex mechanism of the catalytic process; Arrhenius dependence of ln $[H_2]_{lim}$ on $1/T$ could not be applied. Therefore, the interpretation of the "upper" and "lower" limits of catalytic ignition given in the literature should be clarified. The relatively long delay periods of catalytic ignition of hydrogen—n-pentane mixes (tens of seconds) and the absence of the dependence of the periods on the initial temperature allow us to conclude that the catalytic ignition of hydrogen—n-pentane mixes is determined by the transfer of hydrocarbon molecules to the surface of the catalytic wire. Thus, in the oxidation of hydrogen-hydrocarbon blends for "short" hydrocarbons, the main factor determining catalytic ignition is the oxidation reaction of hydrogen on the catalytic surface. With an increase in the number of carbon atoms in the hydrocarbon, the factors associated with the chemical structure, that is, the reactivity of the hydrocarbon in catalytic oxidation, begin to play a significant role; and then the oxidation rate is already determined by the processes of transfer of the hydrocarbon molecules to the catalyst surface.

It was shown that the ignition limits of $2H_2 + O_2$ and $(80\%\ H_2 + 20\%\ CH_4)_{stoich} + O_2$ mixes over Pt wire do not depend on the applied voltage without discharge up to 1200 V. It was shown that in combustion of $(80\%\ H_2 + 20\%\ CH_4)_{stoich} + O_2$ mixes the application of an electric field (1200 V) leads to disappearance of Pt containing particles formed by decomposition of volatile platinum oxide in gas phase from the reaction volume, which indicates that these particles are charged. This may be due to a chemiionization phenomenon observed in the combustion of hydrocarbons. Is was shown that in combustion of $(80\%\ H_2 + 20\%\ CH_4)_{stoich} + O_2$ mix carbon nanotubes practically do not form as distinct from combustion of $(H_2 + C_4H_8)_{stoich} + O_2$ mix.

It was found that an exemplary flame propagation process in a conditional room containing an indoor space with two openings and a flammable material inside shows a wide variety of combustion modes depending on the geometry of this complex volume. The preliminary numerical calculation of the expected flame propagation patterns may not always be successful. Thus, a real experiment under laboratory conditions, assuming the possibility of scaling the process, seems to be the most informative one.

It was shown that under certain conditions Pt catalyst can suppress combustion and thereby show the opposite effect due to the high efficiency of Pt surface coated with a Pt oxide layer in the reaction of chain termination. Therefore, kinetic factors could be the determining ones even under conditions of high turbulence.

The value of effective activation energy of the dark reaction of H_2 oxidation over Pd is evaluated as $E = 4.1 \pm 1$ kcal/mol that is characteristic of a surface process. The value is close to one determined in the literature for the dependence on temperature

of the H_2 fraction at the ignition limit over Pd surface in mixtures with O_2: 3.5 $\pm$ 1 kcal/mol. It was shown that the rate of chain termination determines the value of the critical diameter for flame penetration through Pt or Pd cylinders; the efficiency of Pd surface in chain termination reaction is much greater than that of Pt. Therefore, the action of noble metals on the processes of hydrocarbons oxidation is an effective tool to identify important reaction sets in their kinetic mechanisms.